The development of a cellular model of nephrosis to evaluate nephrotoxic biomarkers

Gareth Marlow

The Development of a Cellular model of Nephrosis to Evaluate Nephrotoxic Biomarkers

Gareth Marlow

Department of Biological Sciences

University of Durham

2005

Abstract

Nephrotoxicity is one of the major causes for compound failure late in the drug development process. Pharmaceutical companies are interested in identifying biomarkers of nephrotoxicity which can be used to identify potential toxic compounds earlier in the development process and hence reduce the overall time and costs involved in bringing a drug to market.

I developed a cellular model of nephrosis, in NRK cells, using the well characterized nephrotoxicant compound puromycin aminonuceloside (PAN). Using this cellular model I examined the expression of kidney specific genes. Two podocyte specific proteins, podoplanin and podocalyxin were found to be specifically down-regulated. Podoplanin showed an almost universal 65% reduction in the level of gene expression after PAN treatment. Podocalyxin showed a dose-dependent reduction in expression, which reached a peak of 85% reduced expression at the highest PAN dose tested.

A cell aggregation assay was developed to quantify the effect of PAN induced nephrosis on the cell adhesion properties of the NRK cells. It was found that PAN nephrosis had a significant effect on the cells ability to aggregate and to remain adhesive. However cells which lost the ability to adhere were still found to be viable. Integrin α3 protein expression was found not be altered in response to PAN treatment as determined by immunofluorescence microscopy however Laminin β2 was found to form aggregates in response to PAN treatment. The actin cytoskeleton was also found to be severely disrupted as a result of PAN induced nephrosis.

Based on these studies podocalyxin has been identified as a potential genetic biomarker of nephrosis, however further study of podocalyxin expression in other models of nephrosis is required before podocalyxin can be routinely used as a predictor of nephrotoxicity.

Declaration

I declare that the work within this thesis is my own work. Any material generated through joint work has been acknowledged and the appropriate publications cited. In all other cases material from the work of others has been acknowledged and quotations and paraphrases suitably indicated.

Signed... Gareth Mahr .....

Date..... 1/12/05 .....

Statement of Copyright

Acknowledgements

There are many people to thank, in getting me to this point. First and foremost I would like to thank my supervisors; Dr Rumaisa Bashir, without whose support and guidance over the last four years this thesis wouldn't have been possible. Dr Uzma Atif and Dr Bronagh Heath at GlaxoSmithkline, whose input during the early meetings got me going and who challenged me to think outside the box.

I would also like to thank Dr Julie Holder who provided me with the invaluable resource of her time and expertise both in the production of this thesis and throughout the last three years. I would also like to thank Julie and everyone within the CPT group for making me feel welcome and for all their support while I used their facilities to image my results and for giving me the opportunity to present my results to a wider audience.

A big thank you to everyone who has helped me, Stephanie Margrett who taught me everything I needed to know about tissue culture, Mike Aylott who very patiently taught me all about statistical analysis, everyone within the ICBL who always made time to answer my questions and discuss ideas, all of Dr Jahoda's group, who kindly shared tissue culture facilities and Dr Chris Thompson and his staff who helped create an enjoyable working environment.

I would like to thank all my friends at Durham, who made three years flyby. But my greatest thanks go to my parents who supported me throughout my time in Durham and during my write-up when I was back at home.

Last but not least I would like to thank the BBSRC and GSK for their generous funding.

Table of Contents

Chapter 2. Materials and Methods 55

Chapter 3. Establishing a Cellular Model which Mimics PAN Nephrosis 75

List of Figures

List of Tables

Abbreviations

CAMS	Cell adhesion molecules
CD2AP	CD2-associated protein
CNF	Congenital nephrotic syndrome of the Finnish type
CNS	Congenital nephrotic syndrome
DDS	Denys-Drash syndrome
DICs	Detergent-insoluble complexes
DIGs	Detergent-insoluble glycosphingolipids
D-MEM	Dulbecco's modified eagle media
DRM	Detergent-resistant membranes
EDTA	Ethylene diamine tetra-acetic acid
EEA1	Early endosomal antigen 1
EGR-1	Early growth response gene 1
EM	Electron microscopy
ER/N	Endoplasmic reticulum/nuclei
ERM	Ezrin/radixin/moesin
ERMAD	ERM-associated domain
ESRD	End-stage renal disease
EST	Expressed sequence tag
FACS	Fluorescence Activated Cell Sorting
FBS	Fetal bovine serum
FDA	US Food and Drug Administration
FISH	Fluorescent *in situ* hybridization
FP	Foot process
FS	Frasier syndrome
FSGS	Focal Segmental Glomerulosclerosis
G3PDH	Glyceraldehyde 3 phosphate dehydrogenase
GBM	Glomerular basement membrane
GLEPP-1	Glomerular epithelial protein 1
GVEC	Glomerular visceral epithelial cells
HBSS	Hank's balanced salt solution
HDM	High density microsomes

Hom	Homogenate
Ig	Immunoglobin
ILK	Integrin-linked kinase
KIM-1	Kidney injury molecule 1
LCM	Laser capture microdissection
LDM	Low density microsomes
mAb	monoclonal antibody
MAGUK	Membrane associated guanylate kinase
MCD	Minimal change disease
MCN	Minimal change nephropathy
MCNS	Minimal change nephrotic syndrome
MN	Membranous nephropathy
NHE3	NA+/H+ exchanger isoform 3
NHERF1	Na+/H+ exchange factor 1
NHERF2	Na+/H+ exchange factor 2
NPHS1	Gene encoding nephrin
NPHS2	Gene encoding podocin
NRK	Normal rat kidney cells
pAb	polyclonal antibody
PAGE	Polyacrylamide gel electrophoresis
PAN	Puromycin aminonuceloside
PBS	Phosphate buffered saline
PCLP	Podocalyxin like protein
PDI	Protein disulfide isomerase
PFA	Paraformaldehyde
PHN	Passive Heymann nephritis
PIP2	Phospatidylinositol 4,5-biphosphate
PM	Plasma membrane
PPGS	Podocalyxin-positive granular structures
RPTP	Receptor protein tyrosine phosphatases
RT-PCR	Reverse transcription Polymerase chain reaction
SD	Slit Diaphragm
SDS	Sodium dodecyl sulphate

SNP	Single nucleotide polymorphism
SRNS	Steroid resistant nephrotic syndrome
TBM	Tubular basement membrane
TJ	Tight junction
WAGR	Wims' tumor, aniridia, genitourinary abnormalities and mental retardation
WT-1	Wilms' tumor suppressor 1
ZO-1	Zonula occludens 1

Chapter 1.
Introduction

1.1. Kidney Structure

1.1.1. Gross Kidney Anatomy

The kidneys are a pair of organs situated in the posterior section of the abdomen behind the peritoneum and located either side of the spine. In humans the kidneys lie between the twelfth thoracic vertebra and the third lumbar vertebra. An average human kidney ranges between 125 – 170 g in men and 115 – 155 g in women. The kidney is approximately 11 – 12 cm in length 5 – 7.5 cm in width and a minimum thickness of 2.5 cm [1].

Located on the medial surface of each kidney is a slit called the hilum, through which passes the renal artery and vein, the renal nerve, the lymphatics and the renal pelvis. The renal pelvis is the funnel shaped upper end of the ureter, it is lined by transitional epithelium. Extensions of the pelvis, the calices, extend towards the papilla of each pyramid.

If a kidney is bisected longitudinally, the cut surface shows two distinct regions. A dark outer region, called the cortex, and a pale inner region, the medulla. The medulla is further divided into renal pyramids, where the apex of each pyramid extends towards the renal pelvis, forming a papilla (Figure 1.1) [2].

On the tip of each papilla are small openings which represent the distal ends of the collecting ducts. Striations can be seen on the renal pyramids, these are medullary rays, which are attributed to the collecting ducts, loops of Henle and blood vessels in this region.

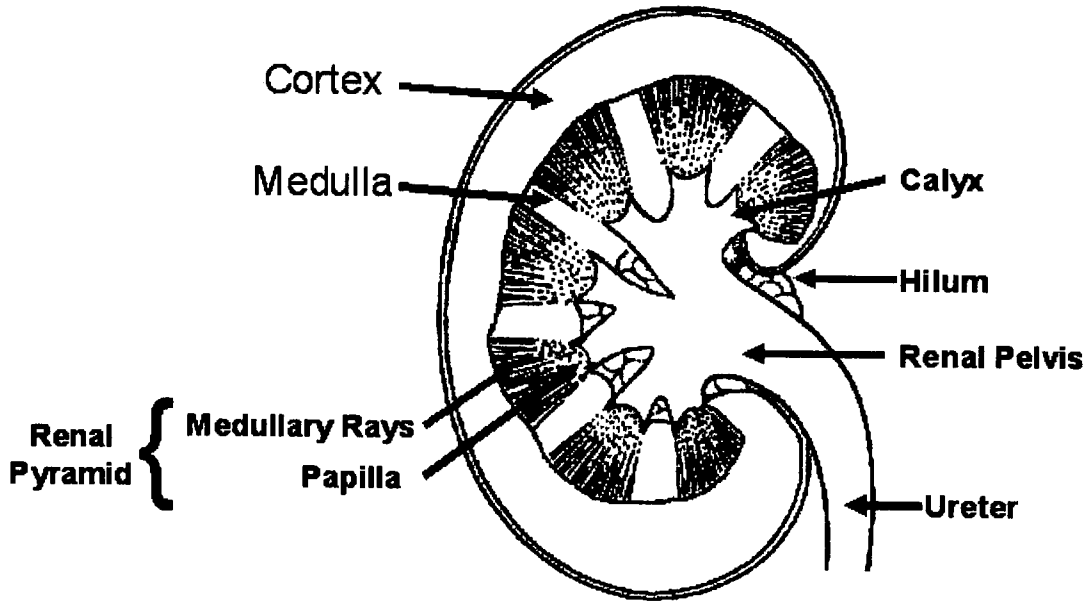

Figure 1. 1. Schematic Representation of a Bisected Kidney

Adapted from fig 2.1 Principles of Renal Physiology [2].

In contrast to humans, rats only posses a single renal pyramid and are therefore termed unipapillate. In a unipapillate kidney, the papilla is directly surrounded by the renal pelvis. Other than this difference rat kidneys resemble human kidneys in their gross anatomy.

The kidneys of rat, as in all mammals, are mainly involved in homeostasis through the regulation of fluid volume, electrolyte composition and acid-base balance. It also has endocrine and metabolic functions, including detoxification. The main functional unit of the kidney is the nephron [1, 2].

1.1.2. The Nephron

Each human kidney contains 1 – 1.5 million nephrons, while a rat has approximately 30,000 – 34,000. A nephron is a blind-ended tube; the blind end forms the Bowman's capsule around a knot of capillaries, the glomerulus. The remaining components of the nephron are the proximal tubule, the loop of Henle and the distal tubule (Figure 1.2). The collecting duct is not classed as part of the nephron because it arises embryologically from the ureteric bud, while the remaining components all originate from the metanephric blastema [1, 2].

There are two main populations of nephron; the juxtamedullary nephrons have long loops of Henle, which pass deeply into the medulla while the cortical nephrons have very short loops of Henle (Figure 1.2). In humans only 15% of nephrons are juxtamedullary, in rats this figure increase to 30%. The length of the loop of Henle is related to the position of the glomerulus. Although there are two basic types of nephron many variations exist depending on their position within the cortex.

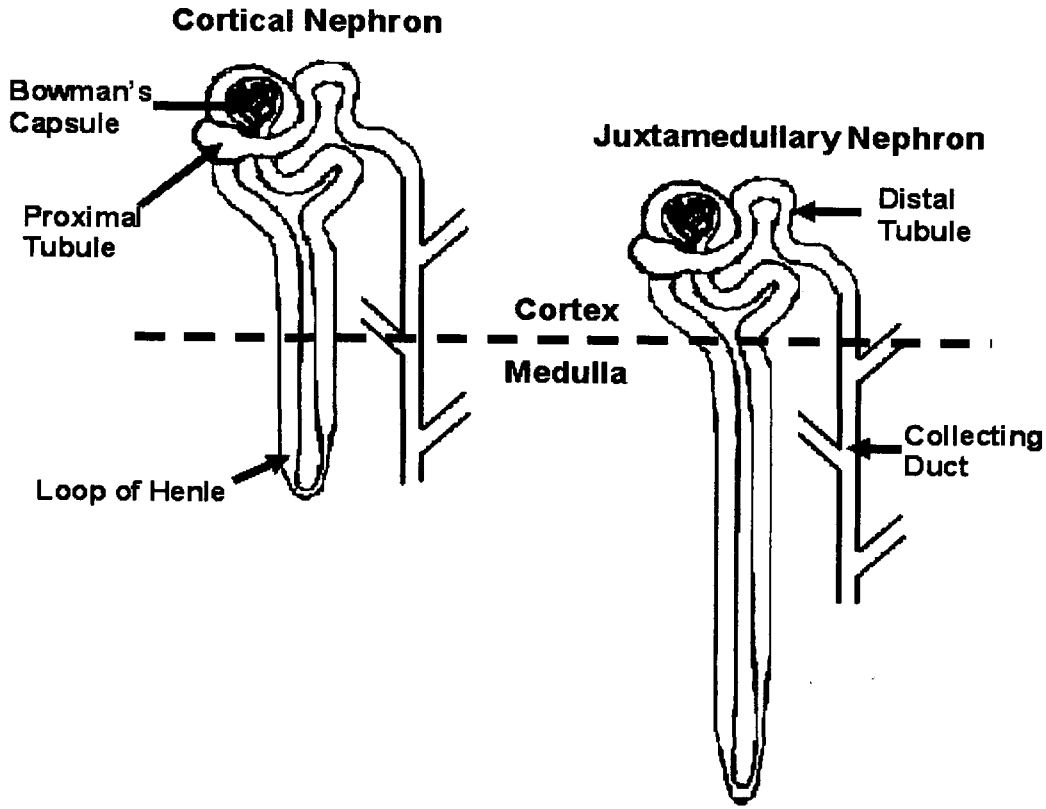

Figure 1. 2. Schematic diagram showing the main components of the two main classes of nephron.

Adapted from fig 2.2 Principles of Renal Physiology [2].

1.1.3. Proximal Tubule

The proximal tubule is the first section of the nephron after the Bowman's capsule. It starts convoluted (pars convoluta) but becomes straight (pars recta) and passes down towards the medulla where it becomes the descending limb of the loop of Henle. It is generally 12 – 25 mm in length with an outside diameter of 70 µm.

The convoluted section of the proximal tubule consists of cuboidal/columnar cells, which have a 'brush border' on their luminal surface; this increases the surface area available for absorption. The cells of the straight part of the proximal tubule are very similar to those of the convoluted section, but have a less dense brush border and fewer mitochondria [2].

Loop of Henle/ Distal tubule:

The loop of Henle is composed of the straight portion of the proximal tubule (pars recta), the thin limb segments, and the straight portion of the distal tubule. The cells of the thin part of the loop of Henle are squamous, and resemble capillary endothelial cells. The ascending thin segment of the loop is up to 15 mm long and the external diameter is 20 µm. The thick ascending segment of the loop is a cuboidal/columnar epithelium, with cells similar in size to those of the proximal tubule. However the cells are lacking a brush border and have few basal infoldings but many infoldings and projections on the luminal surface.

Collecting duct:

Most cells are cuboidal, with a much less granular cytoplasm than that of the proximal tubule cells. In the cortex, each collecting duct receives 6 distal tubules, and as the ducts enter the medulla they join each other in successive pairings to form the duct of Bellini, which drains into a renal calyx.

1.1.4. Glomerulus

The glomerulus also referred to as the renal corpuscle is composed of a capillary network lined by endothelial cells, a central region of mesangial cells, the visceral epithelial cells (podocytes) and the associated basement membrane. The role of the glomerulus is to act as the filtration barrier creating the plasma ultrafiltrate. The average diameter of a human glomerulus is approximately 200 μm while for rats it is 120 μm. Juxtamedullary nephrons have glomeruli which are approximately 20% greater in diameter. The mean area of the filtration surface per glomerulus has been reported to be 0.136 mm^2 in humans and 0.184 mm^2 in rats. Ultrafiltration occurs across the glomerulus into the Bowman's capsule. The filtrate must sequentially cross the fenestrated endothelium, the glomerular basement membrane (GBM) and finally the podocyte slit diaphragms (Figure 1.3) [1].

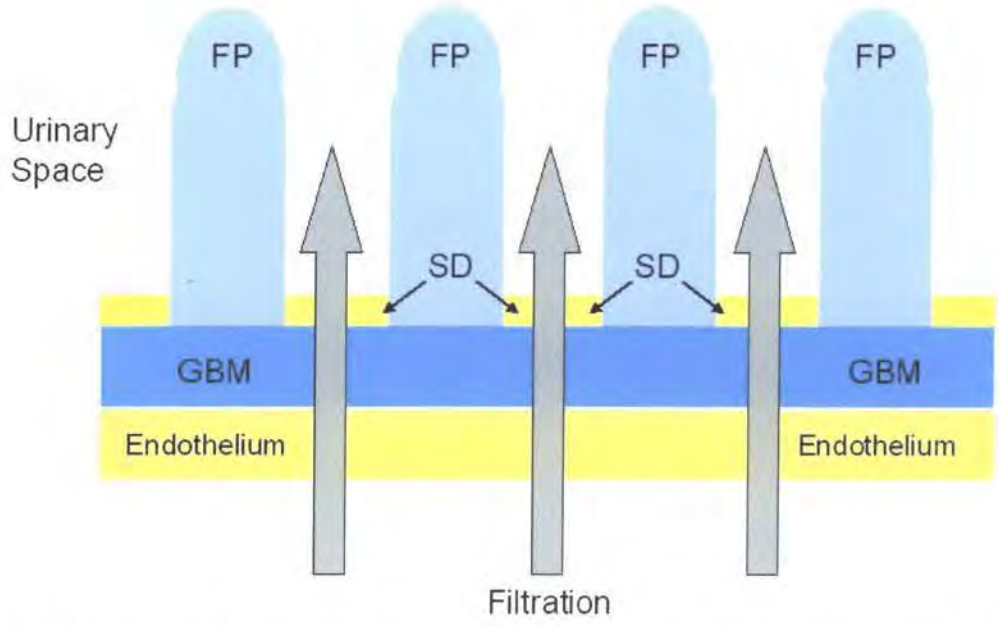

Figure 1. 3. **The main components of the glomerular filtration barrier**. FP – Podocyte Foot Process, SD – Slit Diaphragm, GBM – Glomerular Basement Membrane

1.1.5. Glomerular Basement Membrane

The glomerular basement membrane (GBM) is composed of three layers, a central layer called the lamina densa, which is surrounded by two thinner layers the lamina rara externa and the lamina rara interna. The layered configuration is the result in part of the fusion of endothelial and epithelial basement membranes during development.

The GBM is a molecular scaffold consisting of type IV and type V collagen, laminin, fibronectin, proteoglycans and nidogen which are tightly cross-linked. Several estimates of the thickness of the normal human GBM have been made: Osawa [3] reported it to be 315 nm, Jorgenson [4] 329 nm and Osterby [5] 310 nm, the rat has been found to be 132 nm in thickness.

It is commonly believed that the GBM is the principal structure responsible for the permeability of the glomerulus because it is both a charge-selective and size-selective barrier, however there is increasing evidence that the podocyte slit diaphragms also play a significant role in permeability.

As previously mentioned the glomerular filter functions as both a size and charge-selective barrier, however size is the main factor determining filtration. The filter is freely permeable to molecules with a molecular weight less than 7,000 and is impermeable to molecules of 70,000 or greater, very small quantities of albumin with a molecular weight of 69,000 can pass through the filter [2].

1.1.6. Podocytes

Podocytes also referred to as glomerular visceral epithelial cells (GVEC), are the largest cells in the glomerulus and are unique in location and architecture [6]. Podocytes consist of a cell body and primary processes which extend from the main cell body and form

individual foot processes which come into direct contact with the glomerular basement membrane (GBM) [7].

Podocytes are highly differentiated polarized epithelial cells, consisting of an apical or luminal membrane domain and a basal membrane domain, which corresponds to the sole of the foot processes. The apical membrane domain and the slit diaphragm (SD) are covered by a thick negatively charged glycocalyx rich in sialoglycoproteins including podocalyxin (See Section 1.2.2) and podoendin. The basal cell membrane mediates the interaction between the podocytes and the GBM. Both membranes are heterogeneous with regard to lipid composition and contain cholesterol-rich domains which support the findings of Schwarz [8] and Simons [9] that some podocyte membrane proteins are arranged in lipid rafts.

In the normal glomerulus there is a gap of 25 – 60 nm between adjacent foot processes. This gap referred to as the filtration slit is bridged by the slit diaphragm (SD).

The slit diaphragm is a continuous structure that bridges the filtration slit between neighbouring foot processes. The SD is the only point of cell-cell contact between foot processes of neighbouring podocytes. Detailed studies of the slit diaphragm by Rodewald and Karnovsky in 1974 [10], revealed a zipper-like structure with rows of pores 4 x 14 nm separated by a central bar (Figure 1.4).

The SD also functions to define the boundary between the apical and basolateral membranes of the podocyte [11]. The SD is composed of a growing number of proteins including nephrin, podocin, FAT, ZO-1 and CD2AP which are believed to be critical in maintaining correct structure and function.

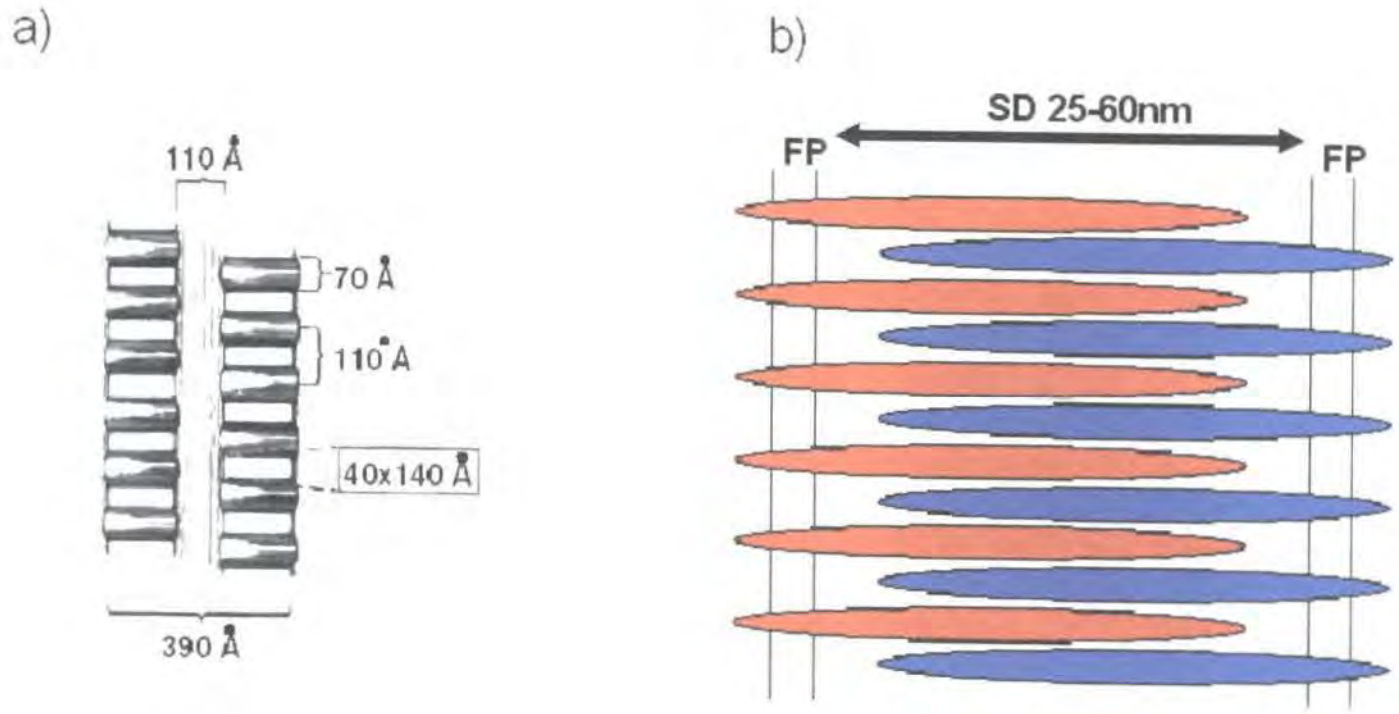

Figure 1. 4. Structural arrangement of nephrin within the SD

a) Original zipper-like structure proposed by Rodewald and Karnovsky. Adapted from [12]
b) Schematic representation of nephrin from adjacent FP's forming the zipper-like structure

It has been suggested that the SD is a modified tight junction (TJ) based on (1) the identification of ZO-1, a tight-junction associated protein, on the cytoplasmic side of the SD, (2) during renal development the SD evolves from the TJ and (3) the TJ-like function of the SD to divide the podocyte apical and basal domains [13].

The podocytes are believed to have several distinct functions, not only do they maintain the size and charge of the glomerular filtration barrier along with the GBM and endothelial cells but they also maintain the GBM by contributing to matrix synthesis, and also have a endocytic function [14].

The podocyte cell body contains a prominent nucleus and lysosomes, mitochondria, a well-developed Golgi apparatus and abundant endoplasmic reticulum, in contrast the cell processes contain very few organelles. The levels of organelles within the cell body indicate a high level of catabolic and anabolic activity and the ability to synthesize the components of the GBM [7].

It is critical for correct podocyte function that the structural integrity of the foot process is maintained, this has resulted in the development of a specialized cytoskeletal organization. To respond to the challenges of the glomerular filtration barrier the podocyte cytoskeleton has a complex structural conformation [7]. The cytoskeleton has to serve both static and dynamic functions and consists of three ultrastructural elements: microfilaments, intermediate filaments and microtubules [15].

The cell body contains a large number of microtubules, microfilaments and intermediate filaments. The foot processes contains a contractile structure consisting of several proteins, including α-actinin, myosin, talin and vinculin and a dense network of actin filaments connected by an array of linker proteins including ZO-1 and CD2AP to the SD complex. The complex is linked to the glomerular basement membrane by α3β1-integrin and dystroglycan (Figure 1.5). F-actin is a highly dynamic

structure with a polar orientation allowing for rapid elongation, branching and disassembly [7, 15].

Podocytes are the injury target of many glomerular diseases including minimal change nephropathy (MCN), chronic glomerulonephritis, focal segmental glomerulosclerosis (FSGS) and diabetes mellitus [6]. Regardless of the underlying disease the initial events of podocyte injury are characterized by either alterations in the molecular composition of the SD without any visible morphological changes or by a visible reorganization of FP structure resulting in filtration slit fusion and apical displacement of the SD.

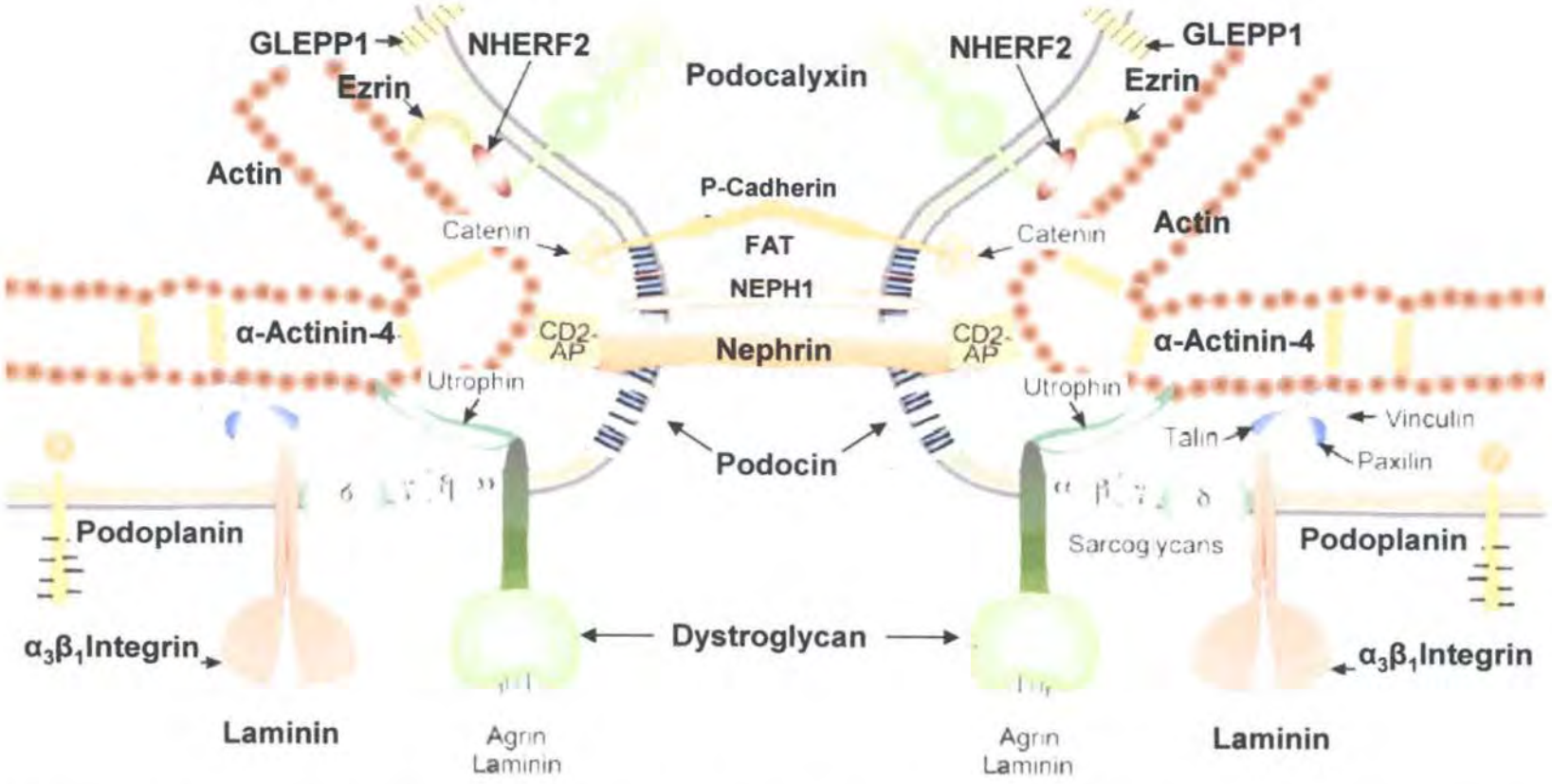

Figure 1. 5. Schematic representation of the SD between two adjacent Foot Processes. Adapted from [16].

1.2. Podocyte Proteins

1.2.1. Podoplanin

Podoplanin is a 43 kDa integral membrane glycoprotein, with a single membrane spanning domain, a short 9 amino acid intracytoplasmic tail and at least 6 O–glycosylation sites in the mucin-like ectodomains. Podoplanin has 2 potential phosphorylation sites, one for protein kinase C and one for cAMP-dependent protein kinase, in the intracytoplasmic tail which also contribute to the larger observed molecular weight, [17]. Molecular cloning showed that the open reading frame of podoplanin is 498 bp long, and encodes for 166 amino acids which should give a protein of approximately 18 kDa [18].

Podoplanin is localized predominantly within the cytoplasm of podocyte foot processes at their origin from the parent processes but also on the apical surface of the parietal epithelial cells of Bowman's capsule [18]. It is believed to have a role in maintaining glomerular permeability and maintaining the structure of podocyte foot processes, which are essential for the correct function of the glomerular filtration barrier, as any effacement of foot processes results in proteinuria [17, 19].

Podoplanin shows extensive sequence identity with glycoproteins in unrelated tissues, including T1α in rat lung, fetal kidney cortex and brain [20], E11 and OTS-8 in rat and mouse osteoblasts [21, 22], gp40 in canine kidney cells, gp36 in humans [23] and GP38 in mouse thymus epithelium [24, 25].

Podoplanin is also found in the lymphatic endothelia and is a promising selective marker for lymphatic endothelium [26] and benign tumour lesions; it is highly expressed in the endothelial cells of Kaposi's sarcoma [27].

It has been shown that in the PAN nephrosis animal model, (see section 1.3.3.1), podoplanin is down-regulated at the transcriptional mRNA level by 70%, these results were supported at the protein level by quantitative immunogold electron microscopy and Western blotting [18].

1.2.2. Podocalyxin

Podocalyxin was originally identified by Kerjaschki *et al.* [28] as the predominant sialoprotein on the apical surface of podocytes, It has subsequently been shown to be expressed on vascular endothelia [29] including high endothelial venules [30] and more recently in hematopoietic cells [31], megakaryocytes and thrombocytes, [32]. Based on its structure podocalyxin has been postulated to have an anti-adhesive role at these locations with the exception of high endothelial venules, where it is proposed to have an adhesive function.

Podocalyxin is a 140 – 165 kDa type 1 transmembrane protein with features typical of membrane-associated mucins, including serine-, threonine-, and proline-rich ectodomains, it is heavily sialylated and extensively O-glycosylated [33]. Structurally it belongs to the sialomucin family, a large family of highly sulphated cell surface glycoproteins of poorly understood function. The amino acid and protein sequence suggest that podocalyxin is most closely related to CD34 and endoglycan [34]. It has been established based on structural similarities that these three proteins belong to the CD34 family of sialomucins [35, 36].

Podocalyxin-like proteins have been successively cloned from rabbit (PCLP1) [37], chicken (thrombomucin) [38], mouse [39] and human (PCLP) [30, 40]. All of these proteins share a high degree of homology in the intracellular and transmembrane domains, while the ectodomain is more heterogeneous by only preserving the mucin-like structure and four conserved cysteines [32]. Using FISH the gene for PCLP, PODXL has been assigned to the long arm of chromosome 7, 7q32-q33 [41].

As mentioned earlier in order for the glomerular filter to work correctly it is critical to maintain the structural integrity of the foot process, this is achieved by podocalyxin. Podocalyxin is the major sialoprotein in the rat glomerulus and accounts for more than 50% of the total glomerular sialic acid content. This gives the glomerular epithelial a very high negative charge which acts to maintain an open filtration pathway between neighbouring foot processes, as well as maintaining the architecture of foot processes and filtration slits [33]. Therefore podocalyxin is proposed to act as an anti-adhesive molecule by charge repulsion, this was subsequently confirmed by Takeda *et al.* [42]. Takeda *et al.* showed that podocalyxin inhibits cell–cell adhesion in an expression dependent manner and this effect was the result of charge repulsion caused by the sialic acid residues, if the sialic acid was removed the cells showed normal adhesion.

In PAN rats, foot process effacement and disorganization of the slit diaphragm is accompanied by a 70% reduction in the sialic acid composition of podocalyxin [43].

Furthermore it has also been shown that podocalyxin associates with the actin cytoskeleton through an interaction with NHERF2 and ezrin (Figure 1.6) [44, 45]. Functional or structural disruption to podocalyxin or to the associated cytoskeletal linker proteins, ezrin and NHERF2 could be a cause of glomerular disorders and serve as viable targets for future studies.

1.2.3. Ezrin

Ezrin is a member of the ezrin/radixin/moesin (ERM) family, which is a subfamily of the protein 4.1 superfamily. ERM proteins have been classically defined in the literature as membrane–cytoskeleton linkers. ERM proteins can bind directly or indirectly to the plasma membrane through the FERM domain. The FERM domain is a 300 amino acid domain found in the N-terminal domain [46].

Ezrin displays 75% amino acid homology to moesin and radixin, and like moesin and radixin interacts with the actin cytoskeleton and the plasma membrane. Members of the ERM family are believed to be critical for cell–cell adhesion and microvilli formation and are characteristically located in dynamic structures that undergo changes in cell shape [47].

Although members of this family have very striking structural and functional similarities, there is a major difference in tissue distribution, ezrin is located primarily in epithelial cells while moesin primarily in endothelial cells. This difference implies that these proteins may have adapted distinct functions to the specific cell types [47].

ERM proteins contain two conserved domains, a NH2-terminal domain containing the membrane targeting domain and the COOH-domain containing the F-actin binding domain [48].

ERM proteins are recruited to the plasma membrane via their NH2-terminal domain which contains both protein and phosphatidylinositol 4, 5-bisphosphate (PIP2) binding sites. The actin binding site is the last 34 amino acids in the COOH-terminal domain. ERM proteins are maintained in the cytoplasm in an inactive conformation [49].

The inactive conformation is due to a masking of both binding sites, caused by an intramolecular N- to C- ERM association domain (ERMAD) interaction. The N-ERMAD has been mapped to the first 296 amino acids

while the C-ERMAD to the last 107 [48]. To generate the active conformation of ERM proteins requires the binding of PIP2 and the phosphorylation of a conserved threonine residue in the C-ERMAD, T567 in the case of ezrin [50].

Ezrin is specifically expressed by podocytes in the glomerulus. Ezrin protein expression is altered in glomerular disease; there is a decrease in the puromycin aminonucleoside model of nephrosis but an increase in the passive Heymann model. However under no circumstances was there a change in mRNA levels [47]. Podocytes undergoing injury and/or proliferation showed strong ezrin expression. The observation that ezrin expression was highest in mitotic, polynucleated podocytes or podocytes completely or nearly detached from the GBM may reflect the need to adapt to injury. If adaptation fails podocytes may become completely detached round up and die. This pathway maybe of relevance to glomerular disease, since loss of podocytes is believed to predispose to progressive scarring [47].

1.2.4. Na^+/H^+ Exchange Regulatory Factor

Na^+/H^+ exchange regulatory factor (NHERF) was originally identified from renal brush-border membranes and identified as a cofactor in cAMP regulation of the renal apical Na^+/H^+ exchanger isoform 3 (NHE3) [51].

There are two isoforms, NHERF-1, also known as ezrin-binding protein of approximately Mr 50,000 (EBP-50) and NHERF-2, also known as NHE3 kinase A regulatory protein (E3KARP) [52]. NHERF-1 and NHERF-2 share an overall homology of 57%, but the two tandem PDZ domains have a much higher degree of identity.

The isoforms have a significantly different distribution in the kidney; in fact there are no areas of overlap, suggesting the proteins have important differences in physiological effects [53]. NHERF-1 is located in the proximal tubule and no expression was detected in the glomerulus. In

contrast NHERF-2 is strongly expressed in the glomerulus and not in the proximal tubule [53].

Takeda et al. [45] showed that NHERF-2 was a member of the podocalyxin-actin complex. Podocalyxin binds to the PDZ2 domain of NHERF-2 via its C-terminal PDZ binding domain DTHL. NHERF-2 binds to the N-terminus of ezrin via its C-terminal ERM-binding domain. Ezrin links the complex to the actin cytoskeleton via its C-terminal actin binding domain [15, 18, 19, 28, 42] (Figure 1.6).

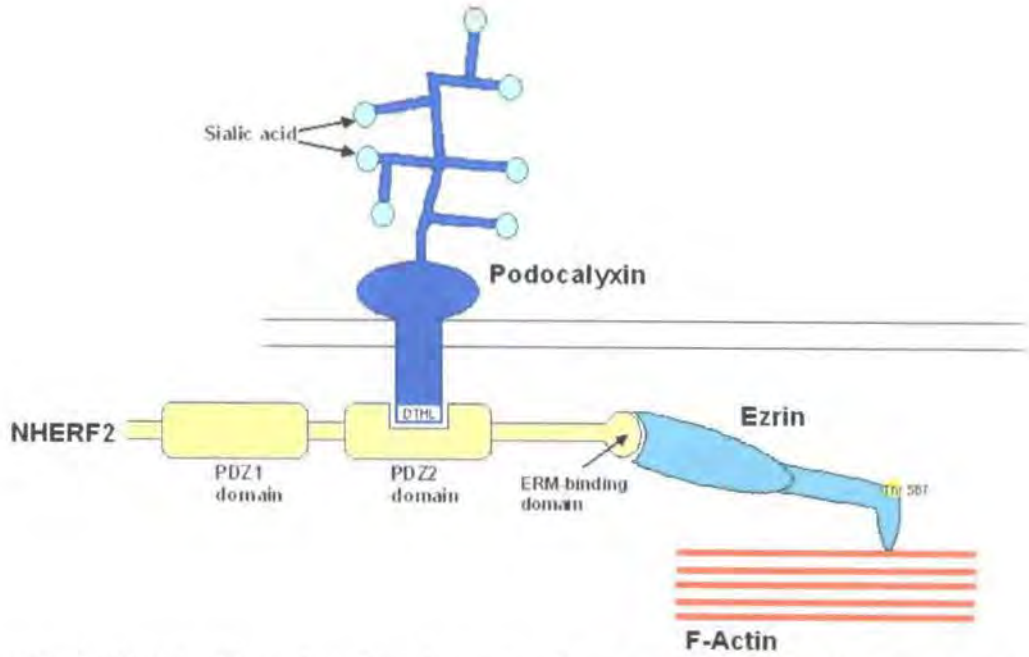

Figure 1. 6. Illustration showing how the Podocalyxin/NHERF2/Ezrin complex interacts with the actin cytoskeleton. Adapted from [45].

1.2.5. Nephrin

Nephrin is a transmembrane protein of the immunoglobulin (Ig) superfamily of cell adhesion molecules (CAMS), which is encoded for by the gene NPHS1. Nephrin was identified in 1998 by Kestila *et al.* [54] as the gene responsible for congenital nephrotic syndrome of the Finnish type. Nephrin was mapped to chromosome 19q13.1 and the gene spans 29 exons [54, 55].

Exon 1 codes for the signal peptide, exons 2 – 20 encode for the 8 extracellular Ig type-c2 motifs, each motif is encoded for by two exons except Ig2 which is encoded by three. Exons 22 and 23 code for a fibronectin type III-like domain. Exon 24 codes for the transmembrane domain and exons 25 – 29 the intracellular cytoplasmic domain, which contains 9 potential tyrosine phosphorylation sites, and 3' UTR [55, 56].

Nephrin contains 1241 amino acids and has a predicted molecular mass of 136 kDa, however extensive N-glycosylation, of the ten potential N-glycosylation sites, contributes to the actual size of 180 kDa. Northern blotting and *in situ* hybridization showed nephrin to be uniquely expressed at the podocyte slit diaphragm, [54, 57-60]. Recent studies have shown that nephrin is also expressed in the brain, testis and pancreas [61-63].

Following the identification and cloning of human nephrin, the rat and mouse homologues were successively cloned [57, 59, 64, 65]. Sequence analysis showed that rat and mouse are 93% identical but only share 83% identity with human nephrin [64, 65]. In addition, nephrin has been identified in *C. elegans* [66].

Kawachi *et al.* [57] showed that nephrin was critical for maintaining the barrier function of the slit diaphragm but was not critical for maintaining the correct ultrastructural morphology of the slit diaphragm. A recent study by Simons *et al.* [9] showed that nephrin was associated with lipid rafts.

From its predicted structure it was suggested that nephrin could homodimerize with neighbouring molecules in an antiparallel, head to head fashion, this was proved in 2003 by Khoshnoodi *et al.* [67], it has also been shown that nephrin can form heterodimers with NEPH1, a recently identified nephrin homologue [68-70].

Two splice variants of nephrin, termed alpha and beta have been identified in both humans and rats. The alpha form produces a soluble truncated, 166 kDa, form of nephrin. The function of the truncated alpha isoform is as yet unknown but has been identified in the urine of rats with PAN induced nephrotoxicity but not in normal rats [11].

Cytoskeletal integrity and N-linked glycosylation are critical for correct nephrin membrane localization [71]. Nephrin, podocin and CD2AP are functionally linked to the cytoskeleton at the cell periphery [72, 73] (Figure 1.7).

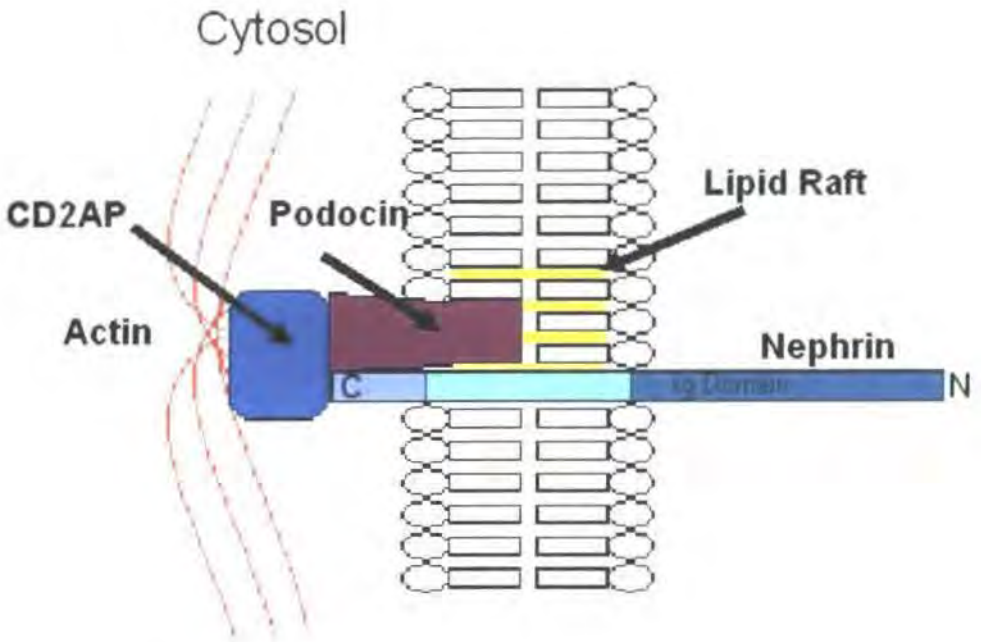

Figure 1. 7. Nephrin, Podocin and CD2AP membrane interactions. Adapted from [9]

Nephrin expression was found to be reduced in several experimental proteinuric diseases including; passive Heymann nephritis (PHN) [74, 75], puromycin aminonuceloside nephrosis (PAN) [76-78] and experimental diabetic nephropathy [79].

Nephrin expression is differentially expressed in human glomerular diseases. In childhood cases of minimal change nephropathy and FSGS nephrin expression was reduced [80]. Doublier *et al.* [81] found a reduction and redistribution of nephrin in minimal change nephrotic syndrome, FSGS and membranous nephropathy (MN). Wang et al. [75] also found a reduction in nephrin expression in membranous nephropathy and IgA nephropathy. However Patrakka et al. [82] found no change in nephrin expression in minimal change nephropathy, FSGS and MN. Although there are differences between these studies, these studies did use differing techniques and patient samples, which could account for the variability in observed nephrin expression. A recent study by Huh et al. [83] offers another explanation of the observed discrepancies in nephrin expression. They found that nephrin expression was only reduced if the foot processes were effaced. As foot process effacement is not uniform in glomerulonephritis, this could result in the differing results observed.

1.2.6. NEPH1

Little has been published regarding NEPH1 but what is known is that NEPH1 is a type-1 transmembrane protein, with important similarities to nephrin. NEPH1 belongs to a family of three closely related proteins; the other members are named NEPH2 and NEPH3. All three proteins belong to the Ig superfamily, and share common domain architecture, consisting of an extracellular domain of 5 Ig-like domains, a transmembrane region and an intracellular region which can interact with podocin [84]. NEPH1 is localized to the slit diaphragm of podocytes and co-localizes with nephrin [68, 70].

Recent studies by Barletta *et al.* [68], Gerke *et al.* [69] and Liu *et al.* [70] have shown that nephrin and NEPH1 are able to form homodimers, but can also interact via their cytoplasmic domains to form a cis-interacting hetero-oligomeric complex, which is believed to be significant in maintaining the slit diaphragm.

Deletion of NEPH1 in mice results in an almost identical phenotype to that observed in nephrin deficient mice [85] suggesting that nephrin and NEPH1 participate in overlapping pathways.

1.2.7. Podocin

A novel gene encoded for by NPHS2 was identified recently [86] by positional cloning, to region 1q25-q31, as the gene mutated in autosomal recessive steroid resistant nephritic syndrome (SRNS) (see section 1.3.1.1). The protein, named podocin due to specific expression in podocytes, is a member of the stomatin protein family of lipid raft-associated proteins [87, 88]. The rat homologue of podocin was cloned in 2003 by Kawachi *et al.* [89] showed 84% identity to human podocin and 93% to mouse. The domain structure of podocin is highly conserved between species.

Podocin is a 42 kDa integral membrane protein of 383 amino acids with a single membrane domain and both N and C-terminals located in the cytosol, [90, 91].

Podocin forms high-order oligomers and was shown to be associated with lipid rafts and hence may act as a scaffold protein in lipid rafts, recruiting nephrin and CD2AP to these microdomains [8, 9].

Podocin is located at the cytoplasmic face of the slit diaphragm, where it is suggested that it acts as a membrane protein anchor and binds via its COOH-terminal domain with the intracellular domain of nephrin and CD2AP [8, 91] (Figure 1.5).

In PAN nephropathy of the rat, podocin showed a shift in localization and a decrease in protein expression but no corresponding decrease in mRNA. This suggests that podocin is either degraded or secreted in urine in proteinuric state [89].

Lipid rafts

Lipid rafts are specialized liquid-ordered membrane microdomains with unique protein and lipid compositions. Lipid rafts are usually enriched in cholesterol and glycosphingolipids [92, 93]. Lipid rafts are biochemically defined as membrane complexes insoluble in non-ionic detergents at low temperatures, because of this definition lipid rafts are also referred to as detergent-insoluble glycosphingolipids (DIGs), detergent-insoluble complexes (DICs) and detergent-resistant membranes (DRM). Lipid rafts are dynamic structures in living cells, which are important in modulating and integrating signals by providing a signalling micro-environment to produce specific biological responses. *In vivo* the only well defined membrane structures with lipid raft microdomains are caveolae.

1.2.8. CD2-Associated Protein

CD2–associated protein (CD2AP) is an 80 kDa cytoplasmic protein that is expressed in all tissues, but primarily in epithelial cells. The human homologue of CD2AP was identified as Cas ligand with multiple SH3 domains (CMS).

CD2AP contains three SH3 domains at the N-terminus, followed by a proline-rich mid-region, which has weak homology to intermediate filaments, a coiled-coil domain and a potential monomeric actin binding domain at the C-terminus. SH3 domains are conserved protein modules of 60 – 70 amino acids that mediate specific protein-protein interactions. Coiled-coil domains are also known to mediate protein-protein interactions [94, 95].

In the kidney CD2AP is expressed in the glomerulus, and specifically the podocyte in a pattern of expression consistent with expression at the foot processes [96]. In vivo CD2AP has been shown to interact with polycystin-2 and nephrin [95, 97, 98]. CD2AP may therefore act as a scaffolding protein in various signalling cascades controlling processes dependent on the actin cytoskeleton for example cell adhesion, morphology and motility [99].

Interestingly mice lacking CD2AP develop nephrotic syndrome [97] resembling diffuse mesangial sclerosis, an infantile nephrotic syndrome [94].

1.2.9. Glomerular Epithelial Protein 1

Glomerular epithelial protein 1 (GLEPP-1) also referred to as protein tyrosine phosphates receptor type O (Ptpro), is a member of the fibronectin type III receptor protein tyrosine phosphatases (RPTP) family and is only located in the kidney and brain. In the kidney it localizes specifically to the apical cell membrane of podocyte foot processes, and has therefore been suggested to have a role in regulating podocyte structure and function [100-102].

GLEPP-1 has a single transmembrane domain, a single intracellular phosphatase domain and a large extracellular domain containing 8 fibronectin type III-like repeats. It is highly conserved in human, rat, mouse and rabbit [102].

GLEPP-1 was first cloned and characterized from rabbit in 1994 by Thomas *et al.* [103] and subsequently identified and cloned in human [104] and more recently in mouse [101]. Nucleotide sequence comparison showed that human and mouse GLEPP-1 are approximately 90% and 80% identical to rabbit; while deduced amino acids analysis indicated higher identity, 97% and 91% [101, 104].

In some forms of human disease, including the collapsing form of focal segmental glomerulosclerosis (FSGS) and crescentic nephritis, GLEPP-1 is completely lost from the podocytes [105] however this is not the case in congenital nephritic syndrome and minimal change disease [100]. Using the established model of puromycin aminonucleoside nephrosis in the rat, which has similarities to minimal change disease and focal segmental glomerulosclerosis, both the studies by Kim [100] and Wang [101] showed that during the early stages of foot process effacement the expression of GLEPP-1 mRNA and protein levels are significantly reduced. Suggesting GLEPP-1 is a sensitive marker of podocyte injury and could be a useful clinical marker for glomerular injury [101].

1.2.10. Synaptopodin

Synaptopodin, previously named "pp44", was first identified as a novel actin binding protein in 1991 by Mundel *et al.* [106] and was subsequently cloned and characterized in 1997 [107]. Synaptopodin is exclusively expressed in podocytes foot processes and dendritic spines in a subset of telencephalic synapses in the brain.

Based on its amino acid composition and tissue distribution, synaptopodin is different from all previously described actin-associated proteins. It is a basic protein encoded by a 685 amino acid polypeptide in humans with a calculated molecular mass of 73.7 kDa. In mice it is 690 amino acids which encode a 74 kDa protein. However due to posttranslational modifications it appears as a 110 kDa band on Western blotting from kidney glomeruli and a 100 kDa band from brain [107].

Synaptopodin is a linear, proline-rich protein without any globular domain. This may result in a side to side arrangement along actin microfilaments similar to that for dystrophin. Synaptopodin shares some properties with VASP, another proline-rich actin-associated protein [107].

Barisoni *et al.* and Kemeny *et al.* reported loss of synaptopodin expression in collapsing focal segmental glomerulosclerosis (FSGS) and HIV nephropathy [108] and the early stages of idiopathic focal segmental glomerulosclerosis [109]. In a later study Srivastava *et al.* [110] showed the expression levels of synaptopodin decrease with increasing severity of nephrotic syndrome. Srivastava also proposed that changes in synaptopodin expression is a secondary effect that reflects the magnitude of damage and as such synaptopodin could be a potential marker to predict steroid response and podocyte damage in idiopathic nephrotic syndrome including minimal change disease (MCD) and focal segmental glomerulosclerosis (FSGS).

1.2.11. FAT

FAT was originally identified as a tumour suppressor gene in Drosophila called fat, its mammalian homologue FAT has been identified in humans and rats. There is 88% amino acid conservation over the entire molecule between the three species [111].

FAT is a novel member of the cadherin superfamily. The extracellular domain of FAT contains 34 tandem cadherin-like repeats, 5 EGF-like (epidermal growth factor) repeats and a laminin A-G domain, which is the same as the extracellular domain motif of protocadherins. The cytoplasmic domain of FAT contains sequences homologous to the β-catenin binding region of the classic cadherins. It is concentrated mainly at cell–cell contacts as a huge 500 kDa transmembrane protein, comparable in size to megalin [111].

FAT is expressed predominantly in epithelial cell layers and in the central nervous system but there is also some expression in endothelial cells and smooth muscle cells. Most FAT expression disappears in adult tissues, suggesting that it is developmentally regulated. However FAT expression remains widely distributed in the kidney and specifically in the podocyte. Using immunoelectron microscopy Inoue *et al.* [111] showed that the FAT

cytoplasmic domain was located at the base of the slit diaphragm and co-localized with ZO-1, based on these findings and the molecular structure of FAT it has been concluded that FAT is a component of the slit diaphragm [111].

1.2.12. Zonula Occludens–1

Zonula Occludens 1 (ZO-1) was first identified by Stevenson *et al.* [112] as a 225 kDa polypeptide, specifically located at the tight junction (TJ). It was subsequently shown that ZO-1 was also expressed at the slit diaphragms of podocytes [113], which therefore reinforces the hypothesis that the SD is a modified TJ.

Willott *et al.* [114] identified two RNA splice variants of ZO-1, which differ in the expression of an 80 amino acid region termed "motif–α". These differing isoforms, ZO-1α^+ and ZO-1α^-, are expressed differentially within the kidney, suggesting different functional properties. Both isoforms are expressed in renal tubule epithelia but only ZO-1α^- is expressed in the slit diaphragms and between the glomerular and peritubular capillary endothelia junctions [115]. It is believed the α–motif has no effect on function but is involved in binding ZO-1 to other proteins associated with the TJ and maintaining their attachment to the tight junction [115].

ZO-1 is a large, asymmetric, monomeric phosphoprotein tightly associated with the tight junction as a peripheral membrane protein. ZO-1 is concentrated at the points of cell-cell contact [116, 117].

ZO-1 has a species-dependent relative mass between 210 and 225 kDa, [112, 116] and is localized at the cytoplasmic face of intercellular junctions. ZO-1 and its homologue ZO-2 are members of the membrane-associated guanylate kinase (MAGUK) protein family. MAGUK proteins share a multidomain organization including one or three PDZ domains, an SH3 domain and a region of homology with the enzyme guanylate kinase [118].

ZO-1 has been demonstrated to interact with the components of cell–cell junctions including occludin and the actin-binding protein spectrin [118]. In mice, ZO-1 and nephrin are closely co-localized in the mature glomerulus, but it has been suggested that they may arrive at their final positions from opposite directions [119].

1.2.13. α-actinin-4

There are four mammalian α-actinin genes ACTN 1 – 4, encoding four highly homologous 100 kDa actin cross-linking proteins. These proteins exist as dimers in a head–to–tail configuration. α-actinin-1 and α-actinin-4 are both expressed in the kidney, but α-actinin-4 expression is more prevalent [120].

α-actinin-4 is an actin binding protein with a role in cross-linking actin filaments into bundles and anchoring actin to the plasma membrane at focal contacts. α-actinin-4 binds to the cytoplasmic domain of β1-integrin, one of the proteins responsible for anchoring podocytes foot processes to the GBM. Redistribution of α-actinin-4 has been observed in nephrotic rats [121]. Indirect evidence that alterations to the expression and/or localization of podocyte cytoskeletal proteins, including α-actinin-4, are responsible for the observed foot process effacement characteristic of nephrotic syndromes was provided by Smoyer *et al.* [122].

Mutations in ACTN4 have been linked to the familial autosomal dominant form of FSGS. These mutations increase the affinity of α-actinin-4 for filamentous actin (F-actin) causing dysregulation of the actin cytoskeleton [123]. Clinical cases of ACTN4–associated FSGS have a mild onset of proteinuria in the teenage years with slow but progressive loss of renal function, some cases do develop end-stage renal disease (ESRD) later in life. This syndrome is not fully penetrant, as some carriers do not develop proteinuria, similarly not all ACTN4 mutant mice were proteinuric [123].

1.2.14. α3β1 Integrin

Integrins are type 1 transmembrane glycoproteins composed of an α and a β subunit and play a critical role in providing the link between the extracellular matrix and the actin cytoskeleton. Currently 18 α and 8 β subunits have been described, the subunits combine to form dimers which have distinct but often overlapping functions and ligand-binding properties [124].

The extracellular domains of the subunits are the ligand binding domains while the cytoplasmic domains are involved in promoting cell anchorage. Integrins are involved in both "outside-in" signalling and "inside-out" signal transduction. Therefore integrins are able to pass signals across the plasma membrane in both directions making them very important signalling receptors. Integrins are involved in modulating cell adhesion, shape, polarity, growth, differentiation and motility which are in turn regulated by and can regulate both gene expression and cell function [124].

α3β1 integrin is an enigmatic member of the integrin family. Due to its basolateral membrane localization in many epithelial cell types, it is suggested to function as a basement membrane receptor [125]. α3β1 integrin was originally identified as a receptor for types I and VI collagen, laminin-1, fibronectin and nidogen. α3β1 integrin is expressed in the skin, brain and kidney. α3β1 is the predominant integrin expressed by podocytes, but α6β1 is also expressed in much lower levels [125, 126].

1.2.15. Wilms' Tumor Suppressor-1

Wilms' tumor, also called nephroblastoma, is a pediatric kidney cancer that affects 1 in 10,000 children with onset usually at 5 years of age, but with genetic predisposition may develop earlier. It is very rare for Wilms' tumor to affect adults [127, 128]. The Wilms' tumor suppressor-1 (WT1) gene was identified as a tumor suppressor gene in a subset of Wilms' tumor patients.

WT1 is one of the transcription factors involved in nephrogenesis, and is crucial for correct kidney development. WT1 expression persists in the podocytes of mature glomeruli [129]. A direct role for WT1 in podocytes function has not been found.

The Wilms' tumor suppressor-1 (WT1) gene was mapped by positional cloning in 1990 to chromosome 11p13 [130, 131]. The WT1 gene contains 10 exons and encodes a protein of 52 – 54 kDa [132]. This protein has two functional domains, 4 C-terminal Kruppel-type Cys_2His_2 zinc finger domain, which shares homology to the early growth response gene 1 (EGR-1) family and a N-terminal proline-glutamine rich domain, typically found in regulatory regions of transcription factors [127, 133].

WT1 is extremely complex and encodes for between 16 and 24 different isoforms [132-134]. The different isoforms are created through a combination of alternative splicing, alternative translational start sites and RNA editing. Two important isoforms are alternative splice I and II. Alternative splice I is generated by an insertion of 17 amino acids encoded for by exon 5 between the transactivation and DNA-binding domains. Alternative splice II results in the insertion of 3 amino acids, lysine, threonine and serine (KTS), between exons 9 and 10, which encode for the third and fourth zinc fingers. The two KTS splice variants, localize to different nuclear compartments, -KTS localizes with the other transcription factors while +KTS associates with components of the pre-mRNA-splicing machinery [135]. The ratio of splice variants is highly conserved, in fact changes in the ratio between WT1 +KTS and WT1 -KTS can lead to developmental abnormalities and Frasier syndrome [132, 135, 136].

Niksic *et al.* [137] showed that both KTS isoforms of WT1 could shuttle from the nucleus to the cytoplasm and both are associated with functional polysomes, suggesting a role in translation. Depending on the cell type, 10 – 50% of total cellular WT1 can be found in the cytoplasm. This result combined with previous knowledge suggests that WT1 may in fact

regulate three steps of gene expression: transcription, RNA processing and translation [137].

WT1 -KTS has been shown to cause a specific up regulation of podocalyxin, other podocytes proteins including podoplanin, nephrin, podocin, CD2AP and α-actinin-4 are not induced by WT1. The rapid and reversal induction of podocalyxin suggests a direct transcriptional mechanism [138]. Recent research by Guo *et al.* [139] and Wagner *et al.* [140] have identified nephrin as a direct transcriptional target of WT-1.

WT1 mutations have been associated with human disease including WAGR syndrome (Wilms' tumour, aniridia, genitourinary abnormalities and mental retardation), Denys-Drash syndrome (DDS) [141, 142] (See Section 1.3.1.2) and Frasier syndrome [143] (See Section 1.3.1.3). WAGR syndrome is due to hemizygous deletion of a chromosomal segment encompassing WT1 and is associated with late onset renal failure [136].

1.3. Nephrotic Syndromes

Podocyte injury occurs in many forms of experimental, including PAN and PHN animal models and human glomerular disease, including minimal change disease (MCD), focal segmental glomerulosclerosis (FSGS), membranous glomerulopathy and diabetes mellitus [14, 144-146].

Regardless of the underlying disease the initial events are characterized by disruption to the slit diaphragm, which can result in a visible reorganization of the foot process structure, including foot process effacement.

If these early changes are not reversed, progressive severe damage occurs, including podocyte vacuolization, pseudocyst formation and podocyte detachment, these irreversible changes ultimately lead to segmental glomerulosclerosis and end-stage renal failure [147, 148].

Four major causes of foot process effacement and subsequent proteinuria have been proposed by several groups, [14, 144-146, 149]:

1. Interference with the SD complex and/or the lipid rafts
2. Interference with the GBM or podocyte-GBM interaction
3. Direct interference with the actin cytoskeleton and the associated protein α-actinin-4
4. Interference with the glycocalyx or GLEPP1

Morphological changes in podocytes resulting from nephrotic syndrome include foot process effacement, cell swelling, occurrence of occluding junctions and detachment of podocytes from the GBM [13]. Nephrotic syndrome also results in changes to the filtration slits and slit diaphragms, resulting in fewer and narrower slits [13].

In 2003 Barisoni and Mundel [149] proposed a new classification for podocytes diseases based on histology Table 1. 1, while Table 1. 2 shows the genetic causes of the common forms of nephrotic syndromes.

Histology	Disease	Targets
Normal	Minimal Change Disease Congenital Nephrotic Syndrome	Dystroglycan Nephrin/ Podocin
Diffuse Mesangial Sclerosis	Denys-Drash Syndrome Frasier Syndrome	WT1
Focal Segmental Glomerulosclerosis	Primary (Idiopathic) Genetic Hyperfiltration	Podocin, CD2AP, α-actinin-4, β1-integrin
Collapsing Glomerulopathy	HIV-1 associated Collapsing Glomerulopathy	

Table 1. 1. Proposed new Classification for Podocyte Disease based on Histology [149].

Disease	Gene Locus	Gene	Protein
CNF	19q12-13	NPHS1	Nephrin
SRNS	1q25-32	NPHS2	Podocin
FSGS1	19q13	ACTN4	α-actinin-4
FSGS2	11q21-22	Unknown	Unknown
DDS	11p13	WT1	WT1

Table 1. 2. Outlining the Genetic causes of Common Kidney Diseases. Adapted from [150].

1.3.1. Genetic Human Diseases

1.3.1.1. Congenital Nephrotic Syndrome

Congenital nephrotic syndrome (CNS) comprises a heterogeneous group of renal diseases that result in defects of the glomerular barrier resulting in massive proteinuria. CNS is primarily associated with defects in the structure and function of podocytes. The onset of clinical symptoms in CNS can vary dramatically between different forms of the disease.

Congenital Nephrotic Syndrome of the Finnish Type (NPHS1)

Congenital Nephrotic Syndrome of the Finnish Type (CNF) is the best characterized of the nephrotic syndromes, it was first described by Hallman *et al.* in 1956. It is an inherited autosomal recessive trait that has a very high prevalence in the Finnish population [150]. CNF affects 1 in 8200 in the Finnish population.

Affected patients exhibit massive proteinuria *in utero* and develop nephrosis soon after birth. The only successful long term form of treatment is renal transplantation. The gene responsible for CNF has been mapped to chromosome 19q13.1 and named NPHS1, it codes for the slit diaphragm protein nephrin (See Section 1.2.5).

To date more than 50 mutations, including deletions, insertions, nonsense, mis-sense, splice site and promoter mutations have been reported in patients suffering from both Finnish and non-Finnish forms of CNF [55, 151, 152].

Kestila *et al.* [54] found that there were two common mutations found in the Finnish population, which account for 90% of the CNS cases in Finland. Fin major, a 2-bp deletion in exon 2 resulting in a truncated 90 residue protein and Fin minor a nonsense mutation in exon 26 resulting in a premature stop codon in the cytoplasmic domain.

Autosomal Recessive Steroid-Resistant CNS (NPHS2)

Autosomal Recessive Steroid-Resistant CNS (SRNS) is an inherited autosomal recessive trait, which is commonly observed in children aged between 3 months and 5 years. As the name suggests patients do not respond to steroid treatment and once proteinuria has developed there is a rapid progression towards end-stage renal disease. The gene responsible, NPHS2, has been mapped to chromosome 1q25-q32 and was isolated by Antignac [153] in 2001, it codes for the podocyte protein podocin (See Section 1.2.7).

Mutations in NPHS2 results in severe glomerular disease commonly referred to as autosomal recessive steroid-resistant nephrotic syndrome (SRNS). SRNS is characterized by early onset nephrotic syndrome with foot process effacement, steroid resistance and progression to end-stage renal disease (ESRD). Subsequently NPHS2 mutations have been identified in sporadic cases of SRNS [154].

In all NPHS2 patients, the defective podocin resulted in significant changes to nephrin and CD2AP localization, shifting from along the GBM to a prominent location in the podocyte cell body [154] [155]. Therefore confirming that podocin is responsible for nephrin and CD2AP targeting to the slit diaphragm.

When first characterized SRNS was described as an autosomal recessive disease, a recent study by Karle [156] showed mutations were heterozygous implying an autosomal dominant mode of inheritance, however based on the family pedigree this is unlikely, what is more likely is that these patients have other mutations in the NPHS2 gene.

R229Q is the most common form of mutation but many novel mutations have been identified, including A284V, R196P, R138Q [86, 156-161].

1.3.1.2. Denys-Drash Syndrome

Denys-Drash syndrome (DDS) is characterized as congenital or early onset nephrotic syndrome associated with malformations in male pseudohermaphroditism and Wilms' tumor.

DDS involves severe early-onset nephropathy and is due to dominant intragenic WT1 mutations, which can be mis-sense or nonsense and primarily affect the C-terminal zinc finger domain [136]. The most common mutation is R394W within the third zinc finger domain, but other point mutations in zinc finger domains 2 and 3 have a similar phenotype [127]. Although only a few deletions, insertions and nonsense mutations result in a truncated protein, all mutations alter the structure of the DNA-binding domain, reducing the ability to bind both DNA and RNA [133]. Increasing evidence shows the mutated protein acts in a dominant – negative way, actively suppressing and inactivating the influence of the wild type allele.

The main feature of DDS is diffuse mesangial sclerosis, a distinct form of glomerulopathy. It is characterized by rapid progression of glomerulosclerosis with end-stage renal failure before the age of 5 years, thickening of the GBM, severe hypertension, podocyte hypertrophy and vacuolation [133]. DDS can in some cases be associated with XY pseudohermaphroditism and predisposition to Wilms' tumourgenesis [136].

1.3.1.3. Frasier Syndrome

Frasier syndrome (FS) is caused by heterozygous intronic mutations that lead to a disruption in the +KTS/-KTS isoform ratios. Frasier syndrome is characterized by an adolescent nephropathy involving focal mesangial sclerosis, predisposition to gonadoblastoma and male – to – female sex reversal [136].

Frasier syndrome is a rare disease affecting phenotypic females, it is characterized by the association of male pseudohermaphroditism and progressive glomerulopathy related to FSGS [162, 163]. Proteinuria is detected in children usually aged 2 – 6. It progresses with age to end-stage renal disease and currently there is no treatment [164].

Mutations have been found in exon 9 of WT1 [143, 165, 166] these mutations resulted in the loss of the +KTS isoform.

Recently a mutation in exon 9 which didn't affect the isoform ratio was identified in two patients diagnosed as having FS [167]. Similarly mutations characteristic of FS have been described in DDS patients. These observations have fuelled a controversy regarding the correct classification of FS and DDS and it has been suggested that FS is an atypical subtype of DDS. The majority of published research distinguishes the syndromes on both clinical and molecular grounds, Table 1. 3. The similarities between the two phenotypes, makes distinction difficult but if classification is done at the molecular level instead of on observed phenotype then classification is possible [133].

	Denys-Drash Syndrome	Frasier Syndrome
Kidney Pathology	Diffuse mesangial sclerosis Kidney failure age 0 – 3 yrs	FSGS Kidney failure 10 – 20 yrs
Gonadal Development	Variable impairment of development, broad spectrum of intersex phenotypes Partially developed gonads	Complete sex reversal in 46, XY individuals, little or no impairment in 46, XX females Streak gonads in 46, XY
Tumor Risk	High risk of Wilms' tumor Gonadoblastomas are rare	No Wilms' tumor reported High risk of gonadoblastomas
WT1 Gene	Mis-sense mutations in the zinc finger domains and premature stop codons <50% WT1 protein function	Mutations in splice donor site in intron 9 No mutant WT1 protein but altered ratio of isoforms

Table 1. 3. Differences between Denys Drash Syndrome and Frasier Syndrome. Adapted from [143].

1.3.2. Acquired Human Diseases

1.3.2.1. Minimal Change Nephrotic Syndrome

Minimal change nephrotic syndrome (MCNS) is also referred to as minimal change nephropathy (MCN) minimal change disease (MCD) and minimal change glomerulonephropathy.

Minimal change nephrotic syndrome (MCNS) is a clinical and pathological entity defined by selective proteinuria and hyboalbuminaemia that occurs in the absence of glomerular infiltrates or immunoglobulin deposits. The only detectable abnormality is podocyte foot process effacement. However vacuolization has also been reported when podocytes were examined under electron microscopy [168]. Foot process effacement is typical of nephrotic syndrome and not specific to MCNS [169].

Minimal change nephrotic syndrome (MCNS) is the most common form of nephrotic syndrome in children, accounting for 90% of cases of nephrotic syndrome in children. MCNS only accounts for 15% of cases in adults [168]. The pathophysiology of MCNS is unknown but has been related to abnormal cytokines [168].

1.3.2.2. Focal Segmental Glomerulosclerosis

Focal Segmental Glomerulosclerosis (FSGS) is a mild form of nephrotic syndrome. This disease is representative of a group of heterogeneous autosomal dominant kidney diseases, which are manifested by proteinuria and slow progression towards segmental sclerosis and finally end-stage renal disease in adulthood [150]. Two loci have been mapped, FSGS1 to 19q13 and FSGS2 to 11q21-22. The gene for FSGS1 has been cloned by Kaplan *et al.* [170] and shown to encode α-actinin-4.

FSGS is believed to be responsible for end-stage renal disease in 5% of adults and 20% of children suffering from ESRD. Both autosomal dominant and recessive forms of familial FSGS have been described [171, 172]. Patients with the autosomal dominant form of the disease tend to

have less severe symptoms and present at a later age [173]. Because FSGS is common occurrence in diverse forms of renal injury, its pathogenesis has been extremely difficult to define and is why the molecular basis is still unknown.

The fact that FSGS and NPHS1 both map to the same region on chromosome 9 is very interesting, because they share similar pathology and clinical manifestations. They both result in foot process effacement and tubular atropathy.

Unlike other conditions, for example minimal change disease, proteinuria and foot process effacement, (podocyte damage) are not reversible in FSGS. This is because the mechanism of podocytes damage differs between these diseases, in MCD the foot process effacement is caused by the reorganization of the actin cytoskeleton while in collapsing FSGS it is the result of the loss of cytoskeletal elements [108].

1.3.2.3. Diabetic Nephropathy

Diabetes is the most common metabolic disorder with an estimated worldwide prevalence of between 1 – 5%. Diabetic nephropathy is one of the most serious complications of diabetes mellitus. Diabetic nephropathy has become the most important cause of terminal renal failure in the world. Diabetic renal disease is the single most common cause of ESRD in the United States, accounting for 43% of new cases [174] [175]. Type 2 diabetes is the single most common cause of End-stage renal disease (ESRD) in diabetic patients [176, 177]. Worryingly the numbers of patients suffering from diabetic nephropathy has been steadily increasing over the past decade.

The earliest sign of diabetic nephropathy is microalbuminuria, which progresses to overt proteinuria or nephrotic syndrome and a subsequent decline in renal function leading to ESRD. Even though the progression of diabetic nephropathy is very slow, 10 – 20 years, many of these patients

require dialysis treatment as a result of ESRD. The prognosis for patients suffering from diabetes nephropathy is not good due to the associated cardiovascular complications [178].

Diabetic nephropathy is characterized by the thickening of the GBM and by an increase in the mesangial matrices. GBM thickening starts 2 – 5 years after the onset of diabetes but doesn't become obvious until after 5 – 10 years. The increase in mesangial matrix leads to mesangial expansion and glomerulosclerosis, which results in the deterioration of glomerular dysfunction. Another morphological change is the thickening of the proximal tubule basement membrane [178].

Until recently it was believed that diabetic nephropathy was progressive and once a patient's excreted urinary protein levels reached 0.5 – 1.0 g/day or higher it was irreversible [178], however increasing evidence suggests that with appropriate and timely intervention diabetic nephropathy is preventable [177].

1.3.3. Experimental Models of Nephrosis

There are several types of model, animal model e.g. PAN nephrosis, perfused rat kidney model or cell culture model, and I will briefly discuss the advantages and disadvantages of each model system before focussing on the PAN nephrosis animal model.

Whole Animal Model

The major advantage of whole animal models over *in vitro* models is that all the components of the kidney are maintained in their natural environment, giving the most accurate model for studies. Furthermore the kidney remains under the influence of the neurohumoral network of the organism which allows the study of nephrotxins whose effects are dependent on extrarenal factors. However this is also the major disadvantage as it is impossible to control all the factors which could influence renal function. Therefore any conclusions based on changes in renal function maybe biased to an unknown extent by functional changes induced independent of the intervention being studied [179].

Isolated Perfused Kidney Model

Originally developed to study renal physiology by Nishiitsuj-Uwo *et al.* (180) and modified by Ross *et al.* (181), the isolated perfused kidney model has contributed substantially to the knowledge of kidney injury susceptibility. The isolated perfused kidney model contains all the structural elements of the kidney, but is missing the extrarenal and neurohumoral influences. The main disadvantage is the model is only functional for a few hours and so can't be used to study chronic renal injury or prolonged pathophysiological processes. It is a relatively simple model but requires a skilled technician, takes three hours per experiment and only one experiment can be run at a time. It is also a costly procedure with each experiment costing $60 [179].

Cell Culture Model

The cellular model can be used to study individual components of the kidney. The advantages of this model are; the ease of use of this model, that it can be used on a large scale to study numerous parameters and can be used to study long term effects. The disadvantage is that it is an isolated model and so doesn't take into account other parameters which could also affect the observed results [179].

1.3.3.1. Puromycin Aminonucleoside

Puromycin aminonuceloside (PAN), a well characterized antibiotic with nephrotoxic properties, has been used since the 1950s to study the mechanisms of proteinuria in rats [180]. The resulting experimental model, called PAN nephrosis of the rat, is similar to the human diseases minimal change nephrosis (MCN) and focal segmental glomerulosclerosis (FSGS) [181].

Despite being a well studied model of nephrosis, the exact mechanism of PAN-induced proteinuria is not fully understood. The two main features of PAN nephrosis are foot process effacement and focal detachment of the podocyte from the glomerular basement membrane [182-184].

Puromycin aminonucleoside consists of puromycin and adenosine, which themselves have toxic effects. Puromycin causes decreased amino acid transport and decreased protein synthesis. Adenosine causes increased cell membrane permeability and increased adenyl cyclase activity and decreased protein and nucleic acid synthesis, however neither constituent alone can cause nephrosis [182, 184]. PAN is known to cause a decrease in protein and RNA synthesis.

Studies by Fishman and Karnovsky [184] and Coers *et al.* [183] showed that PAN resulted in morphological changes to podocytes in culture and a reduction in cell adhesion. A recent study by Luimula *et al.* [78] showed that both podocin and nephrin had reduced protein levels in response to

PAN nephrosis but β1 integrin showed an increase in protein expression, but there was no significant change in mRNA level. Takeda *et al.* [45] showed that PAN disrupts the podocalyxin/NHERF2/ezrin interaction to the actin cytoskeleton, ezrin disassociates from the actin cytoskeleton. By disrupting the sialylation of podocalyxin PAN causes a reduction in the anionic charge, which has been suggested to be the cause of increased permeability leading to proteinuria. PAN nephrosis results in a 70% reduction in the sialic acid composition of podocalyxin [43]. Disialoganglioside expression is also greatly reduced in PAN nephrosis [185].

1.4. Biomarkers of Nephrotoxicity

A biomarker has been defined by the Biomarkers Definitions Working Group as "a characteristic that is objectively measured and evaluated as an indicator of normal biological processes, pathogenic processes, or pharmacological responses to a therapeutic intervention" [186].

Although biomarkers have the greatest value in early efficacy and safety evaluations, for example providing a basis for lead compound selection or dosing, as well as being substitutes for clinical responses. They also have applications as diagnostic tools for the identification of patients, and disease progression, as an indicator of disease prognosis and for predicting and monitoring the response to therapeutic intervention [186].

There has been varying levels of success in identifying and developing biomarkers of renal disorders, including acute renal failure, chronic renal failure and polycystic kidney disease [187].

Biomarkers can be any biological entity which shows changes in response to disease or drug treatment therefore a biomarker could be a gene, protein or metabolite, because of this variety several approaches are used to identify potential biomarkers including Genomics, Pharmacogenetics, Proteomics and Metabolomics/Metabonomics [188].

Genomics:

Genomics is the study of gene expression in cells, tissues or an organism under specific conditions. The main techniques are PCR based or micro-array analysis. Micro-arrays for gene expression analysis has become a very important tool for identifying potential biomarkers, due to the high level of data generated [188].

Pharmacogenetics/Pharmacogenomics:

Pharmacogenetics is an emerging scientific discipline arising from the merging of genetics, biochemistry and pharmacology [189].

Pharmacogenetics studies the role and effect genetic differences have in response to pharmaceutical treatment. Toxicogenetics is the study of individual response to a non-therapeutic foreign substance (xenobiotic). Pharmacogenomics is the fusion of pharmacogenetics with genomics to provide high-throughput data and allows the determination of an individual's genetic profile in respect to disease risk and drug response. Ultimately the goal of pharmacogenetics is to predict a patient's response to a specific treatment and hence therefore provide the best "personalized" medical treatment possible.

Pharmacogenomics correlates phenotypic biomarkers with genetic characterization allowing researchers to identify the actual genetic basis of individual and interracial variation in drug efficiency, metabolism and transport [189]. Individualizing drug therapy with the use of pharmacogenomics holds the potential to revolutionize medicine in the near future and finally allow the doctors to treat the individual rather than the disease. Whether or not this technology does become routine clinical practice, one thing is certain pharmacogenomics has become an increasingly valuable tool in clinical research [189].

Proteomics:

Proteomics has been defined as "the systematic analysis of proteins for their identity, quantity and function" [190]. Proteomics is a rapidly developing field of research, which is a by-product of the human genome project [191].

Proteomics is the study of total protein expression in a cell, tissue or organism under specific conditions. Proteomics provides information on protein abundance, location, modifications and interactions. Proteomics relies on a co-ordinated approach of protein isolation and identification. Common techniques are 2D PAGE, HPLC and mass spectroscopy [192, 193].

Proteomics holds great promise for renal research and clinical nephrology, due to the high-throughput nature of the developing techniques and approaches in identifying proteins and protein interactions [191].

Metabonomics:

Metabonomics is a new area of study, it is a systems approach for studying *in vivo* metabolic profiles and provides information on drug toxicity, disease processes and gene function complementary to other profiling approaches [194]. Metabonomics provides a chemical or biochemical profile of a specific body fluid, organ or tissue over a specified time-course. Overall metabonomics can facilitate the determination of metabolic profiles and the mapping of interactions between metabolic pathways [188].

There is considerable scope for the use of metabonomic approaches in the pharmaceutical industry, from discovery through to clinical development. Metabonomics is now widely recognized as an independent technique for evaluating drug-candidate compound toxicity and has been incorporated into the drug development process by several pharmaceutical companies [194].

Several published studies by pharmaceutical companies have used the approaches outlined above to examine kidney nephrosis models in rats in an attempt to gain a better understanding of the nephrosis process and to identify possible biomarkers of nephrosis to aid compound development and future studies.

GlaxoSmithkline used a proteomic approach, to identify proteins which showed differential expression in compound induced nephrotoxic rats. Two compounds were chosen, puromycin [193] and gentamicin [195]. Puromycin is an aminonuceloside antibiotic which specifically targets glomerular podocytes, causing damage to the glomerular filtration barrier resulting in severe proteinuria. Gentamicin is an aminoglycoside antibiotic which targets the renal proximal tubule causing tubular degeneration.

More than 20 proteins were identified which showed differential expression after gentamicin induced toxicity and could therefore be potential biomarkers. They fall into one of four categories, they are involved in 1) gluconeogenesis and glycolysis 2) fatty acid transport and utilization 3) the citric acid cycle and 4) stress responses [195].

A similar study [196] was conducted by a consortium of universities and pharmaceutical companies. They used genomics to identify genetic markers in compound induced nephrotoxicity of rats. In this study they used puromycin, gentamicin and cisplatin. Cisplatin is an antineoplastic agent, used to treat solid tumours, however its use is limited because it causes severe renal toxicity [197]. This study identified several potential biomarkers, which were up-regulated in a dose and time-dependent manner, they included KIM-1, osteopontin and several ESTs [196].

An Example of a Nephrotoxic Biomarker:

Kidney injury molecule 1 (KIM-1) was first identified and characterized in 1998 by Ichimura *et al.* [198] in humans and rats. The human and rat genes show 44% overall identity, but the similarity increases to 68% in the immunoglobulin (Ig) domain [198]. KIM-1 is a type-1 transmembrane glycoprotein with an ectodomain that contains immunoglobulin and highly O-glycosylated mucin subdomains and multiple N-glycosylation sites. KIM-1 is minimally expressed in the normal rat kidney proximal tubule epithelium but is dramatically up-regulated in the S3 segment of the proximal tubule in the postischemic kidney [199]. Ichimura *et al.* examined KIM-1 expression in three models of nephrotoxicant-induced kidney injury in rats, in addition to seeing increased expression, the KIM-1 ectodomain and fragments of the domain were found in the urine of each model. This indicated that nephron injury resulted in shedding of the ectodomain which would allow for non-invasive monitoring of nephrotoxicity [200]. Taken together the results suggest that KIM-1 is a general biomarker of nephrotoxic injury and maybe used for detection and monitoring of nephrotoxicants as well as for monitoring disease states [200].

As part of a wider nephrotoxicity project, GlaxoSmithkline used TaqMan™ real-time PCR to investigate changes in the expression of selected genes from rat glomeruli subjected to PAN induced nephrosis. The genes chosen for investigation included podoplanin, podocalyxin, nephrin and GLEPP-1.

In brief kidney samples were taken from rats subjected to puromycin aminonuceloside at either low (10mg/kg/day), mid (30mg/kg/day), high (100mg/kg/day) doses or saline control animals. The kidney samples were sectioned, mounted and stained prior to laser capture microdissection (LCM). LCM was used to isolate the glomeruli which were subsequently used for RNA isolation. RT-PCR was used to generate cDNA for each sample. TaqMan™ real-time PCR was then used to quantify the levels of each gene present after normalization with β-actin.

The results from this study correlated with published work, in that podoplanin and podocalyxin both showed a decrease in gene expression at the highest PAN dose. GLEPP-1 showed down-regulation but this result was ambiguous. Based on these experiments, we predicted that podoplanin and podocalyxin could be potential biomarkers of nephrotoxicity and warranted further *in vitro* studies to test this. These studies formed the basis of my hypothesis.

1.5. Aims and Hypothesis

The aims of this thesis are:

1. To develop a cellular model which mimics PAN induced nephrosis
2. To use the cellular model of PAN nephrosis to examine the expression and localization of two podocyte specific proteins, podoplanin and podocalyxin. Evaluate if podoplanin and podocalyxin would be suitable biomarkers of nephrotoxicity.
3. To identify any other potential biomarkers of nephrotoxicity.
4. To use our cellular model to gain a better understanding of the mechanisms involved in PAN induced nephrosis.

To this end our hypothesis is:

PAN causes disruption to the cytoskeletal linked proteins in the podocyte resulting in nephritic injury, but the exact mechanism is unknown. Can a cellular model which mimics PAN nephrosis be developed which would allow us to study and further characterize the mechanism of PAN nephrosis and potential biomarkers of nephrotoxicity.

Chapter 2.
Materials and Methods

2.1. Cell Culture

2.1.1. NRK Cell Maintenance

NRK (Normal Rat Kidney) cells, a fibroblast cell line derived from normal *Rattus norvegius* kidney cells, were a kind gift from GlaxoSmithkline, were routinely cultured and maintained in 75 cm^2 filter-capped flasks (Greiner # 658175), in a humidified 5% CO_2 atmosphere at 37°C. The cells were cultured in D-MEM (Dulbecco's modified Eagle medium, high glucose, with 4500mg/L D-Glucose and sodium pyruvate, without L-Glutamine) (Gibco # 21969-035) supplemented with 10% heat inactivated foetal bovine serum (FBS) (Gibco # 10108-165) and 1% 200 mM Glutamine (Gibco # 21969). The cells were passaged when 70% confluent.

2.1.2. Generating an *in vitro* PAN Nephrosis Model

Based on previous published literature, [182-184] a range of PAN doses were chosen, 0µg/ml, 10µg/ml (3.4 mM), 40µg/ml (13.6 mM), 80µg/ml (27.2 mM), to generate a cellular model of PAN nephrosis. NRK cells were grown for 48 hours under normal conditions, after 48 hours the media was removed, the cells were washed with PBS and fresh media containing PAN at the above doses were added. The cells were cultured as normal in a humidified 5% CO_2 atmosphere at 37°C for 48 or 72 hours.

2.1.3. Cell Viability

Two methods were used to determine cell viability, trypan blue uptake and DAPI staining. For the trypan blue uptake experiments, after PAN treatment the cells were removed from each flask by treatment with trypsin/EDTA and washes in PBS. The cells were centrifuged at 1000 rpm for 5 minutes, the supernatant was discarded. Cells were resuspended in 5 ml of PBS and a 20 µl aliquot of cells was diluted with 20 µl of trypan blue and mixed thoroughly. 10 µl was loaded onto both grids of an improved Neubauer haemocytometer (Figure 2.1.) and

counted in duplicate. Cells which stained blue are dead cells and cells which are not stained are viable. A percentage of viable cells can be calculated by:

(Number of non-stained cells/ total number of cells) X 100

DAPI staining examines DNA damage as the result of PAN treatment. Cells were cultured on 13 mm coverslips under PAN conditions as previously described. The coverslips were inverted and mounted onto slides using Mowiol Mountant (See appendix 1) containing DAPI (Sigma D-9542) which was visualized using the Zeiss LSM510 confocal microscope at Durham University.

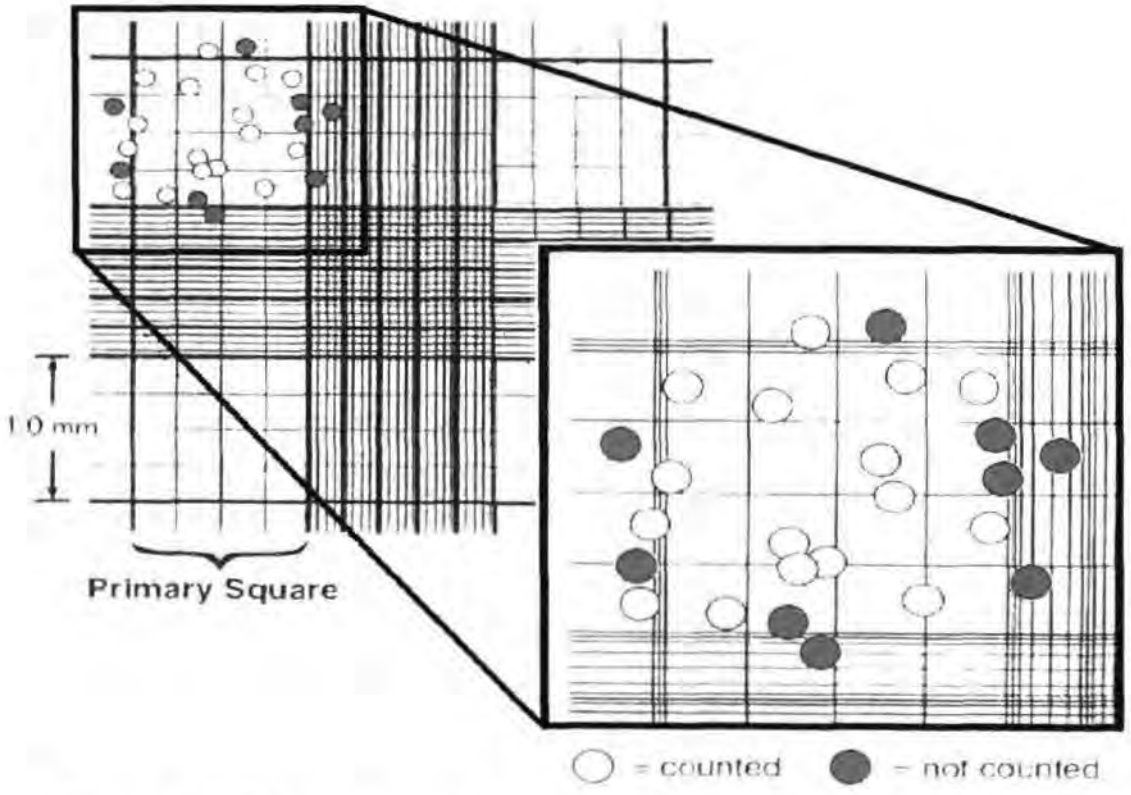

Figure 2. 1. Grid outline of an improved Neubauer haemocytometer.

2.1.4. Cell Aggregation Assay

A cell aggregation assay was established based on the classic cell-aggregation assay first described by Takeichi [201]. NRK cells (passage number 15) were cultured in D-MEM supplemented with 10% FBS and 5% glutamine on 90 mm dishes until 75% confluent. Cells were then cultured in PAN media, as previously described for 48 or 72 hours. At each time point the cells were detached by trypsin/EDTA treatment and re-suspended in Hank's Balanced Salt Solution (HBSS) (Gibco # 14185-045) + 1% BSA following four passages through a 19 gauge syringe, to ensure single cells. Cells were counted on a haemacytometer and 35 X 10^4 cells in a total volume of 1ml were incubated in 12 well plates coated with HBSS + 2% BSA. The cells were allowed to aggregate for 180 min in the presence of 1 mM $CaCl_2$ on a rotating shaker (100rpm) at 37°C. The reaction was stopped by the addition of 0.25 ml 25% glutaraldehyde. Aggregation was quantified by counting six replicates in duplicate of each sample on a haemacytometer using phase-contrast optics, as previously described, section 2.1.3.

% Cell aggregation was estimated by:

(No. of aggregates >3/ total no. of cells) X 100

A paired T-Test was used to analyze PAN treated groups against the control group. All p-values <0.05 were deemed to be statistically significant.

2.1.5. Re-culturing detached NRK cells

After PAN treatment, detached NRK cells were collected from the media by centrifugation. Cells were resuspended in 0.5 ml of media and a viable count was performed. 12 well tissue culture plates were coated with a rat collagen gel (8.5ml collagen solution (kindly supplied by Dr Jahoda, Section 2.1.6), 1ml 10X MEM pH 7.4) at an approximate concentration of 10µg/cm^2 and allowed to set. Equal cell numbers (7.5 x 10^4 cells/ml) at each PAN dose was added to duplicate coated and non-coated plates.

The volume of each well was made up to 1 ml with media. The cells were examined every 24 hours to se if cells were re-attaching to the tissue culture plates and if so were the cells proliferating as normal. Control cells, cells which hadn't detached from the tissue culture plates, were also included for comparison.

2.1.6. Preparation of Collagen from rat tails

This method is based on a protocol by Elsdale and Bard [202]. Rat tails were removed and after washing in non-scented soap were frozen at -20°C. Six tails were defrosted in 70% ethanol and the skin removed. The tendons were stripped and UV irradiated overnight in 70% ethanol. The tendons were weighed and stored in 500 ml 0.5M acetic acid at 4°C for a couple of days. The collagen/acetic acid solution was sterile filtered through gauze and centrifuged at 2000g for 3 hours. The clean collagen solution was decanted and the collagen precipitated using an equal volume of 20% NaCl solution. The solution was centrifuged and the precipitate was redissolved in an equal volume of 1M acetic acid. Store at 4°C for a couple of days. The solution was dialyzed against distilled water for 24 hours. Centrifuged at 2000g for 3 hours. 1 ml of fungizone and gentamicin were added per 100 ml of collagen.

2.2. Gene Expression Analysis

2.2.1. Cell Culture

NRK cells were cultured as previously described with the following alterations. The cells were seeded at 1 x 10^6 and cultured in 90 mm dishes (Greiner) in triplicate for each PAN dose. At each time point the media was removed and the cells were flash frozen in liquid nitrogen and stored at -80 °C.

2.2.2. mRNA Extraction

mRNA was extracted from triplicate plates of 1 x 10^6 NRK cells at each PAN dose, using Quickprep® Micro mRNA Purification kit from Qiagen. In brief 0.4 ml Extraction buffer was added to the plates sequentially and the cells were detached by scraping. 0.8 ml Elution buffer was added and the samples were vortexed. A cleared cellular homogenate was prepared by centrifugation and placed on top of an Oligo(dT)-Cellulose pellet and gently mixed by inversion. Samples were centrifuged and the supernatant discarded. Five High-Salt Buffer washes followed by two Low-Salt Buffer washes were performed. The pellet was re-suspended in 0.3 ml of the Low-Salt Buffer and transferred to a Microspin™ column and following three washes with Low-Salt Buffer mRNA was eluted in 0.4 ml of pre-warmed Elution Buffer. 10 µl of Glycogen Solution and 40 µl potassium acetate Solution was added to each sample. The samples were stored overnight in 95% ethanol at -20 °C.

2.2.3. cDNA Synthesis

mRNA was reverse transcribed using the First Strand cDNA Synthesis Kit from Roche following the recommended protocol. Briefly, a mastermix consisting of 1 µg of mRNA, 10X Reaction Buffer, 5 mM MgCl2, 1 mM dNTP mix, 3.2 µg Random Primer, 50 units RNase inhibitor, 20 units AMV Reverse Transcriptase and sterile DEPC treated water to a total volume of 20 µl, was mixed and centrifuged briefly prior to being incubated at 25°C for 10 minutes, 42°C for 60 minutes and 94°C for 4

minutes. The cDNA was stored at -20°C overnight and subsequently used for RT-PCR (see below).

2.2.4. Polymerase Chain Reaction (PCR)

A PCR reaction mix was set up containing cDNA, 10X Reaction Buffer, 1.5 mM MgCl2, 10 mM of each dNTP, 10 µM of both forward and reverse primers and 0.5 units of Taq polymerase. All reagents were supplied by Promega, the primers were made to order from TAGN and MWG, Table 2.1.

The PCR reactions were carried out using an Omn-E thermal cycler (Hybaid) using the following programme:

94°C	4 min	
94°C	1 min	} 35 cycles
X°C	1 min	
72°C	1 min	
72°C	10 min	

X is the hybridization temperature of the primers being used.

2.2.5. Gel Electrophoresis

PCR products were analysed on 2% agarose gels. Gels were made by dissolving 2% agarose (Bioline) in warm 1X TAE buffer, containing 1 µg/ml ethidium bromide. The gels were poured into BioRad pre-cast gel trays containing a gel comb. Once the gel had set, the comb was removed and the gel was submerged in 1X TAE Buffer. 10 µl of each PCR product was mixed with 5 µl of loading buffer and was electrophoresed in 1X TAE buffer at 60 volts for 45 minutes. Each gel contained 5 units of a DNA ladder (Promega) and a concentration marker to quantify both size and intensity of the PCR product. The DNA was visualized using the BioRad Gel-Doc Ultra Violet Transilluminator at 366 nm, the results were recorded and analysed using the Gel-Doc software.

Gene	Acc. Number	Forward Primer 5' – 3'	Reverse Primer 5' – 3'	Product size bp	Hybridization Temp.
Podoplanin	U96449	AATGGTGCAAAAACCGAGAC	AACTGAAGGCAGTGGATGCT	304	55°C
Podocalyxin	AF109393	GTTCATTTGTGTCCATCCCC	ACCCACCCTTTAGGCAGACT	301	50°C
Nephrin	AF161715	TTCTTCTGATCTCCATGGGC	CACGCCCCTTTTAATTCTGA	271	50°C
Podocin	AY039651	GGGCGAGTGGAC AAGAGTAA	TGAATGATGAGACGACCCAC	214	55°C
WT-1	X69716	GTCCCAGGCAAGAAAGTGTG	CGGCAAACCTGATAGGACTC	154	55°C
G3PDH	AB017801	CTCAGTTGCTGAGGAGTCCC	GGGTGCAGCGAACTTTATTG	153	55°C

Table 2.1. Primers for RT-PCR

2.3. Protein Expression Analysis

2.3.1. Cell Culture

NRK cells were cultured as previously described in 90 mm dishes with the following alterations. After PAN treatment the cells were trypsinized, centrifuged at 1000 rpm for 5 minutes and resuspended in 1 ml of PBS, a 10 µl aliquot was counted, as previously described. The cells were transferred to a sterile 1.5 ml microfuge tube and centrifuged for 30 seconds at 13000 rpm, the supernatant was removed and the cells re-spun. Cells were snap-frozen in liquid nitrogen and stored at -80 °C.

2.3.2. Protein Extraction

The frozen cell pellets were re-constituted in 200 µl of cell lysis buffer (50mM Tris.HCl pH 7.5, 150mM NaCl, 1% NP40, 0.25% Sodium deoxycholate and 1X Protease inhibitor cocktail Sigma # P-8340) per 1 x 10^6 cells and incubated on ice for 10 minutes prior to acetone precipitation. 800 µl 100% acetone (-20 °C) was added to each cell aliquot and incubated at room temperature overnight. The cells were centrifuged at 13000 rpm for 10 minutes. The pellet was washed three times with 80 % acetone (-20 °C) and a final wash in 100 % acetone (-20 °C). The pellet was air-dried for 3 minutes and left to re-hydrate for 3 hours in 200 µl Sample Buffer (8M Urea, 2M Thiourea and 4% CHAPS).

2.3.3. Protein Quantification

The protein levels at each PAN dose were determined by the Bradford Assay. A stock solution of 5 mg/ml BSA (Bovine Serum Albumin) was used to generate a standard curve. Each protein sample was mixed as described (Table 2.2) and analyzed in duplicate. Each sample was mixed thoroughly and incubated for 20 minutes at room temperature. The absorbance was read at 595 nm (A_{595}) using a spectrophotometer and the mean results plotted graphically.

Using the standard curve, the unknown protein concentrations can be calculated using: $Y = m \dot{X}$

Where Y is the protein concentration in µg/µl, m is the gradient of the line and X is the Abs at 595 nm

BSA (µg)	0	5	10	20	40	80	-
BSA stock (µl)	0	1	2	4	8	10	-
Sample (µl)	-	-	-	-	-	-	10
Lysis Buffer (µl)	10	9	8	6	2	0	0
0.1M HCl (µl)	10	10	10	10	10	10	10
dH_20 (µl)	80	80	80	80	80	80	80
Diluted Biorad Reagent (µl)	900	900	900	900	900	900	900

Table 2. 2. BSA Standard Curve for protein quantification.

2.3.4. Western Blotting

Proteins were separated by SDS–PAGE according to size using a Mini-Protean 3 gel system (BioRad). The concentration of the acrylamide resolving gel was dependent upon the size of the protein of interest. A 6% gel was used for Podocalyxin (165 kDa) and Laminin β2 (200 kDa), 8% for Ezrin (80 kDa) and 12% for G3PDH (30 kDa) and Podoplanin (40 kDa). See Table 2.3 for constituents of each SDS–PAGE gel.

Equal volumes of 10 µg protein from each PAN dose were mixed with equal volume of 2X Sample Buffer (see Appendix 1) and electrophoresed for 3 hours at 70v through a mini-gel of 6% acrylamide resolving gel and 5% stacking gel (see Appendix 1), alongside a prestained protein size marker (BioRad). The gels were removed from the plates, rinsed in Transfer buffer (see Appendix 1) and placed into Transfer kit. A sandwich was formed as illustrated in Figure 2.2.

	6% Resolving	8% Resolving	12% Resolving	5% Stacking
Sterile dH_2O	5.8 ml	5.3 ml	4.3 ml	2.72 ml
Acrylamide	1.5 ml	2.0 ml	3.0 ml	625 µl
1.5M Tris pH 8.8	2.5 ml	2.5 ml	2.5 ml	-
0.5M Tris pH 6.8	-	-	-	650 µl
10% SDS	100 µl	100 µl	100 µl	50 µl
10% APS	100 µl	100 µl	100 µl	50 µl
TEMED	4 µl	4 µl	4 µl	5 µl
Total Volume	10 ml	10 ml	10 ml	5 ml

Table 2. 3. Constituents of SDS-PAGE electrophoresis gels.

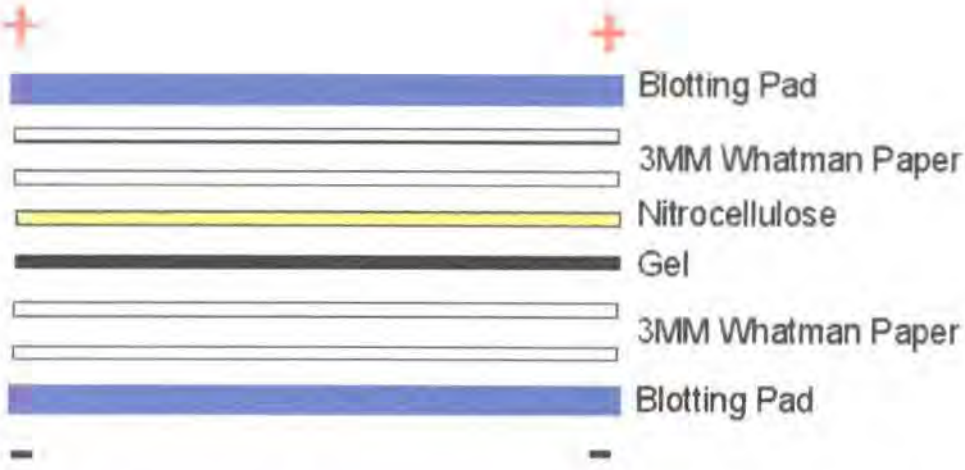

Figure 2. 2. Schematic Representation of Transfer Gel Sandwich.

Protein transfer was performed for 2.5 hours at room temperature at 50v. The nitrocellulose membranes were removed and placed into Block Buffer (see appendix 1) for 2 hours at room temperature. The membranes were incubated with the primary antibody (see table 2.4) diluted in Incubation Buffer (see appendix 1), overnight at 4°C. The nitrocellulose was washed 3X with Washing buffer (see appendix 1) and incubated with the secondary antibody, either donkey anti-mouse or anti-rabbit (see table 2.4) IgG-HRP (Jackson ImmunoResearch) diluted 1:5000. The nitrocellulose was again washed 3X with Wash Buffer and a final PBS wash prior to detection. Detection was carried out in the dark using ECL detection Kit (Amersham) following the recommended protocol. In brief equal volumes of ECL solution 1 and 2 were mixed and incubated for approximately 1 minute. During this time excess PBS was drained from the blot. 0.75 ml of mixed ECL solution was added onto the blot, and spread to cover the whole area. Following two minutes incubation excess reagent was removed and the blot exposed to X-ray film. Depending on the results the exposure time was adjusted accordingly.

Antibody	Concentration	Secondary Ab	Size kDa	% SDS Gel	Supplier	Cat. #
G3PDH	1:16000	Monoclonal	40	12	Abcam	Ab8245
Podoplanin	1:500	Polyclonal	38	12	Sigma	P-1995
Podocalyxin	1:1000	Monoclonal	165	6	Chemicon	MAB430
Ezrin	1:4000	Monoclonal	80	8	Sigma	E-8897
Integrin α3	1:250	Monoclonal	135	6	BD Biosciences	V76720-050
Laminin β2	1:250	Monoclonal	220	6	BD Biosciences	L59920-050
Laminin β2	-	Monoclonal	220	6	Hybridoma Collection	D 18

Table 2. 4. Antibody Details for Western Blotting

2.4. Sub-Cellular Fractionation Studies

2.4.1. Cell Culture

NRK cells were cultured as previously described with the following alterations. NRK cells were cultured in twenty-five 90 mm dishes. The dishes were seeded at 1 x 10^6 and cultured as normal for 48 hours, after 48 hours the normal culture media was removed and PAN media was added. Only the highest dose of 80µg/ml for 72 hours was chosen for this analysis.

2.4.2. Sub-Cellular Fractionation

The sub-cellular fractionation method was based upon an original method first described by Simpson *et al.* [203] to identify the distribution of glucose transporters in rat adipocytes. At 4°C the NRK cells were removed from the plates by scraping and homogenised in 5 ml of HES buffer by hand using a domed homogeniser for a final volume of 25 ml. 100 µl of the homogenate was snap-frozen in liquid nitrogen and stored at -80°C. The remaining homogenate was centrifuged at 19,000g for 20 minutes at 4°C using a Beckman JA-20 rotor. The supernatant is used to prepare the intracellular fractions and the pellet was retained on ice for preparation of the plasma membranes.

Intracellular Fractions:

The 19,000g supernatant is re-centrifuged at 40,000g for 20 minutes at 4°C using a Beckman JA-20 rotor. The pellet obtained containing the high-density microsomes (HDM), including the endoplasmic reticulum, was resuspended in 100 µl of HES buffer and protease inhibitors and 20 µl aliquots were snap-frozen in liquid nitrogen and stored at -80°C. The 40,000g supernatant was transferred to Beckman Ultracentrifuge tubes and centrifuged at 180,000g for 90 minutes at 4°C in a SW-41 rotor. The pellet, containing the low-density microsomes (LDM) predominantly golgi, was resuspended in HES buffer as previously described.

Preparation of Plasma Membranes:

The 19,000g pellet from the initial spin was re-suspended in 800 µl HES buffer and layered onto 10 ml of 1.12 M sucrose (see Appendix 1). The samples were centrifuged at 100,000g for 60 minutes at 4°C in the SW-41 rotor. The fluffy white layer at the interface between the sucrose layers contains the plasma membrane and was carefully aspirated and resuspended in 20 ml of HES buffer. The pellet at the bottom of the sucrose gradient is the nuclei/ mitochondria fraction and was resuspended and stored as previously described. The washed sucrose-free pellets of plasma membranes were obtained by centrifugation at 40,000g for 20 minutes at 4°C in the JA-20 rotor. The pellet was stored as previously described.

2.4.3. Western Blotting

Western blotting was performed on the fractions as previously described for SDS–PAGE with the following alterations to the method. 10 µl of each sub-cellular fraction was mixed with 10 µl of 2X Sample Buffer and 10 µl was loaded onto the gel. The gel was transferred and probed with podocalyxin, podoplanin and ezrin as previously described.

2.5. Immunolabelling

2.5.1. Cell Culture

NRK cells were cultured as previously described with the following alterations. NRK cells were cultured on 13 mm coverslips (SLS # MIC3306) in 90 mm dishes (Greiner # 633171) until 50% confluent. The media was changed for PAN media and the cells were cultured for 48 or 72 hours.

2.5.2. Immunolabelling

The cells were fixed in 4% PFA/ PBS for 20 minutes at 4 °C, washed three times in PBS. To permeabilize, the cells were incubated in 0.2% Triton X /PBS for 5 minutes at 4 °C, after three washes in PBS the cells were incubated in Blocking Buffer (5% FBS/ PBS) for 30 minutes. The cells were dried and briefly incubated with Primary Antibody for 1 hour. Following three washes in blocking buffer the cells were incubated with secondary antibody for 1 hour followed by a further three washes in blocking buffer. The cells were mounted in MOWIOL containing DAPI. The cells were examined using the Olympus Fluoview FV300 laser scanning confocal microscopy system at GlaxoSmithKline.

Antibody	Concentration	Secondary Ab	Supplier	Cat. #
Podoplanin	1:50	Mono	Angiobio Co	11-012
Podocalyxin	1:50	Mono	Chemicon	MAB430
Ezrin	1:100	Mono	Sigma	E-8897
Integrin α3	1:100	Mono	Hybridoma collection	Ralph 3.1
Laminin β2	1:100	Mono	Hybridoma collection	D 18
β -Tubulin	1:100	-	Sigma	C-4585
Actin	1:100	Mono	ICN	691002
EEA-1	1:100	Poly	Abcam	Ab2900
PDI	1:750	Poly	Dr A Benham. Durham University	-
Cellubrevin	1:50	Poly	Abcam	Ab2102
Syntaxin 7	1:100	Poly	Synaptic Systems	110-072
Caveolin 2	1:300	Poly	BD Biosciences	557859

Table 2. 5. Antibody details for Immunofluorescence microscopy

2.6. Confocal Imaging

All images were obtained at GlaxoSmithkline using the Olympus Fluoview V3.3 FV300 laser scanning microscopy system and methods developed by Susanne Moore.

Obtaining a 3D Image

The specimen was focused under brightfield conditions. The appropriate fluorophore and objective, X100 Uplan Apo, were selected and the image size set to 1024 x 768. An initial fast scan of the specimen was used to optimize the image for fluorescence intensity by adjusting the laser intensity, photomultiplier (PMT), gain and offset settings. Once the conditions were optimized an image was obtained using a slow scan speed for increased resolution. The resolution can be further increased by increasing the "Kalman" averaging value upto 16.

A 3D image is obtained by focusing through the specimen until you reach the last visible image, this image is set as zero. Within the "Z –stage" window 0 is entered in the "start Z" box and a value equivalent to the sample thickness in the "stop Z" box. The thickness of sections was set at 0.5 μm and the Kalman value to 4. The "XYZ" option was selected and image capture initiated. Once the Z series was complete the images were saved appropriately. The images can now be viewed as a single image of the merged layers or as a movie showing expression through each layer of the cell.

Obtaining a Dual-stained Image

This follows the same protocol as for a single fluorophore with the exception that two fluorophores are initially selected. The fluorophore with the emission wavelength <570nm was assigned to Channel 1 and the second fluorophore with an emission wavelength >570nm was assigned to Channel 2. The conditions each fluorophore were optimized in turn, using the "Seq123" option and a 3D image obtained as previously described. The images can be saved for each fluorophore independently,

as well as a merged image of both fluorophores to highlight any co-localization.

Chapter 3.

Establishing a Cellular Model which Mimics PAN Nephrosis

3.1. Introduction

Although there are several *in vivo* animal models for studying nephrosis, there are very few *in vitro* models. The two most common *in vitro* models are the isolated perfused rat kidney model and the cell culture model (both primary and immortalized cell lines). Both have advantages and disadvantages as previously discussed, (see Section 1.3.3 Experimental Models of Nephrosis). As we require a model to study the mechanisms of nephrosis and to identify and further characterize potential nephrotoxic biomarkers a cellular model is the most appropriate to use.

There are limitations to using primary or immortalized cultured renal cells. Firstly there are between 15 and 20 cell types within the kidney, before any experiment is initiated it must be ensured that homogeneous cultures have been obtained. Secondly there is little information regarding markers which could be used to identify cell origins/ancestry/lineage. Thirdly, there is always the problem of cells differentiating or dedifferentiating during cell culture. Despite these limitations a cellular model represents a viable alternative to study renal cellular functions and their responses to experimental changes [179].

Unfortunately none of the currently commercially available continuous renal epithelial cell lines fully express all the differentiated functions of their ancestor cells *in vivo*. There are however two experimental models which can be used; (1) Primary cultures of isolated epithelial cells from defined origin and (2) continuous renal epithelial cell lines [179].

Primary cells are less well suited for *in vitro* nephrosis studies as they do not maintain their state of differentiation for more than a few passages. Although primary cultures may be immortalized by transfection, the induced changes in cell function and characteristics have not been fully defined. For this reason it is commonly believed that the well characterized immortalized continuous renal epithelial cell lines are the most suitable for in vitro nephrosis studies. Several cell lines are available

including MDCK, OK, A6 and LLC-PK, but we chose to use normal rat kidney (NRK) cells. NRK cells are a fibroblast cell line with epithelial morphology that has been derived from normal *Rattus norvegius* kidney cells [179].

The most common model of nephrosis, uses the antibiotic puromycin aminonuceloside, (PAN), (see Section 1.3.3.1). The PAN nephrosis model of glomerular disease has been extensively studied since the 1950's. However the majority of these studies have been *in vivo* animal studies, in comparison there have been very few *in vitro* studies [182]. Table 3.1 is a brief summary of the key *in vitro* studies using PAN nephrosis.

Using the published data on *in vitro* and *in vivo* models of PAN nephrosis, we established an *in vitro* cellular model which mimics PAN nephrosis in NRK cells.

Group	Cell Type	PAN Doses	Key Findings	Ref
Bertram *et al.*	Kidney slices	100 and 500µg/ml for 1 – 3 days	PAN effects the ultrastructure of podocytes, including FP and cell body flattening, plasma membrane blebbing and a loss in the number of microvilli on cell bodies	[182]
Coers *et al.*	Rat GVEC's (podocytes)	10, 20 and 50µg/ml for 1 – 2 days	PAN caused cell rounding and detachment, decrease in cell proliferation and a loss of β1-integrin focal adhesions	[183]
Fishman & Karnovsky	Rat GVEC's (podocytes)	10, 20, 40 and 80µg/ml for 1 – 3 days	PAN caused cell rounding, surface blebbing, cells lost ability to adhere to plastic but detached cells remained viable	[184]
Krishnamurti *et al.*	56/10 A1	0.5, 5 and 50µg/ml for 1 – 2 days	PAN caused reduced viability at 50µg/ml only, reduced cell numbers, focal detachment of cells from plastic, reduced expression of α3β1-integrin and increased expression of podocalyxin	[181]
Sanwal *et al.*	Rat GVEC's (podocytes)	5, 10, 20, 50, 100, 200, 500µg/ml for 1 – 2 days	PAN enhances apoptosis in a dose and time dependent manner. PAN induces necrosis at doses >100µg/ml	[204]

Table 3. 1. A Brief summary of the key observations in previous *in vitro* models of PAN nephrosis.

3.2. Determining PAN Doses

Data from three papers, Bertram *et al.* [182], Coers *et al.* [183] and Fishman and Karnovsky [184] (see Table 3.1) which had used PAN to generate nephrosis in cultured renal cells and kidney slices was used to select the range of PAN doses for our studies in NRK cells.

The studies of Coers *et al.* used PAN doses of 10, 20 and 50μg/ml for up to 48 hours to study cytoskeletal organisation and extracellular matrix protein expression in cultured glomerular epithelial cells. These studies showed disturbed cytoskeletal organisation and reduced expression of laminin and β1 integrin protein expression. The PAN doses used were not toxic, cells were found to be >90% viable. Higher PAN doses of 100 and 500μg/ml have been used on rat kidney slices by Bertram *et al.* [182]. Electron microscope (EM) studies showed flattening of podocytes and an increased number of glomeruli which showed membrane blebbing on podocytes. Fishman and Karnovsky [184] showed changes to podocyte ultrastructure by EM using cultured glomerular epithelial cells and PAN doses of 50μg/ml. At this dose membrane blebbing was evident as early as three hours after drug treatment and at twenty hours cell rounding occurred and cells began detaching from the culture plates although they remained viable. These changes mimic PAN nephrosis in vivo.

For our studies it is essential we use PAN doses which display characteristics of nephrosis but without causing cell toxicity. Too high a dose or over exposure of PAN will result in the detection of non-specific effects as a result of toxicity and not nephrosis. We examined the expression of two podocyte markers, podoplanin and podocalyxin, known to have reduced gene expression in the PAN nephrotic rat model.

3.3. Examining Podoplanin and Podocalyxin Gene Expression in NRK cells following PAN Treatment

Podoplanin and podocalyxin have been identified by GlaxoSmithKline as being down-regulated in the rat model of PAN-induced nephrosis. For our cellular model to be an accurate model of PAN nephrosis then these genes must be down-regulated following PAN treatment in our model.

3.3.1. Primer Design

Primers were designed in the specific 3' UTR region for each gene, using Primer3 software (http://www-genome.wi.mit.edu/cgibin/primer/primer3). The primers were designed to give a product between 150 – 300 bp in length, primer details are given in Table 3.2.

3.3.2. Normalization

The house-keeping gene glyceraldehyde-3-phosphate dehydrogenase (G3PDH) was used to normalize our panel of cDNA generated from each PAN dose. The PCR products were electrophoresed on a gel with a DNA marker of known concentration and analysed using the BIO-RAD Geldoc software. Volume analysis software was used to generate a standard curve of DNA concentrations and this curve used to calculate the amount of DNA present in each sample and normalized the panel accordingly.

Gene	Accession Number	Forward Primer 5' – 3'	Reverse Primer 5' – 3'
Podoplanin	U96449	AATGGTGCAAAAACCGAGAC	AACTGAAGGCAGTGGATGCT
Podocalyxin	AF109393	GTTCATTTGTGTCCATCCCC	ACCCACCCTTTAGGCAGACT
Nephrin	AF161715	TTCTTCTGATCTCCATGGGC	CACGCCCCTTTTAATTCTGA
Podocin	AY039651	GGGCGAGTGGAC AAGAGTAA	TGAATGATGAGACGACCCAC
WT-1	X69716	GTCCCAGGCAAGAAAGTGTG	CGGCAAACCTGATAGGACTC
G3PDH	AB017801	CTCAGTTGCTGAGGAGTCCC	GGGTGCAGCGAACTTTATTG

Table 3. 2. Summary of primers for RT-PCR of podocyte genes.

3.3.3. Testing PAN doses of 5 and 10µg/ml

Initially PAN doses of 5µg/ml and 10µg/ml were chosen and cells were exposed for 24 or 48 hours. However with these doses no changes were observed in cell morphology or cell numbers after 24 hours and only 10µg/ml had a limited effect after 48 hours. The lack of any significant changes between the PAN treatments suggested the PAN doses were too low to be causing substantial nephrotic effects.

We found that podoplanin showed little variation in expression at time 0 with PAN treatment but did show an increase in gene expression with increasing PAN doses at both 24 and 48 hours, but a decrease in expression at a given dose between 24 and 48 hours. Podoplanin also showed a large increase in expression at 10µg/ml after 48 hours when compared to control cells (Figure 3.1). Published data shows that podoplanin gene expression is greatly reduced in both the in vitro and in vivo models of PAN nephrosis [18]. In our model podoplanin expression appears to initially increase with response to PAN treatment, peaking after 24 hours before starting to decrease, further time points and higher PAN doses are required to establish exactly how PAN affects podoplanin gene expression.

Podocalyxin showed an initial dose dependent decrease in expression at time 0. At 24 hours there was a decrease in expression at 10µg/ml but at 48 hours there was an increase in expression. Expression of podocalyxin was increased at 10µg/ml over time. Krishnamurti *et al.* [181] found that podocalyxin mRNA expression was increased at 48 hours after PAN treatment with 0.5 or 5µg/ml. This was confirmed at 10µg/ml in my experimental results, but this is in contrast to the results obtained at GlaxoSmithKline, who found podocalyxin gene expression was reduced in the in vivo model of PAN nephrosis.

The fact we didn't observe any of the reported *in vitro* effects associated with PAN nephrosis and the inconsistent data from our initial study of

podoplanin and podocalyxin gene expression suggested that these PAN doses were too low to elicit nephrotic like responses. We therefore increased the PAN doses to 40µg/ml and 80µg/ml and the exposure time to 48 and 72 hours at each dose. We also tested the dose 10µg/ml at the above exposure times.

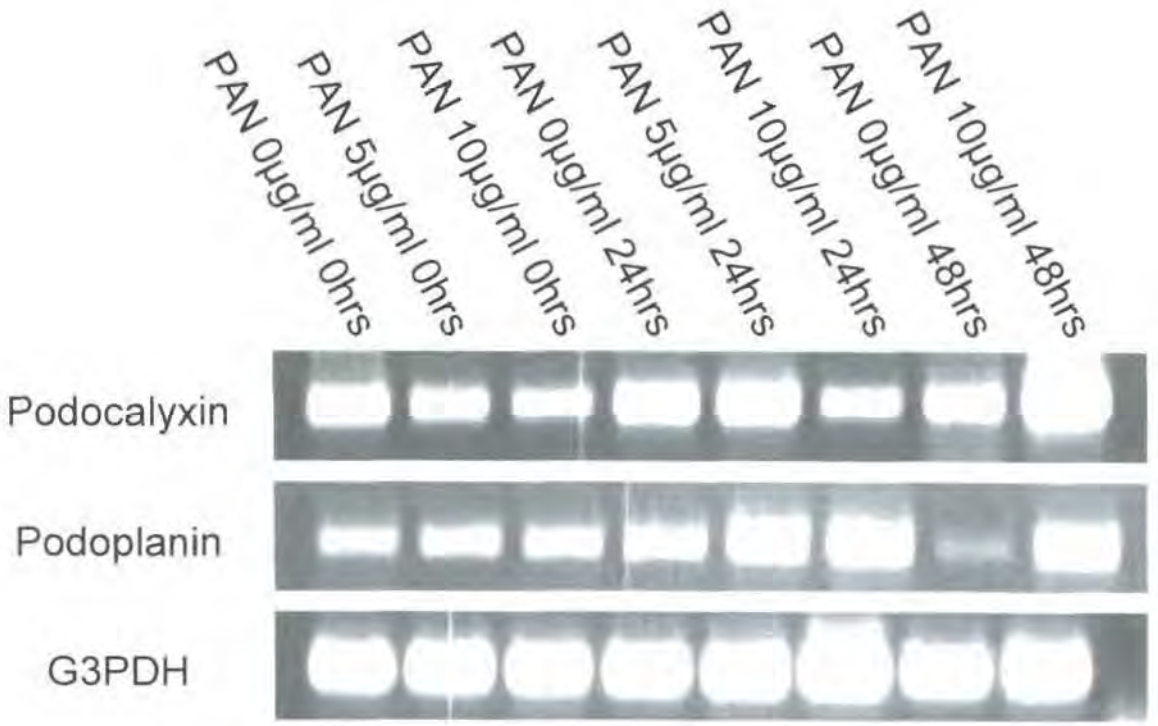

Figure 3. 1. Changes in podoplanin and podocalyxin gene expression in NRK cells following PAN treatment.

Podocalyxin shows decreased expression with respect to PAN treatment at t=0, but shows an increase in expression after 48hrs at the highest (10µg/ml) PAN dose. Podoplanin shows similar initial levels of expression at t=0, which increase with increasing PAN doses at 24hrs. At 48hrs there is a low level of expression in control cells but PAN (10µg/ml) treated cells still have increased expression.

3.3.4. Gene Expression at Increased PAN doses of 40µg/ml and 80µg/ml

The new cDNA panel was normalized as before using G3PDH (Figure 3.2). Increasing the PAN doses to 40µg/ml and 80µg/ml and increasing the exposure time resulted in the downregulation of both podoplanin and podocalyxin genes. Podocalyxin showed a greater reduction in expression and a dose dependent change which wasn't seen for podoplanin (Figure 3.3). Podoplanin showed an almost universal 65% decrease in expression (Figure 3.4), which correlated with the published results of Breitender-Geleff *et al.* [18] who showed that podoplanin was reduced by almost 70% in the PAN nephrosis rat model at the mRNA level. A summary of the reduction in expression of podoplanin and podocalyxin following PAN treatment is shown in Table 3.3.

PAN Dose	% Reduction in Podoplanin Expression	% Reduction in Podocalyxin Expression
10µg/ml 48hrs	65%	63%
40µg/ml 48hrs	65%	78%
80µg/ml 48hrs	65%	80%
10µg/ml 72hrs	25%	68%
40µg/ml 72hrs	65%	85%
80µg/ml 72hrs	65%	86%

Table 3. 3. A summary illustrating the decrease in podoplanin and podocalyxin expression following PAN treatment.

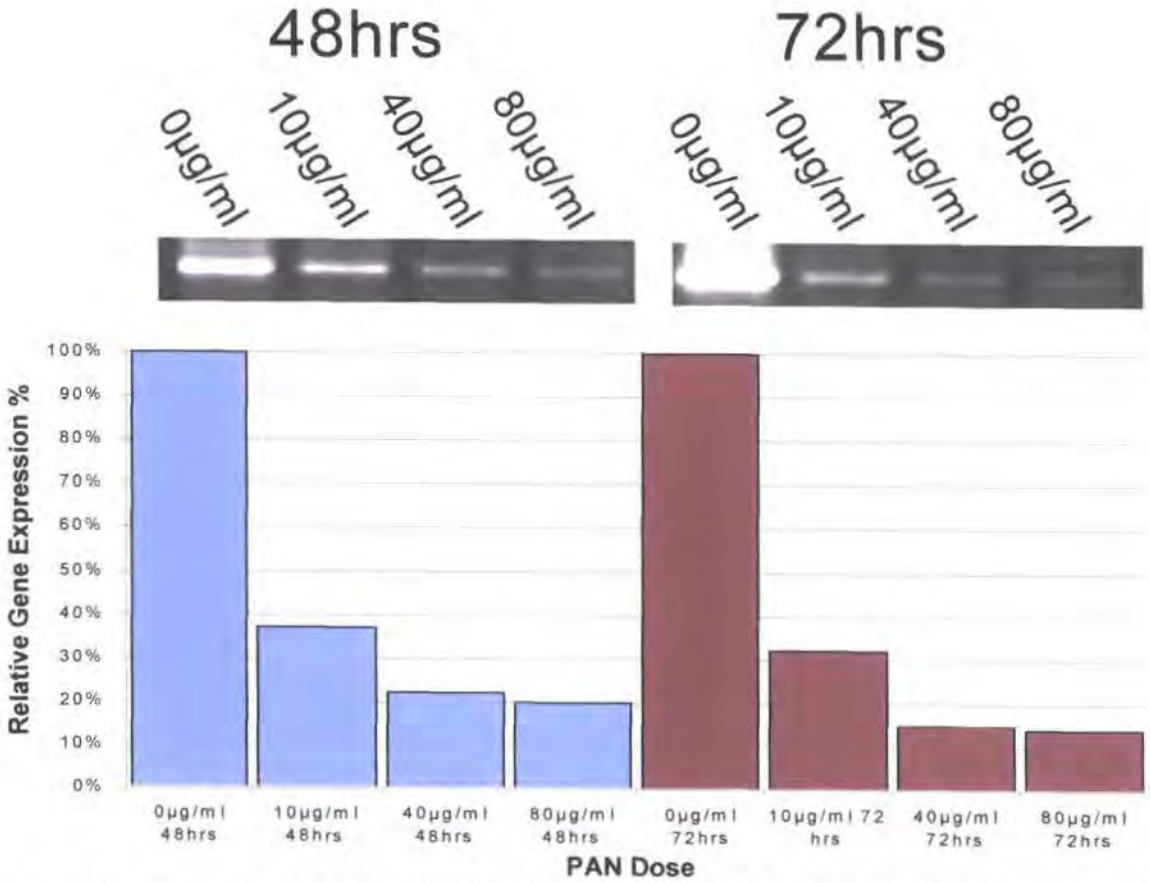

Figure 3. 3. Reduced gene expression of podocalyxin in NRK cells following PAN treatment. Podocalyxin shows a dose-dependent decrease in expression as a result of PAN treatment at both time points.

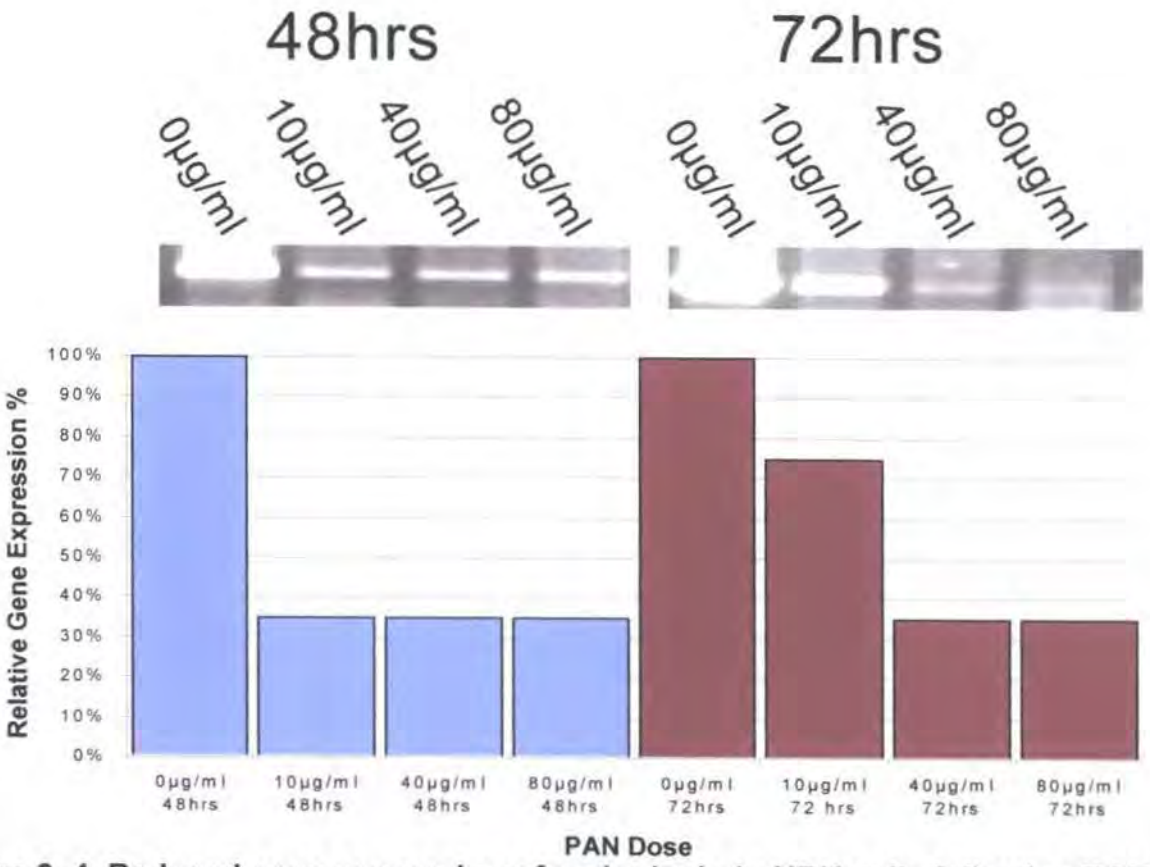

Figure 3. 4. Reduced gene expression of podoplanin in NRK cells following PAN treatment. Podoplanin shows a dose dependent reduction in expression following PAN treatment at 72 hours.

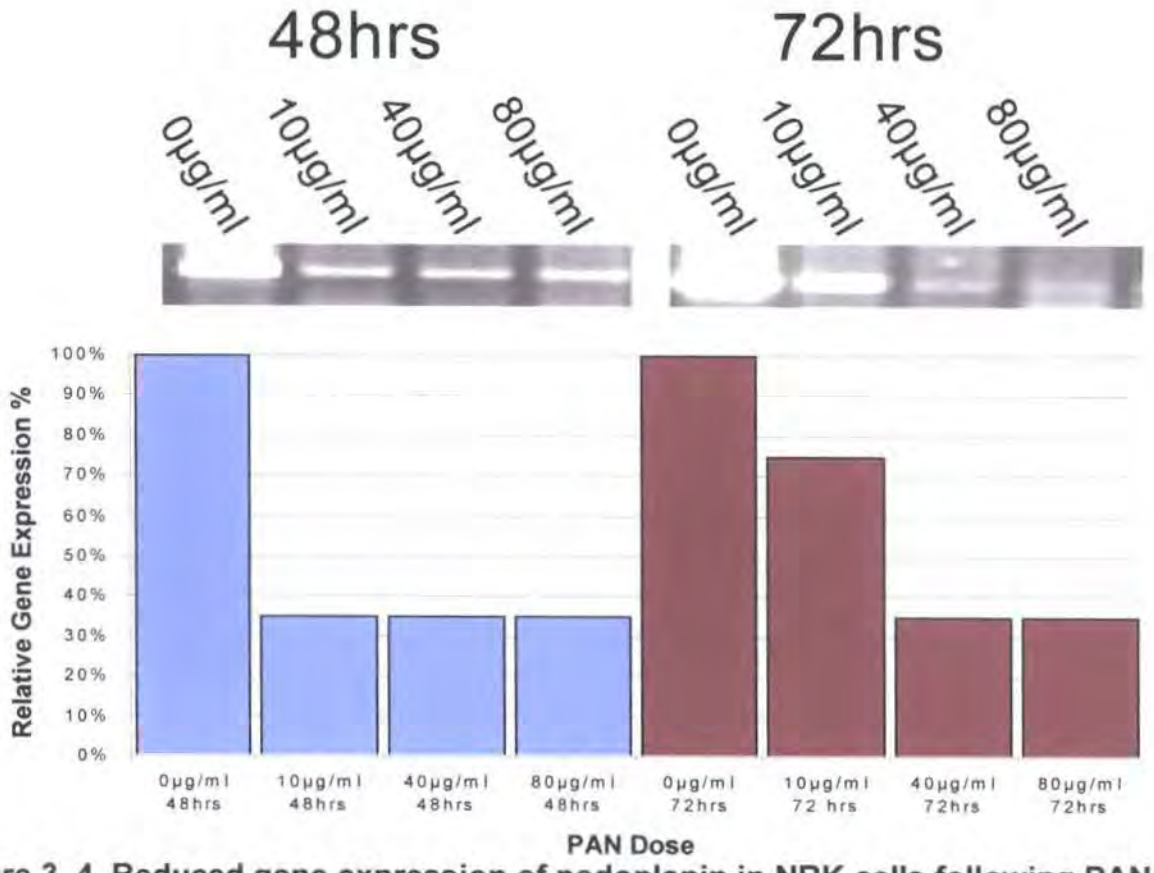

Figure 3. 4. Reduced gene expression of podoplanin in NRK cells following PAN treatment. Podoplanin shows a dose dependent reduction in expression following PAN treatment at 72 hours.

3.4. Examining changes in Expression of other Kidney genes Following PAN Treatment

To show that the reduction in gene expression of podoplanin and podocalyxin was specific and not due to toxicity, we also examined the gene expression of two slit diaphragm proteins, podocin [8, 86, 91] and nephrin [54, 57-60], and the transcription factor WT-1 [129, 138].

Podocin showed reduced gene expression, with a dose response decrease up to the mid PAN dose, but no subsequent reduction in expression from the mid, (40µg/ml), to high, (80µg/ml), doses, (Figure 3.5). However the amplified PCR products did show a mobility shift between the control (0µg/ml) and PAN treated samples, (Figure 3.6), suggesting a change in the size of sequence of the DNA fragment as a result of PAN exposure. To examine whether PAN treatment does result in alterations to the DNA sequence of podocin we sequenced PCR products obtained from cDNA isolated at 0µg/ml and 10µg/ml PAN exposed for 48 hours.

The 0µg/ml DNA product had an additional two nucleotides which were not in the 10µg/ml product and were not in the published sequence (AY039651) however such a small difference should not account for the observed shift, suggesting the observed mobility shift was an artefact. However a consistent G – A change was identified between the sequences and the published rat sequence, which is shown in Appendix 2. This is probably a single nucleotide polymorphism (SNP) but can not account for the shift in mobility as it is observed in both the 0µg/ml and 10µg/ml sequences.

Nephrin amplification was also examined from two replicate experiments in duplicate but despite redesigning the primers and repeating the experiment nephrin expression remained inconsistent. Despite the

inconsistency no significant trend of reduced or increased gene expression was evident for nephrin following PAN treatment, (results not shown). From these results we conclude that nephrin gene expression in our model is not affected by PAN treatment. The podocalyxin transcription factor WT-1, also showed inconsistent PCR amplification. Figure 3.5 shows two gels which were representative of the varying results observed. Overall our results suggest that PAN does not cause a significant increase or decrease in WT-1 gene expression.

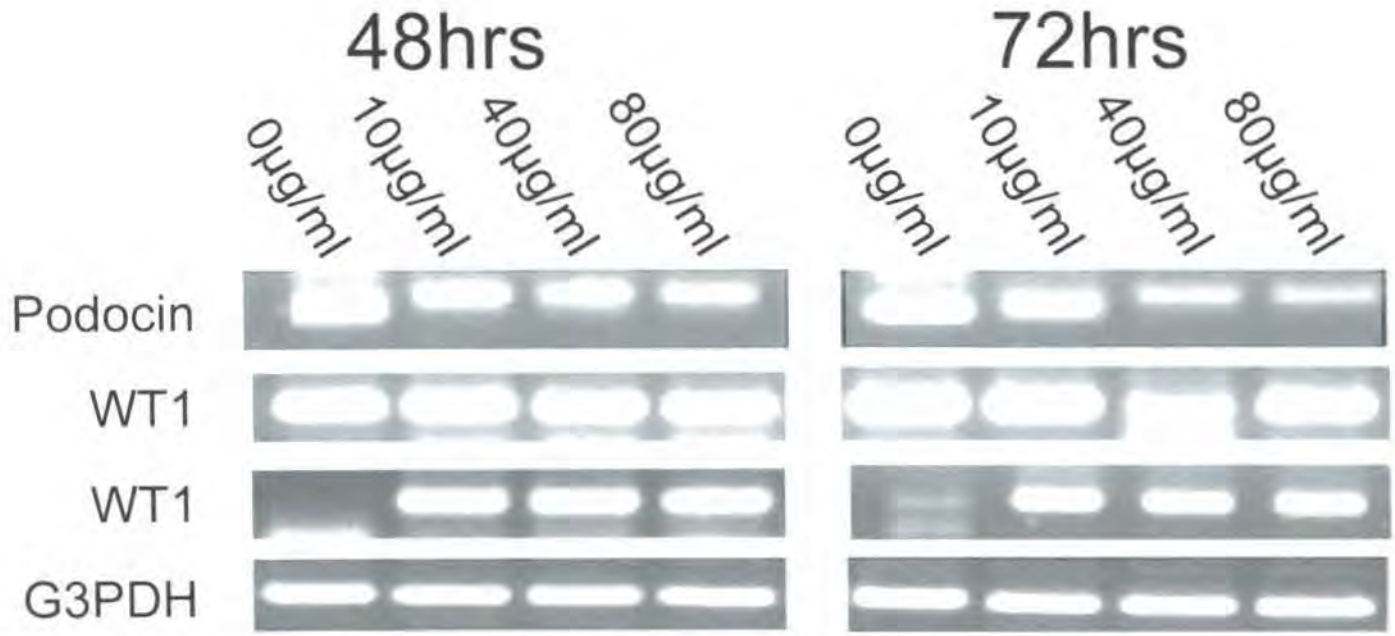

Figure 3. 5. Examining gene expression of podocin and WT-1 in NRK cells following PAN treatment. Podocin shows a mobility shift between control and PAN treated samples and a small reduction in expression following PAN treatment. WT-1 amplification was inconsistent but overall no significant changes in gene expression following PAN treatment were observed.

Figure 3. 6. Mobility shift in podocin DNA following PAN treatment after 48hrs. The change in size is highlighted by the two arrows, blue for PAN doses, green for control.

The fact that we are not seeing a reduction in expression of all the genes examined (Table 3.4) suggests that the doses of PAN we are using are not toxic and that the reduction in gene expression of podoplanin and podocalyxin are specifically as a result of PAN treatment.

Gene	Expression Changes
Podoplanin	Reduction of 65%
Podocalyxin	Dose-dependent Reduction
Podocin	Small Reduction
Nephrin	No change
WT-1	No change

Table 3. 4. The affect of PAN treatment on podocyte specific gene expression in NRK cells.

3.5. Examining Cell Viability following PAN treatment of NRK cells

As mentioned earlier it is critical that the PAN doses we use mimic nephrosis but do not promote apoptosis. At doses of 40µg/ml and 80µg/ml we observed reduced gene expression of known markers of PAN nephrosis however we are yet to confirm if this reduction is a specific effect of nephrosis. To confirm that the above doses are not toxic and the reduced expression is a result of nephrosis we examined the viability of the NRK cells after PAN treatment.

There are several methods of determining cell viability and cell death. DAPI staining was used to detect DNA damage and a trypan blue exclusion assay was used to determine cell viability levels. There was no DNA damage detected at the PAN doses tested using DAPI staining (Figure 3.7). However we did detect a decrease in cell number (see section 3.6).

There was no change in the trypan blue exclusion by adherent NRK cells at any of the PAN doses tested, and the cells were found to be >90% viable. Although there was a small reduction in the viability of detached cells at each PAN dose, this value was not statistically significant when analyzed using the t-Test (Figure 3.8). Overall the detached cells were >65% viable, while the detached cells from the mid and high PAN doses still had a viability level of >80%, this suggested that PAN at these doses is not toxic.

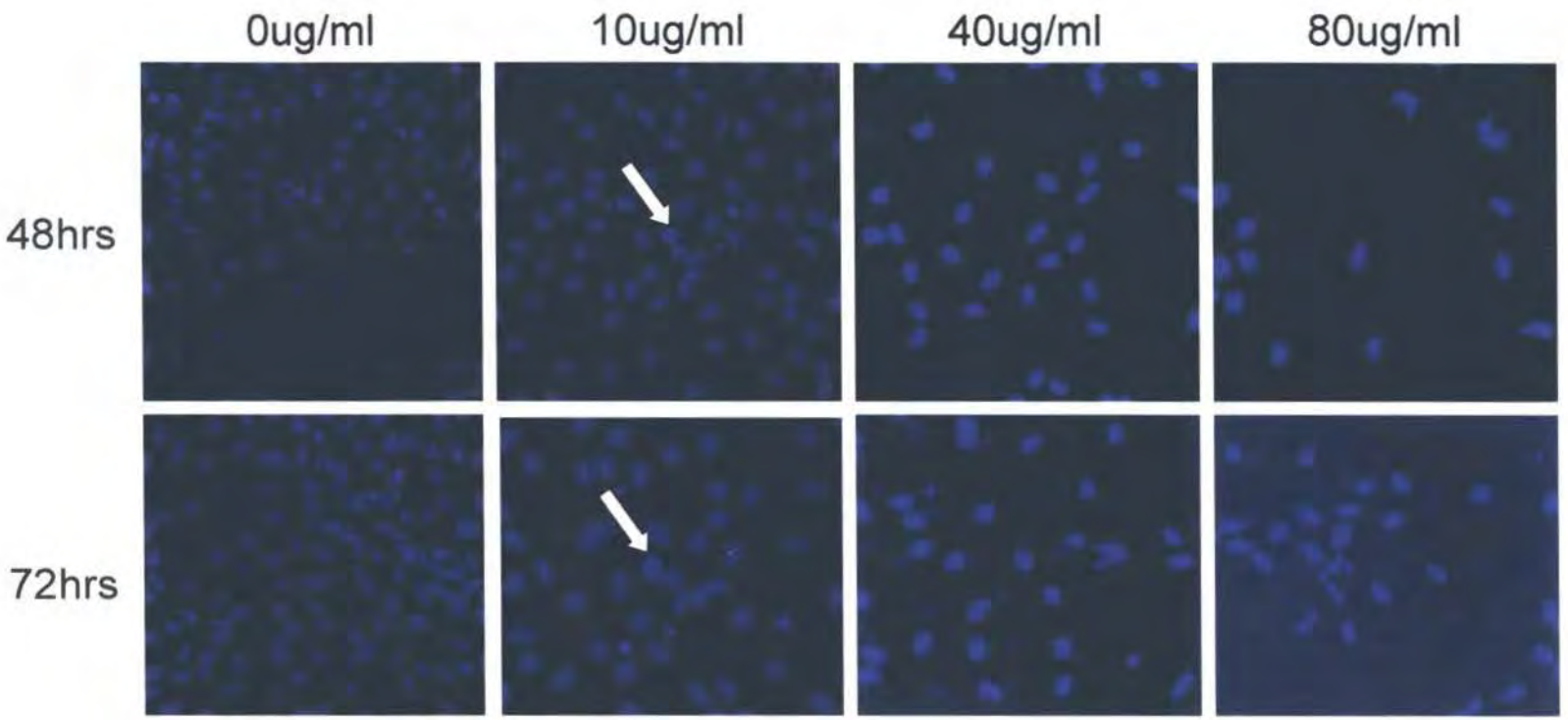

Figure 3. 7. Examining DNA damage by DAPI staining in NRK cells following PAN treatment.

The arrows highlight damaged nuclei.

3.6. Changes in Cell Number

Although the PAN doses were not causing cell death of the attached NRK cells, as shown by trypan blue uptake and DAPI staining, fewer cells were present at the higher PAN doses, (Figure 3.9).

The cells were found to be floating in the media and appeared to be healthy viable cells, suggesting that they were not adhering to the tissue culture plates as efficiently. Using trypan blue staining we performed a viable count upon these floating cells and found that they were indeed still viable (Figure 3.8).

We measured the total number of cells present both attached and detached at each PAN dose and used this total number of cells to calculate the cell proliferation rate, (Table 3.5). As expected a dose dependent decrease in the number of attached cells and a corresponding dose dependent increase in detached cells were observed in response to PAN treatment. PAN also caused a reduction in the cell proliferation rate. The low (10µg/ml) and mid (40µg/ml) PAN doses showed almost identical levels of reduction, 45% after exposure for 48 hours rising to 70% after 72 hours. The high (80µg/ml) PAN dose showed the least reduction in cell proliferation rate 38% and 47% after 48 and 72 hours respectively. The high PAN dose also showed the least reduction in cell proliferation as results to increased exposure to PAN. This suggests that at this dose the effects of PAN on NRK cells are occurring in the first 48 hours, whereas for the lower doses of 10µg/ml and 40µg/ml the effects are cumulative over a longer time course.

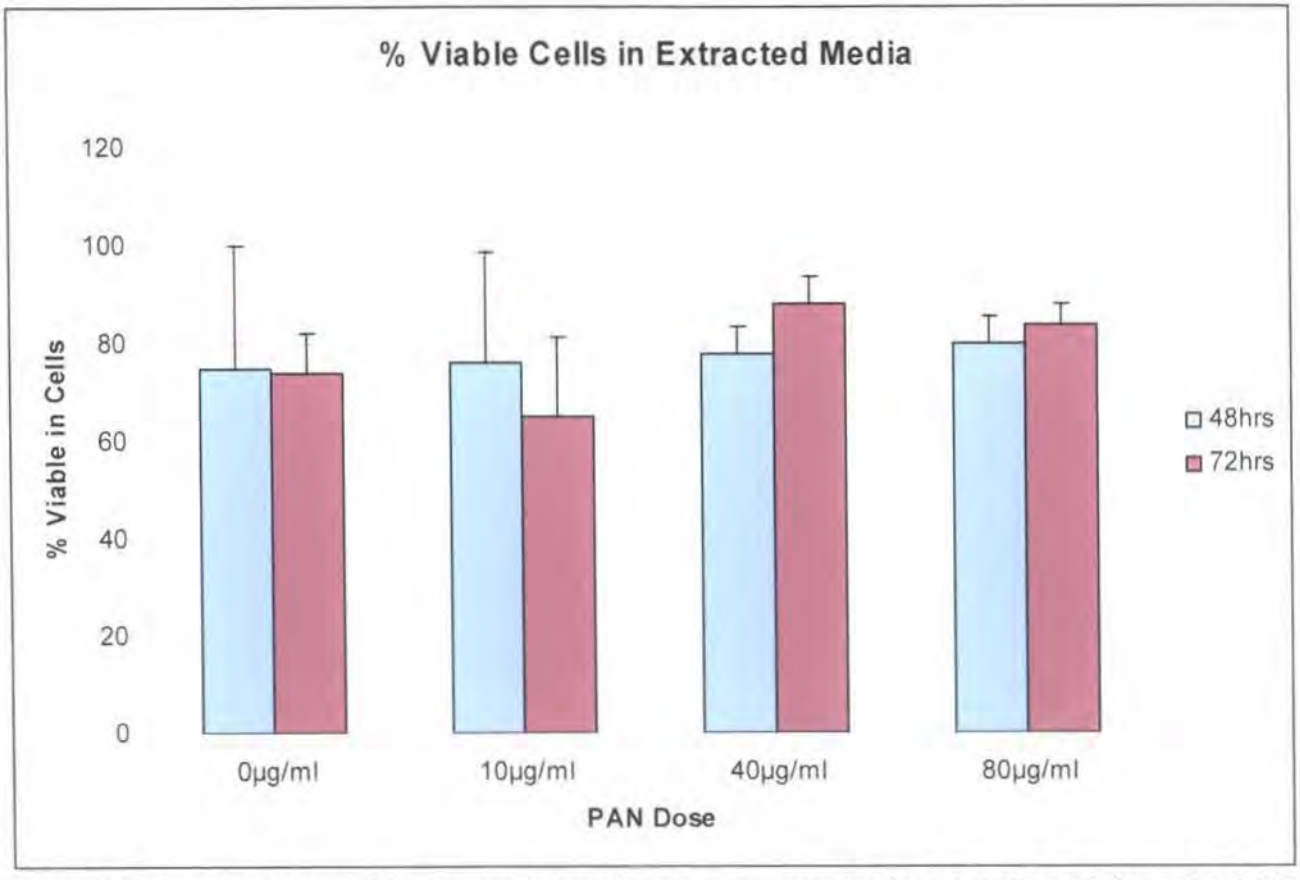

Figure 3. 8. PAN treatment results in non-significant changes in the viability of detached NRK cells.

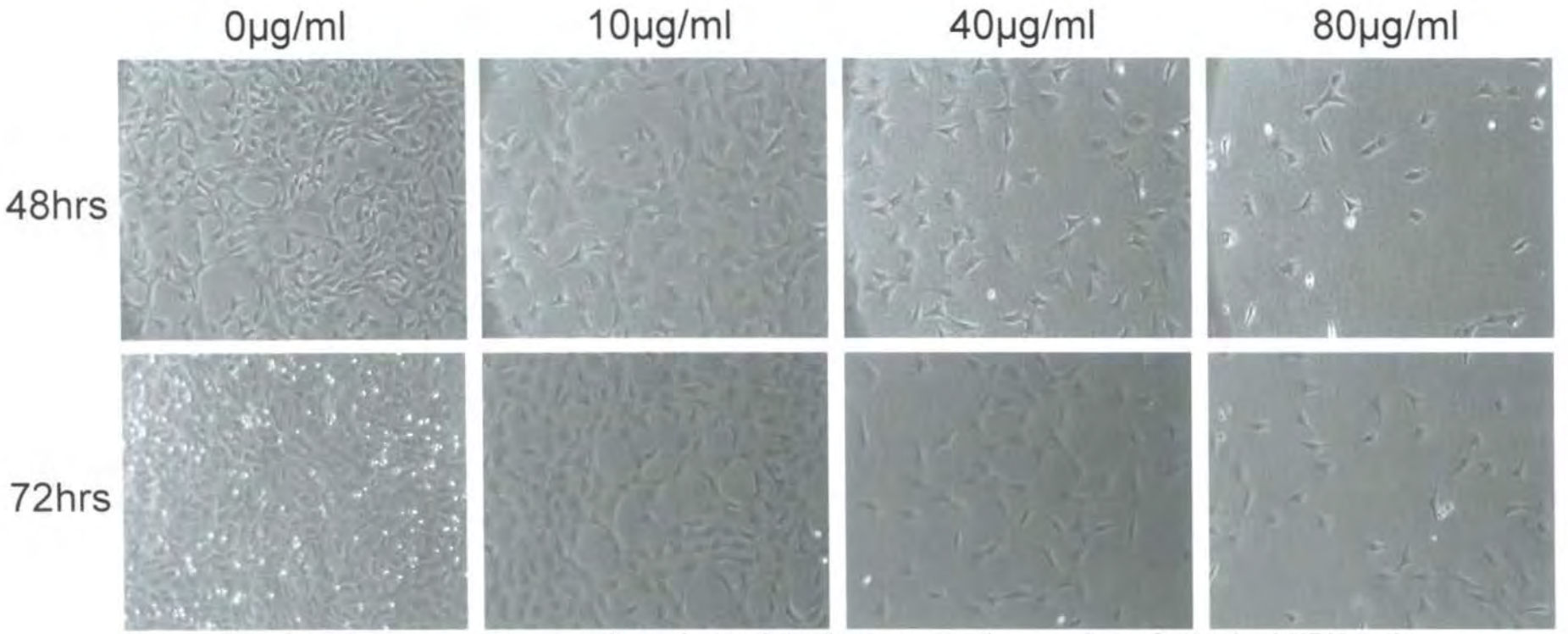

Figure 3. 9. PAN treatment causes a dose-dependent decrease in the number of attached NRK cells.

PAN dose	Attached Cells	Detached Cells	Total Cell Numbers	Cell Proliferation Rate cells/hr
0µg/ml 48hrs	168.34×10^4	26×10^4	194.34×10^4	3.27×10^4
10µg/ml 48hrs	88.69×10^4	39.5×10^4	128.19×10^4	1.89×10^4
40µg/ml 48hrs	57.94×10^4	88.75×10^4	146.69×10^4	2.27×10^4
80µg/ml 48hrs	45.38×10^4	115.75×10^4	161.13×10^4	2.58×10^4
10µg/ml 72hrs	77.78×10^4	44×10^4	121.78×10^4	1.17×10^4
40µg/ml 72hrs	49.13×10^4	58.5×10^4	107.63×10^4	0.97×10^4
80µg/ml 72hrs	28.56×10^4	166×10^4	194.56×10^4	2.18×10^4

Table 3. 5. Total cell numbers present and cell proliferation rates after PAN treatment.

3.7. Conclusions

A cellular model using NRK cells which mimics PAN nephrosis has been established. Using a range of PAN doses we show reduced gene expression of podoplanin and podocalyxin similar to that observed in the *in vivo* rat model of PAN nephrosis [GlaxoSmithKline unpublished] [18]. The changes in gene expression are specific and are not the result of toxicity as determined by the cell viability assay and the observed differential expression of the selected genes. This cellular model will allow us to further study the mechanisms of PAN nephrosis and to identify and characterize biomarkers which subsequently could be used clinically to determine the nephrotoxicity of compounds.

We found no changes in the viability of adherent NRK cells within our model at any of the PAN doses used. This is in agreement with the results published by Coers [183] who found cells were ≥ 95% viable, when treated with PAN doses of 10, 20 and 50 µg/ml for 48 hours and Fishman and Karnovsky [184] who found cells were ≥ 85% viable at PAN doses of 10, 20, 40 and 80µg/ml. Krishnamurti [181] found PAN doses of 0.5 and 5µg/ml for 24 or 48 hours resulted in viability levels of ≥ 97% however 50µg/ml caused a substantial reduction in cell viability and Sanwal [204] found that PAN caused dose dependent apoptosis at doses < 100µg/ml and necrosis at doses > 100µg/ml. However even though there is a dose-dependent reduction in cell viability as a result of PAN treatment, the cells are still 80% viable when treated with 50µg/ml PAN for 48 hours. The variations in levels of cell viability are probably the result of varying exposures of PAN treatment and the differing cell lines used. Sanwal also uses a different method to determine apoptosis, which may result in the lower cell viability observed.

Coers *et al.* [183] and Fishman and Karnovsky [184] both reported a dose and time dependent loss of adhesion, Krishnamurti *et al.* [181] only observed a change in adhesion at the highest dose of 5µg/ml. We observed a reduction in adherent cells in response to PAN treatment in a

dose-dependent fashion and the detached cells were still viable suggesting that PAN is causing a loss of adhesion in a dose and time dependent manner in our model, however this loss of adhesion is yet to be confirmed.

As in my model Fishman and Karnovsky [184] found that detached cells were still viable but would not reattach and grow. On the other hand Coers *et al.* [183] found that detached cells were only 15% viable after PAN treatment of 50µg/ml for 48 hours. Petermann *et al.* found that in both the Passive Heymann Nephritis (PHN) [205] and diabetic nephropathy [206] rat models of nephrosis, that podocytes collected from the urine could be cultured *ex vivo*, thus proving that the detached or shed podocytes remain viable. This has also been shown to be the case in human diseases including diabetic nephropathy [207] and glomerular inflammatory diseases [208]. It is proposed that podocyte excretion could be used as a marker to estimate severity of glomerular injury and a predictor of disease progression.

As previously mentioned the reduction of podoplanin and podocalyxin gene expression observed in my model supports the results obtained from the rat model of PAN nephrosis by GlaxoSmithKline. For podoplanin the decrease in expression of 65% shows a very similar level of reduction, ~70%, to that published by Breitender-Geleff in 1997 [18]. Podocalyxin gene expression has previously been reported to be increased following PAN treatment [181] which is in contrast to our findings and those of GlaxoSmithKline.

In PAN nephropathy of the rat podocin has been shown to shift to a redistributed granular staining pattern upon developing proteinuria and to have decreased protein expression which does not result from a corresponding decrease in mRNA levels [89]. Horinouchi *et al.* [90] found that podocin protein expression was reduced only in FSGS and remained unchanged in minimal change disease and IgA nephropathy. They also discovered a mutated form of the human podocin gene NPHS2, which

contained a 200bp deletion. Podocin has been shown to be downregulated at the protein level in acquired human diseases [209] and in the PAN nephrosis rat model [78] but to show an increase in mRNA expression. We did not examine podocin protein expression but did observe a small reduction in mRNA levels following PAN treatment. The shift in the podocin PCR product we observed appeared to be an artefact as the sequences of the PCR products were 99% similar.

Varying results have been reported regarding changes in nephrin gene and protein expression in human diseases and in experimental models. Nephrin gene expression was found to be reduced in several experimental proteinuric diseases including; passive Heymann nephritis (PHN) [74, 75], puromycin aminonuceloside nephrosis (PAN) [76-78] and experimental diabetic nephropathy [210]. However Aaltonen *et al.* [79] found that nephrin expression was increased in diabetic nephropathy at both the mRNA and protein level.

Nephrin protein expression has been reported to be reduced in minimal change nephropathy, FSGS, [80], [211], membranous nephropathy, [81], [212] and IgA nephropathy [75]. It has also been reported that nephrin expression is unchanged in minimal change nephropathy, FSGS and membranous nephropathy [82, 213]. We observed variable nephrin gene expression but conclude based on the results as a whole that nephrin expression was not significantly reduced by PAN treatment in our model.

WT-1, a transcription factor, which regulates podocalyxin expression in the kidney, showed no significant change in gene expression levels in response to PAN treatment. Although WT-1 has been associated with several human diseases, including WAGR syndrome, Denys-Drash syndrome and Frasier syndrome, it is believed that mutations in the WT-1 gene are responsible for these disorders rather than changes in levels of mRNA expression, [136, 141-143, 214].

Only Guo *et al.* [134] has shown reduced WT-1 expression to be the cause of crescentic glomerulonephritis or mesangial sclerosis. However Guo *et al.* also showed that podocalyxin and nephrin expression was reduced which may ultimately have been the cause of glomerulosclerosis observed.

The work in this chapter provides clear evidence that we have successfully established an *in vitro* cellular model which mimics PAN nephrosis. With this model we can further study the mechanisms of PAN nephrosis and the potential nephrotoxic biomarkers podoplanin and podocalyxin. Table 3.6 is a summary of our cellular model as compared to other *in vitro* models and the *in vivo* rat model of PAN nephrosis. Our model combines the key observations of previous *in vitro* models with that of the *in vivo* model, to give us a model which we can use to further characterize the mechanisms of PAN nephrosis.

In the following chapter we will investigate the apparent effect of PAN on the adhesive properties of the NRK cells in our model.

Characteristic	Our Cellular Model	Other *in vitro* models	GSK *in vivo* rat model
Cell Viability	Unaffected	Unaffected [183,184]	N/A
Cell Detachment	Yes	Yes [181,183,184]	N/A
Podocyte Ultrastructure Changes	N/A	FP flattening, Cell rounding, Membrane blebbing [182,183,184]	N/A
Reduced Podoplanin Gene Expression	Yes 65% reduction	Yes ~70% reduction [18]	Yes
Reduced Podocalyxin Gene Expression	Yes	Increased expression in 56/10 A1 cells [181]	Yes
Non-specific Gene Expression Changes	No	N/A	No

Table 3. 6. Comparison of *in vitro* and *in vivo* models of PAN Nephrosis.

Chapter 4.
PAN Induced Changes in Adhesive Properties of NRK Cells

4.1. Introduction

In establishing a cellular model which mimics PAN nephrosis we found that PAN treated NRK cells were detaching from the surface of the tissue culture plates and floating in the tissue culture media. When these cells were stained with trypan blue they were found to be viable, (section 3.5), suggesting that PAN causes a reduction in cell adhesion in cultured cells, as had previously been reported [183, 184].

Focal detachment of podocytes from the glomerular basement membrane is a prominent morphological feature of PAN-induced nephrosis in the rat model [215, 216], [217-219] and has also been observed in *in vitro* models of PAN nephrosis. Loss of cell adhesion has been shown to occur in cellular models of PAN nephrosis by Coers *et al.* [183], Fishman and Karnovsky [184] and to a lesser extent by Krishnamurti *et al.* [181]. It has also been shown that viable podocytes are shed into the urine of two experimental rat nephrotic models, the diabetic nephropathy model [205, 207] and the PHN induced rat model [206]. Podocytes shed into the urine can be cultured *in vitro* under normal culture conditions [205, 206].

Recently Vogelmann *et al.* [220] showed that podocytes were present in the urine of both healthy individuals and patients suffering from glomerular disease. They observed a difference in the excreted podocytes ability to be cultured *in vitro*. Cells from patients showed the same morphology and growth patterns as glomeruli isolated from whole kidney however cells from healthy subjects had significantly less growth capability and died much sooner. These results suggest that viable podocytes were shed into the urine in diseased states while the podocytes from healthy subjects are shed principally when they are senescent and thus results in their limited ability for replication in culture. These workers don't address the mechanisms by which viable podocytes are shed into the urine in diseased states but it does highlight that the shedding is a response to a sub-lethal damaging stimulus.

It has subsequently been identified that not just podocytes are shed from the glomeruli into the urine, but also podocyte related structures including podocalyxin-positive granular structures (PPGS) and the podocyte apical cell membranes [221].

4.1.1. Integrin

Integrin and dystroglycan complexes provide a critical role in linking podocytes to the glomerular basement membrane (GBM), (Figure 4.1). Both integrins and dystroglycans are coupled via adapter molecules to the podocyte cytoskeleton [222]. If podocytes become detached from the GBM and are shed, then it is highly probable that integrin and/or dystroglycan are involved in whatever changes occur, with experimental evidence indicating that integrins are the most likely molecules to be predominantly responsible.

There is genetic and experimental evidence [223-225], [226] that disruptions of the integrin – mediated podocyte matrix interaction are capable of inducing proteinuria [222]. Integrins have many roles in cells including modulating cell shape, polarity, growth, differentiation and motility but here we will only focus on the modulation of cell adhesion through homophilic and heterophilic interactions.

Ligand binding induces clustering of integrins to form focal adhesions and recruitment of intracellular cytoskeletal proteins. Within the focal adhesion, integrins are connected to the actin cytoskeleton by a number of adapter molecules including, paxillin, vinculin and talin [222]. Focal adhesions have been identified as points of cellular attachment to the underlying matrix [227].

α3β1 is the predominant integrin expressed by podocytes, but α6β1 is also expressed in much lower levels [125, 126]. α3β1 integrin is concentrated at the "sole" of the foot processes facing the GBM and is

thought to be largely responsible for foot processes attachment to the GBM [125] (see Figure 4.1).

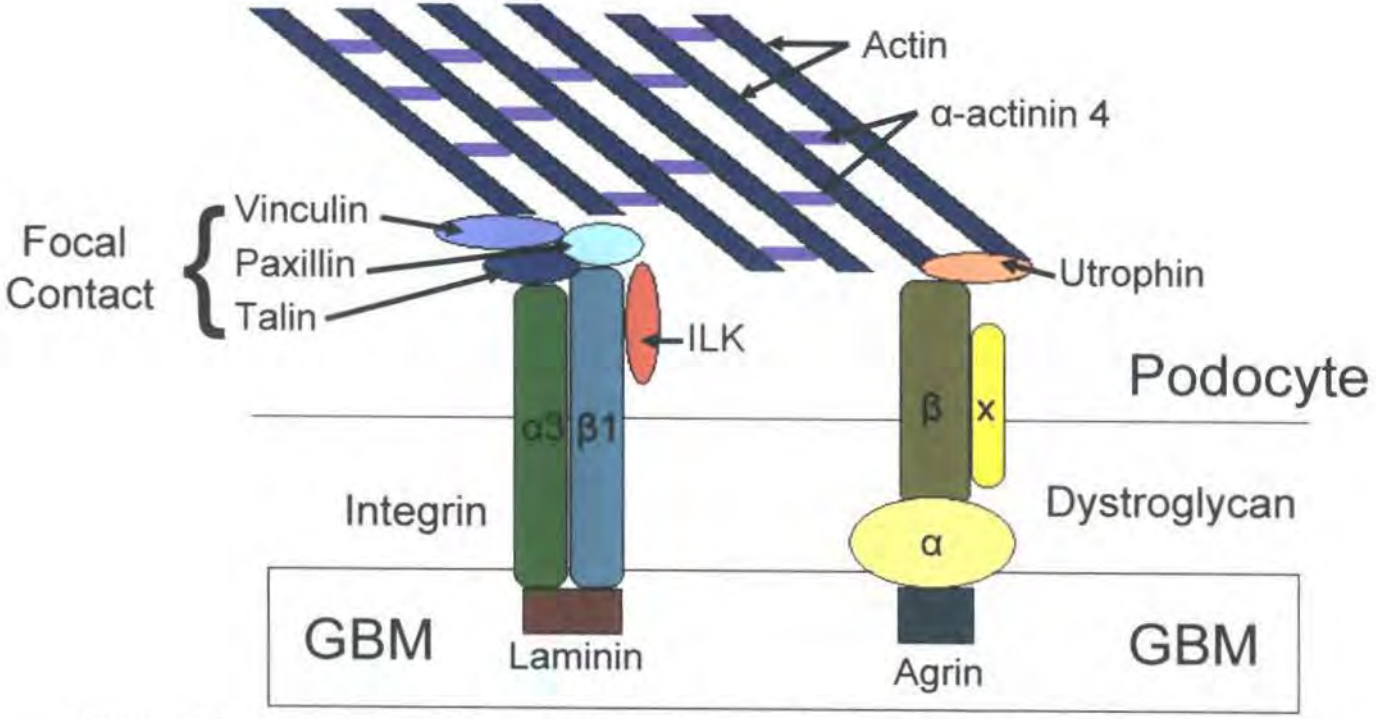

Figure 4.1. Schematic representation showing the podocyte – GBM interaction.
X undefined dystroglycan associated molecule. Adapted from Fig.2. Kretzler *et al.* [223]

α3 integrin deficient mice die the first day after birth with severe kidney and lung abnormalities, highlighting the crucial role of α3β1 integrin in the development of the kidney and lung [223, 228]. They also develop skin blisters as a result of severe disorganization of the epithelial basement membrane extracellular matrix [229]. Although α3 integrin deficient mice are unable to form mature foot processes, in one case of congenital nephrotic syndrome, a disease characterized by lack of foot processes, α3β1 integrin was found to be present in the patient's glomeruli. These results imply that α3β1 integrin maybe necessary but not sufficient for foot process formation. Unfortunately the lethality of the α3 integrin deficient mice precludes using this model for a long-term study on kidney disease [223].

Podocytes deficient in α3β1 integrin are unable to form mature foot processes instead cytoplasmic projections from the podocytes cell body are flattened against the GBM [223]. This is a phenotype more consistent with increased adhesiveness, which may indicate a role for α3β1 integrin in modulating other adhesion receptors, possibly including dystroglycan, so that if there is a defect in α3β1 integrin these other adhesion receptors mediate excess attachment to the GBM [125]. However there is no direct evidence of a relationship between integrin and dystroglycan in podocytes.

Research by Wang *et al.* [227] proved that integrins are required to form the sub-cortical cytoskeleton but integrins are not required to mediate cell-cell contacts. Primary cultures of α3β1 integrin deficient kidney collecting duct cells are indistinguishable from wild type cells, in that they both exhibit the regular cobblestoned appearance of epithelial cells, indicating that cell-cell contacts were unaffected. However cells failed to form the sub-cortical cytoskeleton and instead actin stress fibers were formed.

The concept of integrins as simple adhesion receptors is over simplified, instead integrins can be thought of as receptors that transduce signals on

contact with the extracellular matrix that elicit a specific response. That response could be adhesion, migration and in the case of podocytes foot process assembly, all these responses involve cytoskeletal rearrangement. There is an emerging understanding of how integrin – ECM interactions affect cytoskeletal assembly through the activation of Rho family GTPases [126].

It was initially proposed that integrin activity could be modulated, by phosphorylation, to change the adhesive properties of cells [224]. It was hypothesized by Krishnamurti *et al.* [181] "that the mechanism of PAN-induced detachment involves the inhibition of expression of α3β1 integrin". They found that integrin expression was reduced at both the mRNA and protein levels. As such we would expect to observe a similar pattern of reduced integrin expression in our model and for this reduction to be greatest at the highest PAN dose.

Several studies have examined integrin expression in a variety of diseases and have produced conflicting results regarding α3β1 integrin levels or distribution. Regele *et al.* [230] found no significant changes in β1 integrin expression levels in human minimal change nephrosis (MCN) or focal segmental glomerulosclerosis FSGS. Baraldi *et al.* [231] also detected no changes in MCN or membranous glomerulonephritis. However Shikata *et al.* [232] found a decrease in α3β1 integrin in MCN and Kemeny *et al.* [233] found reduced staining for α3 integrin in FSGS, however only one case was examined. Although Jin *et al.* [234] found there was an increase in integrin staining in human diabetic nephropathy, Chen *et al.* [235] showed a significant reduction in α3β1 integrin expression in both human and rat podocytes with diabetes mellitus and this reduction preceded any observed morphological changes. Regoli *et al.* [236] also found α3β1 integrin was expressed along the luminal membrane as well as the basal plasma membrane and this expression was reduced in diabetic rats.

Similar contradictory results were observed for integrin expression in the PAN nephrosis model. Krishnamurti *et al.* [181] found a dose dependent reduction in integrin expression at both the mRNA and protein levels in PAN induced nephrosis of 56/10 A1 cells at a PAN dose treatment of 0.5μg/ml and 5μg/ml for 48 hours. Smoyer *et al.* [122] found no statistically significant changes in either α3 integrin or β1 integrin protein expression except an increase in α3 integrin expression ten days after induced PAN nephrosis in male Sprague-Dawley rats. Conversely Kojima *et al.* [237] found decreased α3 integrin expression four days after PAN induced nephrosis in male Wistar rats but expression levels returned to normal at day ten, and Luimula *et al.* [78] found a two-fold increase in β1 integrin protein expression at day three and ten after PAN induction in female Sprague-Dawley rats but no corresponding change in mRNA levels. The contradictory results can possibly be explained by variations in each model. Not only were there variations in animal species and sex but also significant variations in the PAN doses. Smoyer *et al.* [122] used a high dose (150mg/kg body weight), Luimula *et al.* [78] a mid dose of (100mg/kg body weight) and Kojima *et al.* [237] a low dose of (50mg/kg body weight). This three-fold change in PAN concentration is likely to have an effect on the severity of nephrosis and hence a subsequent effect on any protein levels affected by PAN.

Integrin Linked Kinase (ILK)

ILK is an ankyrin-repeat containing serine/threonine protein kinase, encoded by a 1.8 kb transcript that is widely expressed in human tissues. ILK interacts with the cytoplasmic domains of β1, β2 and β3 integrin. ILK is involved in "inside-out" and "outside-in" integrin signalling [238].

ILK has been shown to be induced in congenital nephrotic syndrome of the Finnish type. Kretzler *et al.* [239] identified ILK as a candidate signalling molecule linking podocyte function to cell – cell and cell – matrix interaction and if disturbed can lead to proteinuria. The identification of ILK as a potential mediator of glomerular disease has highlighted a novel focus for future drug discovery targets.

4.1.2. Laminin

Laminins are a growing family of heterotrimeric proteins, consisting of one α, one β and one γ chain arranged in a cruciform structure. Fifteen different laminin isoforms have so far been identified, laminin-1 to laminin-15, based on the assembly of the five α, three β and three γ chains. Laminins are mainly localized in basement membranes and have a range of functions, including cell growth and migration, cell adhesion and cell differentiation.

Most laminin chains have been identified in the kidney by immunohistochemical methods, but few laminin heterotrimers have been isolated. It is possible to predict which laminin trimer is present in a given tissue by immunohistochemically colocalizing α, β and γ chains, but this is not proof that the chains assemble into the predicted trimer.

Based on these predictions the following laminin trimers have been "identified" in the kidney. Laminin-1 has been found in proximal tubular basement membranes (TBMs) in the cortex and in the loops of Henle basement membranes in the medulla [240, 241]. Laminin-2 is found in a subset of TBMs at low levels and in the mesangial matrix in mice and humans [241, 242]. In rats laminin-4 is found in the mesangial matrix not laminin-2 [241-244]. Laminin-10 is probably the most abundant trimer in the mature kidney. It is located in all tubular and collecting duct basement membranes [241, 242]. Laminin-11 is only found in GBM and arteriolar basement membranes and is the only trimer which has been shown to be important for correct renal function [245]. Due to its localization at the GBM and its role in maintaining renal function, we will be focussing on Laminin-11. However the existence of laminin-11 in the GBM has been questioned based on *in situ* hybridization studies which showed that α5 and β2 RNAs were not detected within the same cells and so could not form the α5β2γ1 trimer [246]. It is also important to note that only α5, β2 and γ1 chains have been detected in the GBM [240, 242-244, 247, 248] and so based on current knowledge only laminin-11 is possible to be

formed in the GBM. This issue could be resolved by either identifying other laminin chains present at the GBM, therefore giving more possible trimers or by isolating laminin-11 from the glomeruli [249].

Laminin-11 was first identified in rat lung extract [242], but clarification of the specificity of the 4C7 antibody has now identified the heterotrimer originally thought to be laminin-3 [250] from human placenta as now being laminin-11. To examine the function of laminin-11 knockout mice lacking either the β2 or α5 chain have been developed. Mice lacking the β2 chain develop severe morphological and physiological defects at the neuromuscular junction and altered filtration properties of the renal glomerular basement membrane [251], [245]. However with a multi-subunit protein complex it is difficult to assign function. It is not known if the neuromuscular and glomerular filtration defects are the result of the absence of laminin-11 or the absence of the β2 chain. Similarly compensation occurs where β1 substitutes for the missing β2 chain to form a morphologically normal basement membrane [252], [245].

4.1.3. Dystroglycan

Another class of adhesion proteins, the α- and β- dystroglycans have also been localized to the "soles" of podocyte foot processes [230, 253, 254]. It appears that podocytes adhere to the GBM via a dystroglycan complex, consisting of α-dystroglycan, β-dystroglycan, agrin and utrophin, (Figure 4.1).

Dystroglycan consists of two polypeptide chains, which are synthesized as a single precursor and prost-translationally cleaved to form the 43 kDa transmembrane β subunit and the 156 kDa extracellular α subunit. The α subunit has several O-linked sialomucin-like side chains that provide binding sites for laminin G subunits, which are also present in the GBM proteoglycans agrin and perlecan. The α subunit is non-covalently bound to the ectodomain of the β subunit. In the glomerulus β-dystroglycan

binds to the dystrophin homologue utrophin, which directly interacts with actin [230, 255].

Dystroglycan has shown reduced expression in human minimal change nephrosis (MCN) but not in focal segmental glomerulosclerosis (FSGS), two podocyte diseases characterized by extensive foot process effacement and proteinuria. Both Regele *et al.* in 2000 [230] and Kojima and Kerjaschki [254] in 2002 reported that α-dystroglycan protein expression was reduced to 25% and β-dystroglycan to 50% of controls in MCN only. Dystroglycan expression and the reformation of foot processes could be returned to normal with steroid treatment, thus it maybe that dystroglycan levels control foot process formation. The fact that the changes in dystroglycan only occur in MCN suggests that MCN and FSGS have different pathogenic mechanisms of podocyte attachment and foot process deformation.

The expression of the dystroglycan complex is negatively correlated with disease activity in proteinuria in animal models [253] and patients with minimal change disease [230].

In this chapter several techniques are used to analyse the adhesive properties of NRK cells and if these properties are affected by PAN treatment. A cell aggregation assay was developed and used to examine the adhesive properties of NRK cells following PAN treatment. We have also examined if detached cells can be re-cultured *in vitro* and we have determined the expression of two cell adhesion markers α3 integrin and laminin β2 in our cellular model of PAN nephrosis.

4.2. Establishing a Cell Aggregation Assay

As was previously reported during the establishment of our cellular model (see section 3.2), PAN appeared to have a significant effect upon cell adhesion, causing cells to loose the ability to adhere to the tissue culture plastic, this effect was greatest at the highest doses of PAN treatment causing almost three quarters of the cells to become detached.

We developed a cell aggregation assay based on the classic cell-aggregation assay first described by Takeichi [201] and subsequently developed by Takeda *et al.* [42] (section 2.1.6) to examine any changes in cell adhesion as a result of PAN treatment.

Cadherins comprise a large subfamily of Ca^{2+} -dependent glycoproteins that mediate cell-cell adhesion through homophilic interactions. Cadherins can be classified into four main subfamilies; classical cadherins, desmosomal cadherins, protocadherins and cadherin-like proteins [256]. The classical cadherin subfamily consist of the well characterized cadherins; E-cadherin (epithelial cadherin), P-cadherin (placental cadherin) and N-cadherin (neural cadherin). Classical cadherins are found in adherens junctions and typically consist of a highly conserved carboxy-terminal cytodomain, a single transmembrane domain and five extracellular cadherin-motif subdomains, C1-C5. The C1 domain contains a highly conserved tripeptide sequence His-Ala-Val essential for cell-cell adhesion [257, 258].

The cadherins are important for establishing and maintaining intercellular connections. Generally cells with fewer cadherin molecules are less adhesive. As long as cadherins are functioning, inactivation of other adhesion molecules has little effect on cell-cell adhesion, cadherins are therefore the cell-cell adhesion receptors that are most important for the formation of cell-cell associations [259].

Before we were able to develop the cell aggregation assay to meet our needs we needed to determine what was the best way to remove the cells from the tissue culture flasks without damaging the adhesive properties. We tested various concentrations of EGTA, 0.5, 1, 2.5, 5 and 10mM, but we found more cells were damaged using EGTA than our standard protocol of Trypsin/EDTA.

It was found that 2.5 x 10^5 was insufficient to observe significant cell numbers to determine the effects of PAN treatment on cell aggregation. 5 x 10^5 did give significant numbers to perform the assay however after the mid (40µg/ml) and high (80µg/ml) dose treatments of PAN the cell numbers were too low to perform the assay in enough replicates to perform accurate statistical analysis. Therefore a compromise of 3.5 x 10^5 cells was used, this number provided enough cells to observe significant cell numbers but also allowed us to perform the assay in six replicates for statistical analysis.

Next was determining the length of time needed for the cells to aggregate, Takeda *et al.* [42] observed significant aggregation after 1 hour with the results increasing up to 3 hours. Initially, 3.0 x 10^5 cells were incubated for 1, 3 and 6 hours. Results are shown in Table 4.1.

	Incubation Time		
PAN Treatment	**1 hr**	**3 hrs**	**6 hrs**
0µg/ml 48hrs	78%	68%	100%
10µg/ml 48hrs	21%	51%	47%
40µg/ml 48hrs	21%	15%	0%
80µg/ml 48hrs	4%	6%	0%

Table 4. 1. Percentage cell aggregation observed after varying incubation times.

Based on these results, it was determined that an incubation time of three hours was the most suitable.

The speed of rotation during incubation was also tested. 80 rpm was too slow, the cells aggregated together too much and formed large clumps of cells and it was very difficult to gain an accurate count of cells and a true representation of the effects of PAN treatment on the adhesive properties of NRK cells. Similarly above 120 rpm was too fast and cells were not able to aggregate. 100 rpm gave a balance between the two, with both single cells and aggregates and thereby giving a true representation of the effects of PAN treatment on the adhesive properties of NRK cells.

4.3. Changes in cell adhesion properties of NRK cells after PAN nephrosis

We developed a cell aggregation assay (sections 2.1.6 and 4.2) to examine the extent of reduction in cell adhesion and if this reduction was indeed related to the level of PAN.

Briefly at each time point PAN-treated NRK cells were detached by trypsin/EDTA treatment and resuspended in Hank's Balanced Salt Solution (HBSS) + 1% BSA. Cells were separated into single cells by passing through a 19 gauge syringe. 35 X 10^4 cells in a total volume of 1ml were incubated in 12 well plates coated with HBSS + 2% BSA. The cells were allowed to aggregate for 180 minutes in the presence of 1 mM $CaCl_2$ on a rotating shaker (100rpm) at 37°C. Aggregation was quantified by counting six replicates in duplicate of each sample. An aggregate was deemed to be a group of cells greater than three. The percentage cell aggregation was estimated by:

(No. of aggregates ≥3 cells / total no. of cells) X 100

A paired t-Test was used to analyze PAN treated groups against the control group to determine statistical significance (defined as $p < 0.05$ *, $p < 0.01$**, $p < 0.001$ ***).

As expected PAN caused a reduction in the number of cells which aggregated, implying that PAN did result in a reduction in the adhesive properties of NRK cells. This reduction was found to be a dose dependent decrease in cell aggregation (Figure 4.2 and Table 4.2). The reduction in cell aggregation was found to be significant for all doses at a given time point, when analysed using the independent t-Test (Figure 4.2 and Table 4.3).

PAN Treatment	% Cell Aggregation
0µg/ml 48hrs	40.78 ± 15.27
10µg/ml 48hrs	25.41 ± 11.49
40µg/ml 48hrs	24.45 ± 8.74
80µg/ml 48hrs	16.87± 13.42
0µg/ml 72hrs	55.85 ± 14.91
10µg/ml 72hrs	31.45 ± 12.30
40µg/ml 72hrs	30.57 ± 10.38
80µg/ml 72hrs	11.77 ± 8.46

Table 4. 2. PAN treatment results in a decrease in cell aggregation in NRK cells. Data is mean (n = 12) ± SD.

PAN Treatment Comparison		p-value
48hrs	0µg vs 10µg	**0.001** ***
	0µg vs 40µg	**0.001** ***
	0µg vs 80µg	**0.001** ***
72hrs	0µg vs 10µg	**0.001** ***
	0µg vs 40µg	**0.001** ***
	0µg vs 80µg	**0.001** ***
	0µg vs 0µg	**0.01** **
	10µg vs 10µg	0.25
	40µg vs 40µg	**0.05** *
	80µg vs 80µg	Not

Table 4. 3. Statistical significance of cell aggregation assay data. Significant values (* $p < 0.05$, ** $p < 0.01$, *** $p < 0.001$) are highlighted in bold.

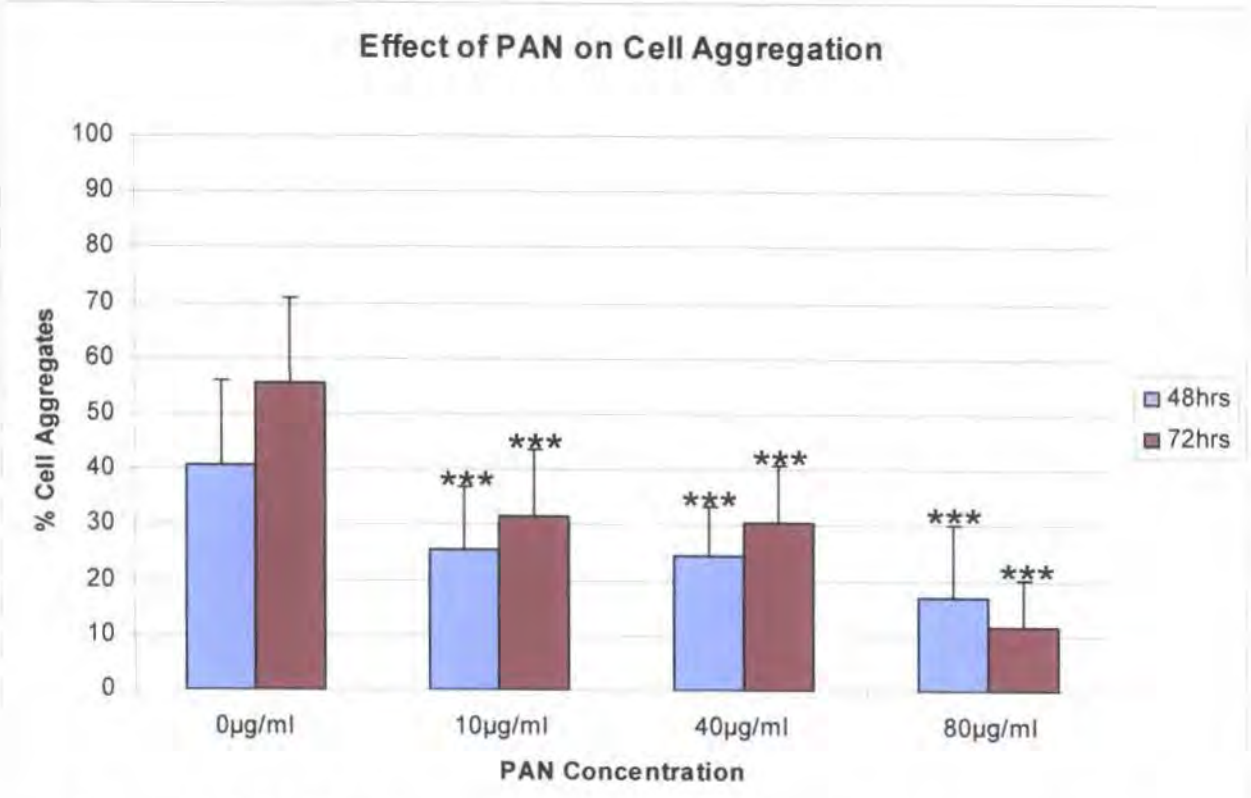

Figure 4. 2. PAN causes a dose dependent decrease in cell aggregation. PAN causes a significant (*** $p < 0.001$ versus control) decrease in cell aggregation at every dose tested.

4.4. Can PAN treated detached NRK cells be recultured *in vitro*?

As previously reported we found that PAN treatment caused a reduction in NRK cells ability to adhere both to each other and to the tissue culture plastic. We found that cells which detached from the surface of the tissue culture plates were still viable when examined by trypan blue exclusion (section 3.5).Therefore we developed a method of testing if these viable cells could recover and reattach to the tissue culture plastic. Briefly detached NRK cells were collected and resuspended in 0.5 ml of media. Equal cell numbers (7.5×10^4 cells/ml) at each PAN dose was added to duplicate non-coated and rat collagen coated 12 well plates and cultured as normal. The cells were examined every 24 hours to see if cells were able to reattach to the tissue culture plates and proliferate as normal. We included cells which had not detached as a positive control to further aid comparisons between control and PAN treated cells.

We found that the cells at the PAN doses of 0µg/ml and 10µg/ml treated for 48 hours reattached to the collagen coated plates and grew as a cluster of cells (Figure 4.3a and b), while very few of the cells reattached at 40µg/ml and 80µg/ml and those which did, appeared to attach and grow as a normal monolayer but displayed a very slow rate of proliferation (Figure 4.3c and d).

We found that no cells reattached after exposure to PAN for 72 hours. We initially thought this was the result of more severe disruption to the cells adhesive properties from greater exposure to PAN but control non-treated cells also did not attach indicating the loss of ability to adhere was not the result of PAN treatment. A possible cause was the higher PAN doses resulted in a lower number of viable cells and maybe the number of cells was too low, to observe a result. However this would not account for why the control cells did not reattach.

There was no difference in cell attachment between coated and non-coated plates, cells attached and formed a monolayer on both, however cells appeared to proliferate faster on non-coated plates after PAN treatment of 10µg/ml and 40µg/ml (Figure 4.4).

We also tested the growth characteristics of control cells, which hadn't been subjected to PAN treatment and which had not detached. These cells formed a confluent monolayer on both collagen coated and non-coated plates (Figure 4.5). On the collagen coated plates the NRK cells formed a confluent monolayer and then started to form a second layer of cells on top of the original layer.

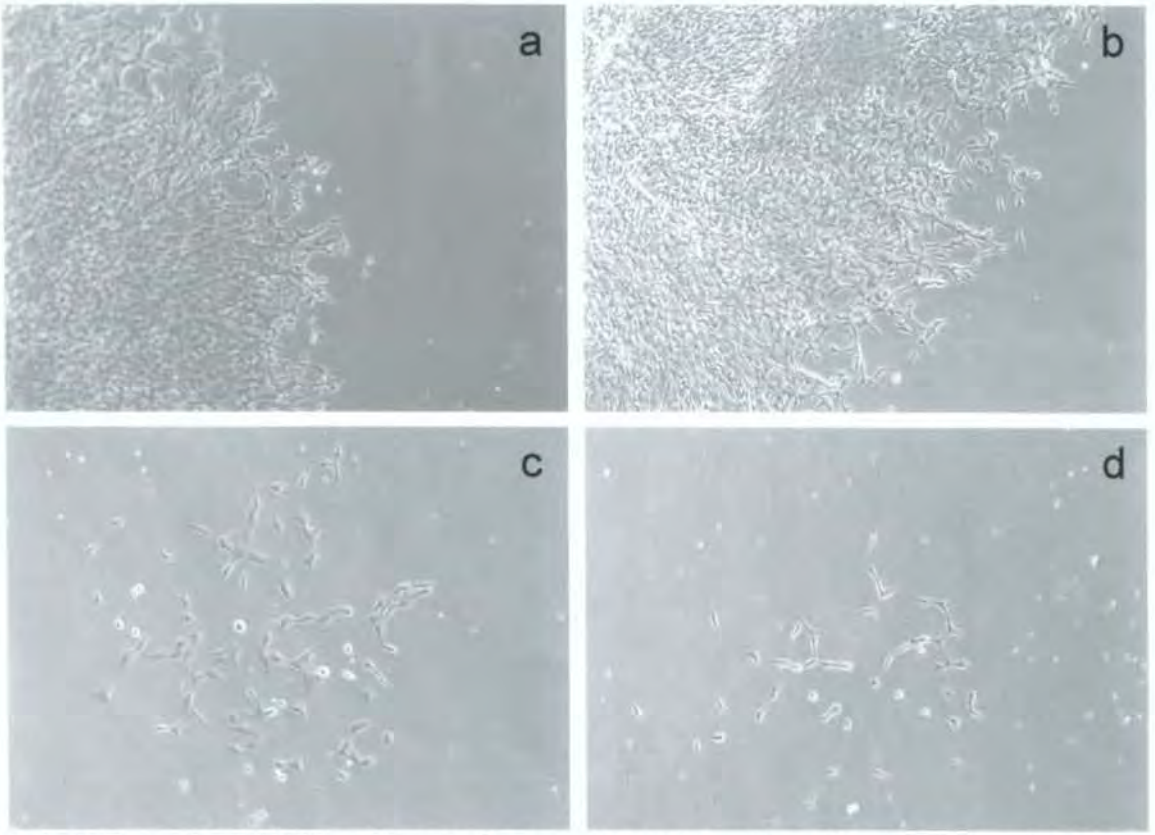

Figure 4. 3. Detached NRK cells can be recultured *in vitro* after PAN treatment.
Phase contrast image (x20) of NRK cells after 48hrs a) 0µgml b) 10µg/ml c) 40µg/ml d) 80µg/ml.

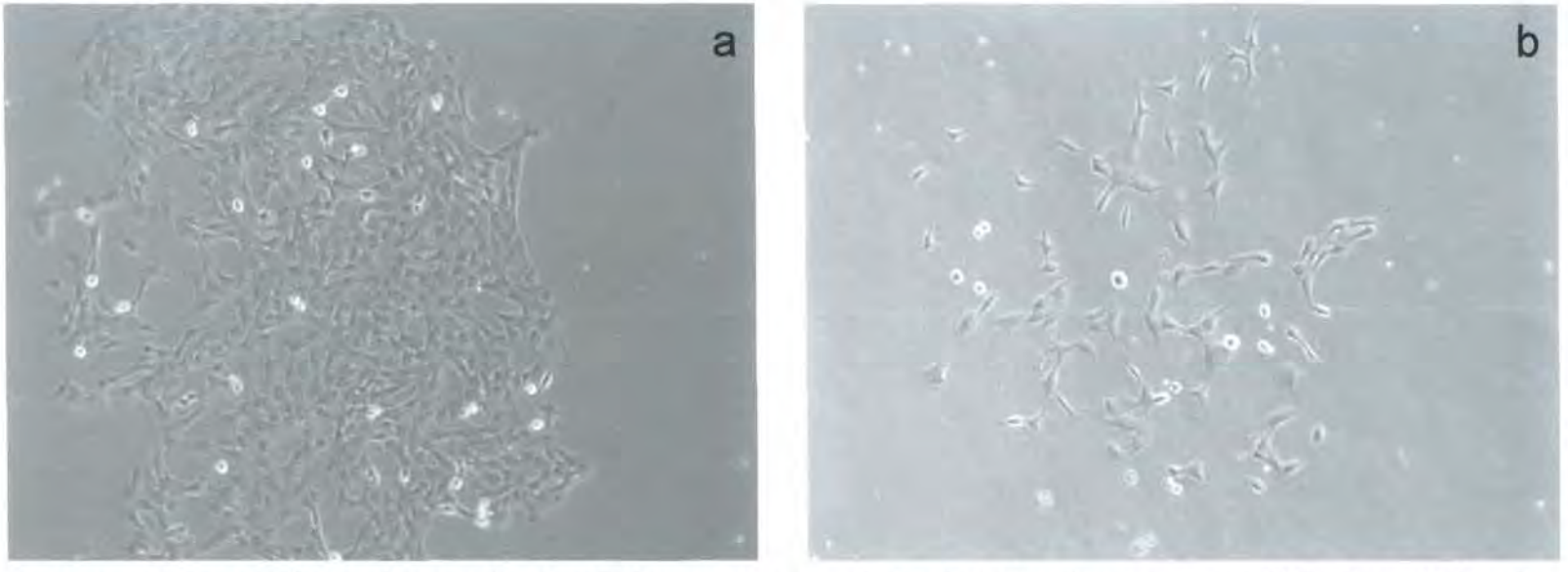

Figure 4. 4. Comparison of NRK cell growth after 72hrs on non-coated (a) and collagen coated (b) plates following 40µg/ml PAN treatment.

Phase contrast image of NRK cells (x20) replated onto coated and non-coated collagen plates after exposure to 40µg/ml PAN treatment for 48hrs. Cells formed a monolayer on each plate, but the cells appeared to attach and replicate faster on the non-coated plate.

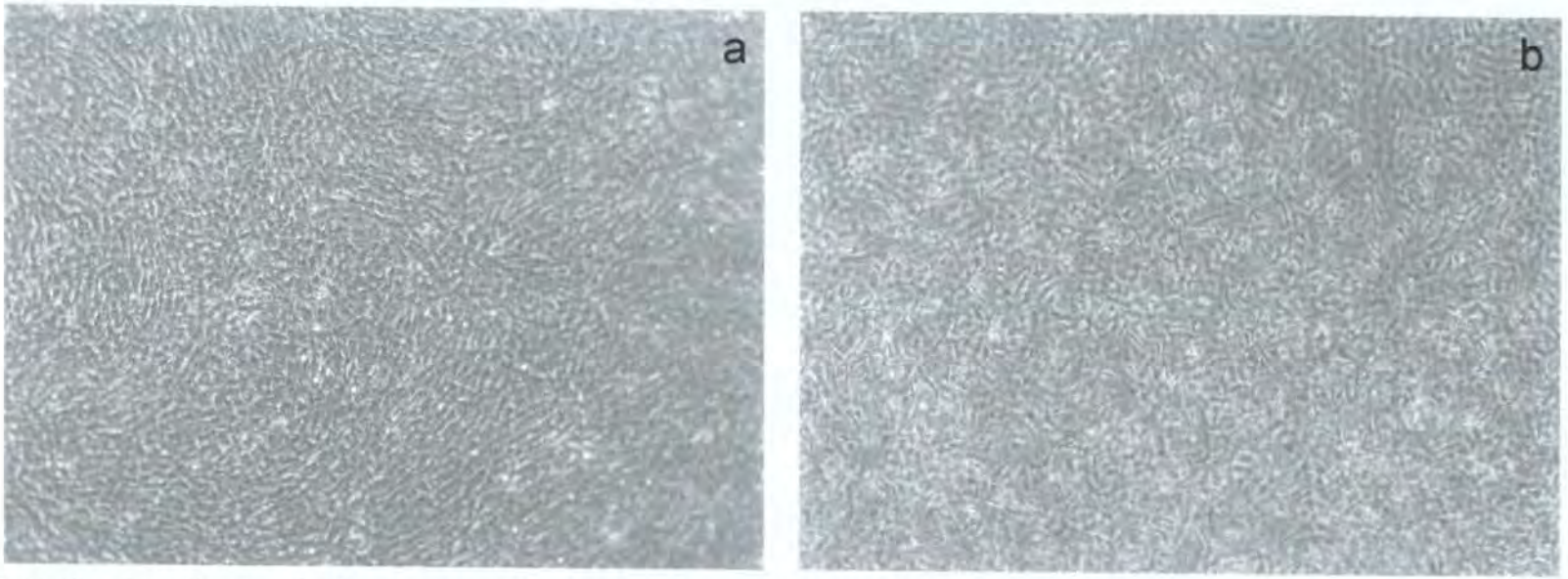

Figure 4. 5. Control NRK cells form a confluent monolayer on both (a) non-coated and (b) collagen coated plates. Phase contrast image of NRK (x20) cells after 48 hours. The cells appeared to be proliferating faster on the collagen coated plates.

4.5. Changes in Protein Expression of α3 Integrin

Since the cell aggregation assay showed that PAN was causing a dose dependent decrease on the cell adhesive properties of NRK cells, we examined the adhesive properties further by determining the protein expression of α3 integrin. It is believed that disruption to the cytoskeleton in nephrotic syndromes can be caused by a disruption or loss of integrin expression [126, 181, 223, 235, 236]. Therefore we hypothesize that PAN treated cells would show a dose dependent decrease in integrin protein expression.

We found a reduction in α3 integrin protein expression by Western blotting at the mid (40μg/ml) and high (80μg/ml) PAN doses, (Figure 4.6). At 48 hours no integrin protein was detected at the mid and high doses, but at 72 hours there were very low levels of integrin protein expression at the mid and high doses of PAN. It is possible that PAN causes an initial decrease in expression which is followed by a period of recovery which results in increased expression. Kojima *et al.* [237] found decreased α3 integrin expression four days after PAN induced nephrosis in male Wistar rats but expression levels returned to normal at day ten, supporting our finding of an initial decrease in expression followed by a subsequent return to normal levels. Similarly Smoyer *et al.* [122] found no statistically significant changes in α3 integrin protein expression except an increase in α3 integrin expression ten days after induced PAN nephrosis in male Sprague-Dawley rats. However Krishnamurti *et al.* [181] found a dose dependent reduction in integrin expression at both the mRNA and protein levels in PAN induced nephrosis of 56/10 A1, an immortalized human glomerular visceral epithelial cell line, at a PAN dose treatment of 0.5μg/ml and 5μg/ml for 48 hours. However only one time point was examined and so any subsequent increase in expression would not have been observed.

Alternatively the contradictory results can possibly be explained by variations in each model. Smoyer [122] and Kojima [237] used a rat model of PAN induced nephrosis while Krishnamurti [181] used 56/10 A1, an immortalized human glomerular visceral epithelial cell line. There were also variations between the two rat models in rat species and PAN doses.

We found no changes in α3 integrin distribution in NRK cells by immunofluorescence microscopy (Figure 4.7). α3 integrin localized diffusely within the NRK cells with slightly increased perinuclear staining at the mid (40μg/ml) and high (80μg/ml) PAN doses, but this was more likely to be the result of a change in cell shape and size as oppose to a genuine increase in expression. There was an increase in α3 integrin expression at 80μg/ml 48hr PAN treatment at the edge of the cell where the cell was detaching from the coverslip. Krishnamurti *et al.* [181] observed no changes in integrin expression by FACS analysis at a PAN dose of 0.5μg/ml for 48 hours but 5μg/ml for 48 hours resulted in a significant reduction in cell-surface expression and overall cell expression of α3 and β1 integrin in 56/10 A1 cells, an immortalized human glomerular visceral epithelial cell line, as detected by FACS analysis and quantitative Western blotting.

The variations we observed between our Western blot data and immunofluorescence data maybe explained by variations in antibody specificity. The antibody we used for immunofluorescence is raised against the extracellular domain of integrin α3 and is specific for rat. While the antibody used for Western blotting is designed against a region towards the N-terminus of mouse VLA-3α (very late antigen) and cross reacts with mouse, rat and dog.

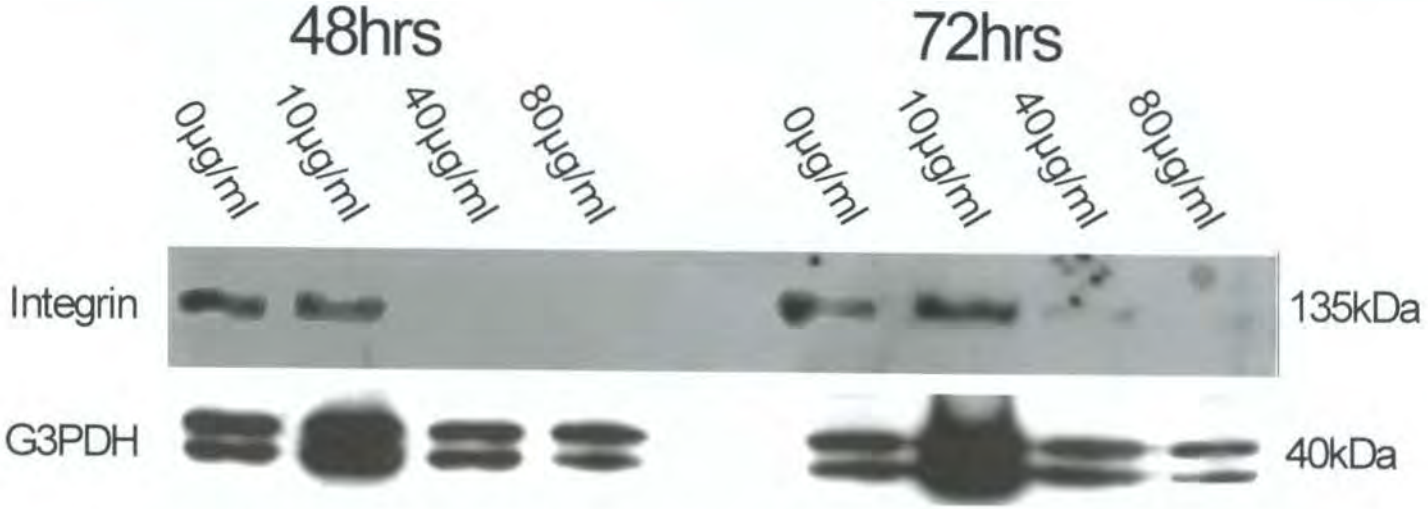

Figure 4. 6. Integrin expression is reduced in NRK cells following PAN treatment.

Figure 4.7. Integrin localization in NRK cells is not affected by PAN treatment.
NRK cells (p4) were cultured for 48hrs in D-MEM + 10% FBS. After 48hrs the medium was replaced with medium containing PAN. The cells were fixed/permeabilized and stained with Ralph3.1 mAb to localize α3 integrin. The cells were then imaged by confocal microscopy at 519nm. Images are merged composite images of layered sections throughout the cell, magnification x200. All microscope and laser settings have been kept constant to allow an accurate comparison of staining intensity. Scale bar 10μm.

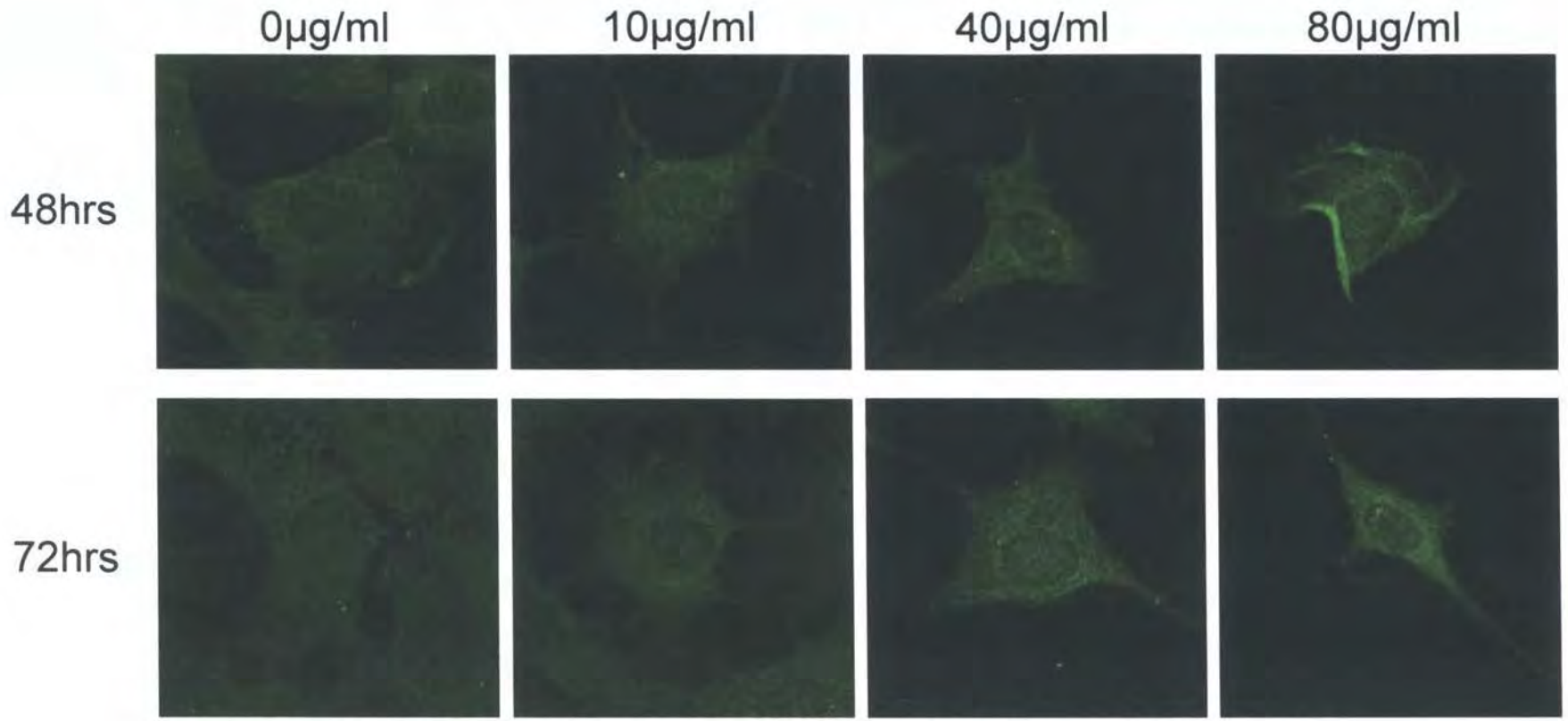

Figure 4. 7. Integrin localization in NRK cells is not affected by PAN treatment.

4.6. Changes in Cell Localization of Laminin β2

We next examined the expression and distribution of laminin β2, another protein involved in cell adhesion, and the effects of PAN treatment in permeabilized NRK cells. We used an antibody raised to the IV domain, the collagen binding domain, of laminin β2. The antibody was specific for human and rat laminin β2 and supplied by BD Biosciences, full experimental and antibody details are provided in section 2.5.

Laminin β2 localization was disrupted and protein expression levels were reduced. Laminin showed a predominantly perinuclear staining pattern in control cells. PAN treatment also resulted in the formation of laminin deposits at the cell periphery, (Figures 4.8 and 4.9). As reported earlier, (section 3.6), PAN treatment results in a loss in cell numbers. Control cells were most confluent and 80μg/ml were the least confluent, the formation of laminin deposits and the change in laminin expression, are not the result of changes in cell density as the deposits are formed after 10μg/ml 48 hours PAN treatment when the cells are almost as confluent as control cells. It is more likely that the changed laminin expression is the result of altered cell morphology.

We were unsuccessful in our attempts to quantify the levels of laminin protein expression by Western blotting. Initially we tried a rat specific monoclonal laminin β2 antibody supplied by The Hybridoma Collection. After numerous experiments proved unsuccessful we tested a second monoclonal laminin β2 antibody supplied by BD Biosciences. Again we were unsuccessful in our attempts.

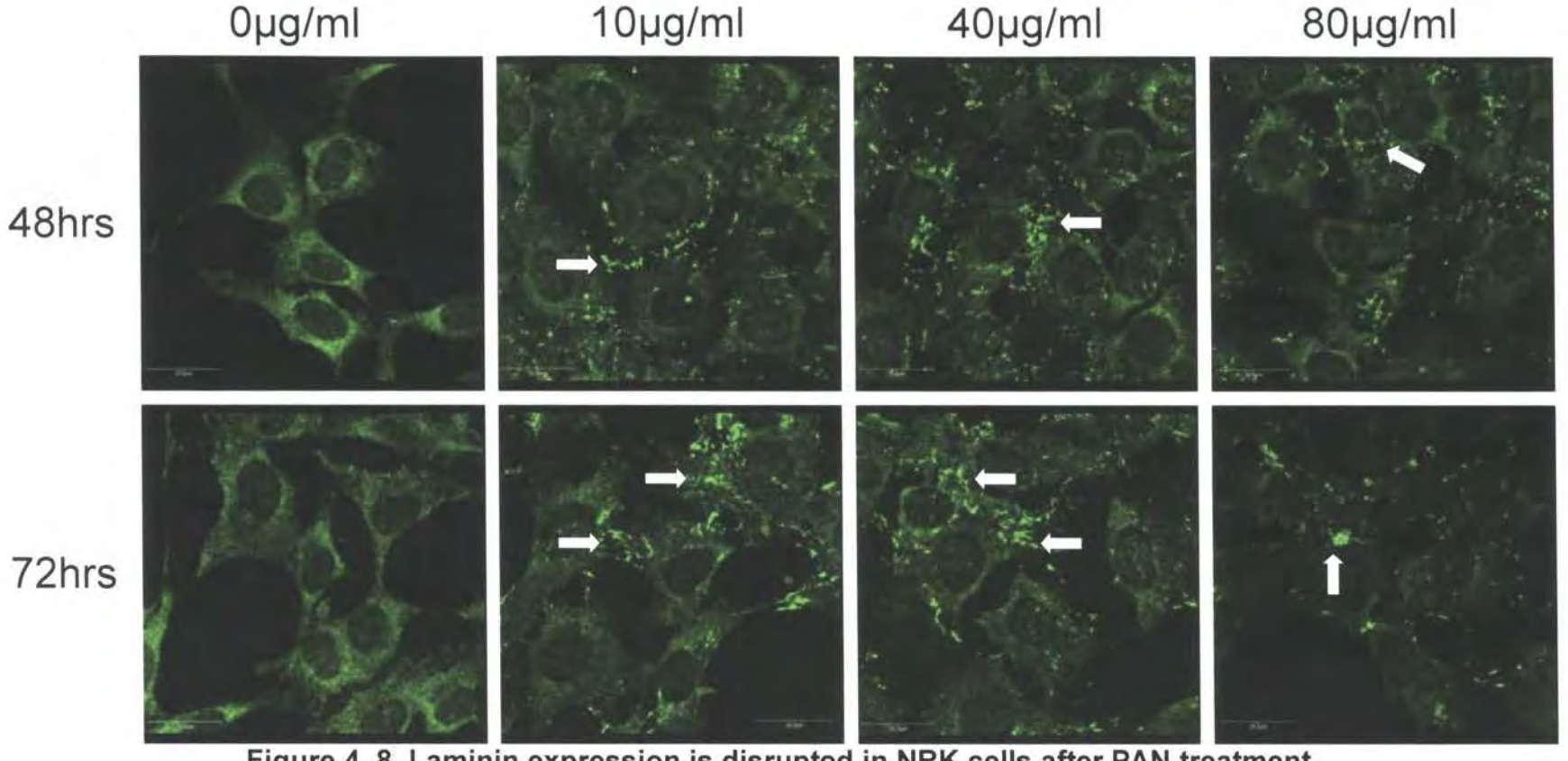

Figure 4. 8. Laminin expression is disrupted in NRK cells after PAN treatment.

Figure 4.8. Laminin expression is disrupted in NRK cells after PAN treatment. Laminin expression is reduced and disrupted by PAN treatment. Laminin deposits form at the cell periphery, highlighted by arrows, after PAN treatment.
NRK cells (p4) were cultured for 48hrs in D-MEM + 10% FBS. After 48hrs the medium was replaced with medium containing PAN. The cells were fixed/permeabilized and stained with a mAb to localize laminin β2. The cells were then imaged by confocal microscopy at 519nm. Images are merged composite images of layered sections throughout the cell, magnification x150. All microscope and laser settings have been kept constant to allow an accurate comparison of staining intensity. Scale bar 20μm.

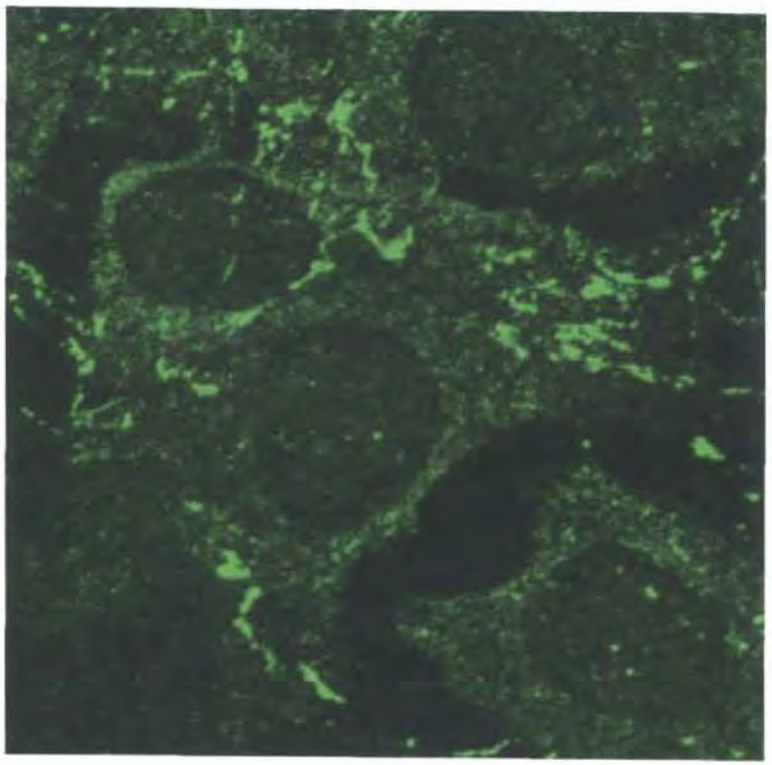

Figure 4. 9. Magnified view of the laminin deposits formed in NRK cells after PAN treatment (40µg/ml 72hrs). As a result of PAN treatment laminin expression was reduced from control levels and the localization changed from perinuclear staining to more diffuse staining throughout the cell with laminin deposits at the cell periphery.

4.7. Conclusions

There are conflicting data on the effect of PAN on integrin protein expression in both animal and cellular models. Krishnamurti *et al.* [181] hypothesized that "the mechanism of PAN-induced detachment involves the inhibition of expression of α3β1 integrin" and found that integrin expression was reduced at both the mRNA and protein levels in PAN induced nephrosis of 56/10 A1 cells at a PAN dose treatment of 0.5μg/ml and 5μg/ml for 48 hours. They also showed that PAN resulted in decreased cellular content of α3β1 integrin rather than redistribution from the cell surface to the cytoplasm. Our results supports the findings of Krishnamurti *et al.* [181] that the adhesive changes observed in kidney cells following PAN treatment may result from reduced integrin expression rather than a redistribution of integrin within the cell.

Smoyer *et al.* [122] found no statistically significant changes in either α3 integrin or β1 integrin protein expression except an increase in α3 integrin expression ten days after induced PAN (150mg/kg body weight) nephrosis in male Sprague-Dawley rats. Conversely Kojima *et al.* [237] found decreased α3 integrin expression four days after PAN (50mg/kg body weight) induced nephrosis in male Wistar rats but expression levels returned to normal at day ten. Luimula *et al.* [78] found a two-fold increase in β1 integrin protein expression at day three and ten after PAN (100mg/kg body weight) induction in female Sprague-Dawley rats but no corresponding change in mRNA levels.

The contradictory results can possibly be explained by variations in each model. Not only were there variations in animal species but also sex as well as variations in the PAN doses. Between these studies there are three-fold differences in the concentration of PAN. This is likely to have an effect on the severity of nephrosis and hence a subsequent effect on any proteins affected by nephrosis.

Our results showed decreased α3 integrin protein expression by Western blotting at mid (40μg/ml) and high (80μg/ml) doses of PAN, which caused the greatest level of cell detachment, and no changes in cellular distribution of integrin. This supports the findings of Krishnamurti *et al.* [181] and Kojima *et al.* [237] that PAN nephrosis results in reduced integrin expression which is responsible for the loss of cell adhesion.

Recently another hypothesis has been proposed regarding the role of integrin in podocyte adhesion. Reiser *et al.* [260] proposed that α3 integrin is not needed for podocytes to adhere to the GBM, but rather α3 integrin is downregulated to increase podocyte attachment. The down-regulation of α3 integrin results in prolonged adhesion and protects against podocyte detachment. Our results do not support this hypothesis. Detailed quantified results are required to confirm that reduced integrin expression prolongs podocyte adhesion. Based on our results and other published data showing reduced integrin expression after PAN treatment of kidney cells I believe that reduced integrin expression results in a loss of adhesion rather than prolonging adhesion.

We found a change in the staining pattern of laminin β2 in response to PAN nephrosis. With increasing PAN dose there was an increase in laminin deposits forming around the edge of the cells. Coers *et al.* [183] also reported similar patterns of change in laminin expression in response to puromycin aminonucleoside and adriamycin treatment of cultured glomerular epithelial cells. They found that the intercellular "pearl chain"-like staining pattern of laminin was lost after 48 hours following treatment of 20μg/ml and 50μg/ml PAN or for 24 hours with 2μg/ml or 5μg/ml ADR. They also showed that β1 integrin focal adhesion formation was disrupted by induced nephrosis.

The work in this chapter provides further evidence that the cellular model I have established mimics PAN-induced nephrosis and that NRK cells adhesive properties are altered after PAN treatment.

In the following chapter we will investigate the effects of PAN on the expression and localization of two podocytes proteins, podoplanin and podocalyxin, which are believed to be potential biomarkers of nephrotic injury.

Chapter 5.
PAN Mediated Effects on Podocyte Proteins

5.1. Introduction

As previously discussed PAN-induced nephrosis specifically targets the podocytes and results in several key findings, including; changes in cell morphology, reduced adhesive ability and changes to podocyte proteins [18, 43, 78, 181-184, 204, 261]. We have shown changes in cell morphology and reduction in adhesive properties of NRK cells in previous chapters. In this chapter we will examine if PAN treatment affects the expression of podocyte proteins.

The genes encoding several podocyte proteins have been identified as showing differential expression in *in vivo* rat models of PAN-induced nephrosis. GlaxoSmithKline using Taqman real-time PCR identified two potential nephrotoxic biomarkers, podoplanin and podocalyxin, which were down-regulated in a rat model of PAN nephrosis. Podoplanin was also shown to be downregulated at the transcriptional mRNA level by 70% and at the protein level by quantitative immunogold electron microscopy and Western blotting by Breiteneder-Geleff *et al.* [18] in the PAN nephrosis animal model. In PAN rats, foot process effacement and disorganization of the slit diaphragm is accompanied by a 70% reduction in the sialic acid composition of podocalyxin [43]. It has also been proposed that functional or structural disruption to podocalyxin or to the associated cytoskeletal linker proteins, ezrin and NHERF2 could be a cause of glomerular disorders and serve as viable targets for future studies [44, 45].

Other podocyte specific proteins including nephrin [76-78], podocin [89], KIM-1 [198, 199] and GLEPP-1 [100, 101] have also been identified as being differentially expressed in the PAN nephrosis model and in nephrotic diseases including minimal change nephropathy and focal segmental glomerulosclerosis.

Of these podocyte proteins nephrin and podocin have been extensively studied and characterized due to their involvement in several diseases,

including diabetic nephropathy, minimal change nephropathy, membranous nephropathy and focal segmental glomerulosclerosis. KIM-1 has previously been identified as a potential biomarker of nephrotoxic injury [200]. GLEPP-1 has been proposed to be a sensitive marker of podocyte injury and therefore could be a useful clinical marker for glomerular injury [101]. Podoplanin and podocalyxin are the least well studied podocyte proteins and show substantial decreases in expression in the rat model of PAN nephrosis and as such we believe they are good candidates for new potential nephrotoxic biomarkers and as such we will focus our studies on their expression and localization in this chapter.

Using several techniques, including Western blotting and immunofluorescence microscopy we analyzed the expression and localization of podoplanin and podocalyxin, to determine if their expression and localization is affected in NRK cells by PAN treatment.

5.2. Podoplanin Expression

We have previously reported a decrease in mRNA expression of podoplanin in response to PAN treatment. Here we examine the corresponding protein expression by Western blotting. Briefly NRK cells were cultured on 90 mm tissue culture dishes as normal. Protein was extracted from each PAN dose overnight by acetone precipitation. Each protein sample was quantified by a Bradford Assay and equal volumes of 10µg of protein were subjected to electrophoresis. Proteins were transferred to a nitrocellulose membrane and incubated with podoplanin antibody overnight, subsequently washed and incubated with secondary antibody. Proteins were detected in the dark by ECL (see section 2.3 for full method).

We only observed a reduction in podoplanin protein expression at the highest dose of 80µg/ml at both 48 and 72 hours, (Figure 5.1). This did not correspond to the level of mRNA reduction we had earlier observed or to the previously published results of Breiteneder-Geleff *et al.* [18] who observed a 70% reduction in expression for both mRNA and protein levels. The two bands observed at the theoretical size, 38 kDa, for podoplanin are believed to be the result of post-translational modification, most likely differing glycosylation or phosphorylation states [18].

We also examined the sub-cellular localization of podoplanin after sub-cellular fractionation of control (0µg/ml) and PAN treated (80µg/ml) NRK cells after 72 hours. Briefly equal NRK cell numbers were subjected to homogenisation followed by fractionation to yield membrane fractions, each fraction was resuspended in 100µl HES buffer, 10µl of each fraction was loaded per well for Western blotting and probed with podoplanin. In control cells podoplanin was detected predominantly in the low density microsome (LDM) and endoplasmic reticulum/nuclei (ER/N) fractions with very low expression in the plasma membrane fraction. After PAN treatment no podoplanin protein was detected in the LDM and plasma membrane fractions and was greatly reduced in the endoplasmic

reticulum/nuclei fraction in comparison to control cells (Figure 5.2). Although this would suggest a change in localization of podoplanin we believe that this result is more representative of an overall reduction in protein expression rather than a translocation. We will confirm if this is the case by examining podoplanin expression by immunofluorescence using our cellular model of PAN nephrosis.

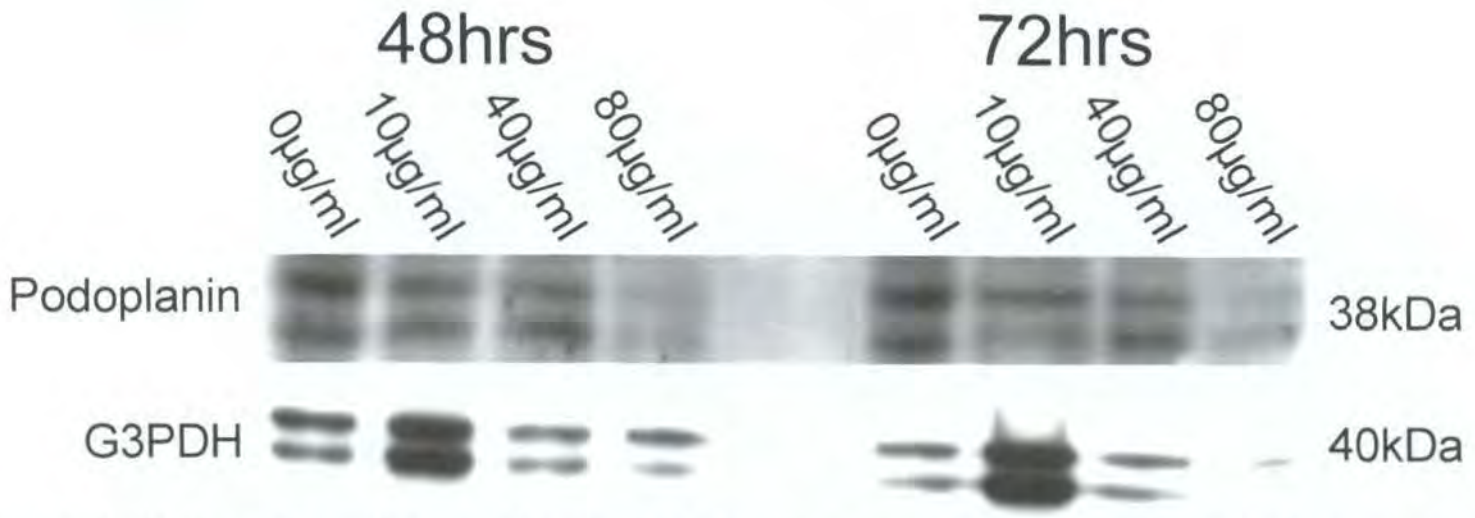

Figure 5. 1. PAN results in decreased podoplanin protein expression as examined by Western blotting.

10µg total protein was loaded per well. Podoplanin expression is greatly reduced at the highest (80µg/ml) PAN dose only.

Figure 5. 2. Sub-cellular fractionation of podoplanin after PAN (80µg/ml 72hrs) treatment. Hom homogenate, HDM High density microsome, LDM Low density microsome, PM Plasma membrane, ER/N endoplasmic reticulum/nuclei fractions. An equal volume of sample, 10µl, based on an equal number of cells was loaded per well, for expression level comparison.

Podoplanin showed a shift in localization from control to PAN treated cells. Podoplanin expression was lost from the LDM fraction and greatly reduced in the ER/N fraction after PAN treatment.

5.3. Podoplanin Localization

We examined the distribution of podoplanin in NRK cells after PAN treatment by immunolabelling followed by confocal microscopy. We examined both intracellular expression and the cell surface expression of podoplanin at all the PAN doses tested.

We found that podoplanin was expressed both at the cell surface, as expected for a membrane glycoprotein but was also observed to be expressed throughout the cellular interior with expression concentrated at the perinuclear regions. Expression became more concentrated around the nucleus with PAN treatment (Figure 5.3).

This pattern of expression can be seen more clearly when we examine cell surface expression in NRK cells that have not been permeabilized (Figure 5.4). More intense podoplanin expression is observed concentrated around the nucleus at 40µg/ml and 80µg/ml PAN treatment for 48 or 72 hours.

Figures 5.5 and 5.6 show podoplanin expression throughout the cell of control (Figure 5.5.) and PAN (80µg/ml 48hrs) treated (Figure 5.6.) NRK cells as visualized by immunofluorescence microscopy. In control cells there is clearly defined podoplanin staining at the perinuclear region (Figure 5.5. c-e). After PAN treatment this staining pattern is lost (Figure 5.6. c-e).

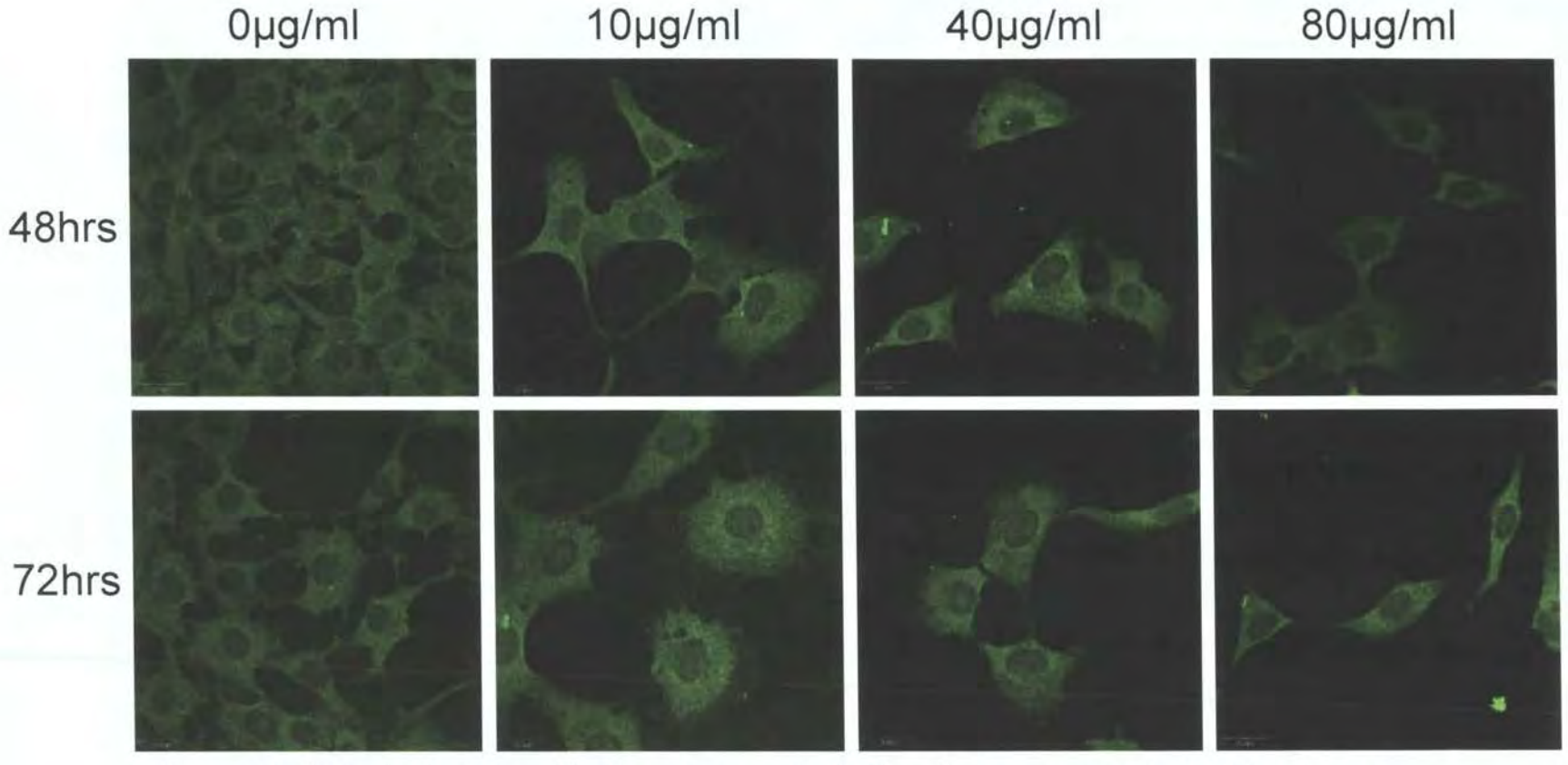

Figure 5. 3. Podoplanin localization changes in NRK cells in response to PAN treatment.

Figure 5.3. Podoplanin localization changes in NRK cells in response to PAN treatment. Podoplanin showed a diffuse staining pattern throughout the cell with increased staining at the perinuclear region at the low (10µg/ml) dose of PAN.
NRK cells (p4) were cultured for 48hrs in D-MEM + 10% FBS. After 48hrs the media was replaced with media containing PAN. The cells were fixed/permeabilized and stained with a mAb to localize podoplanin. The cells were then imaged by confocal microscopy at 519nm. Images are merged composite images of layered sections throughout the cell, magnification x100. All microscope and laser settings have been kept constant to allow an accurate comparison of staining intensity. Scale bar 20µm.

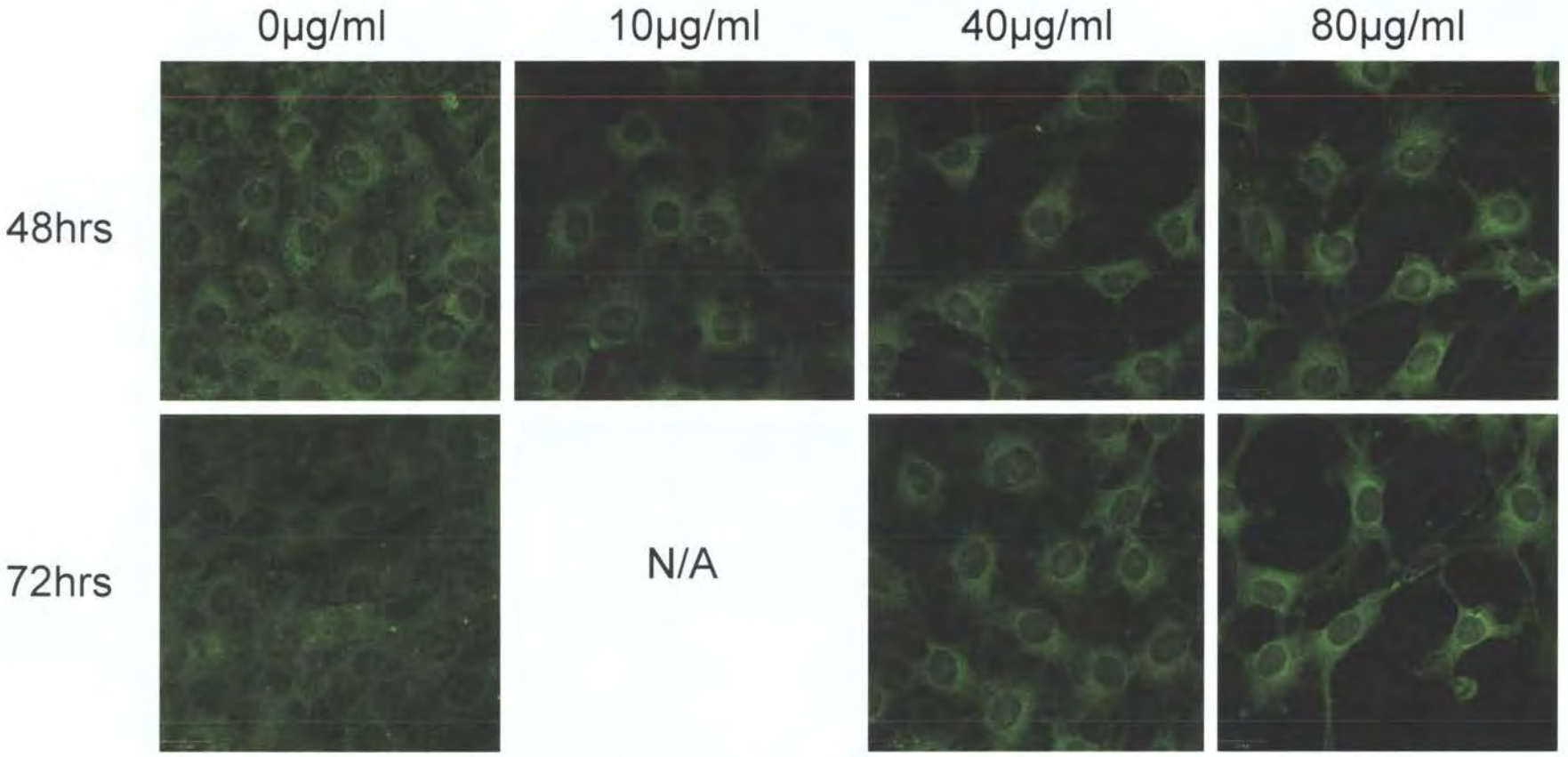

Figure 5. 4. Podoplanin expression in non-permeabilized NRK cells after PAN treatment.

Figure 5.4. Podoplanin expression in non-permeabilized NRK cells after PAN treatment.
NRK cells (p7) were cultured for 48hrs in D-MEM + 10% FBS. After 48hrs the media was replaced with media containing PAN. The cells were fixed and stained with a mAb to localize podoplanin. The cells were then imaged by confocal microscopy at 519nm. Images are merged composite images of layered sections throughout the cell, magnification x100. All microscope and laser settings have been kept constant to allow an accurate comparison of staining intensity. Scale bar 20μm.

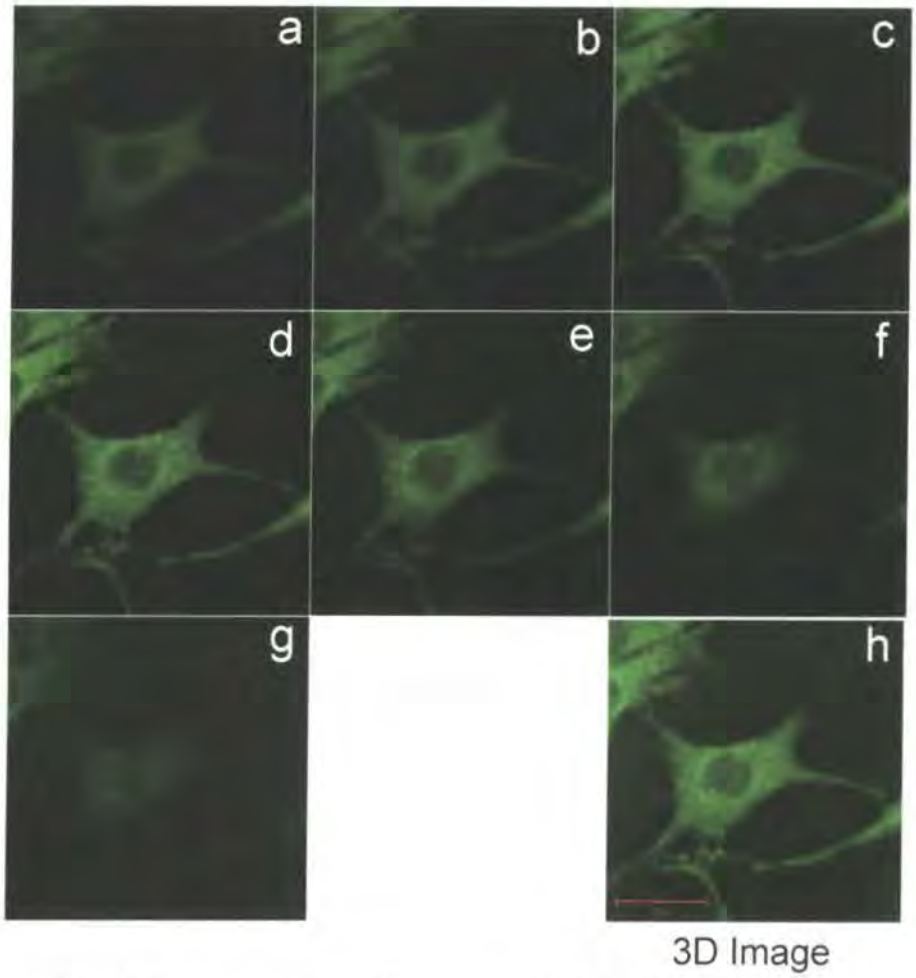

Figure 5. 5. Podoplanin localization in NRK cell layers.
NRK cells (p4) were cultured for 48hrs in D-MEM + 10% FBS. The cells were fixed/permeabilized and stained with a mAb to localize podoplanin. The cells were then imaged by confocal microscopy at 519nm. Images (a-g) are individual layers 0.75µm thick throughout the cell, (h) is the composite image of these layers, magnification x200. All microscope and laser settings have been kept constant to allow an accurate comparison of staining intensity. Scale bar 20µm.

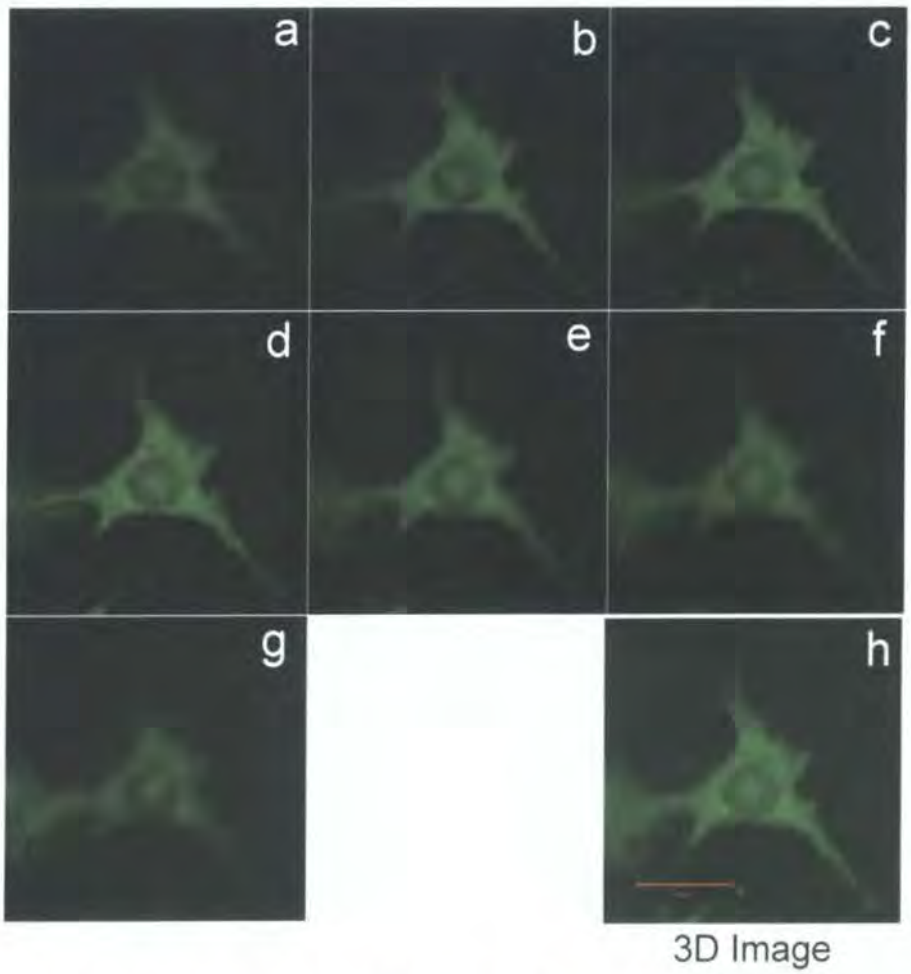

Figure 5. 6. Podoplanin localization in NRK cell layers after PAN treatment.

NRK cells (p4) were cultured for 48hrs in D-MEM + 10% FBS. After 48hrs the media was replaced with media containing 80µg/ml PAN and cultured for 48hrs. The cells were fixed/permeabilized and stained with a mAb to localize podoplanin. The cells were then imaged by confocal microscopy at 519nm. Images (a-g) are individual layers 0.75µm thick throughout the cell, (h) is the composite image of these layers, magnification x200. All microscope and laser settings have been kept constant to allow an accurate comparison of staining intensity. Scale bar 20µm.

5.4. Podocalyxin Expression

We observed a dose-dependent decrease in podocalyxin expression at the mRNA level following PAN treatment. However like podoplanin we did not observe a corresponding reduction in protein expression. Briefly Western blotting was carried out on protein extracted from NRK cells after PAN treatment. Equal volumes of 10µg of protein from each sample as determined by a Bradford Assay were loaded into each well. Proteins were transferred to a nitrocellulose membrane and incubated with podocalyxin antibody overnight, subsequently washed and incubated with secondary antibody. Proteins were detected in the dark by ECL (see section 2.3 for full method).

As with podoplanin we only observed a significant reduction in podocalyxin protein expression at the highest (80µg/ml) PAN dose at both 48 and 72 hours (Figure 5.7). The two bands observed at the theoretical size, 165 kDa, for podocalyxin are believed to be the result of post-translational modifications, based on podocalyxin's structure probably differing glycosylation or sialylation states [33].

We also examined the localization of podocalyxin after sub-cellular fractionation of control (0µg/ml) and PAN treated (80µg/ml) cells after 72 hours. Briefly equal NRK cell numbers were subjected to homogenisation followed by fractionation to yield membrane fractions, each fraction was re-suspended in 100µl HES buffer, 10µl of each fraction was loaded per well for Western blotting and probed with a podocalyxin antibody. In control cells podocalyxin was detected predominantly in the endoplasmic reticulum/nuclei (ER/N) fractions and with some expression in the plasma membrane fraction. After PAN treatment no podocalyxin was detected in the plasma membrane fraction and levels were greatly reduced in the ER/Nuclei fraction and also detected increased expression in the LDM fraction compared to control cells (Figure 5.8). This would suggest that PAN alters the targeting of podocalyxin protein. We will confirm this result

by examining intracellular podocalyxin expression after PAN treatment by immunofluorescence within our cellular model.

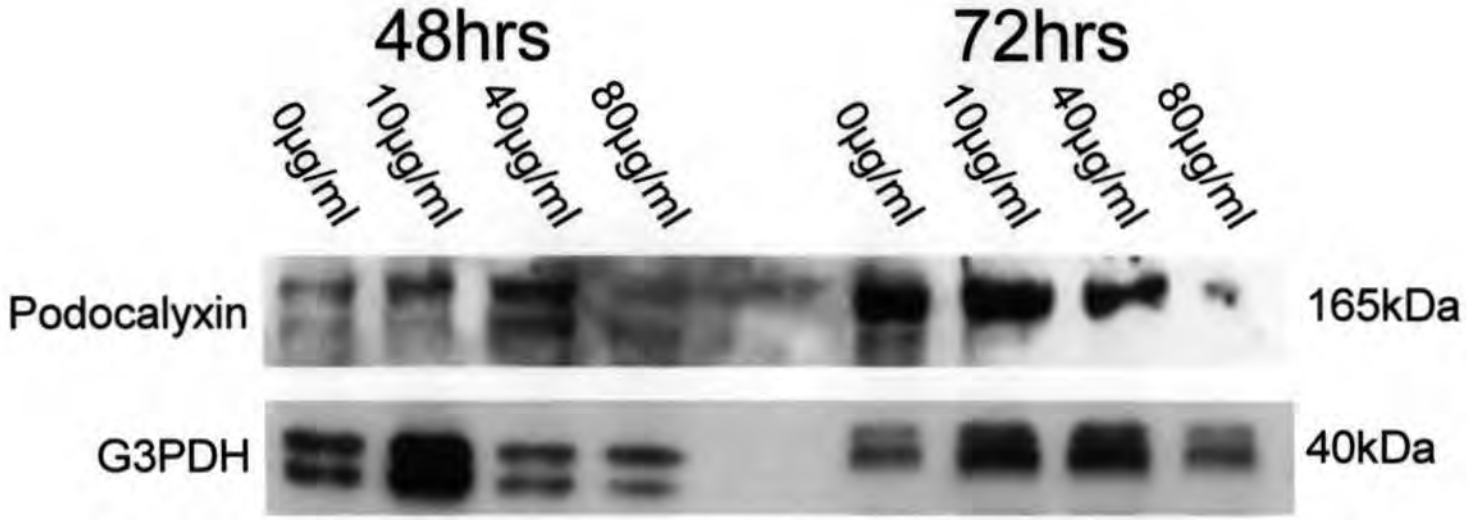

Figure 5. 7. PAN results in decreased podocalyxin protein expression as examined by Western blotting.

10µg total protein was loaded per well. Podocalyxin expression is greatly reduced after PAN treatment of 80µg/ml for 48hrs and almost completely lost after 72 hrs.

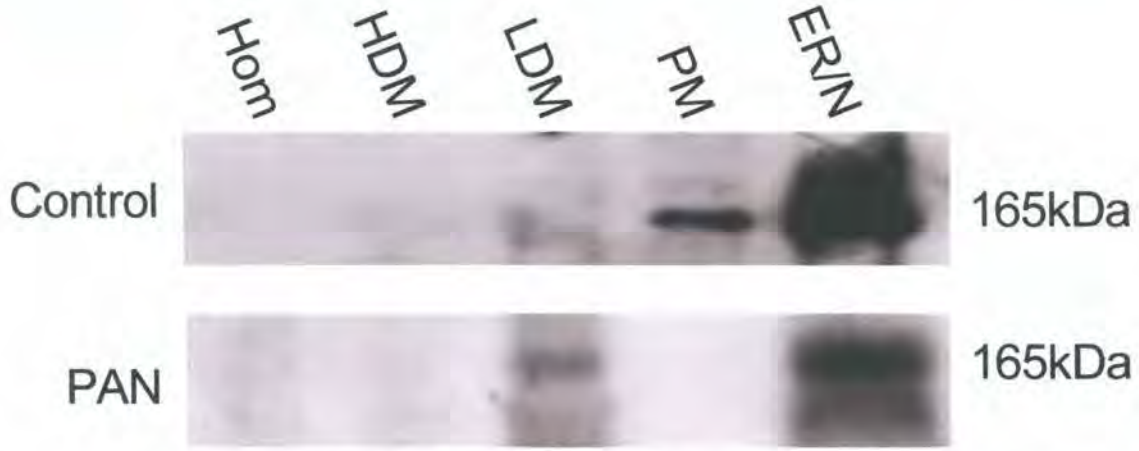

Figure 5. 8. Sub-cellular fractionation of podocalyxin after PAN (80µg/ml 72hrs) treatment. Hom homogenate, HDM High density microsome, LDM Low density microsome, PM Plasma membrane, ER/N endoplasmic reticulum/nuclei fractions. An equal volume of sample, 10µl, based on an equal number of cells was loaded per well, for a comparison of expression levels.

Podocalyxin expression is reduced in the ER/N fraction and shows a shift in localization from the plasma membrane to the LDM fraction after PAN treatment.

5.5. Podocalyxin Localization

We examined changes in podocalyxin protein localization in NRK cells after PAN treatment using immunofluorescence microscopy. We examined both intracellular and cell surface expression.

Podocalyxin expression changed dramatically with changing cell morphology (Figure 5.9), showing progressively increased expression at 48 hours with increasing PAN doses. As the cells develop filapodia at the highest PAN dose (80µg/ml 72hrs) podocalyxin expression is greatly increased. Like podoplanin podocalyxin is concentrated around the nucleus. However podocalyxin does show a more granular pattern of expression. The granular pattern of expression is more clearly shown at the cell surface (Figure 5.10) and in the magnified image (Figure 5.11). The intracellular granular staining pattern led us to investigate if podocalyxin was expressed within vesicles in the cell and not just expressed at the cell surface as previously reported [28, 37, 40].

Figures 5.11 and 5.12 show podocalyxin expression throughout the cell of control (Figure 5.11) and PAN (80µg/ml 48hrs) treated (Figure 5.12) NRK cells as visualized by immunofluorescence microscopy. In both control and PAN treated cells there is clearly defined podocalyxin staining within the golgi complex, but the staining is reduced after PAN treatment. This shows that PAN is not affecting podocalyxin localization but is reducing the levels of podocalyxin expression. This result also adds to our belief that changing cell morphology is responsible for the increased levels of podocalyxin observed after PAN treatment of 80µg/ml for 72hrs rather than a direct result of PAN treatment.

Podocalyxin is heavily sialylated and extensively O-glycosylated, both processes occur when the protein passes through the golgi complex. O-glycosylation occurs in the golgi stack while the addition of sialic acid occurs in the trans-golgi network just prior to the protein being exported from the golgi complex.

Therefore we would expect to see strong podocalyxin expression within the golgi complex. However podocalyxin is a trans-membrane protein and so we would also expect to see strong podocalyxin expression at the cell surface. The fact we see only weak surface expression is most likely a result of using a fibroblast cell line which is phenotypically different from glomerular epithelial cells. However we would encounter a similar problem if we used a podocyte cell line as podocytes in culture do not express cell surface podocalyxin [262].

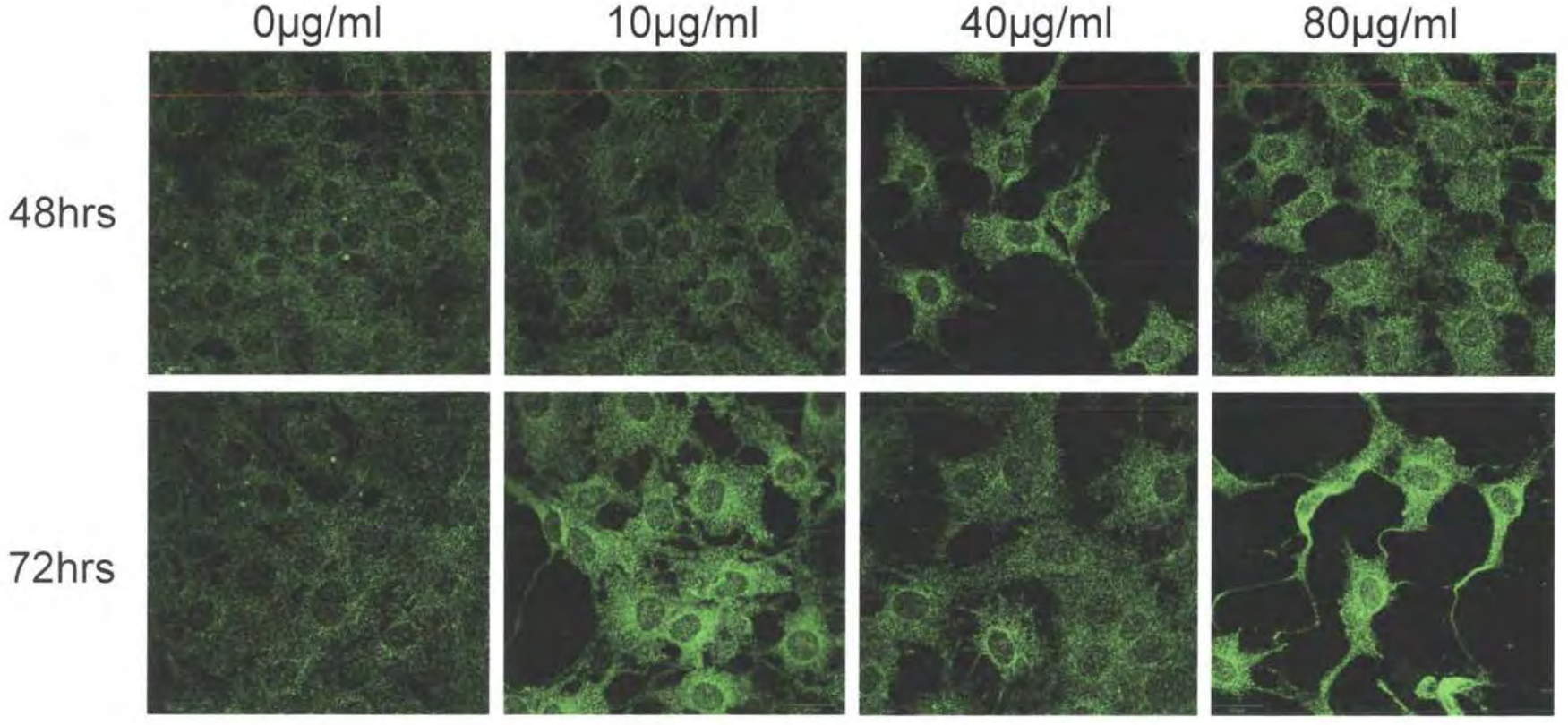

Figure 5. 9. Podocalyxin localization changes in NRK cells in response to PAN treatment.

Figure 5.9. Podocalyxin localization changes in NRK cells in response to PAN treatment.
NRK cells (p4) were cultured for 48hrs in D-MEM + 10% FBS. After 48hrs the media was replaced with media containing PAN. The cells were fixed/permeabilized and stained with a mAb to localize podocalyxin. The cells were then imaged by confocal microscopy at 519nm. Images are merged composite images of layered sections throughout the cell, magnification x100. All microscope and laser settings have been kept constant to allow an accurate comparison of staining intensity. Scale bar 20μm.

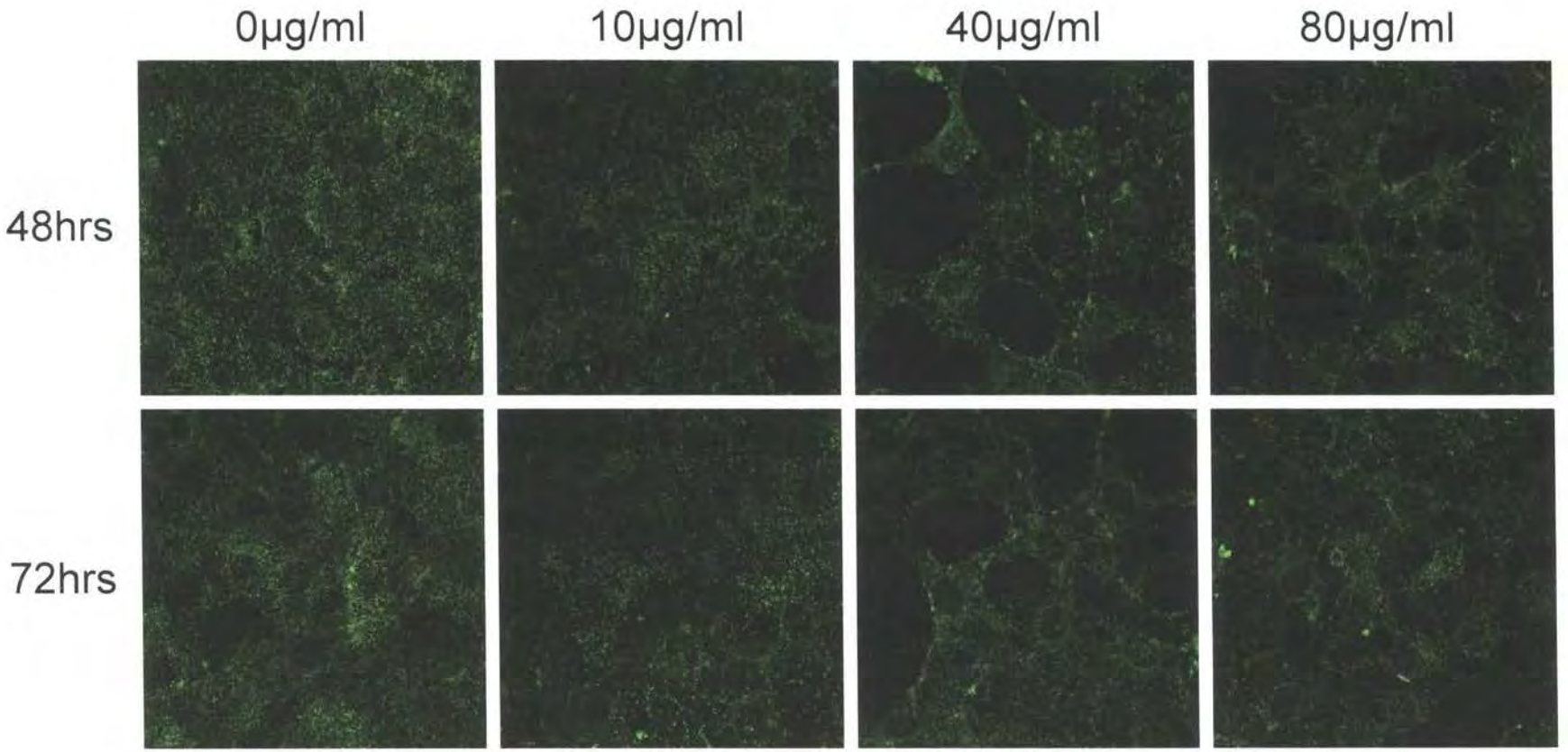

Figure 5. 10. Cell surface localization of podocalyxin in NRK cells after PAN treatment.

Figure 5.10. Cell surface localization of podocalyxin in NRK cells after PAN treatment.
NRK cells (p7) were cultured for 48hrs in D-MEM + 10% FBS. After 48hrs the media was replaced with media containing PAN. The cells were fixed and stained with a mAb to localize podocalyxin. The cells were then imaged by confocal microscopy at 519nm. Images are merged composite images of layered sections throughout the cell, magnification x100. All microscope and laser settings have been kept constant to allow an accurate comparison of staining intensity. Scale bar 20μm.

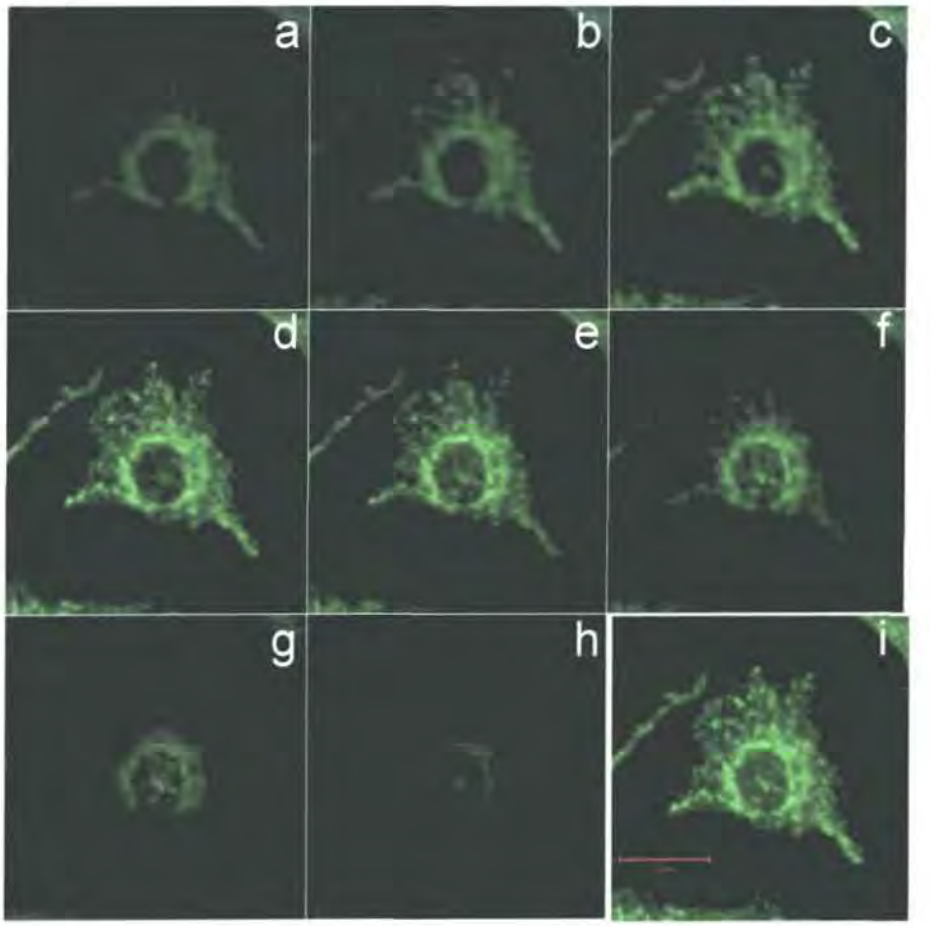

Figure 5. 11. Podocalyxin localization in NRK cell layers.
NRK cells (p4) were cultured for 48hrs in D-MEM + 10% FBS. The cells were fixed/permeabilized and stained with a mAb to localize podocalyxin. The cells were then imaged by confocal microscopy at 519nm. Images (a-h) are individual layers 0.75µm thick throughout the cell, (i) is the composite image of these layers, magnification x200. All microscope and laser settings have been kept constant to allow an accurate comparison of staining intensity. Scale bar 20µm.

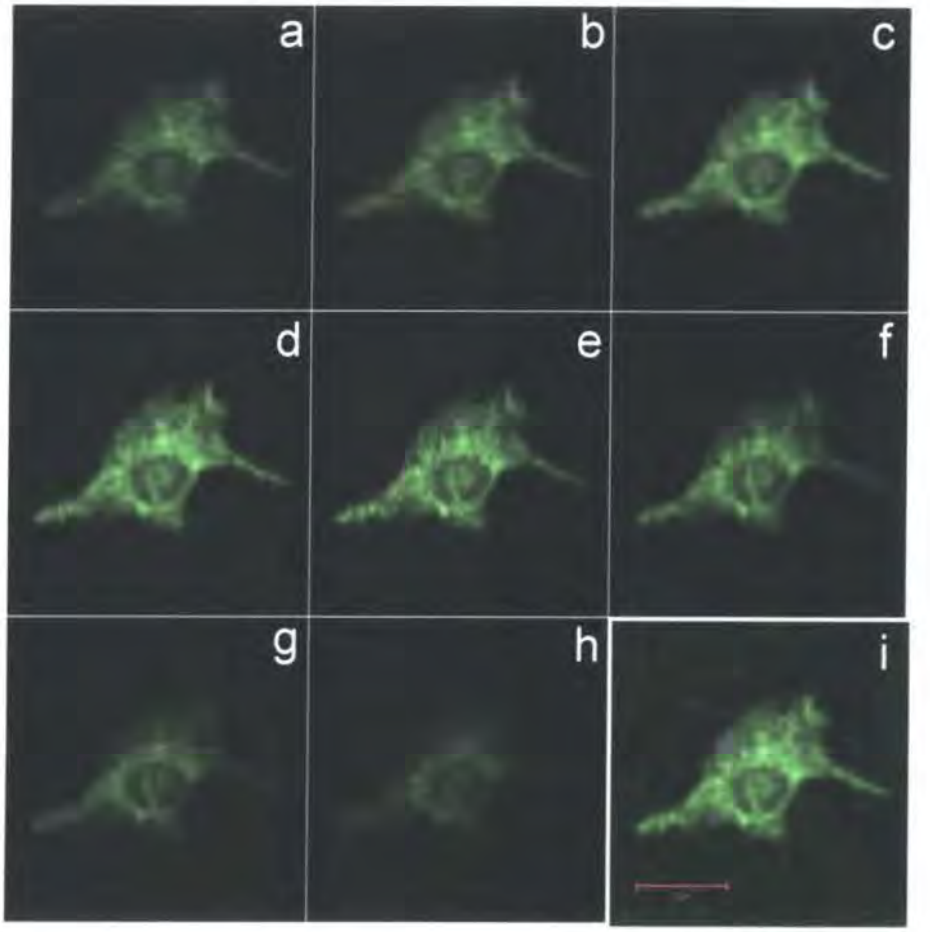

Figure 5. 12. Podocalyxin localization in NRK cell layers after PAN treatment.

NRK cells (p4) were cultured for 48hrs in D-MEM + 10% FBS. After 48hrs the media was replaced with media containing 80µg/ml PAN and cultured for 48hrs. The cells were fixed/permeabilized and stained with a mAb to localize podocalyxin. The cells were then imaged by confocal microscopy at 519nm. Images (a-h) are individual layers 0.75µm thick throughout the cell, (i) is the composite image of these layers, magnification x200. All microscope and laser settings have been kept constant to allow an accurate comparison of staining intensity. Scale bar 20µm.

5.6. Co-localization Studies

The granular intracellular staining pattern of podocalyxin suggested it was expressed within intracellular vesicles. We wanted to establish if this was the case and also wanted to examine any changes in possible vesicle trafficking within the cell in response to PAN treatment. Initially we needed to identify which vesicle podocalyxin was expressed in. To achieve this we carried out dual staining immunofluorescence microscopy using a selection of known characterized vesicle markers including, caveolin for clathrin coated vesicles, cellubrevin for recycling vesicles, EEA-1 for early endosomes, syntaxin7 for late endosomes and lysosomes and protein disulfide isomerase (PDI) for endoplasmic reticulum. In brief NRK cells were cultured, fixed and permeabilized as normal but were then exposed to a primary antibody mixture containing either podoplanin or podocalyxin and a vesicle marker. Subsequently the cells were exposed to both secondary antibodies. The cells were then visualized at both 519nm and 573nm wavelengths to observe the independent staining of each antibody. Co-localization was observed by using software to combine the two images (See Section 2.5.3).

5.6.1. Podoplanin

In each case podoplanin expression was as previously described, staining was in a perinuclear pattern with staining intensity increasing after PAN treatment. Caveolin showed staining around the cell periphery and syntaxin 7 staining was throughout the cell with a concentration at one end of the cell around the nucleus, neither showed any changes in localization or expression and neither co-localized with podoplanin (results not shown). Therefore podoplanin is not expressed in clathrin coated vesicles or late endosomes.

PDI showed increased intensity after 80µgml PAN treatment for 48 hours but no change in localization was detected (Figure 5.13. b, e). There was no co-localization observed at 0µg/ml but due to the increased

concentration of perinuclear podoplanin and increased levels of PDI at 80µg/ml there was a degree of overlapping expression (Figure 5.13. f).

EEA-1 expression became more concentrated at the nucleus after PAN treatment (Figure 5.14. e). There was no co-localization observed between podoplanin and EEA-1 (Figure 5.14. f). As there is no co-localization podoplanin is not present in early endosomes.

Cellubrevin a marker for recycling vesicles showed diffuse staining throughout the cell with marginally increased staining around the nucleus (Figure 5.15. b). Cellubrevin staining was increased within the filapodia of cells after PAN treatment (Figure 5.15. e). There was partial co-localization within these branching cells but not in normal cells (Figure 5.15. f).

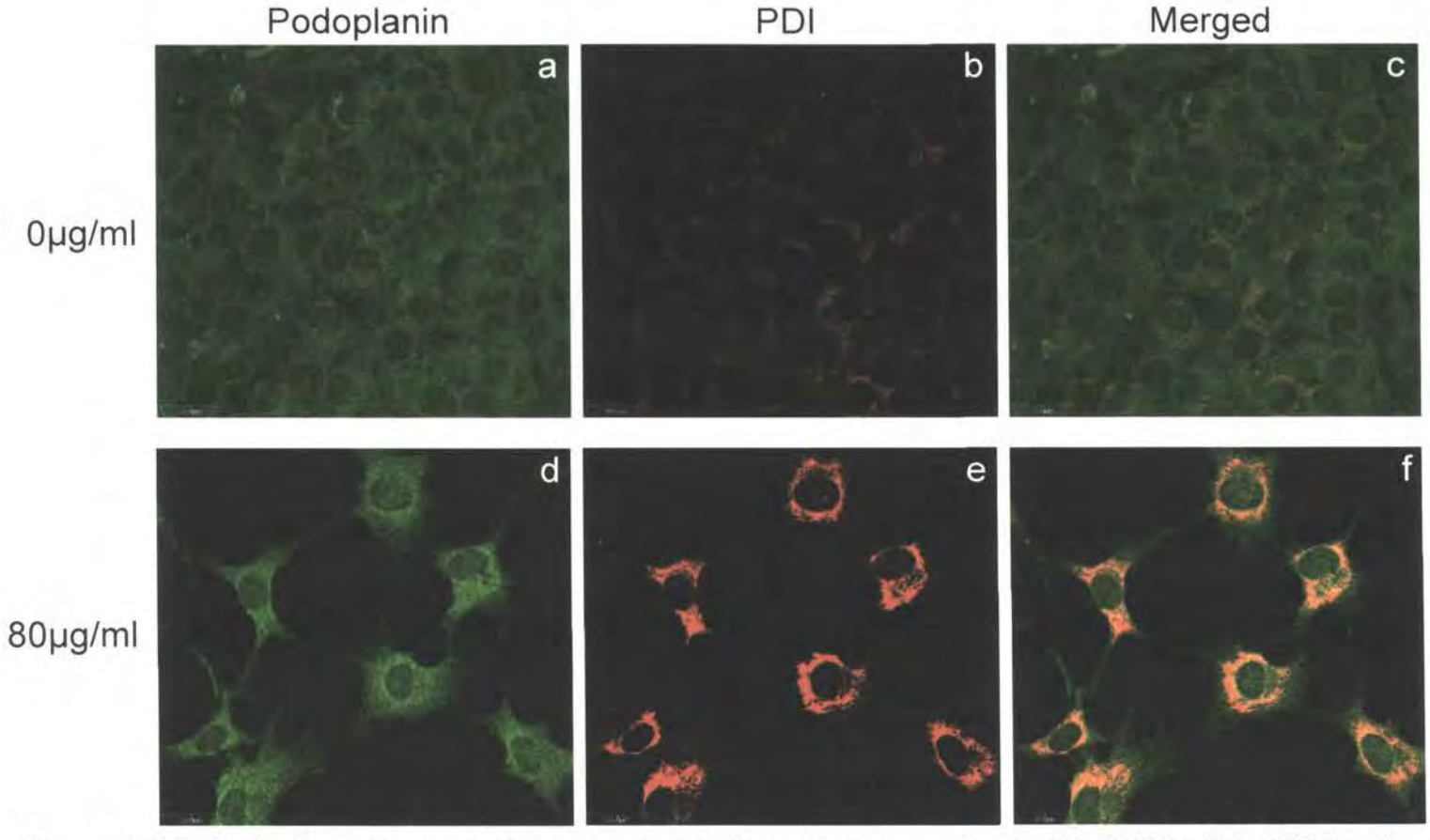

Figure 5. 13. Podoplanin (green) shows partial co-localization (yellow) with PDI (red) in NRK cells after 48hrs PAN treatment.

Figure 5.13. Podoplanin (green) shows partial co-localization (yellow) with PDI (red) in NRK cells after 48hrs PAN treatment.
NRK cells (p6) were cultured for 48hrs in D-MEM + 10% FBS. After 48hrs the media was replaced with media containing PAN. The cells were fixed/permeabilized and stained with a monoclonal Ab to podoplanin (green) and a polyclonal Ab (PDI) to the ER (red). The cells were then imaged by confocal microscopy at 519nm and 573nm. (a, d) show podoplanin expression (b, e) show PDI expression and (c, f) show the co-localization of podoplanin and PDI before and after PAN treatment.

Images are merged composite images of layered sections throughout the cell magnification x100. All microscope and laser settings have been kept constant to allow an accurate comparison of staining intensity. Scale bar 20μm.

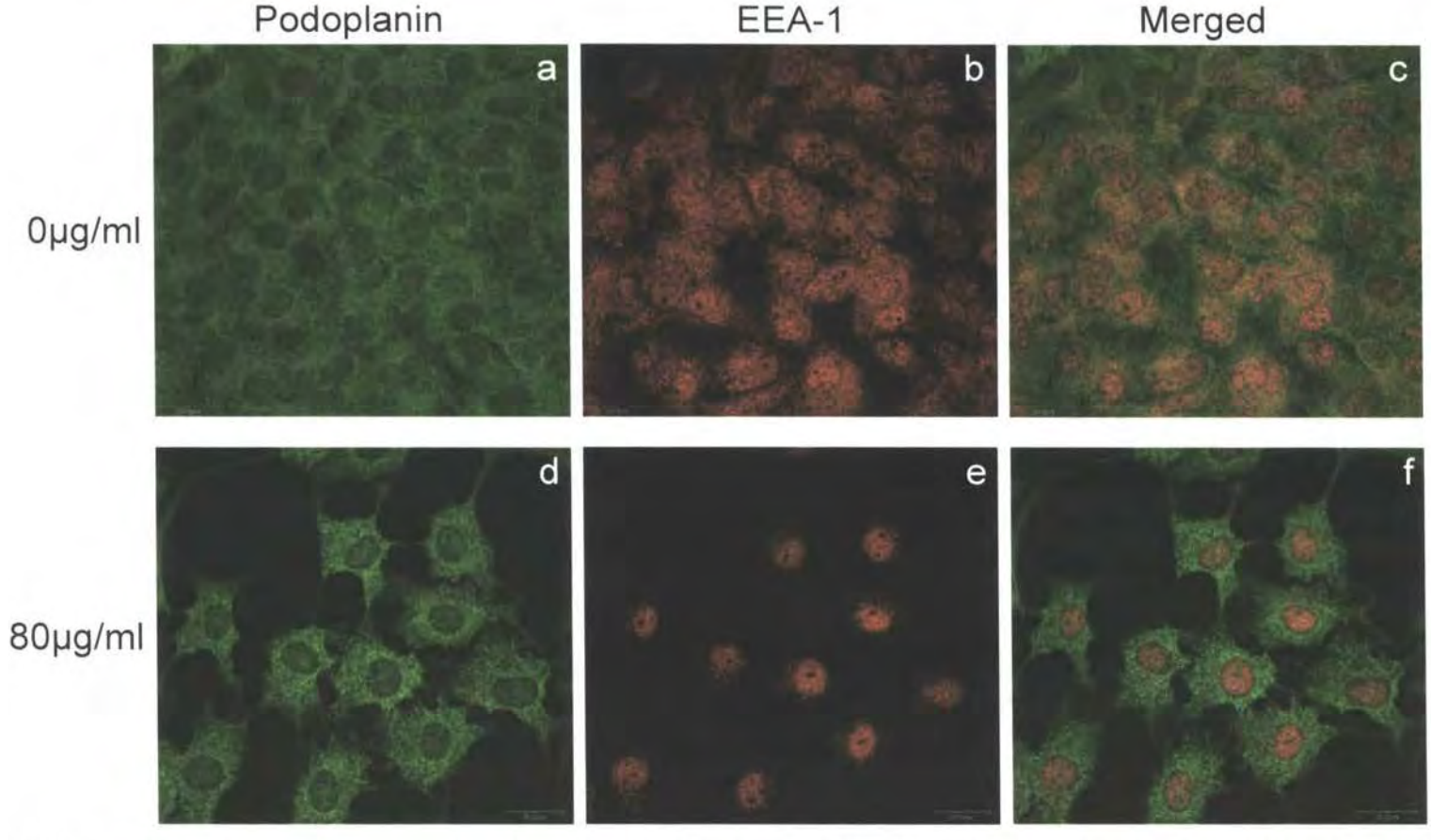

Figure 5. 14 Podoplanin (green) does not co-localize (yellow) with EEA-1(red) in NRK cells after 72hrs PAN treatment.

Figure 5.14. Podoplanin (green) does not co-localize (yellow) with EEA-1(red) in NRK cells after 72hrs PAN treatment.
NRK cells (p6) were cultured for 48hrs in D-MEM + 10% FBS. After 48hrs the media was replaced with media containing PAN. The cells were fixed/permeabilized and stained with a monoclonal Ab to podoplanin (green) and a polyclonal Ab (EEA-1) to the early endosomes (red). The cells were then imaged by confocal microscopy at 519nm and 573nm. (a, d) show podoplanin expression (b, e) show EEA-1 expression and (c, f) show the co-localization of podoplanin and EEA-1 before and after PAN treatment.

Images are merged composite images of layered sections throughout the cell magnification x100. All microscope and laser settings have been kept constant to allow an accurate comparison of staining intensity. Scale bar 20µm.

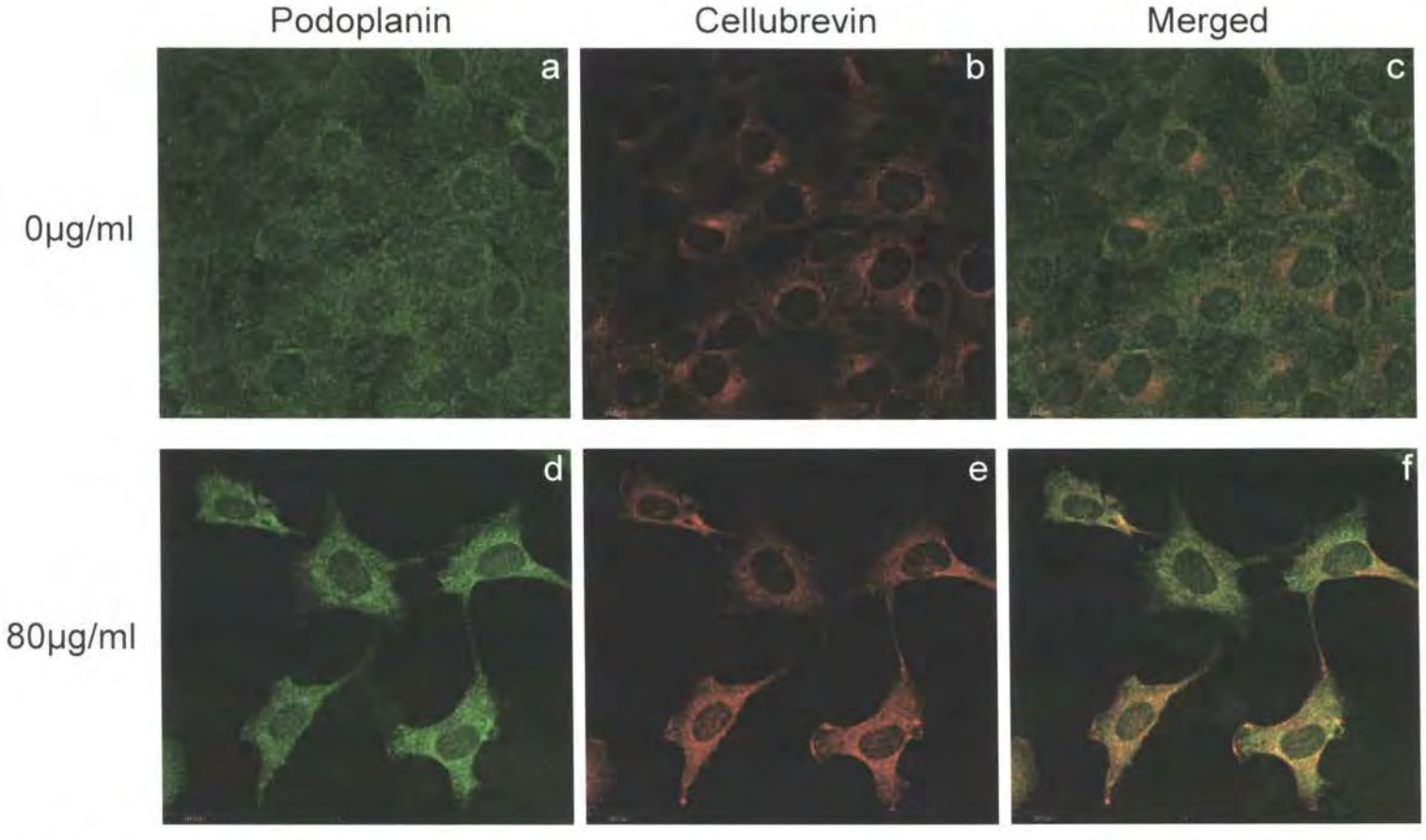

Figure 5. 15. Podoplanin (green) partially co-localizes (yellow) with cellubrevin (red) after 72hrs PAN treatment.

Figure 5.15. Podoplanin (green) partially co-localizes (yellow) with cellubrevin (red) in NRK cells after 72hrs PAN treatment.
NRK cells (p6) were cultured for 48hrs in D-MEM + 10% FBS. After 48hrs the media was replaced with media containing PAN. The cells were fixed/permeabilized and stained with a monoclonal Ab to podoplanin (green) and a polyclonal Ab (cellubrevin) a marker of recycling vesicles (red). The cells were then imaged by confocal microscopy at 519nm and 573nm. (a, d) show podoplanin expression (b, e) show cellubrevin expression and (c, f) show the co-localization of podoplanin and cellubrevin before and after PAN treatment.

Images are merged composite images of layered sections throughout the cell magnification x100. All microscope and laser settings have been kept constant to allow an accurate comparison of staining intensity. Scale bar 20μm.

5.6.2. Podocalyxin

As described earlier podocalyxin localization was predominantly in the perinuclear region with some staining around the edges of the cell with increased staining at 80µg/ml as compared to non-treated cells. The staining pattern is very granular which suggests that podocalyxin is located within a vesicle within the cell.

Like podoplanin, podocalyxin was discretely expressed from EEA-1, with no co-localization observed in normal cells. Co-localization was observed in PAN treated cells which were detaching from the tissue culture surface (results not shown). There was also no co-localization detected for podocalyxin and PDI.

Caveolin was expressed around the cell periphery outlining the cells (Figure 5.16. b, e) with a slight increase in intensity after PAN treatment. Podocalyxin was localized throughout the cell in a granular pattern with increased expression after PAN treatment (Figure 5.16. d). No co-localization was observed at any PAN dose (Figure 5.16. c, f).

Cellubrevin showed diffuse staining throughout the cell with marginally increased staining around the nucleus (Figure 5.17. b). After PAN treatment when the cells elongated and started to form filapodia cellubrevin expression was greatly increased (Figure 5.17. e). This led to almost complete co-localization with podocalyxin (Figure 5.17. f). However this co-localization was only observed when the cells were elongated with filapodia, which was only observed after 80µg/ml PAN treatment for 72 hours (Figure 5.18.).

Syntaxin 7 staining was concentrated at one end of the nucleus and showed no changes in response to PAN treatment (Figure 5.19. b, e). There was some overlap between syntaxin 7 and podocalyxin but no signs of co-localization (Figure 5.20. c, f).

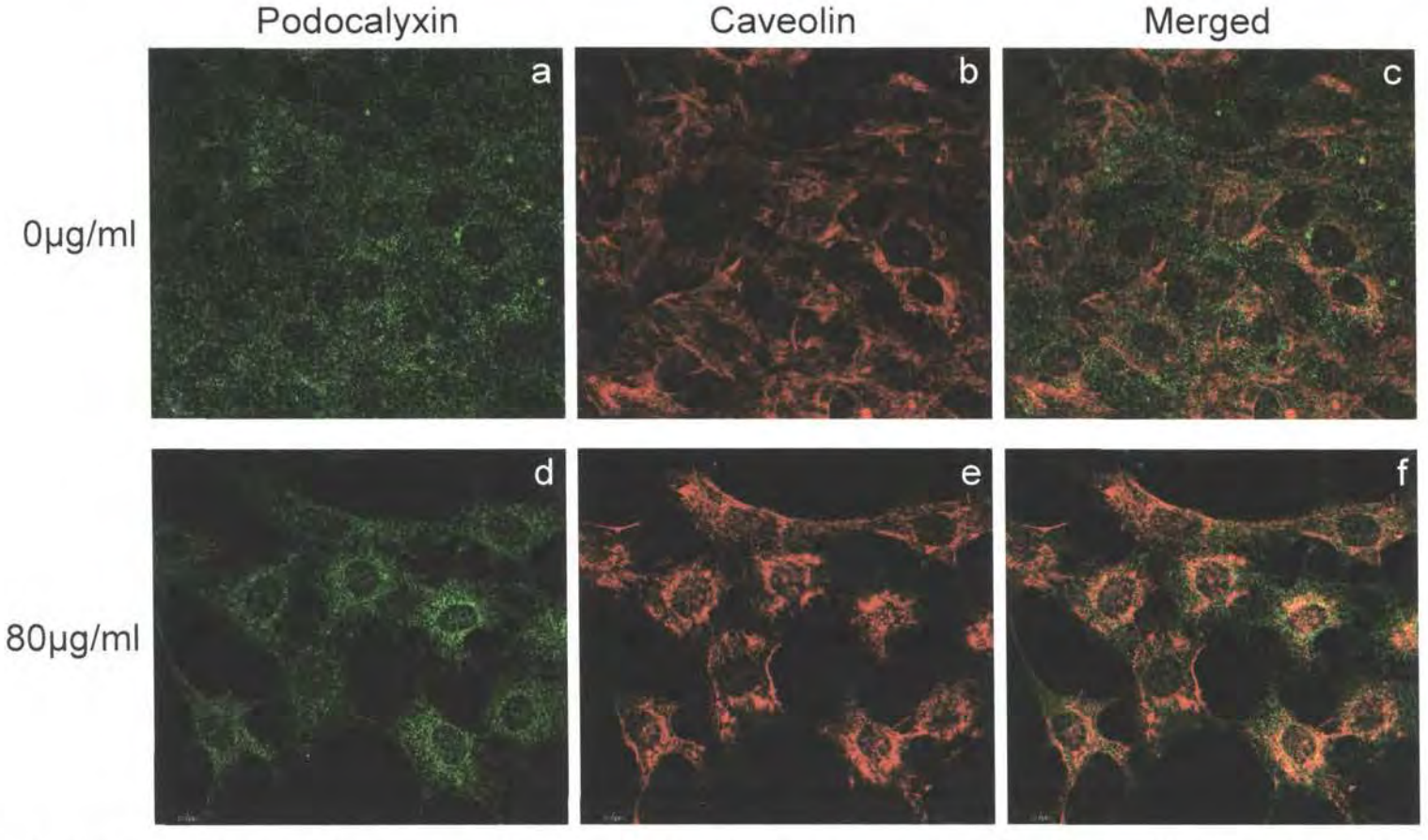

Figure 5. 16. Podocalxyin (green) does not co-localize (yellow) with caveolin (red) in NRK cells after 72hrs PAN treatment.

Figure 5.16. Podocalxyin (green) does not co-localize (yellow) with caveolin (red) in NRK cells after 72hrs PAN treatment.
NRK cells (p5) were cultured for 48hrs in D-MEM + 10% FBS. After 48hrs the media was replaced with media containing PAN. The cells were fixed/permeabilized and stained with a monoclonal Ab to podocalyxin (green) and a polyclonal Ab (caveolin) a marker for clathrin coated vesicles (red). The cells were then imaged by confocal microscopy at 519nm and 573nm. (a, d) show podocalyxin expression (b, e) show caveolin expression and (c, f) show the co-localization of podocalyxin and caveolin before and after PAN treatment.

Images are merged composite images of layered sections throughout the cell magnification x100. All microscope and laser settings have been kept constant to allow an accurate comparison of staining intensity. Scale bar 20μm.

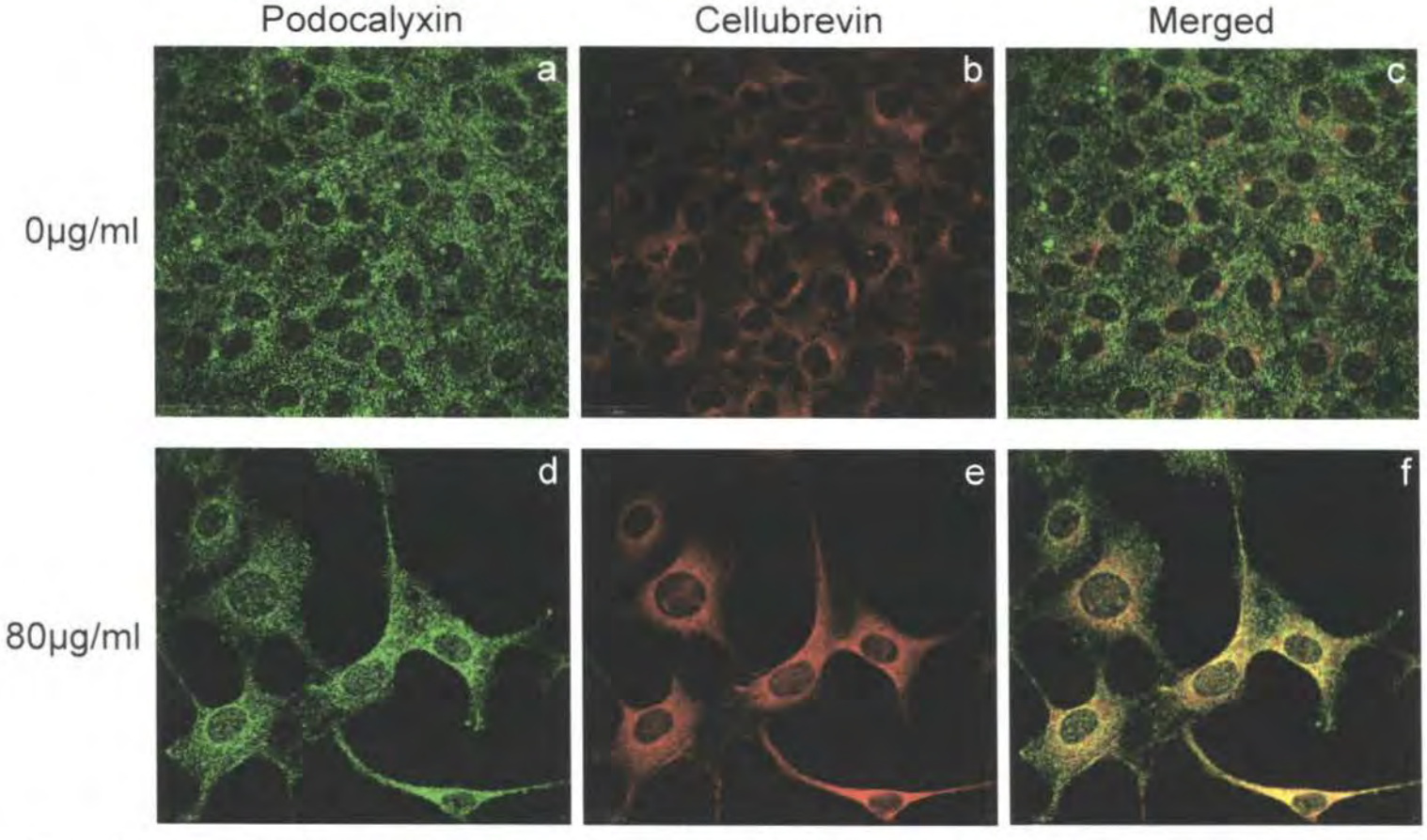

Figure 5. 17. Podocalyxin (green) co-localizes (yellow) with cellubrevin (red) in NRK cells after 48hrs PAN treatment.

Figure 5.17. Podocalyxin (green) co-localizes (yellow) with cellubrevin (red) in NRK cells after 48hrs PAN treatment.
NRK cells (p5) were cultured for 48hrs in D-MEM + 10% FBS. After 48hrs the media was replaced with media containing PAN. The cells were fixed/permeabilized and stained with a monoclonal Ab to podocalyxin (green) and a polyclonal Ab (cellubrevin) a marker of recycling vesicles (red). The cells were then imaged by confocal microscopy at 519nm and 573nm. (a, d) show podocalyxin expression (b, e) show cellubrevin expression and (c, f) show the co-localization of podocalyxin and cellubrevin before and after PAN treatment.

Images are merged composite images of layered sections throughout the cell magnification x100. All microscope and laser settings have been kept constant to allow an accurate comparison of staining intensity. Scale bar 20μm.

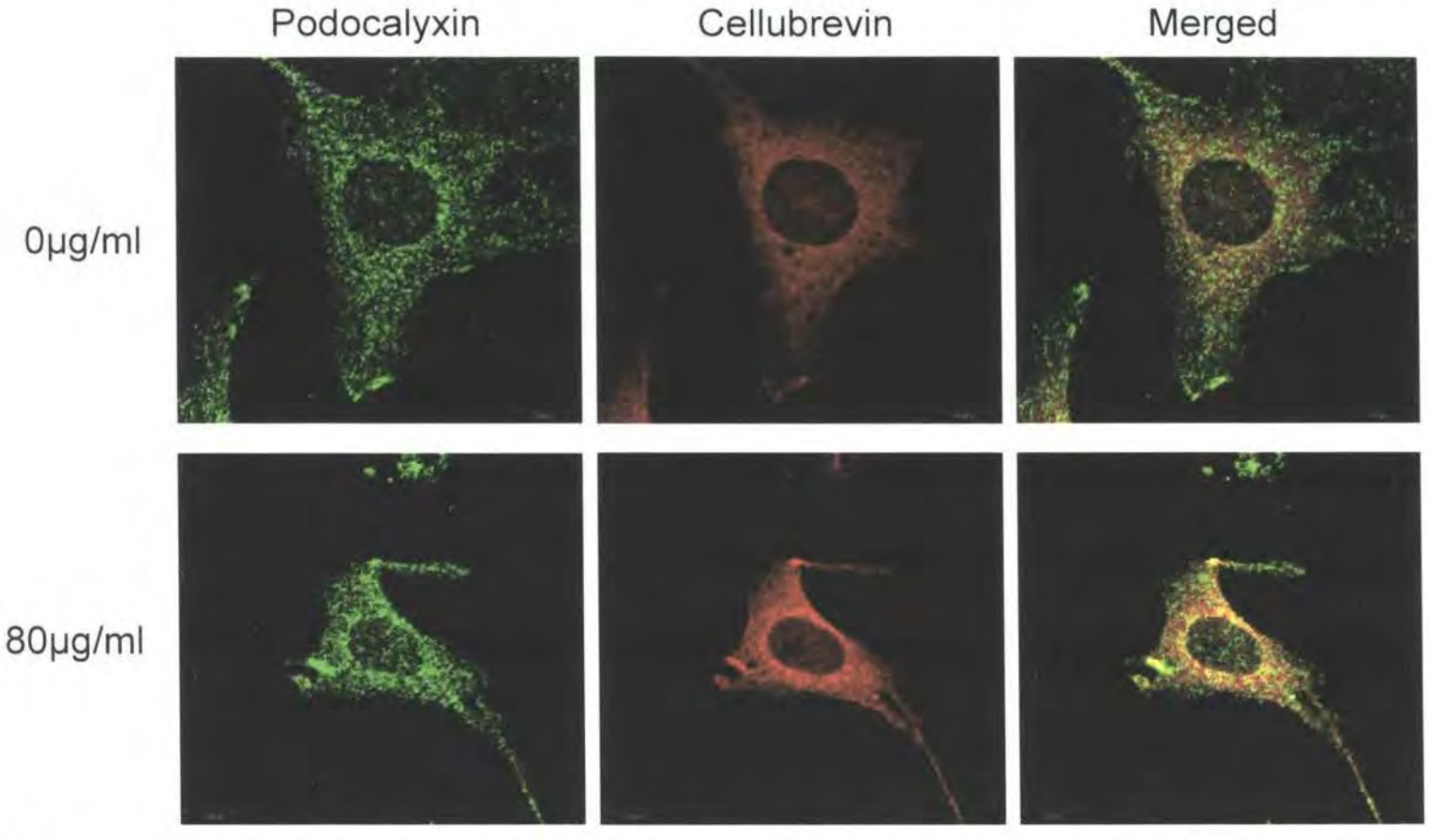

Figure 5. 18. Podocalyxin (green) co-localizes (yellow) with cellubrevin (red) in NRK cells after 48hrs PAN treatment.

Figure 5.18. Podocalyxin (green) co-localizes (yellow) with cellubrevin (red) in NRK cells after 48hrs PAN treatment.
NRK cells (p5) were cultured for 48hrs in D-MEM + 10% FBS. After 48hrs the media was replaced with media containing PAN. The cells were fixed/permeabilized and stained with a monoclonal Ab to podocalyxin (green) and a polyclonal Ab (cellubrevin) a marker of recycling vesicles (red). The cells were then imaged by confocal microscopy at 519nm and 573nm. (a, d) show podocalyxin expression (b, e) show cellubrevin expression and (c, f) show the co-localization of podocalyxin and cellubrevin before and after PAN treatment.

Images are merged composite images of layered sections throughout the cell magnification x200. All microscope and laser settings have been kept constant to allow an accurate comparison of staining intensity. Scale bar 10μm.

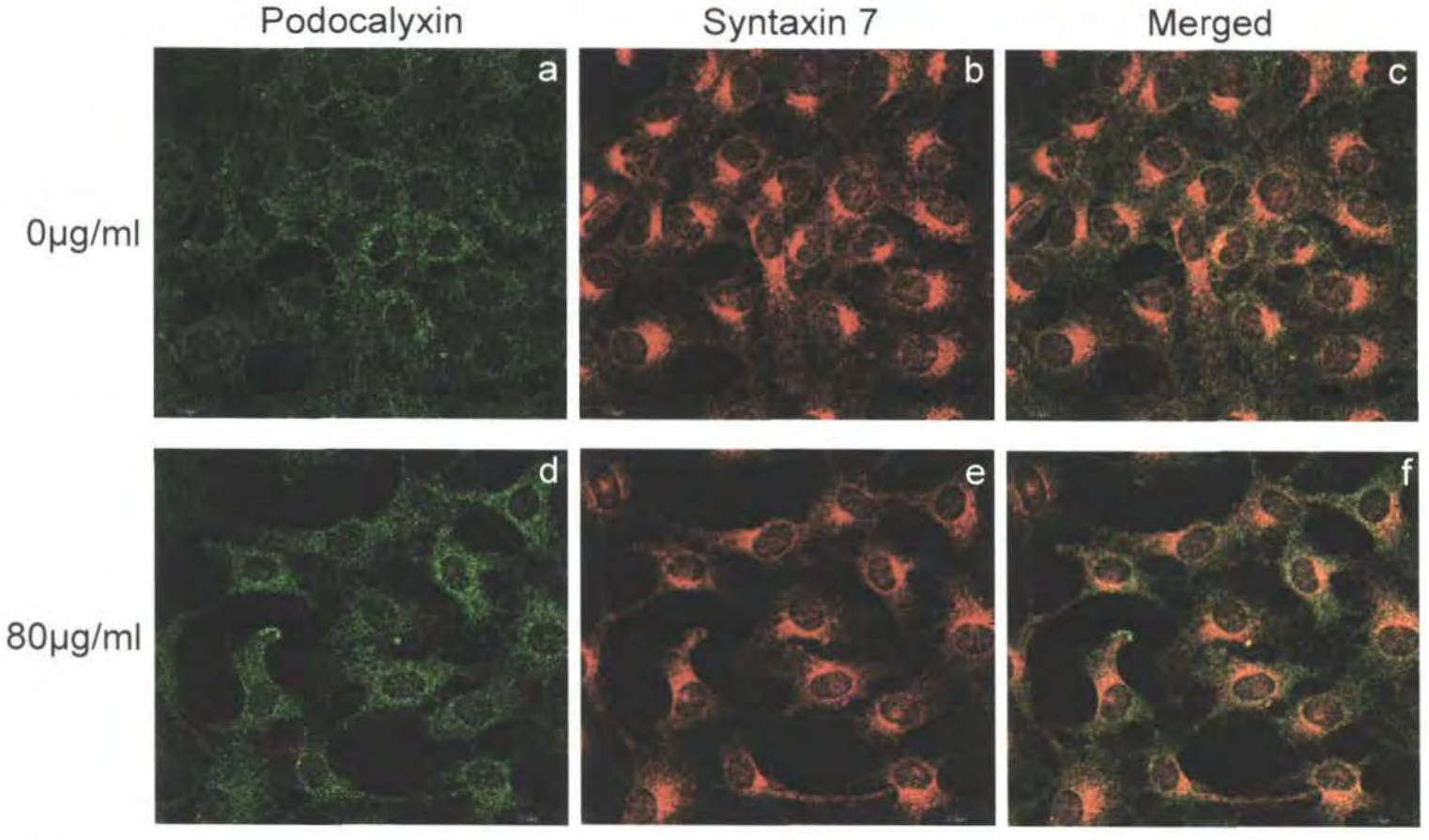

Figure 5. 19. Podocalyxin (green) shows partial co-localization (yellow) with syntaxin7 (red) after 48hrs PAN treatment.

Figure 5.19. Podocalyxin (green) shows partial co-localization (yellow) with syntaxin7 (red) in NRK cells after 48hrs PAN treatment.
NRK cells (p5) were cultured for 48hrs in D-MEM + 10% FBS. After 48hrs the media was replaced with media containing PAN. The cells were fixed/permeabilized and stained with a monoclonal Ab to podocalyxin (green) and a polyclonal Ab (syntaxin7) a marker for late endosomes (red). The cells were then imaged by confocal microscopy at 519nm and 573nm. (a, d) show podocalyxin expression (b, e) show syntaxin7 expression and (c, f) show the co-localization of podocalyxin and syntaxin7 before and after PAN treatment.

Images are merged composite images of layered sections throughout the cell magnification x100. All microscope and laser settings have been kept constant to allow an accurate comparison of staining intensity. Scale bar 20μm.

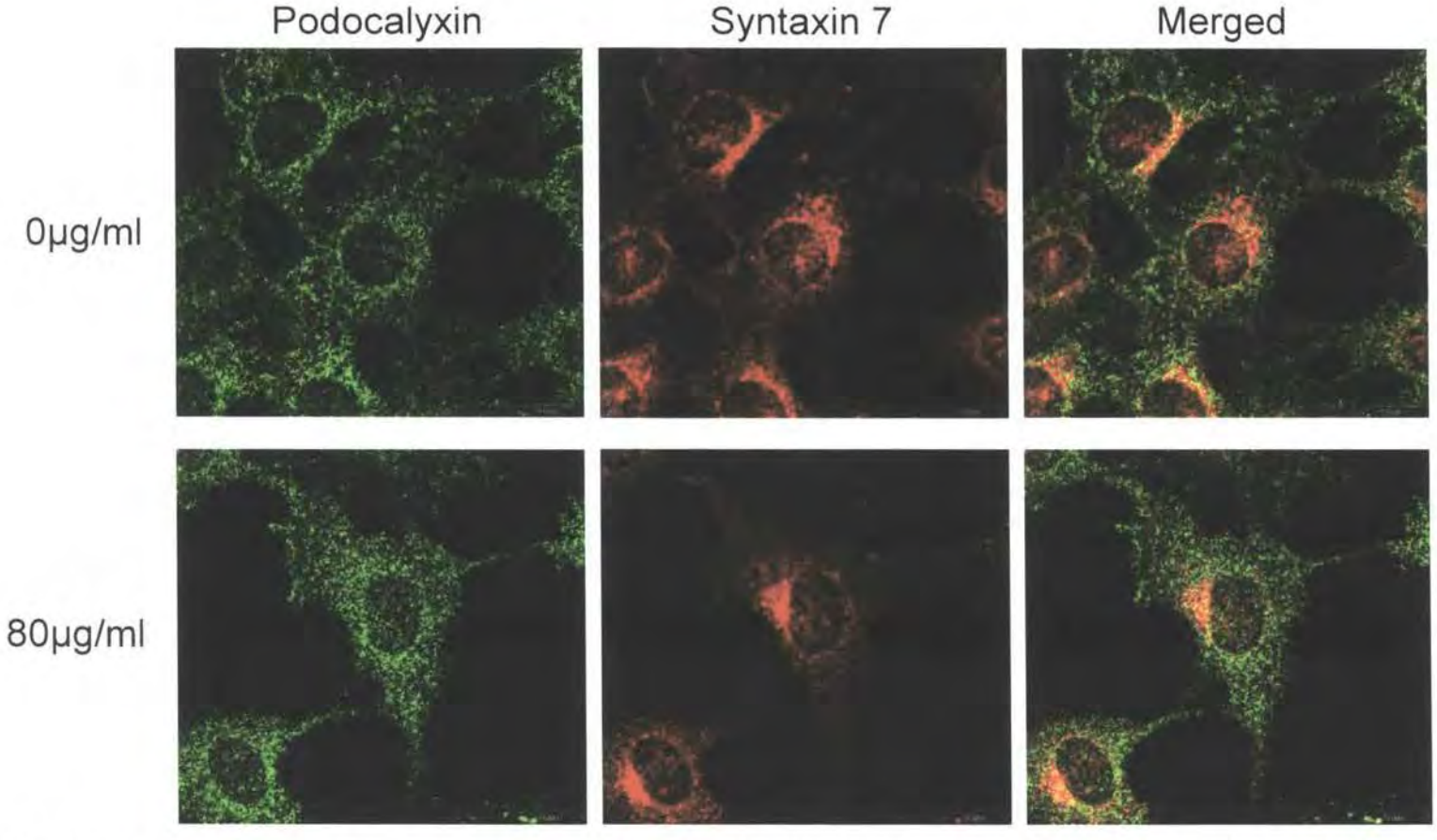

Figure 5. 20. Podocalyxin (green) shows partial co-localization (yellow) with syntaxin7 (red) after 48hrs PAN treatment.

Figure 5.20. Podocalyxin (green) shows partial co-localization (yellow) with syntaxin7 (red) in NRK cells after 48hrs PAN treatment.
NRK cells (p5) were cultured for 48hrs in D-MEM + 10% FBS. After 48hrs the media was replaced with media containing PAN. The cells were fixed/permeabilized and stained with a monoclonal Ab to podocalyxin (green) and a polyclonal Ab (syntaxin7) a marker for late endosomes (red). The cells were then imaged by confocal microscopy at 519nm and 573nm. (a, d) show podocalyxin expression (b, e) show syntaxin7 expression and (c, f) show the co-localization of podocalyxin and syntaxin7 before and after PAN treatment.

Images are merged composite images of layered sections throughout the cell magnification x200. All microscope and laser settings have been kept constant to allow an accurate comparison of staining intensity. Scale bar 10μm.

5.7. Conclusions

In this chapter we have analyzed the effects of PAN treatment on the podocyte specific proteins podoplanin and podocalyxin, examining both expression and localization in an attempt to provide further evidence that these proteins have the potential to be biomarkers of nephrotoxicity.

We only observed a significant reduction in podoplanin and podocalyxin protein expression at the highest dose of 80μg/ml for both 48 and 72 hours. This did not correspond to the previously observed dose-dependent reduction in mRNA expression. Or to the previously published 70% reduction in podoplanin protein expression as determined by quantitative immunogold electron microscopy, immunoblotting and Northern blotting [18].

Podoplanin was found to be expressed both at the cell surface, as expected for a membrane glycoprotein, but also intracellularly. It was found that podoplanin expression was lost from the low density microsome and plasma membrane fractions and greatly reduced in the endoplasmic reticulum/ nuclei fraction after PAN treatment 80μg/ml for 72 hours. However rather than this being an indication of a shift in podoplanin localization as a result of PAN nephrosis, it is more likely to be a reflection of the greatly reduced podoplanin expression overall. This was confirmed by immunofluorescence microscopy. Podoplanin expression intensity levels were changed, with an increase in perinuclear staining, in response to PAN treatment but no shift in localization was observed. This was further confirmed by co-localization studies with vesicle markers. Podoplanin did not co-localize with any of the markers used and showed no shift in localization as a result of PAN treatment.

Podocalyxin was found to be expressed at the cell surface and intracellularly with perinuclear staining. Podocalyxin showed a defined granular pattern of staining suggesting it was expressed within vesicles. Podocalyxin expression was greatly increased when NRK cells

developed filapodia at the highest PAN dose. Podocalyxin was found to be co-localized with cellubrevin in branching NRK cells, which showed filapodia after the highest PAN treatment. There was no co-localization in control cells or in cells not morphologically altered. This implies that in morphologically altered NRK cells podocalyxin is expressed in recycling vesicles.

Podocalyxin also showed changes in its sub-cellular localization as determined by sub-cellular fractionation and Western blotting. Podocalyxin was lost completely from the plasma membrane fraction and greatly reduced in endoplasmic reticulum fraction but was increased in the low density microsome fraction. In contrast to podoplanin, the expression of podocalyxin is both increased and decreased within the profile and therefore it is more likely that this is a true representation of a shift in localization as a result of PAN nephrosis.

In the next chapter we will analyze the effect PAN treatment has on the cytoskeletal structure of NRK cells.

Chapter 6.
PAN Mediated Effects on the Cytoskeleton

6.1. Introduction

Podocytes are the injury target of many glomerular diseases including minimal change nephropathy (MCN), chronic glomerulonephritis, focal segmental glomerulosclerosis (FSGS) and diabetes mellitus [6]. Regardless of the underlying disease the initial events of podocyte injury are characterized by either alterations in the molecular composition of the slit diaphragm (SD) without any visible morphological changes or by a visible reorganization of FP structure resulting in filtration slit fusion and apical displacement of the SD [145]. Based on this common response regardless of the cause of injury it has been suggested that there is a final common pathway which results in foot process effacement [263].

As previously mentioned it is critical for correct podocyte function that the structural integrity of the foot process is maintained. To date four major causes of foot process effacement have been identified; (1) changes in the SD complex and its organization by lipid rafts, (2) interference with the GBM or GBM-podocyte interaction, (3) interference with the negatively charged apical domain of podocytes and (4) reorganization of the actin cytoskeleton and its associated proteins.

We have analyzed the first three causes in previous chapters, in this final chapter we will examine how PAN treatment affects the cytoskeletal organization of NRK cells, paying particular attention to how PAN affects podocalyxin's link to the cytoskeleton as this has been identified by Orlando *et al.* [44] and Takeda *et al.* [45] as a possible cause of glomerular disorders.

The actin cytoskeleton ultimately determines and maintains the structure of the filtration slits. The actin cytoskeleton changes from co-ordinated stress fibers into a dense network with foot process effacement and loss of the filtration slits [264, 265]. Proteins regulating the actin cytoskeleton are of critical importance for sustained glomerular filtration [45, 265, 266]. A growing number of actin-associated proteins have been identified in

podocytes over the last decade, including α-actinin-4, synaptopodin and HSP27, demonstrating the importance of a dynamic actin cytoskeleton in maintaining a functioning intact filtration barrier [265].

Cytoskeleton rearrangement is crucial for tissue remodelling both during kidney development [267] and as a result of pathological conditions [264, 268]. The major cytoskeleton components in foot processes consist of dense actin filament bundles, found predominantly at the central portion of the cytoplasm above the level of the slit diaphragm or cortical actin filament network at the cell periphery, sparse in the apical cytoplasm and dense in the basal cytoplasm [268].

α-actinin-4

α-actinin-4 is an actin binding protein with a role in cross-linking actin filaments into bundles and anchoring actin to the plasma membrane. Induction of α-actinin-4 precedes foot process effacement in the experimental PAN nephrosis rat model [122]. α-actinin-4 has also been shown to be redistributed in nephrotic rats [121] and mutations in the gene encoding α-actinin-4, ACTN4, have been linked to the familial autosomal dominant form of FSGS [123, 269]. In the PAN nephrotic rat model, α-actinin-4 appears to be a target protein for PAN nephrotoxicity [270].

There is also growing evidence that alterations to the expression and/or localization of podocyte cytoskeletal proteins, including α-actinin-4, are responsible for the observed foot process effacement characteristic of nephrotic syndromes [122, 270].

α-actinin-4 can interact with components of the integrin complex at the GBM and with the β-catenin molecule of the SD complex, hence α-actinin-4 may link the two compartments of the FP together, thereby providing a molecular explanation for the observation that the actin cytoskeleton serves as the "common final pathway" organizing FP

effacement independent of the underlying cause of podocyte damage [145, 265].

Synaptopodin

Synaptopodin is a novel actin binding protein which is highly expressed in podocytes [106, 271]. Although synaptopodin was first identified in 1991 and subsequently characterized in 1997 by Mundel *et al.* [107] the precise molecular role for synaptopodin has not been determined.

Barisoni *et al.* and Kemeny *et al.* reported loss of synaptopodin expression in collapsing focal segmental glomerulosclerosis and HIV nephropathy [108] and the early stages of idiopathic focal segmental glomerulosclerosis [109]. In a later study Srivastava *et al.* [110] showed the expression levels of synaptopodin decrease with increasing severity of nephrotic syndrome. Srivastava also proposed that changes in synaptopodin expression is a secondary effect that reflects the magnitude of damage and as such synaptopodin could be a potential marker to predict steroid response and podocyte damage in idiopathic nephrotic syndrome including minimal change disease (MCD) and focal segmental glomerulosclerosis (FSGS).

Hsp27

Small heat shock protein hsp27 is a stress protein with many reported functions including resistance to thermal and metabolic stress, signal transduction, protection from apoptosis and as a molecular chaperone, however it's most well characterized function is that of actin polymerization regulator. Hsp27 has been shown to be an actin-associated protein [272] that inhibits actin polymerization both *in vivo* [273] and *in vitro* [274]. Its inhibition of polymerization has been correlated to its phosphorylation state [275, 276].

Based on the increase in expression and phosphorylation of hsp27 observed in rats with PAN induced foot process effacement [13] it has been hypothesized by Smoyer *et al.* [266] "that hsp27 via regulation of

the actin cytoskeleton has an important role in regulating both normal podocyte structure and the dramatic structural changes in podocytes that occur during nephrotic syndromes" [277].

Podocalyxin

Podocalyxin associates with the actin cytoskeleton through an interaction with NHERF-2 and ezrin. Disruption of this linkage could be a cause of glomerular disorders and serve as viable targets for future studies [44, 45].

NHERF-2 is a Na^+/H^+ exchange regulatory factor which is strongly expressed in the glomerulus [53]. Podocalyxin binds to the PDZ2 domain of NHERF-2 via its C-terminal PDZ binding domain DTHL. In turn NHERF-2 binds to the N-terminus of ezrin via its C-terminal ERM-binding domain. Ezrin links the complex to the actin cytoskeleton via its C-terminal actin binding domain (Figure 6.1) [15, 45].

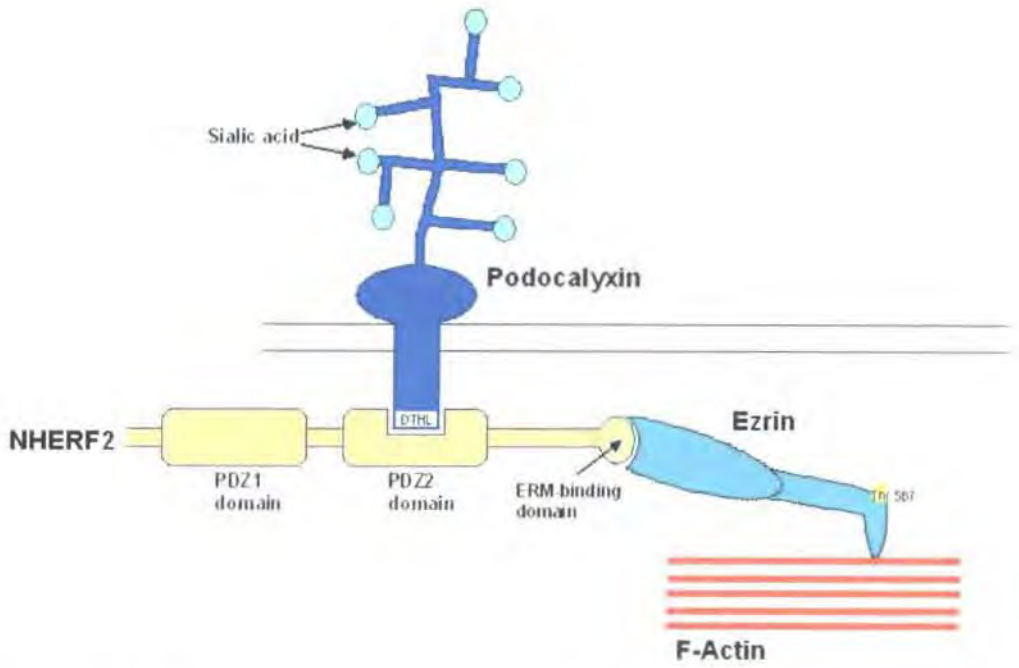

Figure 6. 1. The components of the podocalyxin-actin complex. Adapted from Fig.10 Takeda *et al.* [45]

Ezrin

Ezrin is a member of the ezrin/radixin/moesin family more commonly known as the ERM family, which is a subfamily of the protein 4.1 superfamily. ERM proteins have been classically defined in the literature as membrane–cytoskeleton linkers. Ezrin like moesin and radixin interacts with the actin cytoskeleton and the plasma membrane either directly or indirectly through the FERM domain [46]. Members of the ERM family are believed to be critical for cell–cell adhesion and microvilli formation and are characteristically located in dynamic structures that undergo changes in cell shape [47].

ERM proteins are maintained within the cytoplasm in an inactive conformation [49]. To generate the active conformation of ERM proteins requires the binding of PIP2 and the phosphorylation of a conserved threonine residue in the C-terminus ERM associated domain (C-ERMAD), T567 in the case of ezrin [50].

Although members of this family have very striking structural and functional similarities, there is a major difference in tissue distribution, ezrin is located primarily in epithelial cells while moesin primarily in endothelial cells. This difference suggests that these proteins may have adapted distinct functions for these specific cell types [47].

Ezrin is specifically expressed by podocytes in the glomerulus. Ezrin protein expression is altered in glomerular disease; there is a decrease in the puromycin aminonucleoside model of nephrosis but an increase in the passive Heymann model. However ezrin mRNA levels remained constant in both PAN and PHN glomeruli as determined by *in situ* hybridization [47]. Podocytes undergoing injury and/or proliferation showed strong ezrin expression. The observation that ezrin expression was highest in mitotic, polynucleated podocytes or podocytes completely or nearly detached from the GBM may reflect the need to adapt to injury. If adaptation fails podocytes may become completely detached round up and die. This maybe of relevance in glomerular disease, since loss of

podocytes is believed to lead to glomerulosclerosis and progressive renal failure [47, 145, 278].

In this chapter we will analyze the effects of PAN treatment on the cytoskeletal structure of NRK cells, and confirm the suggested link between podocalyxin and the actin cytoskeleton through ezrin.

6.2. Ezrin Expression

Briefly NRK cells were cultured on 90 mm tissue culture dishes as normal. Protein was extracted from each PAN dose overnight by acetone precipitation. Each protein sample was quantified by a Bradford Assay and equal volumes of 10µg of protein were subjected to electrophoresis. Proteins were transferred to a nitrocellulose membrane and incubated with ezrin antibody overnight, subsequently washed and incubated with secondary antibody. Proteins were detected in the dark by ECL (see section 2.3 for full method).

A dose dependent reduction in ezrin protein expression was observed at both 48 and 72 hours, (Figure 6.2), as has been reported in the puromycin aminonucleoside model of nephrosis by Hugo *et al.* [47]. At 72 hours we observed slightly increased expression at 10µg/ml, which could either be caused by injured cells having greater ezrin expression or could be an artefact of the overall increased protein expression at this dose.

We also examined the sub-cellular localization of ezrin after sub-cellular fractionation of control (0µg/ml) and PAN treated (80µg/ml) cells after 72 hours. Briefly equal NRK cell numbers were subjected to homogenisation followed by fractionation to yield membrane fractions, each fraction was re-suspended in 100µl HES buffer, 10µl of each fraction was loaded per well for Western blotting and probed with Ezrin as previously described. Ezrin was present in all fractions, with greatest expression in the low density microsome fraction. The same pattern of expression was evident in both control and PAN treated cells. In PAN treated cells overall expression was reduced significantly in all fractions except the PM fraction which remained constant. Ezrin expression was almost completely lost from the homogenate and high density microsome fractions (Figure 6.3). The overall distribution profile of ezrin was not altered in response to PAN treatment.

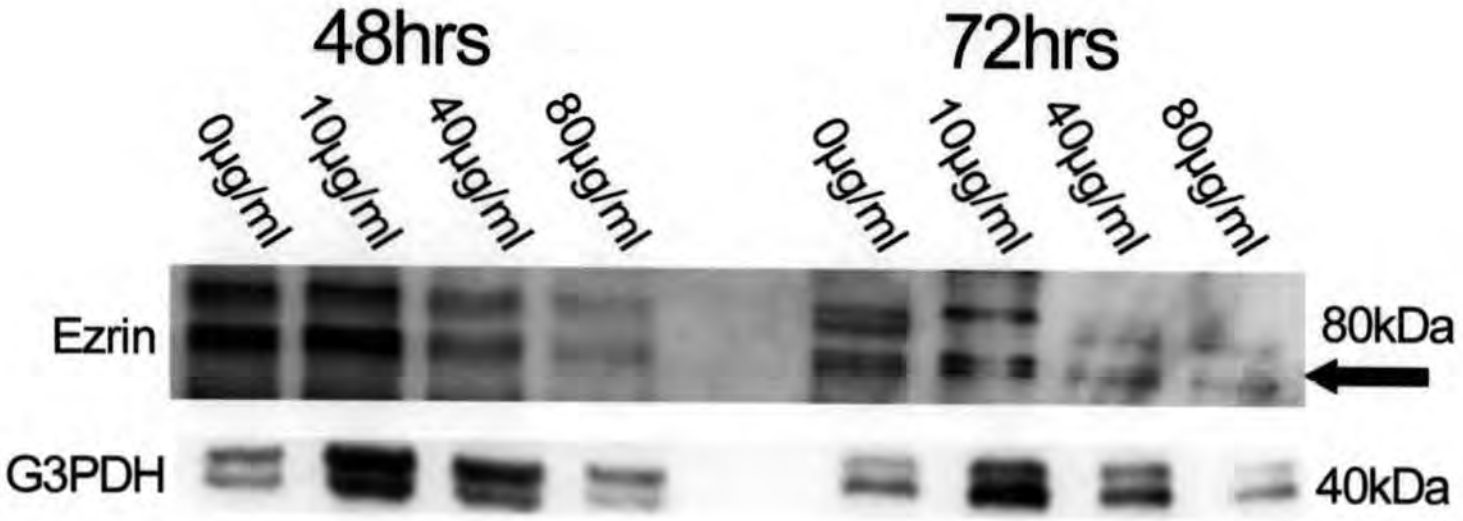

Figure 6. 2. Ezrin expression is reduced in NRK cells after PAN treatment, as determined by Western blotting.

10µg total protein was loaded per well. Ezrin expression shows a dose-dependent reduction after PAN treatment.

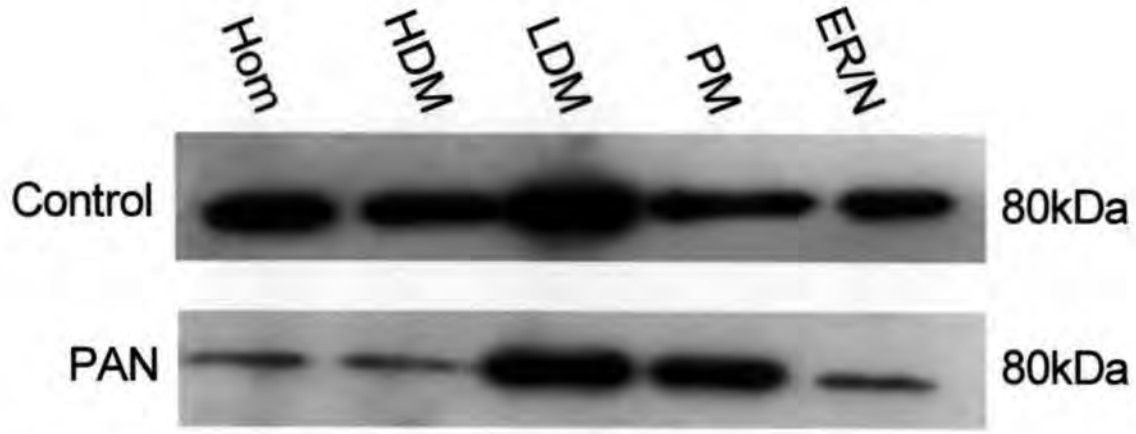

Figure 6. 3. Sub-cellular fractionation of ezrin after PAN (80µg/ml 72hrs) treatment. HDM High density microsome, LDM Low density microsome, PM Plasma membrane, ER/N endoplasmic reticulum/nuclei fractions. 10µl of each sample was loaded per well.
The overall distribution profile of ezrin was not altered in response to PAN treatment.

6.3. Ezrin Localization

Ezrin localization was examined in NRK cells by immunofluorescence microscopy at each PAN dose, as previously described.

The localization of ezrin was unaffected by PAN treatment at the lowest dose (10µg/ml) at both 48 and 72 hours. What was noticeable was the increase in cell size at this dose, the cells have approximately doubled in size (Figure 6.4). The morphology of the NRK cells changes again at the mid (40µg/ml) and high (80µg/ml) PAN treatments. At 48 hours the cells become smaller and more elongated and at the points of elongation there is an increase in the staining of ezrin intensity (highlighted by arrows), this is probably due to the level of ezrin expression remaining constant but being expressed in a smaller cell area resulting in the increased intensity and not a true reflection of an increase in ezrin expression. After 40µg/ml PAN treatment for 72 hours the cells have remained larger in size than in control (0µgml) cells.

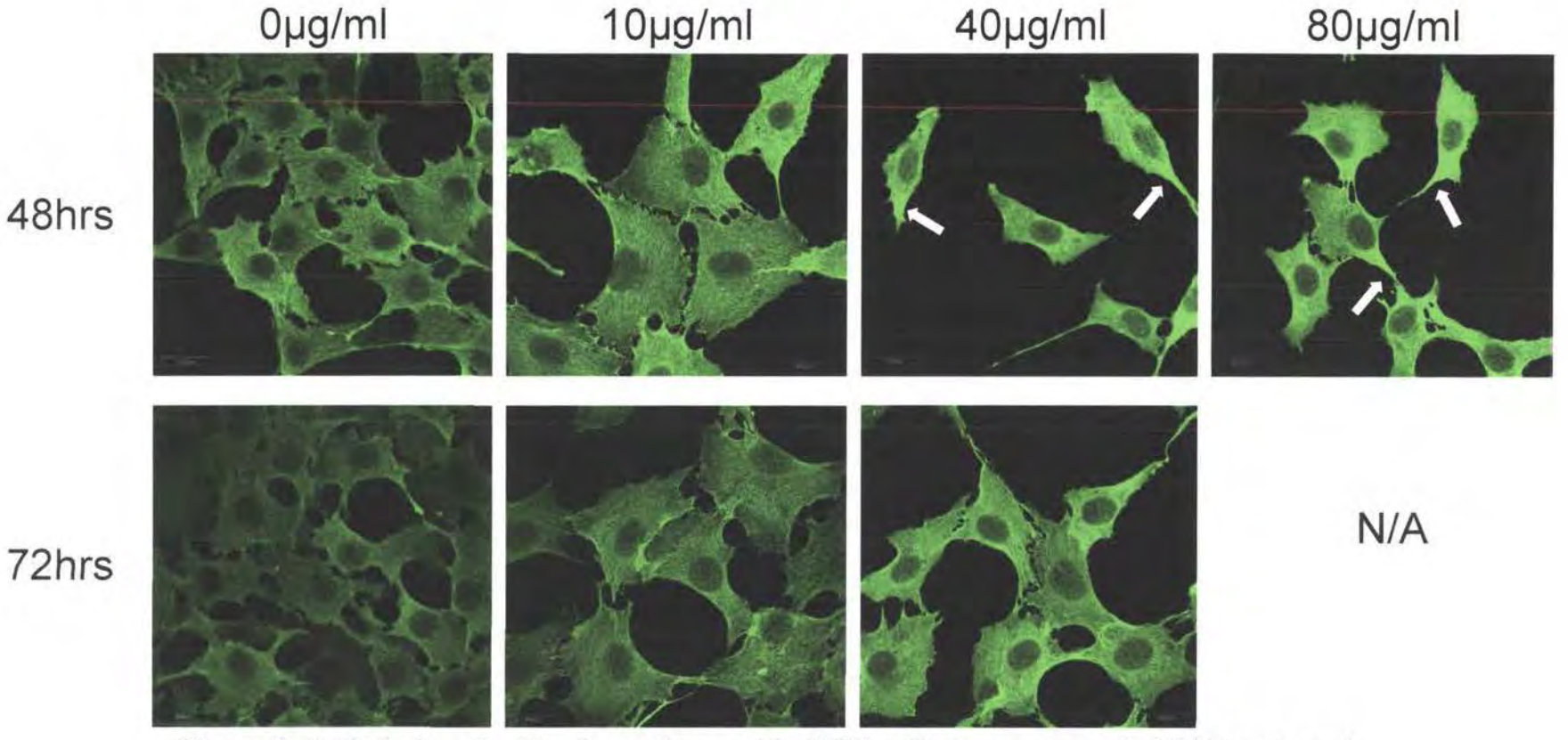

Figure 6. 4. Ezrin localization is unchanged in NRK cells in response to PAN treatment.

Figure 6.4. Ezrin localization is unchanged in NRK cells in response to PAN treatment.
NRK cells (p4) were cultured for 48hrs in D-MEM + 10% FBS. After 48hrs the media was replaced with media containing PAN. The cells were fixed/permeabilized and stained with a mAb to localize ezrin. The cells were then imaged by confocal microscopy at 519nm. Images are merged composite images of layered sections throughout the cell, magnification x100. All microscope and laser settings have been kept constant to allow an accurate comparison of staining intensity. Scale bar 20μm. Arrows show increased ezrin staining at tips of cells.

6.4. Cytoskeletal changes as a result of PAN treatment.

The actin cytoskeleton ultimately determines and maintains the structure of the filtration slits. The actin cytoskeleton has been shown to change from co-ordinated stress fibers into a dense network with foot process effacement and loss of the filtration slits in Masugi Nephritis [264] but cytoskeletal rearrangement is believed to be one of the major causes of foot process effacement in nephrotic syndromes [144, 145, 149, 265]. Proteins regulating the actin cytoskeleton are of critical importance for sustained glomerular filtration [45, 265, 266].

We used antibodies to actin and tubulin to visualize the effects of PAN treatment upon the cytoskeleton by immunofluorescence techniques.

At control (0μg/ml) and low (10μg/ml) PAN doses after either 48 or 72 hours, actin is visualized in a co-ordinated structure consisting of stress fibers which run longitudinally through the cells, this is especially easy to see after 72 hours (Figure 6.5). At mid (40μg/ml) and high (80μg/ml) doses PAN resulted in a reduced level of expression of actin and a change in the actin cytoskeletal architecture was clearly visible. At the mid and high PAN doses actin distribution changes from co-ordinated stress fibers to a dense network of fibers with no defined structure (Figure 6.5). The disruption of the actin cytoskeleton is highlighted in Figure 6.6. There appears to be reduced staining of the longitudinal stress fibers and the actin staining appears weakly at the cell periphery. Therefore PAN treatment is causing a structural rearrangement of the actin cytoskeleton.

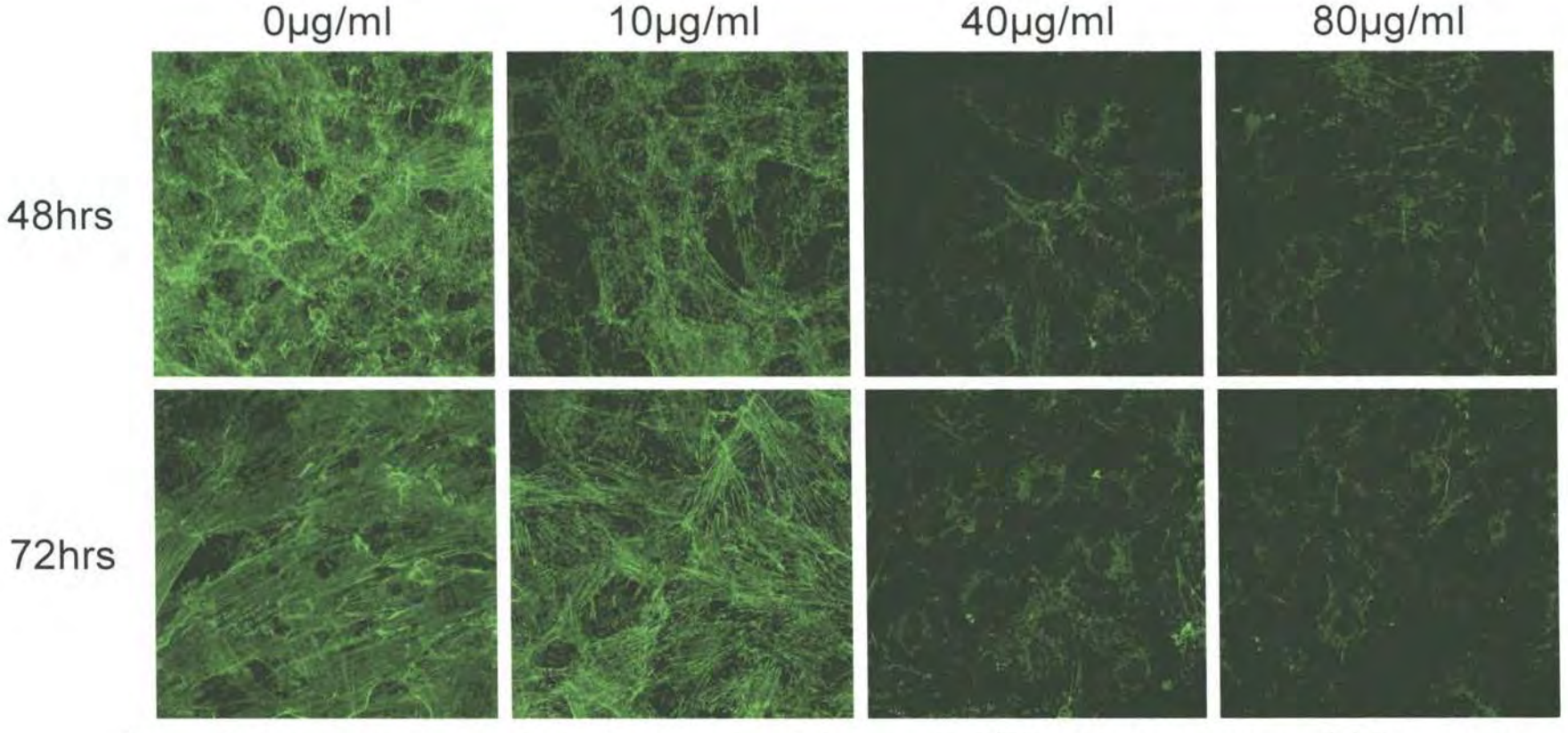

Figure 6. 5. Actin expression is both reduced and disrupted in NRK cells in response to PAN treatment.

Figure 6.5. Actin expression is both reduced and disrupted in NRK cells in response to PAN treatment.
NRK cells (p7) were cultured for 48hrs in D-MEM + 10% FBS. After 48hrs the media was replaced with media containing PAN. The cells were fixed/permeabilized and stained with a mAb to localize actin. The cells were then imaged by confocal microscopy at 519nm. Images are merged composite images of layered sections throughout the cell, magnification x100. All microscope and laser settings have been kept constant to allow an accurate comparison of staining intensity. Scale bar 20μm.

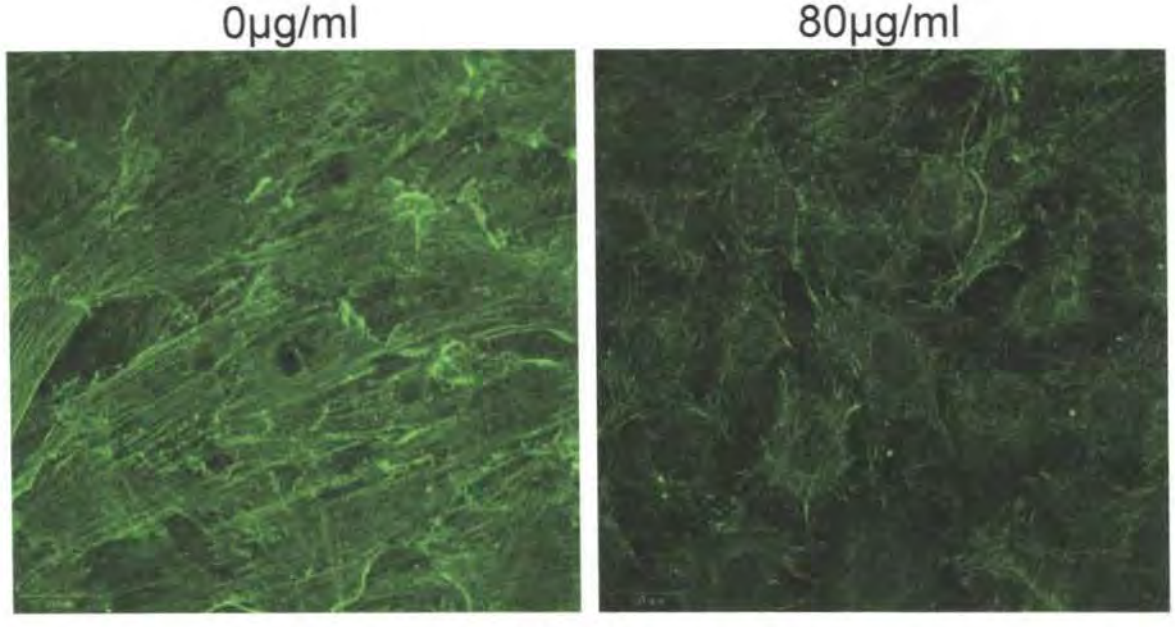

Figure 6. 6. Enlarged image highlighting the disruption to actin caused by PAN treatment.

NRK cells (p7) were cultured for 48hrs in D-MEM + 10% FBS. After 48hrs the media was replaced with media containing 80µg/ml PAN and cultured for 72hrs. The cells were fixed/permeabilized and stained with a mAb to localize actin. The cells were then imaged by confocal microscopy at 519nm. Images are merged composite images of layered sections throughout the cell, magnification x100. All microscope and laser settings have been kept constant to allow an accurate comparison of staining intensity. Scale bar 20µm.

The microtubule cytoskeleton was also affected by PAN treatment but the results I obtained were more ambiguous. Overall the tubulin expression was reduced and altered by PAN treatment (Figure 6.7). Initially tubulin was expressed throughout the cell with a concentration of expression around the nucleus 0µg/ml 48 hours. However there was a huge increase in expression at the low PAN (10µg/ml 48 hours) dose. This increase in expression was so large the microscope laser settings had to be reduced to visualize the expression of tubulin accurately. I can not account for this variation in staining expression, but the results were consistently obtained at this dose and time point. At 72 hours 10µg/ml PAN treatment resulted in the lowest expression observed. At 40µg/ml and 80µg/ml tubulin expression was reduced from control levels and also shifted in expression from within the cell to the cell periphery. A similar pattern of shifting expression was observed when the cells were treated for 72 hours. With the cell filapodia at 80µg/ml showing the highest levels of expression (see Figure 6.7 arrows).

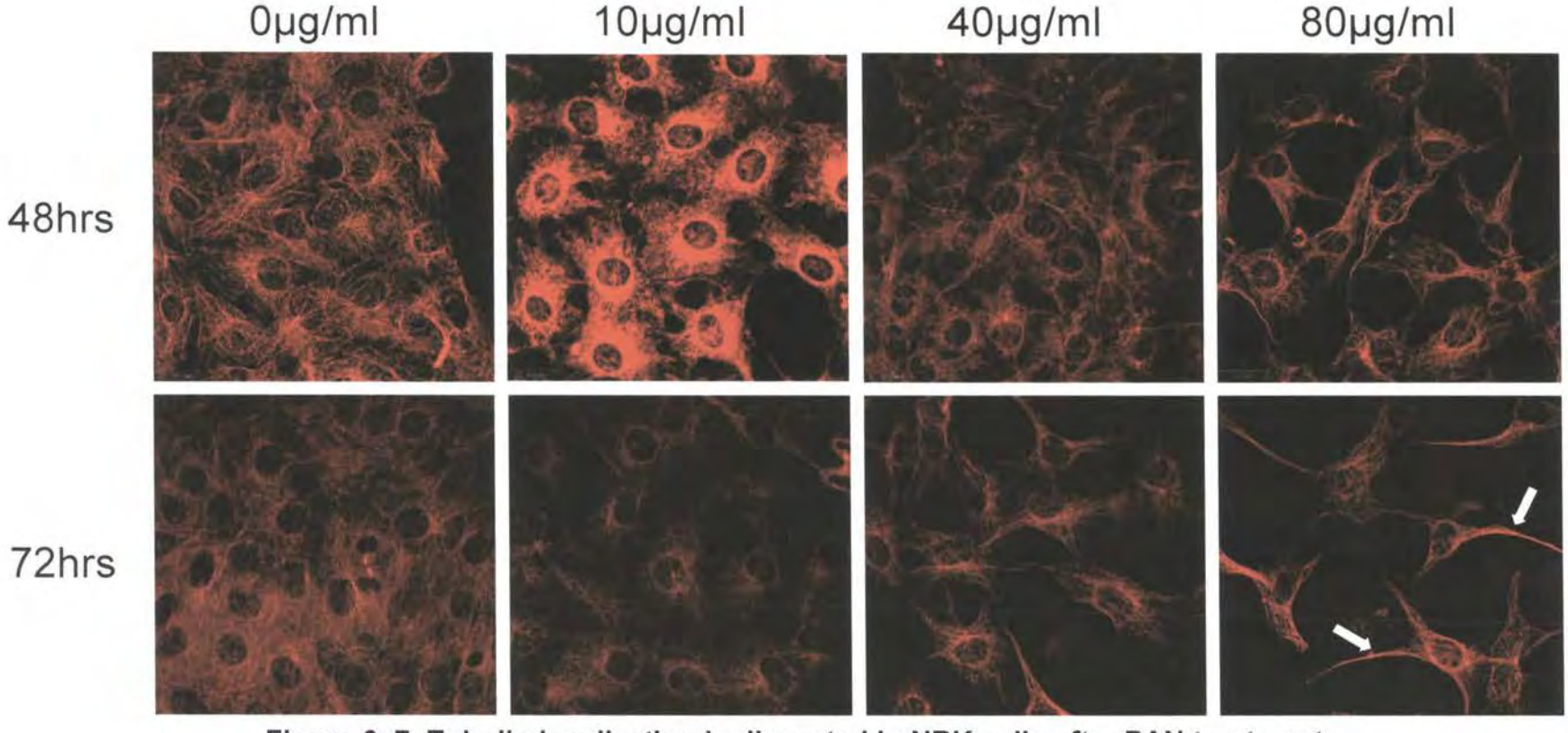

Figure 6. 7. Tubulin localization is disrupted in NRK cells after PAN treatment.

Figure 6.7. Tubulin localization is disrupted in NRK cells after PAN treatment.
NRK cells (p5) were cultured for 48hrs in D-MEM + 10% FBS. After 48hrs the media was replaced with media containing PAN. The cells were fixed/permeabilized and stained with a pAb to localize tubulin. The cells were then imaged by confocal microscopy at 519nm. Images are merged composite images of layered sections throughout the cell, magnification x100. All microscope and laser settings have been kept constant to allow an accurate comparison of staining intensity. Scale bar 20µm.

6.5. Conclusions

Regardless of the underlying cause/disease the initial events of podocyte injury are consistently characterized by molecular alterations to the slit diaphragm or by a visible reorganization of the foot process structure [144-146, 149]. It has been suggested that there is a common pathomechanism involved in podocyte injury. Identification of this mechanism is vital to the development of treatments which would be effective against all causes of podocyte damage. It is believed that the cytoskeleton is a key target leading to podocyte injury pathways and as such the cytoskeleton is regarded as the target for treatment.

Reorganization of the actin cytoskeleton has been shown to be one of the four major causes of foot process effacement [14, 144-146, 149]. However the other causes have also been linked to the cytoskeleton and so the cytoskeleton is a key step in podocyte injury either directly or indirectly. To this end we examined how the actin cytoskeleton is affected by PAN treatment in our cellular model which mimics PAN nephrosis.

We examined the expression of ezrin, part of the multimeric protein complex which links podocalyxin to the actin cytoskeleton [15, 44]. The multimeric protein complex consisting of podocalyxin, NHERF2 and ezrin has previously been shown to be disrupted during podocyte injury [45]. We have previously observed a reduction in podocalyxin protein expression in our cellular model of PAN nephrosis (Section 5.4).

It was found that ezrin showed a dose dependent decrease in protein expression by Western blotting at both 48 and 72 hours, corresponding to the previously published data by Hugo *et al.* [47]. No change was found in the sub-cellular distribution profile of ezrin. This appears to be in contrast to the distribution profile of podocalyxin which was predominantly expressed in vesicles with little expression in the plasma membrane fraction.

Ezrin expression became increased at the cell periphery and at filapodia at several PAN doses (40µg/ml and 80µg/ml). However this maybe the result of the change in cell morphology due to fewer numbers of cells being present as a result of a loss of cell adhesion rather than a direct response to PAN treatment. The membrane filapodia maybe an adaptive response to try to maintain cell – cell contacts to increase survival. Podocalyxin also showed increased expression when cells were elongating and branching and so ezrin and podocalyxin maybe showing a similar pattern of expression due to the linkage between them which has been proposed not to be disrupted in PAN nephrosis [45].

The actin cytoskeleton showed a dramatic change from an organized structured array of fibers running longitudinally through the cells in control and low (10µg/ml) PAN dosed cells to a more disorganized dense network of fibers at the mid (40µg/ml) and high (80µg/ml) PAN doses, which accounts for the greatly reduced staining observed for F-actin. This dramatic change in the cytoskeleton was first reported by Shirato *et al.* [264] in 1996 and last year by Oh *et al.* [265].

In conclusion podocalyxin and ezrin show similar patterns of expression, which differ from the expression of actin, which supports the model proposed by Takeda *et al.* [45] that the podocalyxin/NHERF2/ezrin complex remains intact and separates from the actin cytoskeleton during PAN nephrosis. However we were unable to prove this was the case as we were unable to perform dual labelling studies with podocalyxin and ezrin as they were both monoclonal antibodies.

The dramatic change in the actin cytoskeleton structure suggest that reorganization of the actin cytoskeleton maybe a major cause of foot process effacement in PAN nephrosis. Although other models of nephrosis, such as the PHN rat model and Masugi nephritis are also characterized by a less severe disruption to the actin cytoskeleton [261, 264, 265, 279, 280].

There is indirect/circumstantial evidence that the actin cytoskeleton is involved either directly or indirectly in all causes of foot process effacement. Mundel *et al.* [145] and Oh *et al.* [265] have provided a molecular explanation of how the actin cytoskeleton serves as the "common final pathway" organizing FP effacement independent of the underlying cause of podocyte damage, based upon the ability of α-actinin-4 being able to interact with both the integrin complex at the GBM and with components of the SD complex and hence be a link between the two compartments of the foot processes. Furthermore I don't believe it is possible to have a change in cell shape as substantial as the effacement of foot processes and the loss of slit diaphragms without the cytoskeleton being involved.

Chapter 7.

Final Discussion

Overview

The main aim of my thesis was to develop an *in vivo* cellular model which mimics PAN nephrosis and to use this model to identify and characterize any biomarkers of nephrotoxicity. I have successfully developed a cellular model which mimics PAN nephrosis, an experimental model for human minimal change nephropathy and have used this model to analyze the expression of two potential biomarkers of nephrosis, podoplanin and podocalyxin, and to identify other potential biomarkers of nephrosis.

There have been very few studies based on *in vitro* models of PAN nephrosis and the majority of studies used isolated rat podocytes. In our study we used a rat kidney fibroblast (NRK) cell line. Our model combines the key observations of previous *in vitro* models [181-184] with that of the *in vivo* model used at GlaxoSmithkline. Our model exhibited the previously reported effects of PAN nephrosis *in vitro*; cells lost the ability to adhere to the tissue culture plastic but the cells which detached were found to be viable. We also observed a dose dependent reduction in gene expression of two podocyte specific genes, podoplanin and podocalyxin, but other genes expressed in the kidney were not affected. Although we did not examine ultrastructural changes in cell shape we did observe changes in cell morphology within our cellular model. These observations provide the evidence that we have successfully developed a cellular model which mimics PAN nephrosis.

Using the cellular model, I examined the expression and distribution of two podocyte specific proteins, podoplanin and podocalyxin, potential nephrotoxic biomarkers. Podoplanin and podocalyxin were initially chosen as they had been marked as potential biomarkers after a GlaxoSmithkline nephrotoxicity study showed they were down-regulated in rats in response to PAN treatment. Our studies showed that podoplanin and podocalyxin were down-regulated at the mRNA level. Podoplanin was down-regulated in a dose-dependent manner after exposure to PAN for 72 hours while podocalyxin showed a dose-dependent decrease in expression after 48 and 72 hours. We also found a significant decrease in

protein expression for podoplanin and podocalyxin at the highest dose tested only. There were no significant changes in protein localization of podoplanin and podocalyxin as a result of PAN treatment as determined by immunofluorescence microscopy however podocalyxin did show a change in sub-cellular localization after the highest PAN (80μg/ml 72hrs) treatment.

Mechanisms of Nephrosis

It has been suggested that there is a common pathomechanism involved in podocyte injury. Identification of this mechanism is vital to the development of treatments which would be effective against all causes of podocyte damage. There is indirect evidence that the actin cytoskeleton is involved either directly or indirectly in all causes of foot process effacement. Mundel *et al.* [145] and Oh *et al.* [265] have provided a molecular explanation of how the actin cytoskeleton serves as the "common final pathway" organizing FP effacement independent of the underlying cause of podocyte damage, based upon the ability of α-actinin-4 being able to interact with both the integrin complex at the GBM and with components of the SD complex and hence be a link between the two compartments of the foot processes.

Our model of nephrosis highlighted dramatic changes in the cytoskeleton in response to PAN treatment, adding experimental results to the belief that cytoskeletal changes lead to PAN nephrosis. However this is just one form of nephrosis and so based on these results it is impossible to prove that the cytoskeleton is the "common final pathway" of nephrosis. I personally believe that the cytoskeleton is the final part of the pathways to nephrosis, as you can not have FP effacement without changing cytoskeletal dynamics. More studies are required to examine the organisation of the cytoskeleton in different models of nephrosis resulting from differing mechanisms to definitively show that cytoskeletal changes is the "common final pathway" and hence is the key to developing a universal treatment of nephrosis.

Biomarkers

As for whether podoplanin and podocalyxin are nephrotoxic biomarkers, we must first consider what constitutes a biomarker. A biomarker has been defined by the Biomarkers Definitions Working Group as "a characteristic that is objectively measured and evaluated as an indicator of normal biological processes, pathogenic processes, or pharmacological responses to a therapeutic intervention" [186]. Or put more simply a biomarker is a molecule that indicates an alteration in the physiological state in response to disease or drug treatment [281]. What also must be considered is how easy it is to monitor the biomarker, the most accurate biomarker is of no use if it can't be accessed in a non-invasive manner [282]. Ideally the attributes of a biomarker as defined by the FDA [283] should include:

1. **Clinical relevance**. The biomarker provides evidence to support its use, it is influenced by exposure to a drug which is believed to be related to the intended clinical effect.
2. **Sensitivity and specificity to treatment effects.** The ability to detect the intended change in the target population via a given mechanism.
3. **Reliability.** The ability to analytically measure the biomarker with acceptable accuracy, precision and reproducibility.
4. **Practicality.** How invasive a protocol to obtain the required measurements.
5. **Simplicity.** Can be utilized without the need for sophisticated equipment or skills.

For the case of podoplanin I would have to say it is not an accurate biomarker of nephrotoxicity in that its responses to the severity of modelled nephrosis was not sufficiently dose-dependent. Podocalyxin could be used as genetic biomarker of nephrotoxicity as it showed a good range of dose-dependent expression in response to PAN treatment. However I'm not sure how non-invasive it is to monitor gene expression

and so it may fail at this hurdle to become a clinical biomarker, it could be used as a diagnostic biomarker of nephrosis in research.

Kanno *et al.* [284] used an ELISA test to quantify the levels of urinary sediment podocalyxin to act as a reliable and more accurate marker, than podocyte number, for the estimation of severity of glomerular injury.The patients in this study were children suffering from a variety of glomerular diseases including minimal change nephrosis, membranous nephropathy and IgA nephropathy. As this study covered several diseases it confirms that podocalyxin has a use as a biomarker of glomerular disease.

Overexpression of podocalyxin has been found to be tightly correlated with a poor outcome in a distinct subset of breast tumors and it has subsequently been shown that podocalyxin overexpression is a novel predictor of breast cancer [285].

Our study did highlight other potential research biomarkers of nephrotoxicity. Integrin α3 was found to be down-regulated at the protein level at mid and high doses of PAN treatment. With further study the range of doses which illicit this response could be expanded to give a good dose-dependent range. Laminin β2 and actin localization were found to be severely disrupted by PAN treatment but this is not a quantifiable marker of severity of nephrosis. A further characteristic which could be used as a marker of nephrotoxicity is the number of cells which loose their ability to adhere. It has been proposed that podocyte excretion could be used as a marker to estimate severity of glomerular injury and a predictor of disease progression [207, 208]. Urine samples can be collected from patients and analysed to determine podocyte number, which would offer a non-invasive determination of the severity of glomerular injury, thereby acting as a useful clinical biomarker.

This study only examined one form of nephrotic injury and so any potential biomarkers identified from this study would need to be examined

in other forms of nephrosis arising from different mechanisms e.g. diabetic nephrosis.

There has been varying levels of success in identifying and developing biomarkers of renal disorders, including acute renal failure, chronic renal failure and polycystic kidney disease [187]. Kidney Injury Molecule 1 (KIM-1) is to date the only nephrotoxic biomarker to be identified. KIM-1 has been shown to be expressed in three models of nephrotoxicant-induced kidney injury in rats [200], in addition to seeing increased expression, the KIM-1 ectodomain and fragments of the domain were found in the urine of each model. This indicated that injury resulted in shedding of the ectodomain which would allow for non-invasive monitoring of nephrotoxicity [200]. Therefore suggesting that KIM-1 is a general biomarker of nephrotoxic injury and maybe used for detection and monitoring of nephrotoxicants as well as for monitoring disease states [200].

There is a high level of interest in biomarkers within the pharmaceutical industry, which is faced with increasing research and development costs, and with the growing pressure to accelerate the rate of bringing new drugs to the market. The biggest cost in drug development in financial and time terms is the late point at which the compounds fail due to safety and efficacy concerns. This cost has been recently estimated to be a quarter of the overall cost of drug development at approximately $200 million [282, 286]. The earlier these common biologically-driven failure modes can be detected, the more likely the cost of failure can be reduced [282]. In this context biomarkers show considerable promise for improving the efficiency of drug development [283]. The potential benefit of developing reliable and specific biomarkers that act as early predictors of efficacy or long-term toxicity is to allow earlier, more robust drug safety and efficacy measurements thereby reducing attrition of drugs during clinical phases of development and hence reduce the overall time, size and cost of drug development [281, 282, 287].

The development of new pharmaceutical therapies can be improved with the application of biomarkers in the drug discovery phase and in preclinical and clinical safety assessment phases [288]. In drug discovery the compound screening process can benefit from biomarkers of toxicity. These biomarkers only require internal evaluation within the pharmaceutical company and have inherent intellectual property value for pharmaceutical companies [288]. In preclinical and clinical safety assessment, biomarkers as surrogate endpoints can reduce the time and costs involved in testing but biomarkers must conform to the strict US Food and Drug Administration (FDA) regulations.

Pharmaceutical interest in using biomarkers as surrogate end-points to reduce sample size and duration of phase 3 clinical trials has been high. Actually very few biomarkers have ever attained the status of surrogate end-point for drug approval due to the very stringent regulations of biomarker validation. This fact reflects an underlying biological complexity that makes it unlikely that a biomarker will capture all of the desired and undesired effects of a treatment in a quantitatively predictive manner. A high level of stringency is required when a biomarker is used as a surrogate end-point for a clinical outcome and is used as the basis for regulatory approval of an application for a new drug. However this does not reduce the value of biomarkers in drug development; rather, they must be used in a more sophisticated manner [289]. Biomarkers need not be as rigorously validated in order to play other important roles in drug development, such as improving understanding of disease mechanisms, expediting the development of new drugs and addressing regulatory concerns [283].

In general biomarkers have a much wider range of uses than surrogate end-points. Highly innovative biomarkers used primarily for internal decisions early in drug development do not need to be as thoroughly evaluated as those selected as end-points in clinical trials [289].

There is a general unawareness of the complexity involved in developing biomarkers for the marketplace [289]. Before a biomarker can be introduced to the market, it must be successfully evaluated and validated, this involves costly extended clinical studies, and so the issues regarding medical need and potential return of investment must be considered [281].

Typically validation of a biomarker takes into account;

1. **Sensitivity.** Is the biomarker sensitive enough to reflect a meaningful change in important clinical end-points.
2. **Specificity.** The extent to which the biomarker explains the changes of the clinical end-point.
3. **Reliability.** Bioanalytical assessment of the biomarker in terms of accuracy, precision, reproducibility, range of use and variability.
4. **Probability of false positives.**
5. **Probability of false negatives.**
6. **A PK-PD (pharmacokinetic-pharmacodynamic) model is required**. This establishes the correlation between changes in the biomarker and changes in drug exposure.

There are also patient factors, (age, gender, race and genetics), disease factors (stage and progression) and drug factors (metabolism) that also need to be considered as they may modify treatment effects upon biomarkers but are not directly effected by the treatment [283].

Although biomarkers have the greatest value in early efficacy and safety evaluations, for example providing a basis for lead compound selection or dosing, as well as being substitutes for clinical responses. They also have applications as diagnostic tools for the identification of patients, and disease progression, as an indicator of disease prognosis and for predicting and monitoring the response to therapeutic intervention as surrogate end-points [186] [282].

The use of genomic biomarkers could have an earlier impact on compound efficacy and an assessment of developability hence increasing the probability of success in the preclinical studies by identifying profiles characteristic of unwanted toxicity in early drug candidate screening [287].

Future Experiments

As mentioned above the characteristics I have identified as potential biomarkers are only biomarkers for this model of PAN induced nephrosis, if they are to have a true value as biomarkers of nephrotoxicity they must be shown to be affected in all forms of nephrotic injury. Therefore ideally I would like to replicate theses experiments in other models of nephrotic injury particularly a model of diabetic nephropathy, as this is believed to have a different mechanism of nephrosis. Alternatively these studies could prove a common mechanism exists in all forms of nephrotic injury.

It would also be beneficial to examine a larger dose range of PAN to see at exactly what dose PAN is having an effect. The dose range I chose showed a spectrum of nephrotic characteristics from mild at the low (10μg/ml) dose to severe at the high (80μg/ml) dose, but there is a lot of leeway in between these doses. These dose ranging points are very limited and I think a dose range of 5, 10, 20, 40, 60, 80, 100μg/ml of PAN would give a more detailed picture of the effects of PAN. I did look briefly at a lower PAN dose of 5μg/ml after 24 and 48 hours exposure but found no change in cell morphology and very limited changes in podoplanin and podocalyxin expression, but I did not examine changes in protein expression or localization, which would be very interesting as several proteins showed increased expression after 10μg/ml PAN treatment. I believed that 80μg/ml was the maximal dose I could use to gain enough cell numbers to carryout my experiments, but this wasn't tested.

Similarly I think a larger time course is required to give a true representation of the effects of PAN and to prove if as I suggested for integrin α3 expression that there is a recovery period between 48 and 72

hours. A time course of 24, 48, 60 and 72 hours would address the issue of recovery and show any earlier effects of PAN treatment.

I would also like to use this model of PAN nephrosis to examine other podocyte proteins which have been shown to be differentially expressed in kidney diseases. Nephrin and podocin have both been identified as being genes responsible for forms of congenital nephrotic syndromes, my initial studies examining nephrin gene expression were inconclusive but suggested there was no change in nephrin expression. Podocin expression did show a dose dependent change in expression as a result of PAN treatment and this resulted in changes in protein localization in steroid-resistant nephrotic syndrome (SRNS).

If I could change any part of the work I have done, I would have ideally used a rat podocyte cell line. This was not feasible as a podocyte cell line is not commercially available. In addition, I do not have the experience, time or facilities to generate a podocyte cell line from lab animals. But as it was it worked out as I was able to generate a model of nephrosis using NRK cells which may not be as accurate as using a podocyte cell line but these cells are easier to use and therefore could be more beneficial if it was to be developed into an assay to test for compound nephrotoxicity. I would also have liked to have given definitive quantified results for varying protein localization levels.

Appendix 1

Mowiol Mountant: 2.4 g MOWIOL 4-88, 6 g Glycerol mixed well by stirring. Add 6ml of dH_2O, leave for 4 hours at room temp. Add 12ml 0.2 M Tris pH 8.5 and heat to 50°C for 10 minutes. Centrifuge 5000g for 15 minutes. Add DABCO to 2.5% and 5 µl DAPI 2 mg/ml stock to 10mls. Aliquot into sterile micofuge tubes and store at -20°C.

HES Buffer: To 500ml dH_2O add the following; 255 mM Sucrose, 20 mM HEPES and 1mM EDTA, pH to 7.4 and store at 4°C.

Cell Lysis Buffer: 50 mM Tris.HCl pH 7.5, 150 mM NaCl, 1% NP40, 0.25% Sodium deoxycholate and 1X Protease Inhibitor Cocktail.

Protease Inhibitor Cocktail: 104 mM AEBSF, 80 µM Aprotinin, 2 mM Leupeptin, 4 mM Bestatin, 1.5 mM Pepstatin A, 1.4 mM E-64

Protein Sample Buffer: 8 M urea, 2 M Thiourea and 4% CHAPS

2X Sample Buffer: 0.303 g Tris base, 0.40 g SDS, 6.2 mg DTT, 4ml Glycerol made up to 20ml with dH_2O, pH to 6.8. Add solid bromophenol blue until solution is dark blue in colour. Filter through Whatman no.1 paper. Aliquot into sterile micofuge tubes and store at -20°C.

Transfer Buffer: 3.03 g Tris base, 14.41 g Glycine, 200ml Methanol in 1 L dH_2O, pH to 9.2

Block Buffer: 5% milk, 0.2% Tween20 in PBS

Incubation Buffer: 2.5% milk in PBS

Wash Buffer: 2.5% milk, 0.2% Tween20 in PBS

Appendix 2

Sequence Comparison 0µg/ml vs 10µg/ml Podocin + strand

0µg/ml ccatatnaagccgtatccctgcagcgaggcattcggtccccacg
10µg/ml ccatataaagccgtatccctg-agcgaggcattcggtccccacg

0µg/ml cccaggcccaccctgcccttgttgtttgccttttgagtgtatca
10µg/ml cccaggcccaccctgcccttgttgtttgccttttgagtgtatca

0µg/ml tgtcacaagtatggacacacgcatgagaacacagtgaaatggca
10µg/ml tgtcacaag-atggacacacgcatgagaacacagtgaaatggca

0µg/ml gagaagacatccagccacacaagtgggtcgtctcatcattca
10µg/ml gagaagacatccagccacacaagtgggtcgtctcatcattca

Sequence Comparison 0µg/ml vs 10µg/ml Podocin – strand

0µg/ml gcnggatgtcttctct-ccatttcactgtgttctcatgcgtgtgt
10µg/ml gcnggatgtcttctctgccatttcactgtgttctcatgcgtgtgt

0µg/ml ccatcttgtgacatgatacactcaaaaggcaaacaacaagggcag
10µg/ml ccatcttgtgacatgatacactcaaaaggcaaacaacaagggcag

0µg/ml ggtgggcctgggcgtggggaccgaatgcctcgctcagggatacgg
10µg/ml ggtgggcctgggcgtggggaccgaatgcctcgctcagggatacgg

0µg/ml ctttatatggtgtattcccattactcttgtccactcgccca
10µg/ml ctttatatggtgtattcccattactcttgtccactcgccca

Differences between the two podocin sequences after PAN treatment for 48 hours are highlighted.

Sequence Alignment of published Podocin sequence with the sequences we obtained after PAN treatment.

```
Podocin   ccatataaagccgtatccctg-agcgaggcattcggtccccacg
0µg/ml    ccatataaagccgtatccctgcagcgaggcattcggtccccacg
10µg/ml   ccatataaagccgtatccctg-agcgaggcattcggtccccacg

Podocin   cccaggcccaccctgcccttgttgtttgccttttgagtgtatca
0µg/ml    cccaggcccaccctgcccttgttgtttgccttttgagtgtatca
10µg/ml   cccaggcccaccctgcccttgttgtttgccttttgagtgtatca

Podocin   tgtcacaag-atggacacagcatgagaacgcagtgaaatggca
0µg/ml    tgtcacaagtatggacacagcatgagaacacagtgaaatggca
10µg/ml   tgtcacaagtatggacacagcatgagaacacagtgaaatggca

Podocin   gagaagacatccagccacacaagtgggtcgtctcatcattca
0µg/ml    gagaagacatccagccacacaagtgggtcgtctcatcattca
10µg/ml   gagaagacatccagccacacaagtgggtcgtctcatcattca
```

A consistent G – A change was observed between our PCR products for podocin and the published sequence (AY039651) for rat podocin.

References

1. Tisher CC, M.K., ed. *Anatomy of the Kidney.* The Kidney, ed. R.F. Brenner BM. 1990, Saunders: Philadelphia. 3-75.
2. Lote Christopher J, *Principles of Renal Physiology.* Vol. 4th edition. 2000: Kluwer Academic Publishers.
3. Osawa, G., P. Kimmelstiel, and V. Seiling, *Thickness of glomerular basement membranes.* Am J Clin Pathol, 1966. **45**(1): p. 7-20.
4. Jorgensen, F. and M.W. Bentzon, *The ultastructure of the normal human glomerulus. Thickness of glomerular basement membrane.* Lab Invest, 1968. **18**(1): p. 42-8.
5. Osterby, R., *Quantitative electron microscopy of the glomerular basement membrane. A methodologic study.* Lab Invest, 1971. **25**(1): p. 15-24.
6. Pavenstadt, H., *Roles of the podocyte in glomerular function.* Am J Physiol Renal Physiol, 2000. **278**(2): p. F173-9.
7. Pavenstadt, H., W. Kriz, and M. Kretzler, *Cell biology of the glomerular podocyte.* Physiol Rev, 2003. **83**(1): p. 253-307.
8. Schwarz, K., et al., *Podocin, a raft-associated component of the glomerular slit diaphragm, interacts with CD2AP and nephrin.* J Clin Invest, 2001. **108**(11): p. 1621-9.
9. Simons, M., et al., *Involvement of lipid rafts in nephrin phosphorylation and organization of the glomerular slit diaphragm.* Am J Pathol, 2001. **159**(3): p. 1069-77.
10. Rodewald, R. and M.J. Karnovsky, *Porous substructure of the glomerular slit diaphragm in the rat and mouse.* J Cell Biol, 1974. **60**(2): p. 423-33.
11. Salant, D.J. and P.S. Topham, *Role of nephrin in proteinuric renal diseases.* Springer Semin Immunopathol, 2003. **24**(4): p. 423-39.
12. Tryggvason, K. and J. Wartiovaara, *Molecular basis of glomerular permselectivity.* Curr Opin Nephrol Hypertens, 2001. **10**(4): p. 543-9.
13. Smoyer, W.E. and P. Mundel, *Regulation of podocyte structure during the development of nephrotic syndrome.* J Mol Med, 1998. **76**(3-4): p. 172-83.
14. Barisoni, L. and J.B. Kopp, *Update in podocyte biology: putting one's best foot forward.* Curr Opin Nephrol Hypertens, 2003. **12**(3): p. 251-8.
15. Takeda, T., *Podocyte cytoskeleton is connected to the integral membrane protein podocalyxin through Na+/H+-exchanger regulatory factor 2 and ezrin.* Clin Exp Nephrol, 2003. **7**(4): p. 260-9.
16. Kerjaschki, D., *Caught flat-footed: podocyte damage and the molecular bases of focal glomerulosclerosis.* J Clin Invest, 2001. **108**(11): p. 1583-7.

17. Matsui, K., et al., *Podoplanin, a novel 43-kDa membrane protein, controls the shape of podocytes.* Nephrol Dial Transplant, 1999. **14 Suppl 1**: p. 9-11.
18. Breiteneder-Geleff, S., et al., *Podoplanin, novel 43-kd membrane protein of glomerular epithelial cells, is down-regulated in puromycin nephrosis.* Am J Pathol, 1997. **151**(4): p. 1141-52.
19. Matsui, K., S. Breiteneder-Geleff, and D. Kerjaschki, *Epitope-specific antibodies to the 43-kD glomerular membrane protein podoplanin cause proteinuria and rapid flattening of podocytes.* J Am Soc Nephrol, 1998. **9**(11): p. 2013-26.
20. Rishi, A.K., et al., *Cloning, characterization, and development expression of a rat lung alveolar type I cell gene in embryonic endodermal and neural derivatives.* Dev Biol, 1995. **167**(1): p. 294-306.
21. Nose, K., H. Saito, and T. Kuroki, *Isolation of a gene sequence induced later by tumor-promoting 12-O-tetradecanoylphorbol-13-acetate in mouse osteoblastic cells (MC3T3-E1) and expressed constitutively in ras-transformed cells.* Cell Growth Differ, 1990. **1**(11): p. 511-8.
22. Wetterwald, A., et al., *Characterization and cloning of the E11 antigen, a marker expressed by rat osteoblasts and osteocytes.* Bone, 1996. **18**(2): p. 125-32.
23. Zimmer, G., et al., *Cloning and characterization of gp36, a human mucin-type glycoprotein preferentially expressed in vascular endothelium.* Biochem J, 1999. **341 (Pt 2)**: p. 277-84.
24. Boucherot, A., et al., *Cloning and expression of the mouse glomerular podoplanin homologue gp38P.* Nephrol Dial Transplant, 2002. **17**(6): p. 978-84.
25. Farr, A.G., et al., *Characterization and cloning of a novel glycoprotein expressed by stromal cells in T-dependent areas of peripheral lymphoid tissues.* J Exp Med, 1992. **176**(5): p. 1477-82.
26. Sleeman, J.P., et al., *Markers for the lymphatic endothelium: in search of the holy grail?* Microsc Res Tech, 2001. **55**(2): p. 61-9.
27. Breiteneder-Geleff, S., et al., *[Podoplanin--a specific marker for lymphatic endothelium expressed in angiosarcoma].* Verh Dtsch Ges Pathol, 1999. **83**: p. 270-5.
28. Kerjaschki, D., D.J. Sharkey, and M.G. Farquhar, *Identification and characterization of podocalyxin--the major sialoprotein of the renal glomerular epithelial cell.* J Cell Biol, 1984. **98**(4): p. 1591-6.
29. Horvat, R., et al., *Endothelial cell membranes contain podocalyxin--the major sialoprotein of visceral glomerular epithelial cells.* J Cell Biol, 1986. **102**(2): p. 484-91.
30. Sassetti, C., et al., *Identification of podocalyxin-like protein as a high endothelial venule ligand for L-selectin: parallels to CD34.* J Exp Med, 1998. **187**(12): p. 1965-75.
31. Kerosuo, L., et al., *Podocalyxin in human haematopoietic cells.* Br J Haematol, 2004. **124**(6): p. 809-18.
32. Miettinen, A., et al., *Podocalyxin in rat platelets and megakaryocytes.* Am J Pathol, 1999. **154**(3): p. 813-22.

33. Dekan, G., C. Gabel, and M.G. Farquhar, *Sulfate contributes to the negative charge of podocalyxin, the major sialoglycoprotein of the glomerular filtration slits.* Proc Natl Acad Sci U S A, 1991. **88**(12): p. 5398-402.
34. Doyonnas, R., et al., *Anuria, omphalocele, and perinatal lethality in mice lacking the CD34-related protein podocalyxin.* J Exp Med, 2001. **194**(1): p. 13-27.
35. Fieger, C.B., C.M. Sassetti, and S.D. Rosen, *Endoglycan, a member of the CD34 family, functions as an L-selectin ligand through modification with tyrosine sulfation and sialyl Lewis x.* J Biol Chem, 2003. **278**(30): p. 27390-8.
36. Sassetti, C., A. Van Zante, and S.D. Rosen, *Identification of endoglycan, a member of the CD34/podocalyxin family of sialomucins.* J Biol Chem, 2000. **275**(12): p. 9001-10.
37. Kershaw, D.B., et al., *Molecular cloning, expression, and characterization of podocalyxin-like protein 1 from rabbit as a transmembrane protein of glomerular podocytes and vascular endothelium.* J Biol Chem, 1995. **270**(49): p. 29439-46.
38. McNagny, K.M., et al., *Thrombomucin, a novel cell surface protein that defines thrombocytes and multipotent hematopoietic progenitors.* J Cell Biol, 1997. **138**(6): p. 1395-407.
39. Hara, T., et al., *Identification of podocalyxin-like protein 1 as a novel cell surface marker for hemangioblasts in the murine aorta-gonad-mesonephros region.* Immunity, 1999. **11**(5): p. 567-78.
40. Kershaw, D.B., et al., *Molecular cloning and characterization of human podocalyxin-like protein. Orthologous relationship to rabbit PCLP1 and rat podocalyxin.* J Biol Chem, 1997. **272**(25): p. 15708-14.
41. Kershaw, D.B., et al., *Assignment of the human podocalyxin-like protein (PODXL) gene to 7q32-q33.* Genomics, 1997. **45**(1): p. 239-40.
42. Takeda, T., et al., *Expression of podocalyxin inhibits cell-cell adhesion and modifies junctional properties in Madin-Darby canine kidney cells.* Mol Biol Cell, 2000. **11**(9): p. 3219-32.
43. Kerjaschki, D., A.T. Vernillo, and M.G. Farquhar, *Reduced sialylation of podocalyxin--the major sialoprotein of the rat kidney glomerulus--in aminonucleoside nephrosis.* Am J Pathol, 1985. **118**(3): p. 343-9.
44. Orlando, R.A., et al., *The glomerular epithelial cell anti-adhesin podocalyxin associates with the actin cytoskeleton through interactions with ezrin.* J Am Soc Nephrol, 2001. **12**(8): p. 1589-98.
45. Takeda, T., et al., *Loss of glomerular foot processes is associated with uncoupling of podocalyxin from the actin cytoskeleton.* J Clin Invest, 2001. **108**(2): p. 289-301.
46. Mangeat, P., C. Roy, and M. Martin, *ERM proteins in cell adhesion and membrane dynamics.* Trends Cell Biol, 1999. **9**(5): p. 187-92.
47. Hugo, C., et al., *The plasma membrane-actin linking protein, ezrin, is a glomerular epithelial cell marker in glomerulogenesis, in the adult kidney and in glomerular injury.* Kidney Int, 1998. **54**(6): p. 1934-44.

48. Gautreau, A., D. Louvard, and M. Arpin, *Morphogenic effects of ezrin require a phosphorylation-induced transition from oligomers to monomers at the plasma membrane.* J Cell Biol, 2000. **150**(1): p. 193-203.
49. Fievet, B.T., et al., *Phosphoinositide binding and phosphorylation act sequentially in the activation mechanism of ezrin.* J Cell Biol, 2004. **164**(5): p. 653-9.
50. Pujuguet, P., et al., *Ezrin regulates E-cadherin-dependent adherens junction assembly through Rac1 activation.* Mol Biol Cell, 2003. **14**(5): p. 2181-91.
51. Weinman, E.J., et al., *Identification of the human NHE-1 form of Na(+)-H+ exchanger in rabbit renal brush border membranes.* J Clin Invest, 1993. **91**(5): p. 2097-102.
52. Voltz, J.W., E.J. Weinman, and S. Shenolikar, *Expanding the role of NHERF, a PDZ-domain containing protein adapter, to growth regulation.* Oncogene, 2001. **20**(44): p. 6309-14.
53. Wade, J.B., et al., *Differential renal distribution of NHERF isoforms and their colocalization with NHE3, ezrin, and ROMK.* Am J Physiol Cell Physiol, 2001. **280**(1): p. C192-8.
54. Kestila, M., et al., *Positionally cloned gene for a novel glomerular protein--nephrin--is mutated in congenital nephrotic syndrome.* Mol Cell, 1998. **1**(4): p. 575-82.
55. Lenkkeri, U., et al., *Structure of the gene for congenital nephrotic syndrome of the finnish type (NPHS1) and characterization of mutations.* Am J Hum Genet, 1999. **64**(1): p. 51-61.
56. Tryggvason, K., *Unraveling the mechanisms of glomerular ultrafiltration: nephrin, a key component of the slit diaphragm.* J Am Soc Nephrol, 1999. **10**(11): p. 2440-5.
57. Kawachi, H., et al., *Cloning of rat nephrin: expression in developing glomeruli and in proteinuric states.* Kidney Int, 2000. **57**(5): p. 1949-61.
58. Holthofer, H., et al., *Nephrin localizes at the podocyte filtration slit area and is characteristically spliced in the human kidney.* Am J Pathol, 1999. **155**(5): p. 1681-7.
59. Holzman, L.B., et al., *Nephrin localizes to the slit pore of the glomerular epithelial cell.* Kidney Int, 1999. **56**(4): p. 1481-91.
60. Ruotsalainen, V., et al., *Nephrin is specifically located at the slit diaphragm of glomerular podocytes.* Proc Natl Acad Sci U S A, 1999. **96**(14): p. 7962-7.
61. Liu, L., et al., *Nephrin is an important component of the barrier system in the testis.* Acta Med Okayama, 2001. **55**(3): p. 161-5.
62. Palmen, T., et al., *Nephrin is expressed in the pancreatic beta cells.* Diabetologia, 2001. **44**(10): p. 1274-80.
63. Putaala, H., et al., *The murine nephrin gene is specifically expressed in kidney, brain and pancreas: inactivation of the gene leads to massive proteinuria and neonatal death.* Hum Mol Genet, 2001. **10**(1): p. 1-8.
64. Putaala, H., et al., *Primary structure of mouse and rat nephrin cDNA and structure and expression of the mouse gene.* J Am Soc Nephrol, 2000. **11**(6): p. 991-1001.

65. Ahola, H., et al., *Cloning and expression of the rat nephrin homolog.* Am J Pathol, 1999. **155**(3): p. 907-13.
66. Teichmann, S.A. and C. Chothia, *Immunoglobulin superfamily proteins in Caenorhabditis elegans.* J Mol Biol, 2000. **296**(5): p. 1367-83.
67. Khoshnoodi, J., et al., *Nephrin Promotes Cell-Cell Adhesion through Homophilic Interactions.* Am J Pathol, 2003. **163**(6): p. 2337-46.
68. Barletta, G.M., et al., *Nephrin and Neph1 co-localize at the podocyte foot process intercellular junction and form cis hetero-oligomers.* J Biol Chem, 2003. **278**(21): p. 19266-71.
69. Gerke, P., et al., *Homodimerization and heterodimerization of the glomerular podocyte proteins nephrin and NEPH1.* J Am Soc Nephrol, 2003. **14**(4): p. 918-26.
70. Liu, G., et al., *Neph1 and nephrin interaction in the slit diaphragm is an important determinant of glomerular permeability.* J Clin Invest, 2003. **112**(2): p. 209-21.
71. Yan, K., et al., *N-linked glycosylation is critical for the plasma membrane localization of nephrin.* J Am Soc Nephrol, 2002. **13**(5): p. 1385-9.
72. Saleem, M.A., et al., *Co-localization of nephrin, podocin, and the actin cytoskeleton: evidence for a role in podocyte foot process formation.* Am J Pathol, 2002. **161**(4): p. 1459-66.
73. Yuan, H., E. Takeuchi, and D.J. Salant, *Podocyte slit-diaphragm protein nephrin is linked to the actin cytoskeleton.* Am J Physiol Renal Physiol, 2002. **282**(4): p. F585-91.
74. Furness, P.N., et al., *Glomerular expression of nephrin is decreased in acquired human nephrotic syndrome.* Nephrol Dial Transplant, 1999. **14**(5): p. 1234-7.
75. Wang, S.X., et al., *Patterns of nephrin and a new proteinuria-associated protein expression in human renal diseases.* Kidney Int, 2002. **61**(1): p. 141-7.
76. Luimula, P., et al., *Alternatively spliced nephrin in experimental glomerular disease of the rat.* Pediatr Res, 2000. **48**(6): p. 759-62.
77. Luimula, P., et al., *Nephrin in experimental glomerular disease.* Kidney Int, 2000. **58**(4): p. 1461-8.
78. Luimula, P., et al., *Podocyte-associated molecules in puromycin aminonucleoside nephrosis of the rat.* Lab Invest, 2002. **82**(6): p. 713-8.
79. Aaltonen, P., et al., *Changes in the expression of nephrin gene and protein in experimental diabetic nephropathy.* Lab Invest, 2001. **81**(9): p. 1185-90.
80. Srivastava, T., et al., *Podocyte proteins in Galloway-Mowat syndrome.* Pediatr Nephrol, 2001. **16**(12): p. 1022-9.
81. Doublier, S., et al., *Nephrin redistribution on podocytes is a potential mechanism for proteinuria in patients with primary acquired nephrotic syndrome.* Am J Pathol, 2001. **158**(5): p. 1723-31.
82. Patrakka, J., et al., *Expression of nephrin in pediatric kidney diseases.* J Am Soc Nephrol, 2001. **12**(2): p. 289-96.

83. Huh, W., et al., *Expression of nephrin in acquired human glomerular disease.* Nephrol Dial Transplant, 2002. **17**(3): p. 478-84.
84. Sellin, L., et al., *NEPH1 defines a novel family of podocin interacting proteins.* Faseb J, 2003. **17**(1): p. 115-7.
85. Donoviel, D.B., et al., *Proteinuria and perinatal lethality in mice lacking NEPH1, a novel protein with homology to NEPHRIN.* Mol Cell Biol, 2001. **21**(14): p. 4829-36.
86. Boute, N., et al., *NPHS2, encoding the glomerular protein podocin, is mutated in autosomal recessive steroid-resistant nephrotic syndrome.* Nat Genet, 2000. **24**(4): p. 349-54.
87. Snyers, L., E. Umlauf, and R. Prohaska, *Oligomeric nature of the integral membrane protein stomatin.* J Biol Chem, 1998. **273**(27): p. 17221-6.
88. Salzer, U. and R. Prohaska, *Stomatin, flotillin-1, and flotillin-2 are major integral proteins of erythrocyte lipid rafts.* Blood, 2001. **97**(4): p. 1141-3.
89. Kawachi, H., et al., *Cloning of rat homologue of podocin: expression in proteinuric states and in developing glomeruli.* J Am Soc Nephrol, 2003. **14**(1): p. 46-56.
90. Horinouchi, I., et al., *In situ evaluation of podocin in normal and glomerular diseases.* Kidney Int, 2003. **64**(6): p. 2092-2099.
91. Roselli, S., et al., *Podocin localizes in the kidney to the slit diaphragm area.* Am J Pathol, 2002. **160**(1): p. 131-9.
92. Brown, D.A. and E. London, *Functions of lipid rafts in biological membranes.* Annu Rev Cell Dev Biol, 1998. **14**: p. 111-36.
93. Danielsen, E.M. and G.H. Hansen, *Lipid rafts in epithelial brush borders: atypical membrane microdomains with specialized functions.* Biochim Biophys Acta, 2003. **1617**(1-2): p. 1-9.
94. Shaw, A.S. and J.H. Miner, *CD2-associated protein and the kidney.* Curr Opin Nephrol Hypertens, 2001. **10**(1): p. 19-22.
95. Shih, N.Y., et al., *CD2AP localizes to the slit diaphragm and binds to nephrin via a novel C-terminal domain.* Am J Pathol, 2001. **159**(6): p. 2303-8.
96. Li, C., et al., *CD2AP is expressed with nephrin in developing podocytes and is found widely in mature kidney and elsewhere.* Am J Physiol Renal Physiol, 2000. **279**(4): p. F785-92.
97. Shih, N.Y., et al., *Congenital nephrotic syndrome in mice lacking CD2-associated protein.* Science, 1999. **286**(5438): p. 312-5.
98. Palmen, T., et al., *Interaction of endogenous nephrin and CD2-associated protein in mouse epithelial M-1 cell line.* J Am Soc Nephrol, 2002. **13**(7): p. 1766-72.
99. Lehtonen, S., F. Zhao, and E. Lehtonen, *CD2-associated protein directly interacts with the actin cytoskeleton.* Am J Physiol Renal Physiol, 2002. **283**(4): p. F734-43.
100. Kim, Y.H., et al., *GLEPP1 receptor tyrosine phosphatase (Ptpro) in rat PAN nephrosis. A marker of acute podocyte injury.* Nephron, 2002. **90**(4): p. 471-6.

101. Wang, R., et al., *Molecular cloning, expression, and distribution of glomerular epithelial protein 1 in developing mouse kidney.* Kidney Int, 2000. **57**(5): p. 1847-59.
102. Wharram, B.L., et al., *Altered podocyte structure in GLEPP1 (Ptpro)-deficient mice associated with hypertension and low glomerular filtration rate.* J Clin Invest, 2000. **106**(10): p. 1281-90.
103. Thomas, P.E., et al., *GLEPP1, a renal glomerular epithelial cell (podocyte) membrane protein-tyrosine phosphatase. Identification, molecular cloning, and characterization in rabbit.* J Biol Chem, 1994. **269**(31): p. 19953-62.
104. Wiggins, R.C., et al., *Molecular cloning of cDNAs encoding human GLEPP1, a membrane protein tyrosine phosphatase: characterization of the GLEPP1 protein distribution in human kidney and assignment of the GLEPP1 gene to human chromosome 12p12-p13.* Genomics, 1995. **27**(1): p. 174-81.
105. Yang, D.H., et al., *Glomerular epithelial protein 1 and podocalyxin-like protein 1 in inflammatory glomerular disease (crescentic nephritis) in rabbit and man.* Lab Invest, 1996. **74**(3): p. 571-84.
106. Mundel, P., P. Gilbert, and W. Kriz, *Podocytes in glomerulus of rat kidney express a characteristic 44 KD protein.* J Histochem Cytochem, 1991. **39**(8): p. 1047-56.
107. Mundel, P., et al., *Synaptopodin: an actin-associated protein in telencephalic dendrites and renal podocytes.* J Cell Biol, 1997. **139**(1): p. 193-204.
108. Barisoni, L., et al., *The dysregulated podocyte phenotype: a novel concept in the pathogenesis of collapsing idiopathic focal segmental glomerulosclerosis and HIV-associated nephropathy.* J Am Soc Nephrol, 1999. **10**(1): p. 51-61.
109. Kemeny, E., et al., *Distribution of podocyte protein (44 KD) in different types of glomerular diseases.* Virchows Arch, 1997. **431**(6): p. 425-30.
110. Srivastava, T., et al., *Synaptopodin expression in idiopathic nephrotic syndrome of childhood.* Kidney Int, 2001. **59**(1): p. 118-25.
111. Inoue, T., et al., *FAT is a component of glomerular slit diaphragms.* Kidney Int, 2001. **59**(3): p. 1003-12.
112. Stevenson, B.R., et al., *Identification of ZO-1: a high molecular weight polypeptide associated with the tight junction (zonula occludens) in a variety of epithelia.* J Cell Biol, 1986. **103**(3): p. 755-66.
113. Schnabel, E., J.M. Anderson, and M.G. Farquhar, *The tight junction protein ZO-1 is concentrated along slit diaphragms of the glomerular epithelium.* J Cell Biol, 1990. **111**(3): p. 1255-63.
114. Willott, E., et al., *The tight junction protein ZO-1 is homologous to the Drosophila discs-large tumor suppressor protein of septate junctions.* Proc Natl Acad Sci U S A, 1993. **90**(16): p. 7834-8.
115. Kurihara, H., J.M. Anderson, and M.G. Farquhar, *Diversity among tight junctions in rat kidney: glomerular slit diaphragms and endothelial junctions express only one isoform of the tight junction protein ZO-1.* Proc Natl Acad Sci U S A, 1992. **89**(15): p. 7075-9.

116. Anderson, J.M., et al., *Characterization of ZO-1, a protein component of the tight junction from mouse liver and Madin-Darby canine kidney cells.* J Cell Biol, 1988. **106**(4): p. 1141-9.
117. Stevenson, B.R. and B.H. Keon, *The tight junction: morphology to molecules.* Annu Rev Cell Dev Biol, 1998. **14**: p. 89-109.
118. Mitic, L.L. and J.M. Anderson, *Molecular architecture of tight junctions.* Annu Rev Physiol, 1998. **60**: p. 121-42.
119. Kawachi, H., et al., *Developmental expression of the nephritogenic antigen of monoclonal antibody 5-1-6.* Am J Pathol, 1995. **147**(3): p. 823-33.
120. Kos, C.H., et al., *Mice deficient in alpha-actinin-4 have severe glomerular disease.* J Clin Invest, 2003. **111**(11): p. 1683-90.
121. Lachapelle, M. and M. Bendayan, *Contractile proteins in podocytes: immunocytochemical localization of actin and alpha-actinin in normal and nephrotic rat kidneys.* Virchows Arch B Cell Pathol Incl Mol Pathol, 1991. **60**(2): p. 105-11.
122. Smoyer, W.E., et al., *Podocyte alpha-actinin induction precedes foot process effacement in experimental nephrotic syndrome.* Am J Physiol, 1997. **273**(1 Pt 2): p. F150-7.
123. Michaud, J.L., et al., *Focal and segmental glomerulosclerosis in mice with podocyte-specific expression of mutant alpha-actinin-4.* J Am Soc Nephrol, 2003. **14**(5): p. 1200-11.
124. Pozzi, A. and R. Zent, *Integrins: sensors of extracellular matrix and modulators of cell function.* Nephron Exp Nephrol, 2003. **94**(3): p. e77-84.
125. Kreidberg, J.A., *Functions of alpha3beta1 integrin.* Curr Opin Cell Biol, 2000. **12**(5): p. 548-53.
126. Kreidberg, J.A. and J.M. Symons, *Integrins in kidney development, function, and disease.* Am J Physiol Renal Physiol, 2000. **279**(2): p. F233-42.
127. Lee, S.B. and D.A. Haber, *Wilms tumor and the WT1 gene.* Exp Cell Res, 2001. **264**(1): p. 74-99.
128. Stanhope-Baker, P., et al., *The Wilms tumor suppressor-1 target gene podocalyxin is transcriptionally repressed by p53.* J Biol Chem, 2004. **279**(32): p. 33575-85.
129. Yang, Y., et al., *WT1 and PAX-2 podocyte expression in Denys-Drash syndrome and isolated diffuse mesangial sclerosis.* Am J Pathol, 1999. **154**(1): p. 181-92.
130. Call, K.M., et al., *Isolation and characterization of a zinc finger polypeptide gene at the human chromosome 11 Wilms' tumor locus.* Cell, 1990. **60**(3): p. 509-20.
131. Gessler, M., et al., *Homozygous deletion in Wilms tumours of a zinc-finger gene identified by chromosome jumping.* Nature, 1990. **343**(6260): p. 774-8.
132. Schedl, A. and N. Hastie, *Multiple roles for the Wilms' tumour suppressor gene, WT1 in genitourinary development.* Mol Cell Endocrinol, 1998. **140**(1-2): p. 65-9.
133. Mrowka, C. and A. Schedl, *Wilms' tumor suppressor gene WT1: from structure to renal pathophysiologic features.* J Am Soc Nephrol, 2000. **11 Suppl 16**: p. S106-15.

134. Guo, J.K., et al., *WT1 is a key regulator of podocyte function: reduced expression levels cause crescentic glomerulonephritis and mesangial sclerosis.* Hum Mol Genet, 2002. **11**(6): p. 651-9.
135. Laity, J.H., H.J. Dyson, and P.E. Wright, *Molecular basis for modulation of biological function by alternate splicing of the Wilms' tumor suppressor protein.* Proc Natl Acad Sci U S A, 2000. **97**(22): p. 11932-5.
136. Patek, C.E., et al., *Murine Denys-Drash syndrome: evidence of podocyte de-differentiation and systemic mediation of glomerulosclerosis.* Hum Mol Genet, 2003. **12**(18): p. 2379-94.
137. Niksic, M., et al., *The Wilms' tumour protein (WT1) shuttles between nucleus and cytoplasm and is present in functional polysomes.* Hum Mol Genet, 2004. **13**(4): p. 463-71.
138. Palmer, R.E., et al., *WT1 regulates the expression of the major glomerular podocyte membrane protein Podocalyxin.* Curr Biol, 2001. **11**(22): p. 1805-9.
139. Guo, G., et al., *WT1 activates a glomerular-specific enhancer identified from the human nephrin gene.* J Am Soc Nephrol, 2004. **15**(11): p. 2851-6.
140. Wagner, N., et al., *The major podocyte protein nephrin is transcriptionally activated by the Wilms' tumor suppressor WT1.* J Am Soc Nephrol, 2004. **15**(12): p. 3044-51.
141. Natoli, T.A., et al., *A mutant form of the Wilms' tumor suppressor gene WT1 observed in Denys-Drash syndrome interferes with glomerular capillary development.* J Am Soc Nephrol, 2002. **13**(8): p. 2058-67.
142. Schumacher, V., et al., *Spectrum of early onset nephrotic syndrome associated with WT1 missense mutations.* Kidney Int, 1998. **53**(6): p. 1594-600.
143. Klamt, B., et al., *Frasier syndrome is caused by defective alternative splicing of WT1 leading to an altered ratio of WT1 +/-KTS splice isoforms.* Hum Mol Genet, 1998. **7**(4): p. 709-14.
144. Asanuma, K. and P. Mundel, *The role of podocytes in glomerular pathobiology.* Clin Exp Nephrol, 2003. **7**(4): p. 255-9.
145. Mundel, P. and S.J. Shankland, *Podocyte biology and response to injury.* J Am Soc Nephrol, 2002. **13**(12): p. 3005-15.
146. Reiser, J., et al., *Novel concepts in understanding and management of glomerular proteinuria.* Nephrol Dial Transplant, 2002. **17**(6): p. 951-5.
147. Kriz, W., N. Gretz, and K.V. Lemley, *Progression of glomerular diseases: is the podocyte the culprit?* Kidney Int, 1998. **54**(3): p. 687-97.
148. Somlo, S. and P. Mundel, *Getting a foothold in nephrotic syndrome.* Nat Genet, 2000. **24**(4): p. 333-5.
149. Barisoni, L. and P. Mundel, *Podocyte biology and the emerging understanding of podocyte diseases.* Am J Nephrol, 2003. **23**(5): p. 353-60.
150. Khoshnoodi, J. and K. Tryggvason, *Congenital nephrotic syndromes.* Curr Opin Genet Dev, 2001. **11**(3): p. 322-7.

151. Aya, K., H. Tanaka, and Y. Seino, *Novel mutation in the nephrin gene of a Japanese patient with congenital nephrotic syndrome of the Finnish type.* Kidney Int, 2000. **57**(2): p. 401-4.
152. Beltcheva, O., et al., *Mutation spectrum in the nephrin gene (NPHS1) in congenital nephrotic syndrome.* Hum Mutat, 2001. **17**(5): p. 368-73.
153. Antignac, C., *Genetic models: clues for understanding the pathogenesis of idiopathic nephrotic syndrome.* J Clin Invest, 2002. **109**(4): p. 447-9.
154. Zhang, S.Y., et al., *In vivo expression of podocyte slit diaphragm-associated proteins in nephrotic patients with NPHS2 mutation.* Kidney Int, 2004. **66**(3): p. 945-54.
155. Huber, T.B., et al., *Molecular basis of the functionalpodocin-nephrin complex: mutations in the NPHS2 gene disrupt nephrin targeting to lipid raft microdomains.* Hum Mol Genet, 2003. **12**(24): p. 3397-405.
156. Karle, S.M., et al., *Novel mutations in NPHS2 detected in both familial and sporadic steroid-resistant nephrotic syndrome.* J Am Soc Nephrol, 2002. **13**(2): p. 388-93.
157. Caridi, G., et al., *Prevalence, genetics, and clinical features of patients carrying podocin mutations in steroid-resistant nonfamilial focal segmental glomerulosclerosis.* J Am Soc Nephrol, 2001. **12**(12): p. 2742-6.
158. Caridi, G., et al., *Broadening the spectrum of diseases related to podocin mutations.* J Am Soc Nephrol, 2003. **14**(5): p. 1278-86.
159. Caridi, G., et al., *Podocin mutations in sporadic focal-segmental glomerulosclerosis occurring in adulthood.* Kidney Int, 2003. **64**(1): p. 365.
160. Carraro, M., et al., *Serum glomerular permeability activity in patients with podocin mutations (NPHS2) and steroid-resistant nephrotic syndrome.* J Am Soc Nephrol, 2002. **13**(7): p. 1946-52.
161. Tsukaguchi, H., et al., *NPHS2 mutations in late-onset focal segmental glomerulosclerosis: R229Q is a common disease-associated allele.* J Clin Invest, 2002. **110**(11): p. 1659-66.
162. Demmer, L., et al., *Frasier syndrome: a cause of focal segmental glomerulosclerosis in a 46,XX female.* J Am Soc Nephrol, 1999. **10**(10): p. 2215-8.
163. Denamur, E., et al., *Mother-to-child transmitted WT1 splice-site mutation is responsible for distinct glomerular diseases.* J Am Soc Nephrol, 1999. **10**(10): p. 2219-23.
164. Salomon, R., M.C. Gubler, and P. Niaudet, *Genetics of the nephrotic syndrome.* Curr Opin Pediatr, 2000. **12**(2): p. 129-34.
165. Barbaux, S., et al., *Donor splice-site mutations in WT1 are responsible for Frasier syndrome.* Nat Genet, 1997. **17**(4): p. 467-70.
166. Kikuchi, H., et al., *Do intronic mutations affecting splicing of WT1 exon 9 cause Frasier syndrome?* J Med Genet, 1998. **35**(1): p. 45-8.

167. Kohsaka, T., et al., *Exon 9 mutations in the WT1 gene, without influencing KTS splice isoforms, are also responsible for Frasier syndrome.* Hum Mutat, 1999. **14**(6): p. 466-70.
168. Fogo, A.B., *Minimal change disease and focal segmental glomerulosclerosis.* Nephrol Dial Transplant, 2001. **16 Suppl 6**: p. 74-6.
169. Grimbert, P., et al., *Recent approaches to the pathogenesis of minimal-change nephrotic syndrome.* Nephrol Dial Transplant, 2003. **18**(2): p. 245-8.
170. Kaplan, J. and M.R. Pollak, *Familial focal segmental glomerulosclerosis.* Curr Opin Nephrol Hypertens, 2001. **10**(2): p. 183-7.
171. Mathis, B.J., et al., *A locus for inherited focal segmental glomerulosclerosis maps to chromosome 19q13.* Kidney Int, 1998. **53**(2): p. 282-6.
172. Nakazato, H., et al., *Another autosomal recessive form of focal glomerulosclerosis with neurological findings.* Pediatr Nephrol, 2002. **17**(1): p. 16-9.
173. Winn, M.P., et al., *Clinical and genetic heterogeneity in familial focal segmental glomerulosclerosis. International Collaborative Group for the Study of Familial Focal Segmental Glomerulosclerosis.* Kidney Int, 1999. **55**(4): p. 1241-6.
174. Susztak, K., et al., *Genomic strategies for diabetic nephropathy.* J Am Soc Nephrol, 2003. **14**(8 Suppl 3): p. S271-8.
175. Caramori, M.L. and M. Mauer, *Diabetes and nephropathy.* Curr Opin Nephrol Hypertens, 2003. **12**(3): p. 273-82.
176. Hostetter, T.H., *Prevention of the development and progression of renal disease.* J Am Soc Nephrol, 2003. **14**(7 Suppl 2): p. S144-7.
177. Ritz, E., *Nephropathy in type 2 diabetes.* J Intern Med, 1999. **245**(2): p. 111-26.
178. Makino, H., Y. Nakamura, and J. Wada, *Remission and regression of diabetic nephropathy.* Hypertens Res, 2003. **26**(7): p. 515-9.
179. De Broe, M., *Clinical Nephrotoxins: Renal Injury from Drugs and Chemical.* 1998: Kluwer Academic Publishers.
180. Hjalmarsson, C., M. Ohlson, and B. Haraldsson, *Puromycin aminonucleoside damages the glomerular size barrier with minimal effects on charge density.* Am J Physiol Renal Physiol, 2001. **281**(3): p. F503-12.
181. Krishnamurti, U., et al., *Puromycin aminonucleoside suppresses integrin expression in cultured glomerular epithelial cells.* J Am Soc Nephrol, 2001. **12**(4): p. 758-66.
182. Bertram, J.F., A. Messina, and G.B. Ryan, *In vitro effects of puromycin aminonucleoside on the ultrastructure of rat glomerular podocytes.* Cell Tissue Res, 1990. **260**(3): p. 555-63.
183. Coers, W., et al., *Puromycin aminonucleoside and adriamycin disturb cytoskeletal and extracellular matrix protein organization, but not protein synthesis of cultured glomerular epithelial cells.* Exp Nephrol, 1994. **2**(1): p. 40-50.

184. Fishman, J.A. and M.J. Karnovsky, *Effects of the aminonucleoside of puromycin on glomerular epithelial cells in vitro.* Am J Pathol, 1985. **118**(3): p. 398-407.
185. Holthofer, H., et al., *Decrease of glomerular disialogangliosides in puromycin nephrosis of the rat.* Am J Pathol, 1996. **149**(3): p. 1009-15.
186. Biomarkers Definitions Working Group, *Biomarkers and surrogate endpoints:Preferred definitions and conceptual framework.* Clinical Pharmacology and Therapeutics, 2001. **69**(3): p. 89-95.
187. Chevalier, R.L., *Biomarkers of congenital obstructive nephropathy: past, present and future.* J Urol, 2004. **172**(3): p. 852-7.
188. Ilyin, S.E., S.M. Belkowski, and C.R. Plata-Salaman, *Biomarker discovery and validation: technologies and integrative approaches.* Trends Biotechnol, 2004. **22**(8): p. 411-6.
189. Mancinelli, L., M. Cronin, and W. Sadee, *Pharmacogenomics: the promise of personalized medicine.* AAPS PharmSci, 2000. **2**(1): p. E4.
190. Peng, J. and S.P. Gygi, *Proteomics: the move to mixtures.* J Mass Spectrom, 2001. **36**(10): p. 1083-91.
191. Knepper, M.A., *Proteomics and the kidney.* J Am Soc Nephrol, 2002. **13**(5): p. 1398-408.
192. Neet, K.E. and J.C. Lee, *Biophysical characterization of proteins in the post-genomic era of proteomics.* Mol Cell Proteomics, 2002. **1**(6): p. 415-20.
193. Cutler, P., et al., *An integrated proteomic approach to studying glomerular nephrotoxicity.* Electrophoresis, 1999. **20**(18): p. 3647-58.
194. Nicholson, J.K., et al., *Metabonomics: a platform for studying drug toxicity and gene function.* Nat Rev Drug Discov, 2002. **1**(2): p. 153-61.
195. Charlwood, J., et al., *Proteomic analysis of rat kidney cortex following treatment with gentamicin.* J Proteome Res, 2002. **1**(1): p. 73-82.
196. Amin, R.P., et al., *Identification of putative gene based markers of renal toxicity.* Environ Health Perspect, 2004. **112**(4): p. 465-79.
197. Kramer, J.A., et al., *Overview on the application of transcription profiling using selected nephrotoxicants for toxicology assessment.* Environ Health Perspect, 2004. **112**(4): p. 460-4.
198. Ichimura, T., et al., *Kidney injury molecule-1 (KIM-1), a putative epithelial cell adhesion molecule containing a novel immunoglobulin domain, is up-regulated in renal cells after injury.* J Biol Chem, 1998. **273**(7): p. 4135-42.
199. Han, W.K., et al., *Kidney Injury Molecule-1 (KIM-1): a novel biomarker for human renal proximal tubule injury.* Kidney Int, 2002. **62**(1): p. 237-44.
200. Ichimura, T., et al., *Kidney injury molecule-1: a tissue and urinary biomarker for nephrotoxicant-induced renal injury.* Am J Physiol Renal Physiol, 2004. **286**(3): p. F552-63.

201. Takeichi, M., *Functional correlation between cell adhesive properties and some cell surface proteins.* J Cell Biol, 1977. **75**(2 Pt 1): p. 464-74.
202. Elsdale, T. and J. Bard, *Collagen substrata for studies on cell behavior.* J Cell Biol, 1972. **54**(3): p. 626-37.
203. Simpson, I.A., et al., *Insulin-stimulated translocation of glucose transporters in the isolated rat adipose cells: characterization of subcellular fractions.* Biochim Biophys Acta, 1983. **763**(4): p. 393-407.
204. Sanwal, V., et al., *Puromycin aminonucleoside induces glomerular epithelial cell apoptosis.* Exp Mol Pathol, 2001. **70**(1): p. 54-64.
205. Petermann, A.T., et al., *Podocytes that detach in experimental membranous nephropathy are viable.* Kidney Int, 2003. **64**(4): p. 1222-31.
206. Petermann, A.T., et al., *Viable podocytes detach in experimental diabetic nephropathy: potential mechanism underlying glomerulosclerosis.* Nephron Exp Nephrol, 2004. **98**(4): p. e114-23.
207. Nakamura, T., et al., *Urinary excretion of podocytes in patients with diabetic nephropathy.* Nephrol Dial Transplant, 2000. **15**(9): p. 1379-83.
208. Hara, M., et al., *Urinary excretion of podocytes reflects disease activity in children with glomerulonephritis.* Am J Nephrol, 1998. **18**(1): p. 35-41.
209. Koop, K., et al., *Expression of podocyte-associated molecules in acquired human kidney diseases.* J Am Soc Nephrol, 2003. **14**(8): p. 2063-71.
210. Kelly, D.J., et al., *Expression of the slit-diaphragm protein, nephrin, in experimental diabetic nephropathy: differing effects of anti-proteinuric therapies.* Nephrol Dial Transplant, 2002. **17**(7): p. 1327-32.
211. Kim, B.K., et al., *Differential expression of nephrin in acquired human proteinuric diseases.* Am J Kidney Dis, 2002. **40**(5): p. 964-73.
212. Yuan, H., et al., *Nephrin dissociates from actin, and its expression is reduced in early experimental membranous nephropathy.* J Am Soc Nephrol, 2002. **13**(4): p. 946-56.
213. Guan, N., et al., *Expression of nephrin, podocin, alpha-actinin, and WT1 in children with nephrotic syndrome.* Pediatr Nephrol, 2003. **18**(11): p. 1122-7.
214. Ruf, R.G., et al., *Prevalence of WT1 mutations in a large cohort of patients with steroid-resistant and steroid-sensitive nephrotic syndrome.* Kidney Int, 2004. **66**(2): p. 564-70.
215. Ryan, G.B. and M.J. Karnovsky, *An ultrastructural study of the mechanisms of proteinuria in aminonucleoside nephrosis.* Kidney Int, 1975. **8**(4): p. 219-32.
216. Caulfield, J.P. and M.G. Farquhar, *Distribution of annionic sites in glomerular basement membranes: their possible role in filtration and attachment.* Proc Natl Acad Sci U S A, 1976. **73**(5): p. 1646-50.

217. Venkatachalam, M.A., M.J. Karnovsky, and R.S. Cotran, *Glomerular permeability. Ultrastructural studies in experimental nephrosis using horseradish peroxidase as a tracer.* J Exp Med, 1969. **130**(2): p. 381-99.
218. Venkatachalam, M.A., R.S. Cotran, and M.J. Karnovsky, *An ultrastructural study of glomerular permeability in aminonucleoside nephrosis using catalase as a tracer protein.* J Exp Med, 1970. **132**(6): p. 1168-80.
219. Venkatachalam, M.A., et al., *An ultrastructural study of glomerular permeability using catalase and peroxidase as tracer proteins.* J Exp Med, 1970. **132**(6): p. 1153-67.
220. Vogelmann, S.U., et al., *Urinary excretion of viable podocytes in health and renal disease.* Am J Physiol Renal Physiol, 2003. **285**(1): p. F40-8.
221. Hara, M., et al., *Apical cell membranes are shed into urine from injured podocytes: a novel phenomenon of podocyte injury.* J Am Soc Nephrol, 2005. **16**(2): p. 408-16.
222. Kretzler, M., *Regulation of adhesive interaction between podocytes and glomerular basement membrane.* Microsc Res Tech, 2002. **57**(4): p. 247-53.
223. Kreidberg, J.A., et al., *Alpha 3 beta 1 integrin has a crucial role in kidney and lung organogenesis.* Development, 1996. **122**(11): p. 3537-47.
224. Adler, S., *Integrin receptors in the glomerulus: potential role in glomerular injury.* Am J Physiol, 1992. **262**(5 Pt 2): p. F697-704.
225. Adler, S. and X. Chen, *Anti-Fx1A antibody recognizes a beta 1-integrin on glomerular epithelial cells and inhibits adhesion and growth.* Am J Physiol, 1992. **262**(5 Pt 2): p. F770-6.
226. O'Meara, Y.M., et al., *Nephrotoxic antiserum identifies a beta 1-integrin on rat glomerular epithelial cells.* Am J Physiol, 1992. **262**(6 Pt 2): p. F1083-91.
227. Wang, Z., et al., *(Alpha)3(beta)1 integrin regulates epithelial cytoskeletal organization.* J Cell Sci, 1999. **112 (Pt 17)**: p. 2925-35.
228. Sheppard, D., *In vivo functions of integrins: lessons from null mutations in mice.* Matrix Biol, 2000. **19**(3): p. 203-9.
229. DiPersio, C.M., et al., *alpha3beta1 Integrin is required for normal development of the epidermal basement membrane.* J Cell Biol, 1997. **137**(3): p. 729-42.
230. Regele, H.M., et al., *Glomerular expression of dystroglycans is reduced in minimal change nephrosis but not in focal segmental glomerulosclerosis.* J Am Soc Nephrol, 2000. **11**(3): p. 403-12.
231. Baraldi, A., et al., *Very late activation-3 integrin is the dominant beta 1-integrin on the glomerular capillary wall: an immunofluorescence study in nephrotic syndrome.* Nephron, 1992. **62**(4): p. 382-8.
232. Shikata, K., et al., *Distribution of extracellular matrix receptors in various forms of glomerulonephritis.* Am J Kidney Dis, 1995. **25**(5): p. 680-8.

233. Kemeny, E., et al., *Podocytes loose their adhesive phenotype in focal segmental glomerulosclerosis.* Clin Nephrol, 1995. **43**(2): p. 71-83.
234. Jin, D.K., et al., *Distribution of integrin subunits in human diabetic kidneys.* J Am Soc Nephrol, 1996. **7**(12): p. 2636-45.
235. Chen, H.C., et al., *Altering expression of alpha3beta1 integrin on podocytes of human and rats with diabetes.* Life Sci, 2000. **67**(19): p. 2345-53.
236. Regoli, M. and M. Bendayan, *Alterations in the expression of the alpha 3 beta 1 integrin in certain membrane domains of the glomerular epithelial cells (podocytes) in diabetes mellitus.* Diabetologia, 1997. **40**(1): p. 15-22.
237. Kojima, K., K. Matsui, and M. Nagase, *Protection of alpha(3) integrin-mediated podocyte shape by superoxide dismutase in the puromycin aminonucleoside nephrosis rat.* Am J Kidney Dis, 2000. **35**(6): p. 1175-85.
238. de Paulo, V., et al., *Functional consequences of integrin-linked kinase activation in podocyte damage.* Kidney Int, 2005. **67**(2): p. 514-23.
239. Kretzler, M., et al., *Integrin-linked kinase as a candidate downstream effector in proteinuria.* Faseb J, 2001. **15**(10): p. 1843-5.
240. Sorokin, L.M., et al., *Differential expression of five laminin alpha (1-5) chains in developing and adult mouse kidney.* Dev Dyn, 1997. **210**(4): p. 446-62.
241. Klein, G., et al., *Role of laminin A chain in the development of epithelial cell polarity.* Cell, 1988. **55**(2): p. 331-41.
242. Miner, J.H., et al., *The laminin alpha chains: expression, developmental transitions, and chromosomal locations of alpha1-5, identification of heterotrimeric laminins 8-11, and cloning of a novel alpha3 isoform.* J Cell Biol, 1997. **137**(3): p. 685-701.
243. Miner, J.H. and J.R. Sanes, *Collagen IV alpha 3, alpha 4, and alpha 5 chains in rodent basal laminae: sequence, distribution, association with laminins, and developmental switches.* J Cell Biol, 1994. **127**(3): p. 879-91.
244. Sanes, J.R., et al., *Molecular heterogeneity of basal laminae: isoforms of laminin and collagen IV at the neuromuscular junction and elsewhere.* J Cell Biol, 1990. **111**(4): p. 1685-99.
245. Noakes, P.G., et al., *The renal glomerulus of mice lacking s-laminin/laminin beta 2: nephrosis despite molecular compensation by laminin beta 1.* Nat Genet, 1995. **10**(4): p. 400-6.
246. Durbeej, M., et al., *Expression of laminin alpha 1, alpha 5 and beta 2 chains during embryogenesis of the kidney and vasculature.* Matrix Biol, 1996. **15**(6): p. 397-413.
247. Sorokin, L.M., et al., *Monoclonal antibodies against laminin A chain fragment E3 and their effects on binding to cells and proteoglycan and on kidney development.* Exp Cell Res, 1992. **201**(1): p. 137-44.

248. Ekblom, M., et al., *Transient and locally restricted expression of laminin A chain mRNA by developing epithelial cells during kidney organogenesis.* Cell, 1990. **60**(2): p. 337-46.
249. Miner, J.H., *Renal basement membrane components.* Kidney Int, 1999. **56**(6): p. 2016-24.
250. Engvall, E., et al., *Distribution and isolation of four laminin variants; tissue restricted distribution of heterotrimers assembled from five different subunits.* Cell Regul, 1990. **1**(10): p. 731-40.
251. Noakes, P.G., et al., *Aberrant differentiation of neuromuscular junctions in mice lacking s-laminin/laminin beta 2.* Nature, 1995. **374**(6519): p. 258-62.
252. Patton, B.L., et al., *Distribution and function of laminins in the neuromuscular system of developing, adult, and mutant mice.* J Cell Biol, 1997. **139**(6): p. 1507-21.
253. Raats, C.J., et al., *Expression of agrin, dystroglycan, and utrophin in normal renal tissue and in experimental glomerulopathies.* Am J Pathol, 2000. **156**(5): p. 1749-65.
254. Kojima, K. and D. Kerjaschki, *Is podocyte shape controlled by the dystroglycan complex?* Nephrol Dial Transplant, 2002. **17 Suppl 9**: p. 23-4.
255. Henry, M.D. and K.P. Campbell, *Dystroglycan inside and out.* Curr Opin Cell Biol, 1999. **11**(5): p. 602-7.
256. Koch, A.W., K.L. Manzur, and W. Shan, *Structure-based models of cadherin-mediated cell adhesion: the evolution continues.* Cell Mol Life Sci, 2004. **61**(15): p. 1884-95.
257. Humphries, M.J. and P. Newham, *The structure of cell-adhesion molecules.* Trends Cell Biol, 1998. **8**(2): p. 78-83.
258. Steinberg, M.S. and P.M. McNutt, *Cadherins and their connections: adhesion junctions have broader functions.* Curr Opin Cell Biol, 1999. **11**(5): p. 554-60.
259. Takeichi, M., *Cadherin cell adhesion receptors as a morphogenetic regulator.* Science, 1991. **251**(5000): p. 1451-5.
260. Reiser, J., et al., *Podocyte Migration during Nephrotic Syndrome Requires a Coordinated Interplay between Cathepsin L and {alpha}3 Integrin.* J Biol Chem, 2004. **279**(33): p. 34827-34832.
261. Whiteside, C.I., et al., *Podocytic cytoskeletal disaggregation and basement-membrane detachment in puromycin aminonucleoside nephrosis.* Am J Pathol, 1993. **142**(5): p. 1641-53.
262. Holthofer, H., K. Sainio, and A. Miettinen, *Rat glomerular cells do not express podocytic markers when cultured in vitro.* Lab Invest, 1991. **65**(5): p. 548-57.
263. Shirato, I., *Podocyte process effacement in vivo.* Microsc Res Tech, 2002. **57**(4): p. 241-6.
264. Shirato, I., et al., *Cytoskeletal changes in podocytes associated with foot process effacement in Masugi nephritis.* Am J Pathol, 1996. **148**(4): p. 1283-96.
265. Oh, J., J. Reiser, and P. Mundel, *Dynamic (re)organization of the podocyte actin cytoskeleton in the nephrotic syndrome.* Pediatr Nephrol, 2004. **19**(2): p. 130-7.

266. Smoyer, W.E. and R.F. Ransom, *Hsp27 regulates podocyte cytoskeletal changes in an in vitro model of podocyte process retraction.* Faseb J, 2002. **16**(3): p. 315-26.
267. Kurihara, H., et al., *Monoclonal antibody P-31 recognizes a novel intermediate filament-associated protein (p250) in rat podocytes.* Am J Physiol, 1998. **274**(5 Pt 2): p. F986-97.
268. Ichimura, K., H. Kurihara, and T. Sakai, *Actin filament organization of foot processes in rat podocytes.* J Histochem Cytochem, 2003. **51**(12): p. 1589-600.
269. Kaplan, J.M., et al., *Mutations in ACTN4, encoding alpha-actinin-4, cause familial focal segmental glomerulosclerosis.* Nat Genet, 2000. **24**(3): p. 251-6.
270. Goto, H., et al., *Renal alpha-actinin-4: purification and puromycin aminonucleoside-binding property.* Nephron Exp Nephrol, 2003. **93**(1): p. e27-35.
271. Mundel, P. and W. Kriz, *Cell culture of podocytes.* Exp Nephrol, 1996. **4**(5): p. 263-6.
272. Miron, T., M. Wilchek, and B. Geiger, *Characterization of an inhibitor of actin polymerization in vinculin-rich fraction of turkey gizzard smooth muscle.* Eur J Biochem, 1988. **178**(2): p. 543-53.
273. Schneider, G.B., H. Hamano, and L.F. Cooper, *In vivo evaluation of hsp27 as an inhibitor of actin polymerization: hsp27 limits actin stress fiber and focal adhesion formation after heat shock.* J Cell Physiol, 1998. **177**(4): p. 575-84.
274. Miron, T., et al., *A 25-kD inhibitor of actin polymerization is a low molecular mass heat shock protein.* J Cell Biol, 1991. **114**(2): p. 255-61.
275. Lavoie, J.N., et al., *Modulation of actin microfilament dynamics and fluid phase pinocytosis by phosphorylation of heat shock protein 27.* J Biol Chem, 1993. **268**(32): p. 24210-4.
276. Lavoie, J.N., et al., *Modulation of cellular thermoresistance and actin filament stability accompanies phosphorylation-induced changes in the oligomeric structure of heat shock protein 27.* Mol Cell Biol, 1995. **15**(1): p. 505-16.
277. Smoyer, W.E., et al., *Altered expression of glomerular heat shock protein 27 in experimental nephrotic syndrome.* J Clin Invest, 1996. **97**(12): p. 2697-704.
278. Kim, Y.H., et al., *Podocyte depletion and glomerulosclerosis have a direct relationship in the PAN-treated rat.* Kidney Int, 2001. **60**(3): p. 957-68.
279. Saran, A.M., et al., *Complement mediates nephrin redistribution and actin dissociation in experimental membranous nephropathy.* Kidney Int, 2003. **64**(6): p. 2072-2078.
280. Topham, P.S., et al., *Complement-mediated injury reversibly disrupts glomerular epithelial cell actin microfilaments and focal adhesions.* Kidney Int, 1999. **55**(5): p. 1763-75.
281. Zolg, J.W. and H. Langen, *How industry is approaching the search for new diagnostic markers and biomarkers.* Mol Cell Proteomics, 2004. **3**(4): p. 345-54.

282. Lewin, D.A. and M.P. Weiner, *Molecular biomarkers in drug development.* Drug Discov Today, 2004. **9**(22): p. 976-83.
283. Lesko, L.J. and A.J. Atkinson, Jr., *Use of biomarkers and surrogate endpoints in drug development and regulatory decision making: criteria, validation, strategies.* Annu Rev Pharmacol Toxicol, 2001. **41**: p. 347-66.
284. Kanno, K., et al., *Urinary sediment podocalyxin in children with glomerular diseases.* Nephron Clin Pract, 2003. **95**(3): p. C91-9.
285. Somasiri, A., et al., *Overexpression of the anti-adhesin podocalyxin is an independent predictor of breast cancer progression.* Cancer Res, 2004. **64**(15): p. 5068-73.
286. Caldwell, G.W., et al., *The new pre-preclinical paradigm: compound optimization in early and late phase drug discovery.* Curr Top Med Chem, 2001. **1**(5): p. 353-66.
287. Frank, R. and R. Hargreaves, *Clinical biomarkers in drug discovery and development.* Nat Rev Drug Discov, 2003. **2**(7): p. 566-80.
288. Goodsaid, F.M., *Identification and measurement of genomic biomarkers of nephrotoxicity.* J Pharmacol Toxicol Methods, 2004. **49**(3): p. 183-6.
289. Rolan, P., A.J. Atkinson, Jr., and L.J. Lesko, *Use of biomarkers from drug discovery through clinical practice: report of the Ninth European Federation of Pharmaceutical Sciences Conference on Optimizing Drug Development.* Clin Pharmacol Ther, 2003. **73**(4): p. 284-91.